INVESTIGATING THE CELLULAR AND MOLECULAR EFFECTS OF CITRUS FLAVONOIDS TANGERETIN AND NOBILETIN IN HUMAN CANCER CELLS

(Spine title: Anticancer effects of citrus flavonoids, tangeretin and nobiletin)

(Thesis format: Monograph)

by

Karen L. Morley

Graduate Program
in
Microbiology and Immunology

Thesis submitted in partial fulfillment
of the requirements for the degree of
Doctor of Philosophy

Faculty of Graduate Studies
The University of Western Ontario
London, Ontario, Canada

Your file Votre référence
ISBN: 978-0-494-39311-6
Our file Notre référence
ISBN: 978-0-494-39311-6

THE UNIVERSITY OF WESTERN ONTARIO
FACULTY OF GRADUATE STUDIES

CERTIFICATE OF EXAMINATION

Supervisor	Examiners
Dr. James Koropatnick	Dr. Gregor Reid
Supervisory Committee	Dr. Wayne Flintoff
Dr. Gabriel DiMattia	Dr. David Bailey
Dr. Murray Huff	Dr. Gopinadhan Paliyath

The thesis by

Karen L. Morley

entitled:

Investigating the cellular and molecular effects of citrus flavonoids, tangeretin and nobiletin, in human cancer cells

is accepted in partial fulfillment of the
requirements for the degree of
Doctor of Philosophy

Date_____

_____
Chair of the Thesis Examination Board

Abstract

Flavonoids are a class of secondary metabolites found in all plants including fruits and vegetables. Research over the past 50 years has found increased flavonoid intake correlates with decreased risk and occurrence of chronic diseases like cancer. The anticancer properties of flavonoid compounds such as soy isoflavones have been well established, however others, such as citrus flavonoids have not been. In this thesis, I show a common physiological response in cancer cells of different origins to two citrus flavonoids, tangeretin and nobiletin. Cell cycle and apoptosis analysis using flow cytometry found tangeretin inhibited proliferation by inducing G1 accumulation in MDA-MB-435, MCF-7 and HT-29 cells without inducing death. Nobiletin had a similar effect at low concentrations, however, treatment with higher concentrations resulted in apoptosis. When concentrations of tangeretin and nobiletin that induced cell cycle accumulation (and apoptosis in the case of nobiletin) were used, cells recovered and proliferated similar to untreated controls following removal of these flavonoids. Analysis of gene expression in tangeretin-treated MDA-MB-435 cells using microarrays found expression changes consistent with cell cycle accumulation and a lack of apoptosis. Additionally, I report the selection and characterization of cancer cells resistant to a naturally occurring flavonoid, tangeretin. These cells displayed a lack of resistance to a panel of chemotherapy drugs demonstrating specific resistance to tangeretin. P-glycoprotein overexpression did not confer resistance to tangeretin or nobiletin which is consistent with findings from the cross-resistance analysis. Tangeretin also induced G1 accumulation of tangeretin-resistant cells, however, this effect disappeared by 4 days. Preliminary gene expression analysis identified expression changes in cell cycle regulators different than those identified in parental cells. The present study demonstrated that tangeretin and nobiletin reduced proliferation of human cancer cells of disparate origin in a reversible, non-toxic manner, by modulating expression of cell cycle and apoptosis regulatory genes resulting in induction of cell cycle accumulation and, in some cases, apoptosis. These and other compounds that inhibit proliferation of human

cancers without inducing irreversible toxicity may be advantageous in treating human tumors by restricting proliferation in a manner unlikely to permanently harm non-tumor host cells.

Keywords

Flavonoid, tangeretin, nobiletin, anticancer, cell cycle, apoptosis, cytostatic, cytotoxic

For the Morley Family

I dreamed the impossible dream,
It came true,
And it was all because of you.

Acknowledgements

Thanks to my thesis supervisor, Dr. Jim Koropatnick, for allowing me the freedom to find my way. His talent for putting the proverbial silver lining on dark clouds was much appreciated and admired. My committee members, Dr. Gabe DiMattia and Dr. Murray Huff, always provided me with unique perspectives and I appreciate their guidance and encouragement. Thank you to Dr. Joe Mymryk for his obvious care and interest in the training of graduate students which I benefited from through Journal Club, Ivey Lectures and random chats in the hallways of LRCP about science and weird news like diamonds made from the ashes of loved ones. It is my hope that he continues his unique brand of mentorship of graduate students at LRCP. Thanks also to Dr. Peter Ferguson for his guidance and assistance with the design and execution of experiments.

Special thanks to Wendy Brown, Mike Keeney and all the other members of the LHSC Flow Cytometry Unit (Karin, Sylvia, Leslie, Luigi and Janice) for their assistance with cell cycle and apoptosis analyses. I appreciate their patience and willingness to help me and for always making me feel welcomed whenever I visited the flow lab. I also thank Joe Andrews for being my go-to guy for assistance with microarray data analysis. Undoubtedly without his help with GeneSpring, I would be hairless and in the looney bin by now.

I have had a blast working with all the past and present members of the Koropatnick lab, most notably Tracey Jason, Shireen Fard, René Figueredo, Farzana Haq, Wendy Kennette, Alayne Brisson, Meghan Mahoney, Faiyaz Notta, Aleksandra Pandyra and Tracy Wong. You have all contributed in some way to my personal and professional growth. I am proud and honored to call all of you friends. You have helped me brave the failures and successes of graduate training. I would also like to acknowledge the scientists, students and staff of the LRCP Cancer Research Labs for providing a supportive and fun work environment.

Most importantly, I thank the Morley family who have sacrificed so much for me to get where I am today. Truly, without you, none of this would have been possible. I am inspired by your strength, faith, perseverance, and selflessness.

And to my amazing Chris, and my beautiful Savannah, thank you for your unconditional love and support. You are my foundation.

This work was supported by a CIHR University-Industry Scholarship in conjunction with KGK Synergize Inc., London, Ontario.

Table of Contents

List of Tables

List of Figures

List of Appendices

List of Abbreviations

^3H	tritium
5-FU	5-fluorouracil
5-FUdR	5-fluorodeoxyuridine
18S	18S rRNA
α	alpha
ABC	ATP-binding cassette
AIF	apoptosis inducing factor
AIP	2-amino-indan-2-phosphonic acid
α-MEM	minimal essential media, alpha
ANOVA	analysis of variance
AP-1	activator protein-1
APAF-1	apoptotic protease-activating factor-1
ara-C	cytosine arabinoside
ATM	ataxia-telangiectasia mutated
ATP	adenosine triphosphate
ATR	ATM and Rad3-related
β	beta
BCRP	breast cancer resistance protein
cAMP	cyclic adenosine monophosphate
CCNE2	cyclin E2
Cdc	cell division cycle
CDK	cyclin-dependent kinase
cDNA	complementary DNA
cGMP	cyclic guanosine monophosphate
Chk1/2	checkpoint kinase
CIP/KIP	CDK inhibitor family
CKI	CDK inhibitor
cm	centimeter
CO_2	carbon dioxide
CoA	Coenzyme A
CoASH	Coenzyme A

COMT	catechol-O-methyl-transferase
CREM	cAMP responsive element modulator
cRNA	complementary RNA
C_t	threshold cycle
CYP3A4	cytochrome P450 enzyme, group 3A, member 4
Cyt c	cytochrome c
d	day
DMBA	7,12-dimethylbenz[a]anthracene
DMSO	dimethyl sulfoxide
DNA	deoxyribonucleic acid
DR	death receptor
DUSP6	dual specificity phosphatase 6
E2F	transcription factor family
ECG	epicatechin gallate
EGCG	epigallocatechin gallate
EGF	epidermal growth factor
EGFR	epidermal growth factor receptor
ER	estrogen receptor
ERK	extracellular signal-regulated kinase
FAA	flavone-8-acetic acid
FADD	Fas-associated protein *via* death domain
FITC	fluorescein isothiocyanate
g	gram
G	gap phase
GADD45	growth arreast and DNA damage family
GBE	Gingko biloba extract
GSH	glutathione
GST	glutathione-S-transferase
h	hour
H&E	hematoxylin and eosin staining
HDAC	histone deacetylase
i.v.	intravenous
IAP	inhibitor of apoptosis protein

IC_{50}	inhibitive concentration 50%
INK4	inhibitor of cyclin-dependent kinase 4
IPA	Ingenuity pathways analysis
IPKB	Ingenuity pathways knowledge base
kg	kilogram
lb	pound
LD_{50}	lethal dose 50%
LPH	lactate-phlorizin hydrolase
M	mitosis phase
MAPK	mitogen activated protein kinase
Mdm2	murine double minute 2 oncogene
MDR	multi-drug resistance
MEK	MAPK kinase
mg	milligram
ml	milliliter
mM	millimolar
min	minute
µg	microgram
µl	microliter
µM	micromolar
mRNA	messenger ribonucleic acid
MRP	multidrug resistance protein
NADPH	nicotinamide adenine dinucleotide phosphate
NC	no colonies
NF-κB	nuclear factor kappa beta
nm	nanometer
Nob	nobiletin, 3',4',5,6,7,8-hexamethoxyflavone
NP40	nonidet P40
NPAT	nuclear protein mapped to the AT locus
NBS1	Nijmegan breakage syndrome 1
O_2	oxygen
P	P value
p53	tumor protein or protein 53, tumor suppressor

P450	cytochrome P450 enzymes
PAL	phenylalanine ammonia-lyase
PARP	poly(ADP-ribose) polymerase
PBS	phosphate buffered saline
PC	positive control
PCR	polymerase chain reaction
P-gp	P-glycoprotein
PI	propidium iodide
PI3K	phosphoinositide-3-kinase
PKC	protein kinase C
PMF	polymethoxyflavone
P-PST	phenol sulfotransferase
pRb	retinoblastoma protein
QR	quinone reductase
R^2	r squared
RNA	ribonucleic acid
rpm	rotations per minute
RT	reverse transcription
S	synthesis phase
SCF	Skp1/Cullin/F-box protein
SEM	standard error of the mean
SULT1	sulfotransferase
Tan	tangeretin, 4',5,6,7,8-pentamethoxyflavone
TGF-β	transforming growth factor beta
TNFAIP3	TNFα -induced protein 3 or A20
Tris	Tris(hydroxymethyl)-aminomethane hydrochloride
TS	thymidylate synthase
UC	untreated control
UDP	uridine diphosphate
UGT	UDP glucuronosyl transferase
UV	ultraviolet
V	volt
VC	vehicle control

v/v	volume to volume
VEGF	vascular endothelial growth factor
x g	times gravity

Chapter 1
INTRODUCTION

1.1. History of flavonoids

Flavonoids have been studied since the early 1600s in the form of plant pigments. Although they were not yet known as flavonoids. Early investigation was concerned with the morphological and histological distribution of plant and flower pigmentation. The earliest account of these plant pigments was by Robert Boyle in 1664. He described the colour changes that occurred when acids or bases were added to plant and flower extracts [28] (as reviewed by Muriel Wheldale Onslow in 1916 [300]). In 1682, Nehemiah Grew, in papers read before the Royal Society in London, discussed solubility properties of plant pigments and their behaviour towards acids and bases [98] (as reviewed in [300]). The terms "anthocyanin" and "anthoxanthin" were introduced 150 years later by Marquart in 1835 to describe the red, blue and violet, and the yellow pigments of plants, respectively [179] (as reviewed in [300]). The term "anthocyanin" persists today to describe one class of flavonoid.

Following the observations of these early scientists, other lines of investigation began to emerge. Studies over the next two centuries focused mainly on determining function, chemical composition and formation of plant pigmentation. The view that anthocyanins have a protective function in plants arose from work by Pringsheim in 1880, which showed that an artificially applied red screen prevented chlorophyll bleaching by intense light (as reviewed in [263]). The first hints of anthocyanin composition came from Morot in 1849, who isolated the blue pigment of cornflower and found it contained carbon, hydrogen and oxygen [192] (as reviewed in [300]). Wigand in 1862 provided insight into the formation of anthocyanins, suggesting they arose from the oxidation of colourless tannin-like chromogens [302] (as reviewed in [300]). These examples are by no means an exhaustive account of work in the areas of plant pigment formation, composition and function, but they demonstrate the early interest and observations about one particular class of compounds (anthocyanins) that came to be applied to flavonoids in general.

The early 1900s saw further study into the role of anthocyanins in the inheritance of colour in plants, and those studies eventually led to further insight into the chemical nature and structure of anthocyanins. In 1905 Bateson, Saunders and Punnett found that crossing two white-flowered sweet pea plants produced a purple-flowered plant [17] (as reviewed in [300]). They proposed the presence of three factors. Two main factors were hypothesized to be primarily responsible for flower color, the loss of which resulted in albino flowers. The third was a modifying factor that produced blue or purple flowers in the presence of the other two factors. Work by Muriel Wheldale in 1909 supported the idea of chemical substances that were combined or modified to produce variety in flower colour [299] (as reviewed in [300]). Filhol and his colleagues had observed colourless plant pigments that reacted with alkali to produce a bright yellow colour [82] (as reviewed in [300]). In 1905, Bidgood identified these colourless substances as "flavones" [22] (as reviewed in [300]) derived from the Latin word for yellow, flavus. These were likely the same yellow pigments Marquart referred to as anthoxanthins. In fact, the term "flavone" had appeared 10 years earlier in a paper by von Kostanecki and Tambor [290] (as reviewed in [25]).

Besides anthocyanins and flavones, there are mentions of other types of flavonoids as early as the 1820's. For example, hesperidin, a flavanone glycoside, was first described by Lebreton in 1828 [164] (as reviewed in [263]). Phlorodzin (a dihydrochalcone), was isolated by de Koninck from apple root bark in 1835 [63] (as reviewed in [25]). Isoflavones were isolated by de Laire and Tiemann in 1893 from the rhizomes of irises [64] (as reviewed in [25]). The first chalcone described was carthamin, isolated from safflowers [135] (as reviewed in [25]). Aurones were first described by Geissman and Heaton in 1944 [91] (as reviewed in [25]).

The Hungarian scientist and Nobel prize-winner Albert Svent-Györgyi is credited with the serendipitous discovery of the biological activities of flavonoids. While working to characterize the benefits of vitamin C, a patient developed bleeding gums which Szent-Györgyi believed was associated with vitamin C deficiency. He administered a partially-purified preparation of vitamin C,

successfully treating the bleeding. Thinking that a fully purified preparation would work even faster, he treated a second patient with purified vitamin C which failed to alleviate that patient's symptoms. Szent-Györgyi hypothesized the impure preparation contained an additional factor and, in 1935 he isolated a substance from lemon juice that decreased permeability and increased resistance of capillary walls [232]. He first called it "citrin", and later "vitamin P" to indicate its therapeutic value to patients with vascular purpura. Later that year, Szent-Györgyi determined citrin was actually a mixture of hesperidin and eriodictyol glycoside [268]. The essential nature of flavonoids could not be substantiated, and in 1950 the Joint Committee on Biochemical Nomenclature recommended that the term "vitamin P" be discontinued [287]. The terms "flavonoid" and "bioflavonoid" (coined by biochemist BL Oser) first appeared in literature in the late 1940s just prior to the discontinuation of vitamin P [14]. Nevertheless, Szent-Györgyi was credited with highlighting the potential health benefits of flavonoids in humans, and his work in the 1930s shifted the focus of flavonoid research from merely characterizing the structure and function of these plant pigments to assessing their role in the prevention and treatment of human diseases.

1.2. Flavonoid chemistry

1.2.1. Structure

Flavonoids are a large group of secondary metabolites ubiquitously produced in plants of both terrestrial and aquatic locale [228]. They are the most abundant polyphenols found in plants [309] and over 8,000 compounds have been isolated and identified to date [217]. The basic flavonoid structure is a 15-carbon skeleton that consists of two benzene rings connected by a three carbon bridge (Figure 1) [25]. The two benzene rings are labeled A and B with the intervening carbon bridge (which is most often cyclic) designated C. A multitude of substitutions can occur at any of nine different sites in the A and B rings however, substitutions occur more frequently at positions 5, 7, 3', 4' and 5' [25]. It is this variety in substitutable positions which accounts for the large numbers of individual compounds given that these sites can be hydroxylated, methoxylated, alkylated,

Figure 1. Basic flavonoid structure showing ring designations (A, B, and C), and the carbon numbering system (2-8 on rings A and C; 2'-6' on ring B). More commonly substituted positions are indicated by a period (■).

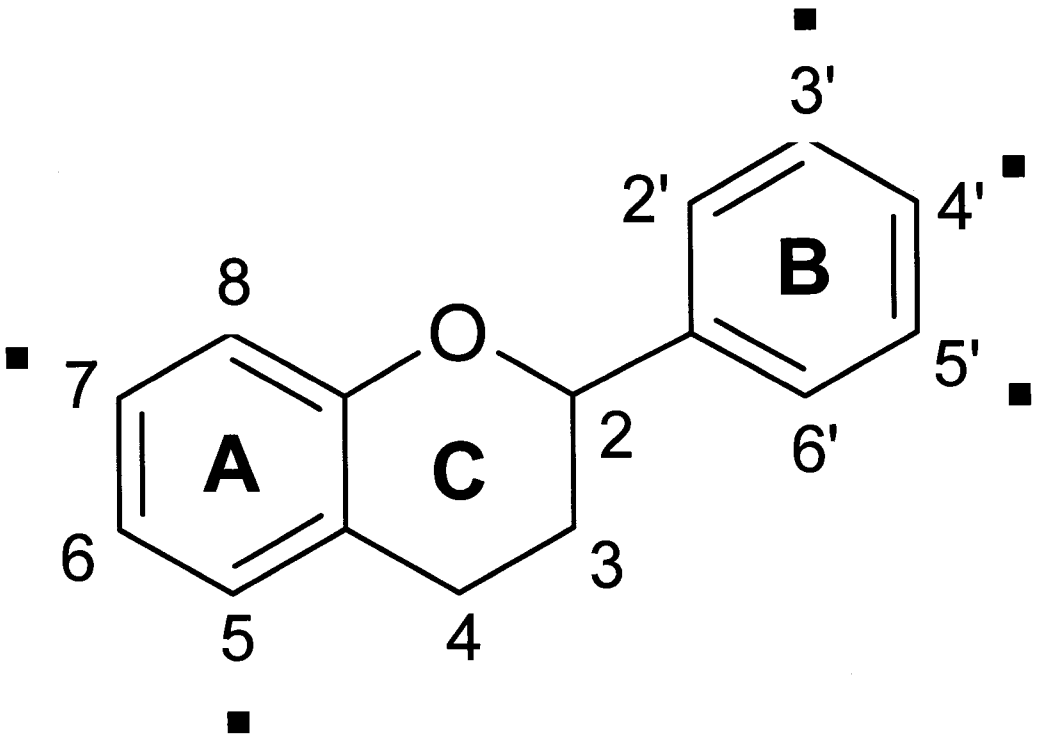
3'
2'
4'
B
8
O
5'
7
2
A
C
6'
6
3
5
4

glycosylated, acylated and sulfated [25]. Based on the potential numbers and kinds of substitutions that are possible, it is estimated that more than $2x10^6$ different flavonoid species could, in theory, exist in nature [113].

Flavonoids most frequently occur in plants as glycosides in vacuoles of flowers, seeds, stems, leaves and roots [61]. They are typically attached to glucose or rhamnose but can also be attached to galactose, arabinose, xylose, glucuronic acid or other sugars [4,139]. Glycosylation increases the polarity and solubility of the flavonoid molecule, both of which are necessary for storage in plant cell vacuoles [4]. Flavonoids not attached to sugars are called aglycones and they are found in the wax on leaves, barks and buds of plants [61].

1.2.2. Classification

While patterns of substitution of the A- and B-rings distinguish compounds within a class, it is substitutions and oxidation level of the C-ring that distinguishes one class of flavonoid from another. The common classes of flavonoids are: flavones, flavonols, flavanones, flavanols (catechins), anthocyanidins, isoflavones and chalcones (Figure 2) [139]. These classes can be further divided based on substitutions or polymerization for a more extensive list of classes. For example, flavanonols, aurones, coumarins and biflavones are also listed as flavonoid subgroups [217].

Compounds belonging to the flavone class have the basic flavonoid structure with substitutions of the A- and B-ring. Flavones can be found in all parts of the plant: stem, bud, leaves, bark, root, rhizomes, flowers, fruit, seeds and resin [180]. Examples of flavones are apigenin and luteolin, commonly found in parsley, thyme, celery and sweet red peppers [227]. Flavones also include tangeretin and nobiletin (commonly found in citrus fruits) which are the focus of this study. Table 1 shows substituents and positions of substituents for the abovementioned flavones.

Flavonols (i.e. 3-hydroxyflavones) are closely related to flavones in structure with the only difference being hydroxylation at the carbon-3 position. Flavones and flavonols are the most commonly occurring flavonoids [30] and

Figure 2. General structures of seven classes of flavonoids.

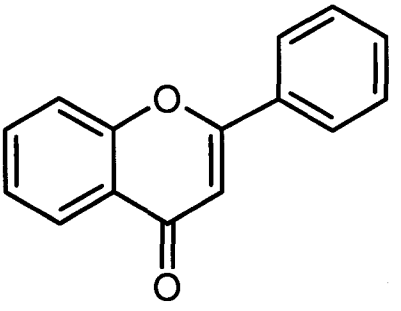

Flavones

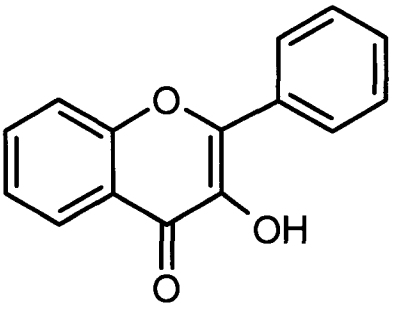

Flavonols

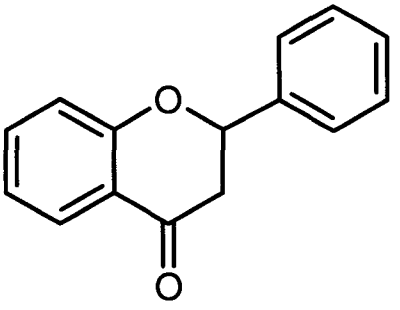

Flavanones

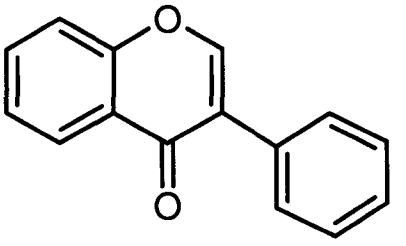

Isoflavones

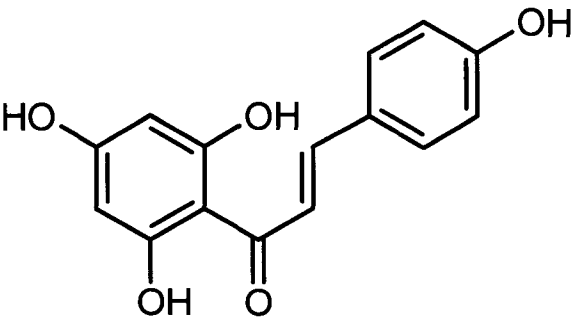

Chalcones

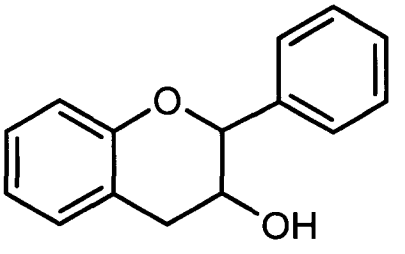

Flavanols

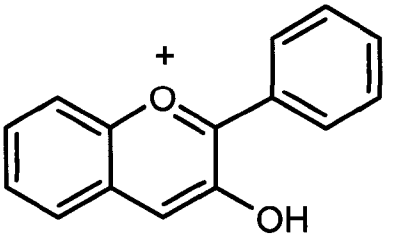

Anthocyanidins

Table 1. Substitutions of the A- and B-ring of the basic flavone structure for several representative flavones, including tangeretin and nobiletin.

	Ring position of carbon						
Flavonoid	**5**	**6**	**7**	**8**	**3'**	**4'**	**5'**
apigenin	OH	H	OH	H	H	OH	H
luteolin	OH	H	OH	H	OH	OH	H
tangeretin	OCH_3	OCH_3	OCH_3	OCH_3	H	OCH_3	H
nobiletin	OCH_3	OCH_3	OCH_3	OCH_3	OCH_3	OCH_3	H

exist mainly as colourless pigments in the leaves of plants. They control light admittance to leaves, playing an important role in UV protection and photosynthesis, and are the cause of leaf color changes in the fall. Examples of flavonols are quercetin and kaempferol which are found at high levels in onions, broccoli, apples, cherries and tea [227].

Flavanones are the main type of flavonoids found in citrus fruits and juices [177], and are largely responsible for their bitter taste. Some examples of flavanones are naringenin and hesperidin. Common food sources are citrus fruits and prunes.

Flavanols are a unique class of flavonoids as they are present in the diet in monomeric (catechins) or polymeric (proanthocyanidins) forms [175,177]. Another feature of this class is that they are never found attached to a sugar moiety [177]. Some examples of flavanols are epicatechin and gallocatechin. Flavanols are commonly found at high levels in green and black tea, apples, wine and cocoa [310].

Anthocyanidins are an important group of water soluble plant pigments that provide colour (ranging from red to blue) to flowers and fruits which makes them the most conspicuous class of flavonoids. They are important for attracting pollinators and dispersers to plants. Examples of anthocyanidins are cyanidin, malvidin and pelargonidin which are commonly found in cherries and grapes.

Isoflavones are one of the most highly studied classes of flavonoids. Structurally, the B-ring of isoflavones is attached to the heterocyclic C-ring at the carbon-3 position of the flavone molecule, as opposed to carbon-2 attachment in other classes. Hydroxyl groups occur at positions 7 and 4, similar to estradiol, which confers pseudohormonal abilities to these compounds and thus they are referred to as phytoestrogens [177]. Some well-known members are genistein and diadzein and foods high in isoflavonoid content include soya beans and other legumes.

Chalcones are another class of plant pigments, providing yellow color to the flowers and leaves of higher plants. The C-ring of chalcones is not closed;

position 1 is hydroxylated resulting in an opening of the heterocyclic C-ring. Phloretin and arbutin are two examples of chalcones which are found in apples, pears, strawberry and wheat.

1.2.3. Flavonoid biosynthesis in plants

All flavonoids are derived from a common biosynthetic pathway and are a combination of two basic plant metabolites: malonyl-CoA and *p*-coumaroyl-CoA. Malonyl-CoA is a product of the acetate pathway (Figure 3B) and *p*-coumaroyl-CoA is derived from the shikimate pathway (Figure 3A) [263]. The C6-C3-C6 backbone requires condensation of 3 molecules of malonyl-CoA and one of *p*-coumaroyl-CoA [180]. The *p*-coumaroyl-CoA molecule becomes the B-ring and the central heterocyclic C-ring, and the methyl and carboxyl groups of the three malonyl-CoA molecules become the A-ring, producing a chalcone intermediate. Chalcones are converted to flavanones by the activity of chalcone isomerase and flavanones are the starting point for synthesis of all other classes of flavonoids (Figure 4) [306]. Flavones, isoflavonoids and dihydro-flavonols (which become flavonols) are directly synthesized from flavanones but flavan-3-ols and anthocyanidins are synthesized *via* intermediate compounds.

1.2.4. Food content and intake

The estimation of flavonoid content in foods is difficult due to the structural diversity of flavonoids. Levels of flavonoids in food can be influenced by genetic factors such as plant variety or species, environmental factors such as light, maturity or ripeness of the food, and post-harvest processing [4]. Flavonoids found at the highest amounts in the human diet are: soy isoflavones (e.g. genistein, diadzein and biochanin A), flavonols (e.g. quercetin, keampferol and myricetin) and flavones (e.g. luteolin and apigenin) [227,310]. Table 2 shows estimates of flavonoid levels in several common foods [239].

Precise quantification of flavonoid intake by humans is difficult due to the large variety of flavonoids, their broad distribution and the diversity of human consumption. Measurement of intake depends on the method and criteria of the

Figure 3. Synthesis of *p*-coumaroyl-CoA via the shikimate pathway (A) and malonyl-CoA via the acetate pathway (B). These compounds are the starting point for the synthesis of all classes of flavonoids.

A

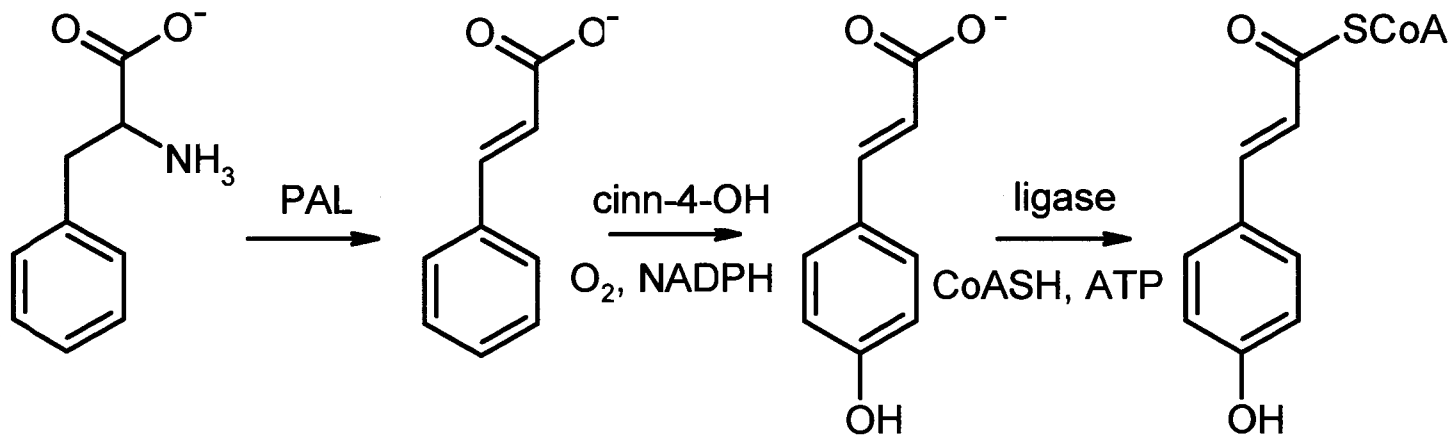
PAL
cinn-4-OH
O_2, NADPH
ligase
CoASH, ATP
L-phenylalanine
cinnamate
p-coumarate
p-coumaroyl-CoA

B

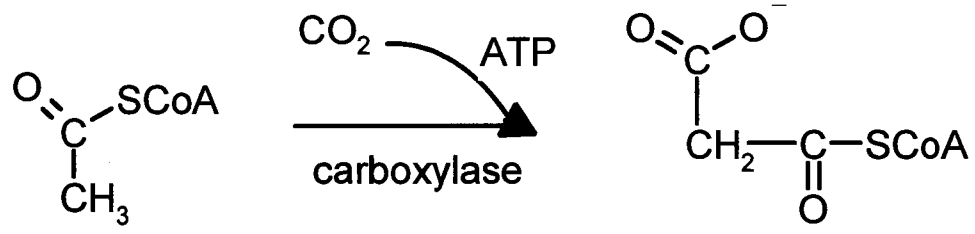
CO_2
ATP
carboxylase
acetyl-CoA
malonyl-CoA

Figure 4. Schematic of the flavonoid biosynthesis pathway in plants (adapted from Martens *et al.* [171]).

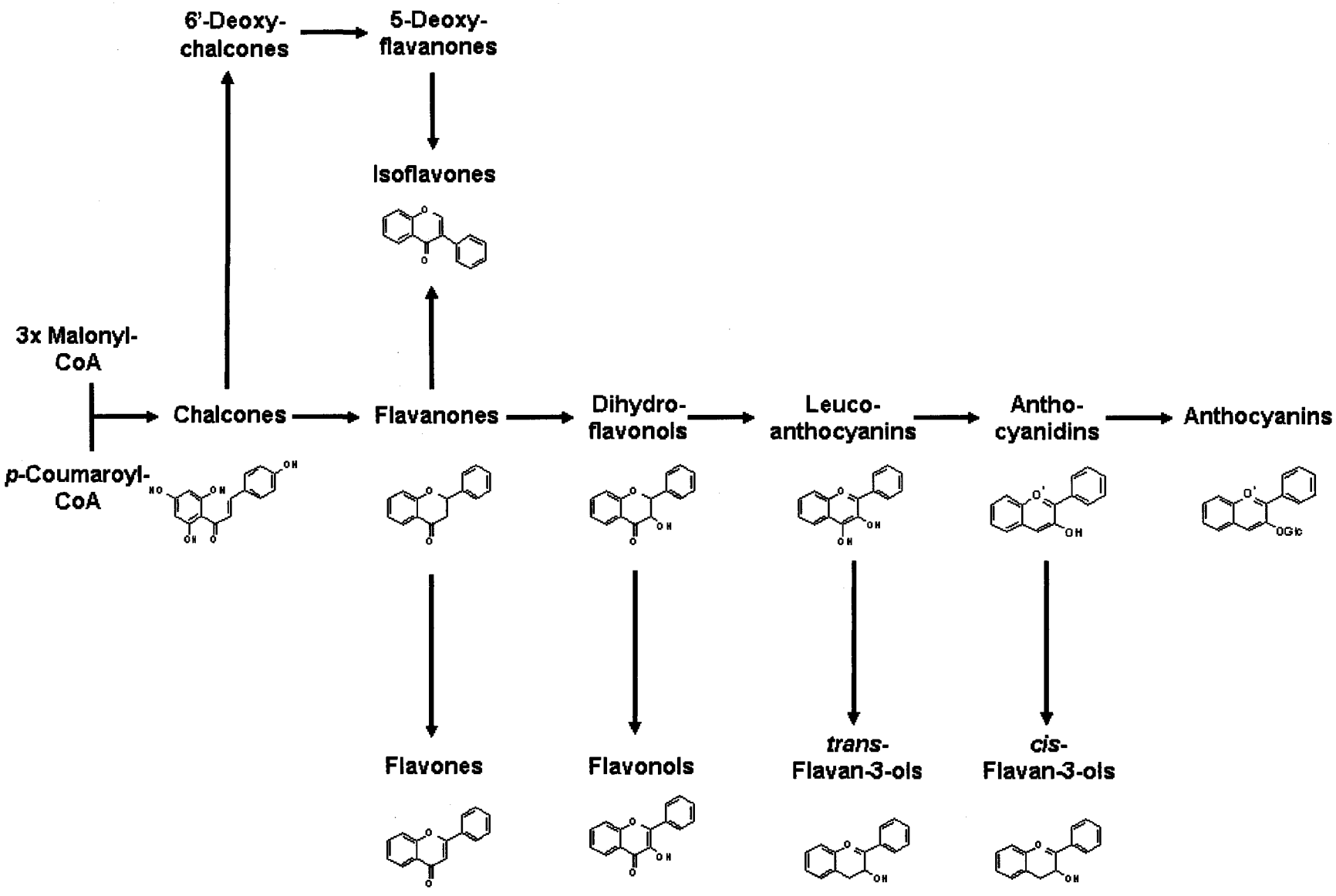
6'-Deoxy-chalcones
5-Deoxy-flavanones
Isoflavones
3x Malonyl-CoA
p-Coumaroyl-CoA
Chalcones
Flavanones
Dihydro-flavonols
Leuco-anthocyanins
Antho-cyanidins
Anthocyanins
Flavones
Flavonols
trans-Flavan-3-ols
cis-Flavan-3-ols

Table 2. Estimates of flavonoid levels in commonly consumed foods and beverages (adapted from Scalbert *et al.* [227]).

Food	Flavonoid content (mg/100g)
Vegetables	
tomato	0.5
lettuce	1.0
onion	35
Fruits	
apple	114
cherry	478
Other	
dark chocolate	510
Beverages (mg/100ml)	
orange juice	22
red wine	68
black tea	69

survey, the population, and the flavonoids selected for analysis. In 1976, Kuhnau estimated the daily intake of flavonoids in the United States to be 1g/d (expressed as glycosides) or 650 mg/d expressed as aglycones [158]. It has been suggested that this was an overestimation due to the unreliability of analytical methods available in the 1970s [122]. More recent estimates of daily intakes have been determined at much lower levels in diets from numerous countries and typically are in the range of tens to hundreds of mg per day [122,239]. The estimated daily intake of flavonoids varies considerably, depending on geographical location (Table 3).

1.2.5. Absorption, metabolism and bioavailability

The processing of flavonoids for cellular absorption begins in the stomach with the cleavage of polymeric forms to monomers. The monomeric forms move on to the small intestine where they are more easily absorbed. It was once thought that the absorption of flavonoids in the intestine was negligible as they exist primarily as glycosides in nature, and that there were no enzymes secreted or present in the intestines to break the β-glycosidic linkage between the aglycone and sugar [99]. Only lipophilic, sugar-free aglycones were thought to be absorbed, *via* passive diffusion across the gut wall [67]. It was assumed that glycosides passed through the small intestine to the large intestine where they underwent hydrolysis by colonic microflora, releasing aglycones and smaller phenolic acid products for absorption and excretion [62]. However, it was determined that quercetin glycosides were absorbed two times better than quercetin aglycones (52% vs. 24%) in ileostomy patients [120], demonstrating previously unrecognized absorption of glycosides in the small intestine. It is now clear that glycosides can be hydrolysed at the brush border of the small intestine through the action of lactate-phlorizin hydrolase (LPH), a membrane bound β-glucosidase enzyme present on the luminal side of the brush border [62]. Quercetin glycosides were determined to be up to 81% hydrolysed to quercetin aglycones by β-glucosidase activity prior to uptake [293].

Country	Intake (mg/d)
Denmark	23-46
Finland	24
Holland	73
Japan	63
United States	20-34

Once flavonoids are absorbed by intestinal cells, metabolism continues with the conjugation of methyl, glucuronide or sulphate groups to the aglycone, following a pathway common to the metabolism of drugs (Figure 5). Glucuronidation appears to be the primary type of conjugation of flavonoids carried out in intestinal cells, followed by methylation [214]. Flavonoids are then bound to albumin and transported to the liver *via* the hepatic portal vein [176] where the majority of flavonoid metabolism occurs. In the liver, additional conjugations can occur including glucuronidation, sulfation and methylation. The added conjugations increase the clearance time of these compounds, aiding in their quick elimination from the circulatory system. The main enzymes responsible for glucuronidation, methylation and sulfation of flavonoids in the liver are the phase II metabolizing enzymes UDP glucuronosyl transferase (UGT), catechol-O-methyl-transferase (COMT) and phenol sulfotransferases (SULT1 and P-PST), respectively [239]. After conjugation in the liver, flavonoids can either enter the circulation where they can access cells and tissues of the body, or they can be eliminated from the liver *via* renal or biliary excretion. Bile (synthesized and secreted by hepatocytes *via* the canaliculi duct system and then stored in the gall bladder) provides a route for excretion of conjugates to the large intestine. Flavonoids in bile are returned to the colon, degraded by colonic microflora, and are reabsorbed by intestinal cells or excreted in feces [103].

Flavonoids circulating in the blood (already conjugated in the intestines and liver) that are absorbed by cells and tissues of the body may undergo further metabolism. This "intracellular metabolism" includes: 1) thiol conjugation, particularly with GSH, 2) oxidative metabolism (involving hydroxylation to a more polar compound), and 3) metabolism by P450 enzymes [304].

Only approximately 5-10% of food-borne flavonoid is absorbed in the small intestine [53]. The remaining 90-95% continues on to the large intestine where it is degraded by colonic microflora for absorption and excretion. Of the 5-10% absorbed in the small intestine, 90-95% is conjugated (in intestinal lumen or liver cells) and does not remain in its original form [53].

Figure 5. Pathways of flavonoid absorption and metabolism in humans (adapted from Manach *et al.* [166]).

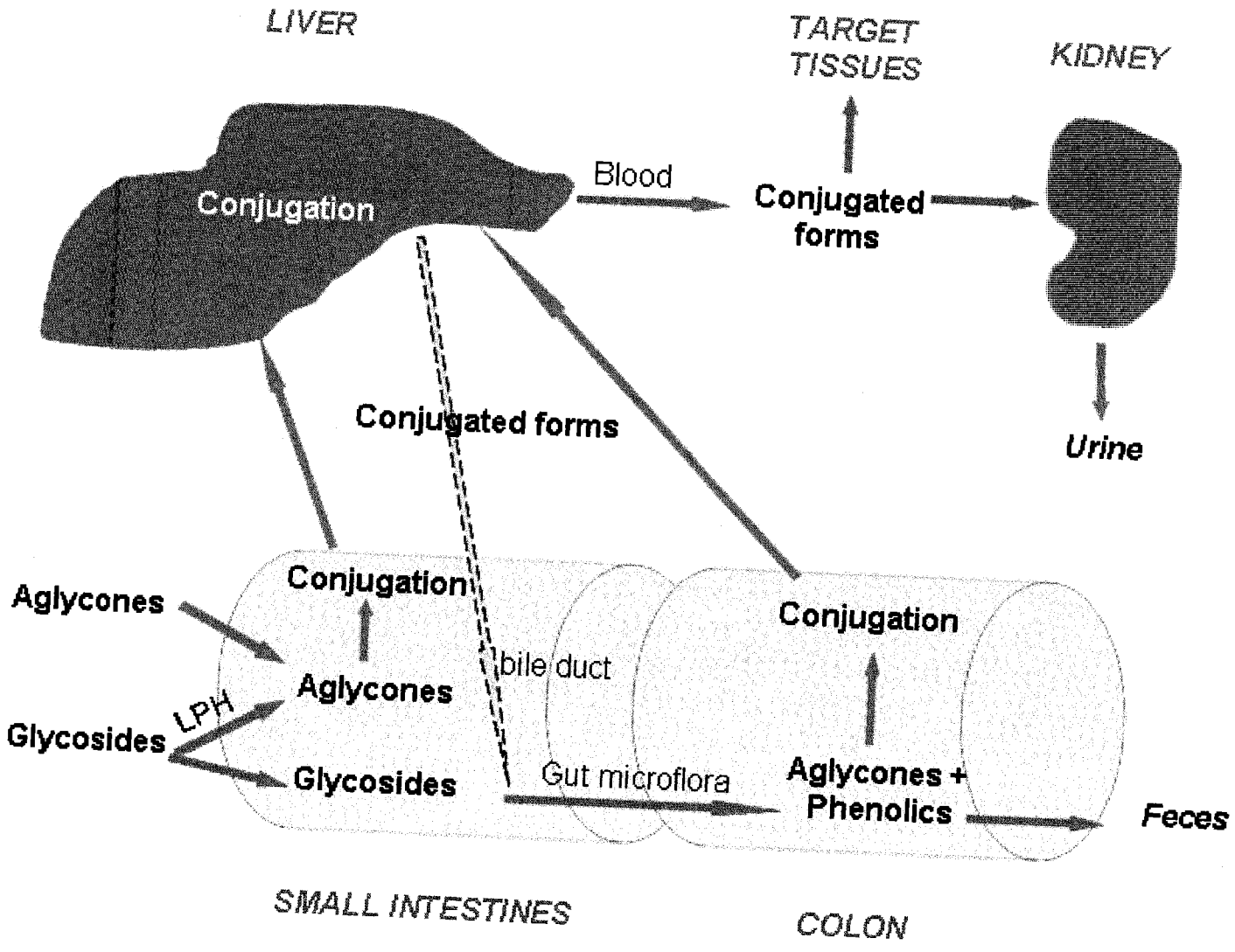
LIVER
TARGET TISSUES
KIDNEY
Conjugation
Blood
Conjugated forms
Conjugated forms
Urine
Aglycones
Conjugation
Conjugation
bile duct
Aglycones
LPH
Glycosides
Glycosides
Gut microflora
Aglycones + Phenolics
Feces
SMALL INTESTINES
COLON

For example, following consumption of a few milligrams of catechin (comparable to amounts found in moderate servings of red wine), the majority of circulating catechin was conjugated with only small amounts of free compound detectable [72]. Although it has been assumed that the biological effects of flavonoids result from activity of the free compounds, there is evidence suggesting that conjugated forms (glucuronides, sulphates, and O-methylates) may contribute to the bioactivity of flavonoids [100,260,261]. This does not mean that free flavonoids are never found in circulation. After consumption of a large dose of catechin (2 g), free catechin was detectable in plasma [104].

The maximum concentration of flavonoids found in blood plasma following normal dietary consumption ranges from 0.07-5.0 μM, depending on the flavonoid [239], but it rarely exceeds 1-2 μM. These concentrations peak 1-2 h after ingestion [12] with the exception of flavonoids requiring microbial metabolism which can reach maximum concentrations hours later. Levels of rutin (a quercetin rhamnoside which can only be metabolized by colonic bacteria) reached a maximum concentration 9 h after ingestion [121]. Higher levels of flavonoids in plasma were achieved following consumption of concentrated dietary supplements or after i.v. administration of flavonoids. For example, plasma concentration of tangeretin and metabolites ranged between 16-67 μM in hamsters fed a 3% PMF diet over 30 days [160], and following a single i.v. administration of a water-soluble prodrug of quercetin in humans, plasma levels of total quercetin peaked at 19.9±11.8 μM [193].

There are few studies concerning the disposition of tangeretin and nobiletin in the human body. The major cytochrome P450 enzyme known to metabolize tangeretin is CYP1A2 [31] (no comparable data on nobiletin could be found). It has also been shown that methoxylation increased metabolic stability and membrane transport in the intestine and liver, thus improving the oral bioavailability compared to hydroxylated compounds [292].

1.2.6. Safety of flavonoids

With increased interest in alternative medicine, flavonoids are being ingested at much higher levels by some members of the general population. Concentrated flavonoid preparations are available as unregulated herbal remedies or dietary supplements, thus raising the question of the safety of these compounds when consumed at doses far in excess of those found in normal diets. In rats, the LD_{50} of flavonoids was determined to be 2g/kg when administered intravenously [40]. A safety study of green tea polyphenols found that consumption of 800 mg/d of a flavanol, epigallocatechin gallate (EGCG), (equivalent to 8-16 cups of green tea) induced no deleterious effects in healthy individuals [48,49]. Consumption of 300-600 mg/d of genistein and diadzein (soy isoflavones) over 3 months by men with prostate cancer was not associated with significant toxicity [85]. In another pharmacokinetic study of genistein, consumption of up to 8 mg/kg (equivalent to 800 mg for a 220 lb male) resulted in plasma concentrations of up to 16.3 μM total genistein and was not associated with any toxicities [271]. This evidence indicates that ingesting high doses of flavonoids does not result in severe toxicities and it is assumed that consumption of flavonoids at these levels is relatively safe.

Another concern arising from the consumption of high doses of flavonoids is the potential for lethal flavonoid-drug interactions. Flavonoids are known to interact with phase I and II drug metabolizing enzymes [191] in ways that may be beneficial to humans (see section 1.3.2.3). They can also interact with certain members of this class in ways that are not. For example, naringenin (a flavanone found in grapefruit juice) inhibited the activity of CYP3A4 when administered simultaneously, impairing the metabolism of calcium channel blockers such as felodipine, and verapamil [87]. CYP3A4 is the predominant hepatic and intestinal cytochrome P450 responsible for metabolizing 50% of all therapeutic drugs [88]. Altered drug pharmacokinetics as a result of reduced drug metabolism could lead to accumulation of drugs and subsequent toxicity [88]. Regular high dosing of flavonoids could result in sustained levels in the circulation, greatly increasing the

chances of adverse flavonoid-drug interactions. On the other hand, some flavonoids have been found to stimulate metabolism by CYP3A4. For example, tangeretin stimulated midazolam 1'-hydroxylation by CYP3A4 in human liver microsomes [13], an effect that could potentially reduce the effectiveness of the drug.

1.3. Function of flavonoids

1.3.1. Function in plants

Flavonoids are synthesized in plants and are functional molecules in this locale. A primary function of flavonoids in plants is to provide pigmentation to flowers, which serves as an attractant to pollinators such as insects and birds for pollination [297]. Potential pollinators can be attracted simply by the color of the flower; for example, bees prefer blue and yellow flowers while hummingbirds prefer red [25]. In addition, pollinators can be attracted by patterns of pigmentation that act as nectar guides [15]. Not only do flavonoids play a role in attraction of pollinators for cross pollination, they are also involved in pollen development and germination [189]. A flavonoid-deficient mutant petunia was sterile due to the failure of pollen germination [280].

Flavonoids were hypothesized to block UV radiation in plants early on in plant pigment research (Pringsheim 1880 as reviewed in [263]). UV-B radiation, within the ultraviolet spectrum of sunlight, is a shorter wavelength (280-315 nm), high energy radiation that induces oxidative damage in nucleic acids and degradation of photosynthetic tissue [305]. Flavonoids, which are universally present in all structures of plants, absorb in the 280-320 nm region which makes them capable of acting as UV filters [108]. *Arabadopsis thaliana* mutants lacking epidermal flavonoids became sensitive to damage by UV-B radiation [210], supporting a role in UV protection. Furthermore, when flavonoid synthesis was blocked in red cabbage by treatment with 2-amino-indan-2-phosphonic acid (AIP), plants were twice as sensitive to UV-B damage as wild-type, untreated plants [93].

Flavonoids play a role in protecting plants from attack by herbivores, bacteria, viruses and fungi. Flavonoids protect plants in two ways: 1) previously synthesized flavonoids are used to discourage organisms from attacking (allelopathy). Allelopathy is demonstrated in the rice plant which uses three flavone glycosides present in the phloem sap as deterrents to the sucking behavior of the brown plant hopper pest, *Niloparvata lugens* [97]. 2) *de novo* synthesized flavonoids induced in response to infection by pathogenic organisms act as toxins to invading organism (phytoalexin). Phytoalexins mediate disease resistance by disrupting the growth and development of pathogens [16]. An example of flavonoid phytoalexins can be found in the legume *Astragalus cicer L.* where mucronulatol (7,3'-dihydroxy-2',4'-dimethoxyisoflavan) was induced following inoculation with fungal spores [181].

Flavonoids also play a role in the symbiotic relationship between the roots of leguminous plants and nitrogen fixing *Rhizobium* bacteria as well as mycorrhizal fungi. Flavonoids secreted from the roots of legumes activate nod genes in bacteria, inducing the secretion of Nod factors which trigger nodule development in the roots of these plants [264]. The nodules are subsequently colonized by rhizobial bacteria which "fix" nitrogen for the plant. Low nitrate conditions producing nutritional stress induced the accumulation of flavonoids in root exudates [71] leading to increased interaction with nitrogen fixing bacteria. The colonization of soybean roots by mycorrhizal fungi was enhanced by external application of genistein, diadzein and coumestral [264]. The colonization of roots by these bacterial and fungal organisms provide essential nutrients (nitrogen and phosphorous) to plants, and flavonoids play an important role in the establishment of this relationship.

1.3.2. Function in humans

1.3.2.1. General beneficial health effects in humans

Research into the beneficial effects of flavonoid consumption on human health began with Szent-Györgyi's work on treatment for the side effects of vitamin C deficiency. Since then, much research has been done on the role

flavonoids play in human health [310]. These compounds have demonstrated numerous biological activities that are beneficial to humans including antioxidant [107,217], antiviral [142,168], antiparasitic [183], antibacterial [27,198], anti-arthritic [101], antilipoperoxidant [273], antiatherogenic [11,133], hypoglycemic [47], antiallergic [148], anti-ischemic [230], antiplatelet [276], antiangiogenic [151,216], anti-inflammatory [187,235,274], and anticancer [136,172] effects, the latter being the focus of this study.

Flavonoids mediate their anticancer effects by influencing cellular processes important in tumor development and progression. This includes differentiation [56], cell cycle [254], cell adhesion and migration [226], proliferation [95], and apoptosis [106]. They modulate the activity of a large number of intracellular molecules directly and indirectly involved in the above-mentioned processes such as lipoxygenase [124,161], cyclooxygenase [124,161], monooxygenase [253], phospholipase A2 [92], xanthine oxidase [57], mitochondrial ATPase [26], succinoxidase [26,118], NADPH oxidase [26,118], EGF receptor kinase [146], MAP kinase [156], protein kinase C [3,80], DNA topoisomerase [50], cGMP and cAMP phosphodiesterase [202], aldose reductase [199], reverse transcriptase [209] and DNA polymerase [209]. Effects at the molecular and cellular levels mediate the biological effects listed above, however, only ones relevant to the anticancer activity of flavonoids will be discussed in the following section.

1.3.2.2. Anticancer effects

There is a correlation between diets high in fruits and vegetables and decreased risk of cancer [147,223]. High consumption of fruits and vegetables is significantly protective against risk of cancers arising in the lung, colon, ovary, esophagus, breast, cervix, bladder, pancreas, oral cavity and stomach [24]. Flavonoids are the largest class of polyphenolic compounds in fruits and vegetables, so it is not surprising that there is also evidence supporting a correlation between high flavonoid intake and decreased risk of cancer. In a 25-year cohort study in Finland, flavonoid consumption was inversely associated with decreased incidence of cancers to all sites of the body [153]. The same

researchers also found that in Finnish males, high intakes of quercetin and myricetin was associated with decreased risk of lung and prostate cancer, respectively [154]. A case-control study in Hawaii observed an inverse correlation between consumption of apples, grapefruit and onions and risk of lung cancer [163]. They also found quercetin intake inversely correlated with lung cancer risk. In another case-control study, flavonoid consumption decreased the risk of cancers of the oral cavity, pharynx, larynx and esophagus [65]. A 12-year cohort study of nearly 35,000 post-menopausal, cancer-free females found high consumption of catechin decreased the incidence of rectal cancer [9]. These studies suggest a protective role for flavonoids against cancers of various sites in the body, although there are studies in which flavonoid intake does not correlate with risk of specific cancers [8,89].

Consistent with the anticancer effects established by epidemiological studies, flavonoids are potent inhibitors of tumor cell growth *in vitro*, effectively inhibiting the growth of human cancer cell lines originating from various organs and tissues of the body including skin [60,138,225], prostate [213], bone marrow [117,265], stomach [144], colon [159], lung [60], and breast [60,259]. Even though flavonoids are effective antiproliferative agents in cancer cells, these compounds typically do not inhibit the growth of non-transformed normal cells [115,116,144,265] suggesting a tumor-specific anticancer effect.

Flavonoids have also demonstrated anticancer activity *in vivo*, affecting initiation, promotion and progression of tumorigenesis [75,272]. Initiation involves the uptake, distribution and metabolic activation of carcinogens leading to genotoxic damage to cells that results in loss of growth inhibition, resistance to apoptosis, enhanced invasion, and other characteristics of malignant cells; promotion is the accumulation of these damaged cells through proliferation; and progression involves the relatively uncontrolled growth and spread of cells, and addition of secondary characteristics mediating increased malignancy [266]. In an aflatoxin B1 induced-hepatocarcinogenesis model in rats, flavonoids (flavone, flavanone, quercetin and tangeretin) administered throughout the initiation period decreased formation of prenoplastic foci [252]. Flavonone administered during

phenobarbital-induced promotion also decreased preneoplastic formation. A study of DMBA-induced mammary tumorigenesis found citrus juices and their component flavonoids delayed development of tumors and decreased tumor burden in rats [259]. EGCG inhibited the growth of and reduced the size of human prostate and breast tumors after they had been injected in a mouse xenograft model [170]. Similarly, in a mouse xenograft model of advanced prostate cancer, silibinin decreased tumor volume and size in mice fed the flavonoid pre- and post-injection of tumor cells [255]. These *in vitro* and *in vivo* data indicate that flavonoids do have potential as anticancer agents, and that their anticancer activity can be mediated at any stage of cancer development which is consistent with the vast numbers of molecular interactions that have been documented for these compounds.

1.3.2.3. Anticancer mechanisms

At the cellular and molecular level, flavonoids have a broad range of effects and interactions that contribute to their ability to inhibit tumorigenesis at the various stages of development. These effects constitute the anticancer mechanisms of action for these compounds and can be categorized as chemopreventive and antiproliferative.

As chemopreventive agents, flavonoids inhibited tumor initiation by serving as powerful antioxidants and preventing oxidative damage to cells [107], and by inhibiting phase I xenobiotic metabolizing enzymes such as cytochrome-P450 [191,314]. Cytochrome P450 enzymes metabolize procarcinogens into reactive intermediates capable of binding to and damaging cellular DNA leading to carcinogenesis [55]. Flavonoids also prevented initiation of carcinogenesis by inducing phase II detoxification enzymes such as glutathione-S-transferase (GST), quinine reductase (QR) [316], and UDP glucuronyltransferase (UGT) [294]. Phase II enzymes metabolize and inactivate carcinogens thus aiding in their rapid removal from the body [303]. Once tumors are initiated by carcinogens, prooxidant processes producing reactive oxygen species can lead to the promotion of tumor growth [10]. Flavonoids inhibited the activity of

Figure 6. A schematic overview of cell cycle regulation including cell cycle phases and the cyclin/CDK complexes that control progression through each phase (adapted from Vermeulen *et al.* [273]).

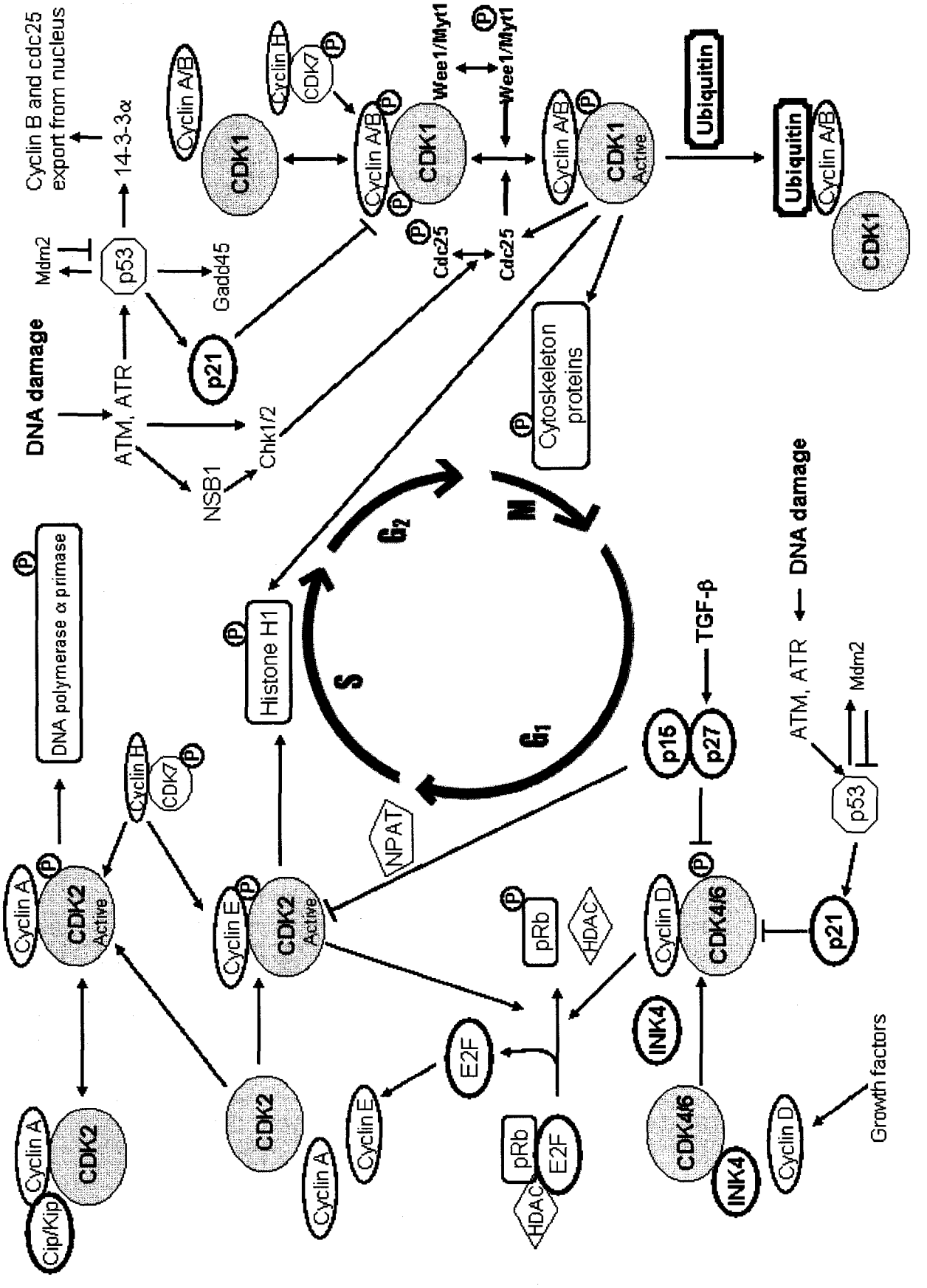
Cyclin B and cdc25 export from nucleus
14-3-3α
Mdm2
p53
Gadd45
DNA damage
ATM, ATR
p21
NSB1
Chk1/2
Cyclin A/B
CDK1
Cyclin H
CDK7
Wee1/Myt1
Cdc25
Cytoskeleton proteins
Ubiquitin
DNA polymerase α primase
Histone H1
S
G2
M
G1
Cyclin A
CDK2 Active
Cyclin E
NPAT
pRb
HDAC
E2F
Cip/Kip
CDK2
TGF-β
p15
p27
Cyclin D
CDK4/6
INK4
Growth factors
ATM, ATR
DNA damage
Mdm2
p53
p21

Figure 7. The molecular mechanisms of apoptosis (adapted from Bremer *et al.* [27])

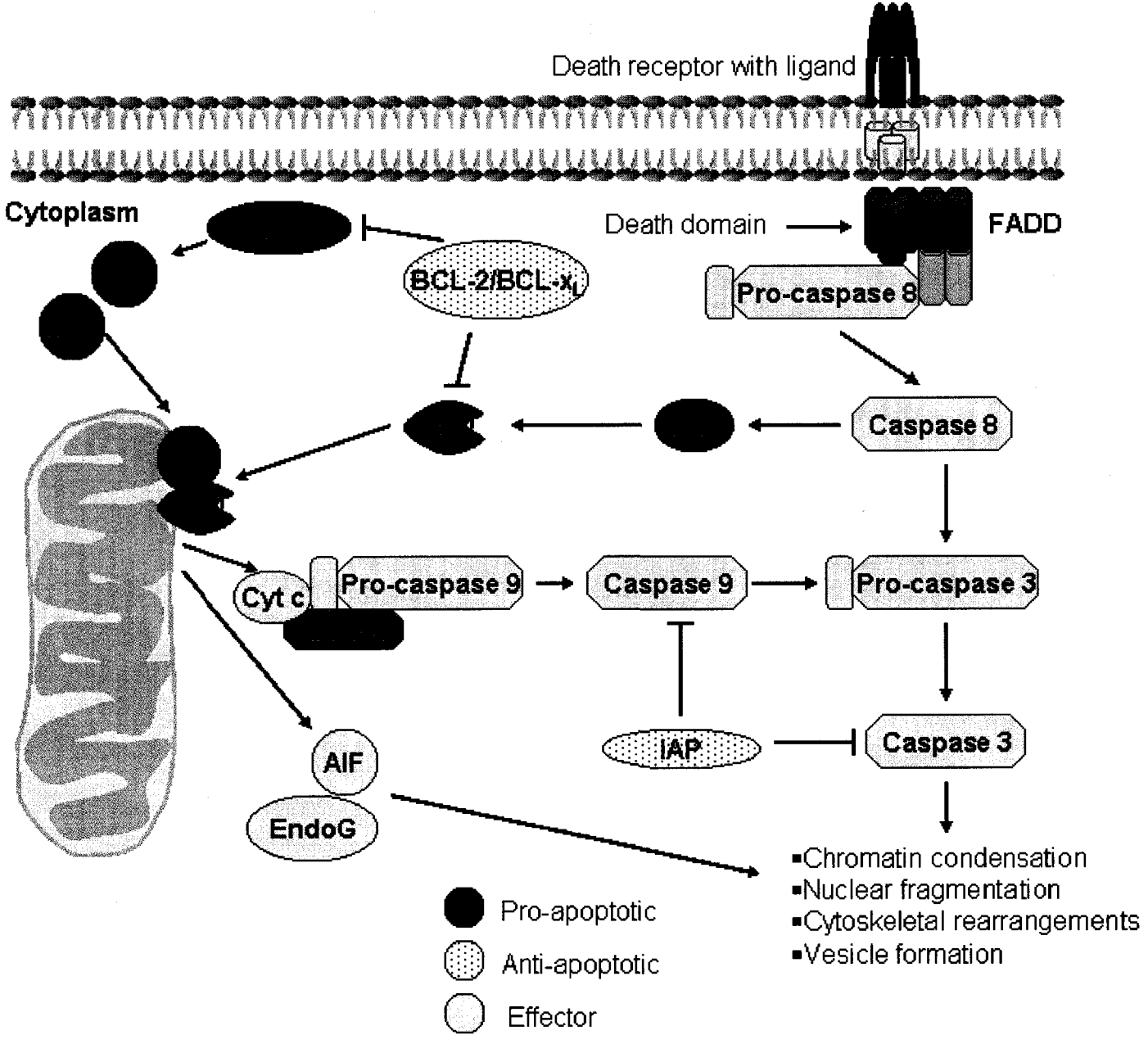
Death receptor with ligand
Cytoplasm
Death domain
FADD
BCL-2/BCL-x$_L$
Pro-caspase 8
Caspase 8
Cyt c
Pro-caspase 9
Caspase 9
Pro-caspase 3
IAP
Caspase 3
AIF
EndoG
▪Chromatin condensation
▪Nuclear fragmentation
▪Cytoskeletal rearrangements
▪Vesicle formation
Pro-apoptotic
Anti-apoptotic
Effector

Apoptosis is another cellular event whose control is often subverted in cancer. Cancer cells frequently acquire inactivating mutations of pro-apoptotic proteins or upregulate antiapototic proteins in order to evade cell death and proliferate uncontrollably [204]. Re-instating the capacity of these cells to undergo cell death is second method of controlling unchecked growth of cancer. Flavonoids induced apoptosis in a variety of human cancer cell lines including oral carcinoma [233], and colon cancer [159]. Apoptosis is an organized form of cell death that functions to maintain tissue homeostasis and genetic integrity of normal cells by eliminating unwanted or damaged cells [132]. Apoptosis induction can occur via two major pathways: the intrinsic mitochondrial, and the extrinsic death receptor pathway [220]. The intrinsic pathway is used by most chemotherapeutic drugs and is controlled by Bcl-2 family proteins, caspases, and inhibitors of apoptosis proteins (IAPs) (Figure 7). The extrinsic pathway consists of transmembrane death receptors and caspases. At the molecular level, flavonoid-induced apoptosis occurs primarily through modulation of regulatory molecules of the intrinsic pathway. For example, apoptosis induced by the flavonoids wogonin and fisetin involved caspase 3 activation, induction of the pro-apoptotic Bax and suppression of the anti-apoptotic Mcl-1 proteins [166]. Also, apigenin-induced apoptosis was associated with altered Bax/Bcl-2 ratio favoring apoptosis, induction of apoptotic protease-activating factor-1 (Apaf-1), and increased caspase 3, 9 and poly(ADP-ribose) polymerase (PARP) cleavage [250]. Flavonoids can also induce apoptosis through the extrinsic, death receptor pathway. For example, death receptor 5 (DR5) upregulation played a role in apoptosis induced by luteolin [123]. The apoptosis inducing effect of flavonoids in cancer cells provides another means for controlling the unchecked proliferation of these cells.

Modulation of intracellular signaling pathways central to cellular proliferation is another mechanism through which flavonoids exert their antiproliferative effects on cancer cells. These include pathways mediated by receptor tyrosine kinases such as EGFR, and intracellular kinases such as MAPK, PI3 kinase and PKC which can activate transcription factors such as NF-κB and AP-1. EGFR

signaling controls various cell activities, including cell proliferation, apoptosis, cell mobility, and angiogenesis [307]; MAPK signaling is involved in the control of gene expression, cellular proliferation, and programmed cell death [41]; PI-3 kinase signaling regulates cellular processes such as proliferation, differentiation, apoptosis, membrane trafficking and cytoskeleton organization [275,283]; and PKC is involved in a vast array of cellular processes including proliferation, cell cycle control and apoptosis [119]. Representatives from six classes of flavonoids (e.g. myreciten, apigenin, luteolin, quercetin and fisetin) inhibited the activities of PKC, EGFR and PI 3-kinase [3]. Apigenin inhibition of thyroid cancer cell growth was associated with inhibition of EGFR and MAPK phosphorylation [311]. The physiological manifestations of flavonoid modulation of these intracellular signaling pathways are the cell cycle arrest and apoptosis discussed above.

The antiestrogenic effect of isoflavonoids in hormone-responsive cancers has been well documented. Isoflavonoids like genistein demonstrated a biphasic effect on ER^+ breast cancer cells; it stimulated growth at concentrations below 10 μM and inhibited growth at concentrations above 10 μM [295]. Isoflavones, which have weak estrogenic potential [195], are antiestrogenic because they outcompete 17-β-estradiol for binding at the ER thereby decreasing endogenous estrogen-stimulated growth [1]. Flavonoids other than isoflavones are also antiestrogenic due to their ability to inhibit the activity of enzymes involved in estrogen production. Aromatase or CYP19 is a cytochrome P450 complex which catalyses the biosynthesis of estradiol from androgens. Apigenin, chrysin and hesperetin were among 28 flavonoids that inhibited CYP19 activity [129]. Inhibition of aromatase activity reduced the growth stimulatory effect of estrogens in hormone responsive cancers [33].

1.3.3. Anticancer effects of tangeretin and nobiletin

Tangeretin (4',5,6,7,8-pentamethoxyflavone) and nobiletin (3',4',5,6,7,8-hexamethoxyflavone) are polymethoxylated flavones found in the oily extract of citrus fruits (Figure 8). Tangeretin was first isolated from tangerine oil in 1934 and nobiletin from orange peel in 1938. They are among the most effective citrus

Figure 8. Structure of tangeretin and nobiletin.

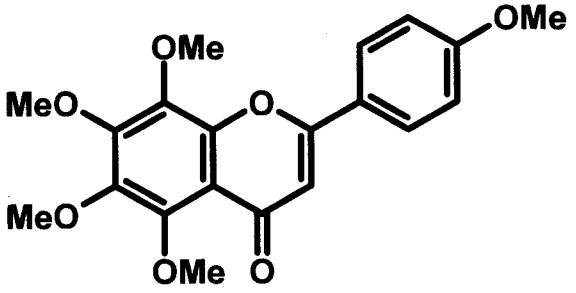

Tangeretin

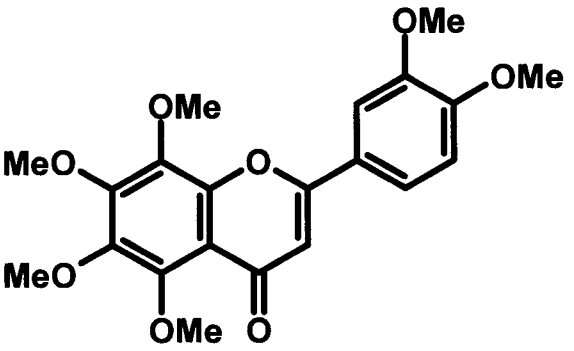

Nobiletin

flavonoids at inhibition of human cancer cell proliferation [178]. Tangeretin and nobiletin inhibited proliferation of human cancer cell lines derived from squamous cell carcinoma [137,138], gliosarcoma [137], leukemia [116,144], melanoma [225,308], colorectal cancer [211], gastric carcinoma [144], and lung carcinoma [144]. In addition, they have been reported to decrease the incidence of chemically induced tumors in mice and rats [194,252,267]. There is only a single *in vivo* xenograft treatment model reported in literature for tangeretin which found tangeretin did not inhibit the growth of human breast cancer in mice, and in fact it neutralized the growth inhibitory effect of tamoxifen when used in combination [29]. Unlike tangeretin, there are no reports of *in vivo* xenograft treatment models for nobiletin. Thus, evidence for or against a growth inhibitory effect of tangeretin and nobiletin in *in vivo* xenograft models is too sparse to be conclusive.

The anticancer effect of tangeretin and nobiletin is mediated by the same cellular and molecular effects discussed in section 1.3.2.3. These flavonoids are not reported to have estrogenic activity, so this investigation of their anticancer mechanism of action focuses on cellular effects (cell cycle and apoptosis induction) and the molecular interactions that might mediate those effects. Tangeretin has been reported to: induce apoptosis in HL-60 cells [116], induce G1 arrest in colorectal cancers by inhibiting Cdk2 and Cdk4 and elevating levels of the Cdk inhibitors p21 and p27 [211], and to inhibit ERK 1/2 phosphorylation in mammary cancer cells [281]. Likewise, nobiletin has been shown to: induce apoptosis in colorectal [317] and leukemia cancer cells [166], induce G1 arrest and apoptosis in gastric cancer cells [312], induce G2/M arrest and apoptosis in hepatocellular cancer cells [207], and inhibit MEK 1/2 phosphorylation in fibrosarcoma [188].

1.4. Flavonoids in cancer chemotherapy clinical trials

Flavopiridol (Figure 9) is a synthetic flavonoid derived from an alkaloid, rohitukine, which was isolated from plants indigenous to India [241]. Flavopiridol has been the subject of research since the early 1990s when it was found that it induced cell cycle arrest [143] mediated by CDKs [38] eventually leading to its

Figure 9. Structure of two synthetic flavonoids in past and current clinical trials.

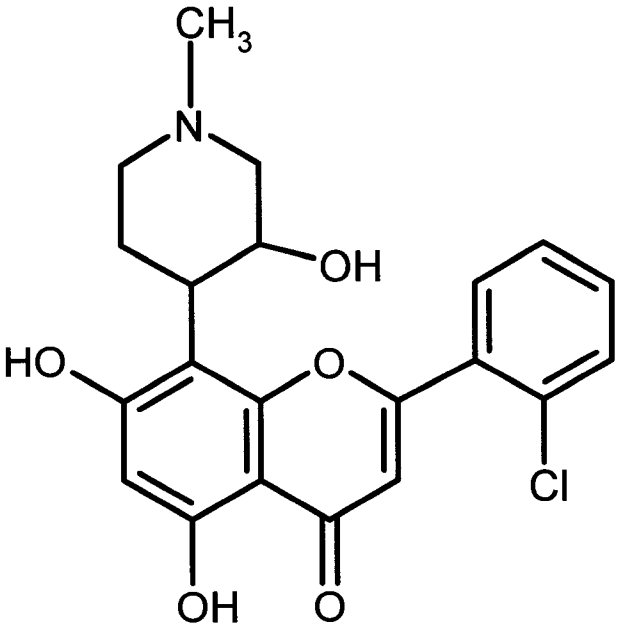

Flavopiridol

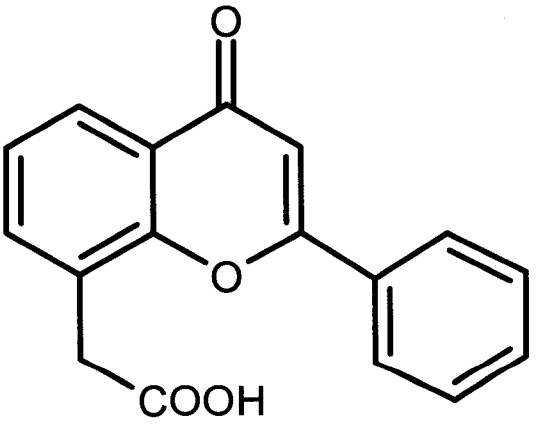

Flavone-8-acetic acid

establishment as a pan-CDK inhibitor [243]. It has been reported to be an effective anticancer agent in preclinical *in vitro* and *in vivo* models [7,212]. Consequently, it was the first small molecule CDK inhibitor to be assessed in clinical trials in the late 1990s [242]. It quickly moved into phase II clinical trials where it was assessed as a single agent against advanced colorectal cancer [5], metastatic renal cancer [262], untreated malignant melanoma [34], untreated, metastatic, hormone-refractory prostate cancer [171], advanced gastric cancer [240], untreated non-small cell lung cancer [247], mantle cell lymphoma [157], and refractory solid tumors [301]. Unfortunately, it failed to demonstrate activity in any of these trials of its effectiveness as a single agent. More recently, flavopiridol has been in phase I clinical trials in combination with other chemotherapy drugs (ara-C, mitoxantrone, irinotecan, cisplatin and carboplatin) with encouraging results [21,140,244].

Another synthetic flavonoid that has progressed to clinical trials is flavone-8-acetic acid (FAA), a benzopyrone derivative (Figure 9). It preceded flavopiridol in clinical trials by a few years, although at that time its mechanism of action was unknown [112]. However, it was assessed in human patients on the basis of promising activity in murine solid tumor models [59,205]. It was in clinical trials for 4 years with only one phase II trial in which the effectiveness observed in mice did not translate to antitumor activity in humans [251]. Since then, FAA has been returned to the preclinical stage where it and several analogues are being evaluated for their anti-angiogenic activity [19].

Some naturally occurring flavonoids have been evaluated in phase I and II clinical trials. A phase I trial of the flavonol quercetin found it was safely administered by i.v. and that there was evidence of antitumor acvtivity [81]. This same research group later developed and evaluated a water-soluble prodrug of quercetin in phase I trials due to the unsuitability of the vehicle used in the first trial (DMSO) for clinical development [193]. Gingko biloba extract (GBE or EGb 761 containing approximately 24% flavone glycosides) was evaluated for efficacy in phase II clinical trials against advanced colorectal cancer following treatment with 5-fluorouracil [111]. Survival for patients administered GBE was comparable

to that of standard second-line treatment for advanced colorectal cancer, suggesting a favorable benefit-risk ratio for its use as second-line therapy for advanced colorectal cancer. Findings were similar in an earlier phase II trial of GBE in combination with 5-FU against pancreatic cancer [110]. A phase II clinical trial evaluated the efficacy of green tea in patients with androgen independent prostate cancer and determined it had limited antineoplastic activity in these patients [128]. The pharmacokinetics of an immunoconjugate of genistein (B43-Genistein) was evaluated in phase I clinical trials and it was found to be well tolerated with an acceptable toxicity profile in leukemia patients [43,277]. Another immunoconjugate, EGF-Genistein, is currently in clinical trials [296].

All of the flavonoid compounds (synthetic or natural) entered into clinical trials to date appears to have met with little success so far. The best illustration of this unexpected lack of success is exemplified by flavopiridol which has been in clinical trials for almost 10 years, with only modest performance in phase II trials. Flavopiridol's disappointing performance was explored in a recent article by Blagosklonny who suggested that flavopiridol's myriad molecular and cellular effects are the result of potent inhibition of global transcription, in essence suggesting that critical molecular targets of this agent have not all been identified [23]. Other explanations for flavopiridol's disappointing performance in clinical trials include sub-optimal drug doses, sequences or schedules; and sub-optimal pharmacokinetic parameters [96].

1.5. Treatment resistance in tumor cells as a potential limitation to flavonoid chemotherapy

1.5.1. Flavonoid resistance

Development of resistance to the effects of drugs is a common occurrence in the treatment of cancers. Resistance may be pre-existent in a subpopulation of heterogenous cancer cells, or it may be acquired as a cellular response to drug exposure. Cells can mediate resistance to drugs in several ways including: altered membrane transport involving upregulation of ATP-binding cassette (ABC) drug efflux transporters like P-glycoprotein; altered intracellular targets

(e.g. mutated topoisomerase II); decreased drug activation in cases utilizing prodrugs; increased drug degradation due to upregulated expression of drug-metabolising enzymes; drug inactivation due to increased intracellular drug metabolism, for example increased glutathione conjugation; decreased target availability due to subcellular redistribution; enhanced DNA repair resulting in increased survival; and failure to apoptose as a result of mutated cell cycle and apoptosis regulatory proteins such as p53 [174].

To date, there is no evidence in the literature of resistance to any naturally occurring flavonoid. There are, however, reports of resistance to the synthetic flavonoid, flavopiridol, which has undergone several clinical trials. Flavopiridol resistance was first reported in an ovarian cancer cell line that spontaneously developed resistance to flavopiridol upon prolonged passage *in vitro* [20]. Since then, flavopiridol-resistant breast [224] and colon [258] cancer cell lines were deliberately developed by exposing cells to incrementally increased concentrations of drug *in vitro*. The flavopiridol-resistant MCF-7 breast cancer cells, generated in this way and characterized by Robey *et al.*, were reported to overexpress the ABC half-transporter, breast cancer resistance protein (BCRP), at both the mRNA and protein level [224]. Further, MCF-7cells artificially induced to overexpress BCRP by transfection with an expression vector were also resistant to flavopiridol. *In vivo*, leukemic blast cells (from adult acute myeloid leukemia patients) that overexpressed BCRP mRNA were found to be less sensitive to flavopiridol-induced cytotoxicity and apoptosis [200]. This data suggests overexpression of BCRP correlates with flavopiridol resistance.

It can be argued that incrementally increasing the concentration of flavopiridol selected for a pre-existing sub-population of BCRP overexpressing cells (versus inducing overexpression) to mediate resistance to the drug. Developing resistant cell lines by this method takes time, at least in the case of the breast cancer cells, as levels of BCRP protein in parental MCF-7 cells were not detectable by the methods used in that study [224].

1.5.2. Flavonoids and reversal of multidrug resistance (MDR)

The success of cancer chemotherapy is plagued by the development of multi-drug resistance (MDR) whereby exposure of cancer cells to a single cytotoxic agent results in cross-resistance to other structurally and mechanistically diverse anticancer agents [162]. The MDR phenotype is mediated most often by members of the ABC membrane transporters, P-glycoprotein (P-gp, MDR1), multidrug resistance protein (MRP1) [162], and more recently BCRP [94]. These transporters hydrolyse ATP to remove drugs from the cell cytoplasm or plasma membrane to the exterior, effectively decreasing the intracellular accumulation of drugs [94]. Substrates of ABC transporters include vinca alkaloids (e.g. vincristine), anthracyclines (e.g. doxorubicin), epipodophytllotoxins (e.g. etoposide), taxol, mitomycin C [6], mitoxantrone, flavopiridol [73] and glutathione conjugates [145].

Since the discovery of the involvement of ABC transporters in MDR, efforts have been made to find compounds that inhibit their activity and allow re-accumulation of drugs intracellularly, reinstating sensitivity or reversing resistance. Flavonoids have been investigated for their ability to inhibit ABC transporter efflux activity and it was found that some flavones, flavonols and chalcones had the capacity to reverse multidrug resistance in mammalian cells *in vitro* [51,58]. For example, myricetin increased the accumulation of vincristine in MDR1 and MRP1 transfected MDCK cells, and restored sensitivity to vincristine [282]. Similarly, tangeretin and nobiletin among other citrus flavonoids inhibited the P-gp-mediated transport of talinolol in intestinal Caco-2 cells [185]. Tangeretin also inhibited P-gp efflux of vinblastine and enhanced uptake in intestinal Caco-2 cells [269]. Two other flavonoids, biochanin A and chrysin inhibited BCRP activity in BCRP-overexpressing, mitoxantrone resistant breast and lung cancer cells which resulted in intracellular accumulation of, and restoration of sensitivity to mitoxantrone [315]. There is also evidence that flavonoids are capable of MDR reversal *in vivo* as well. In a xenograft model, treatment of P-gp mediated doxorubicin resistant tumors with EGCG enhanced doxorubicin efficacy and increased its concentration in the tumors [221].

The mechanisms involved in the reversal of P-gp mediated MDR by flavonoids are well established and include: inhibition of P-gp activity by direct binding to its nucleotide binding domain [69]; inhibition of expression of multidrug resistance gene 1 [150]; and inhibition of ATP hydrolysis and energy-dependent drug interaction with transporter-enriched membranes [68,246].

While flavonoids are capable of inhibiting drug efflux transporters, it is reported that they themselves are potential substrates of these transporters. Treatment of Caco-2 and Chinese hamster ovary cells with inhibitors of P-gp and MRP2 efflux activity (MK-571) resulted in intracellular accumulation of a green tea flavonoid, epicatechin gallate (ECG) [279] suggesting that ECG is a substrate of P-gp and MRP2. Transfection of BCRP into LLC-PK1 cells increased export of [^{3}H] genistein. However, treatment with a BCRP inhibitor abolished the increased transport [126] which suggests genistein is a substrate of BCRP. In a more recent study investigating the effect of several flavonoids on P-gp mediated [^{3}H] talinolol transport across Caco-2 cells and their ability to displace [^{3}H] talinolol from its P-gp binding site, it was found that while these flavonoids decreased secretion of [^{3}H] talinolol (inhibited P-gp activity), none of them were able to displace its binding to P-gp and act as substrates [206]. There is evidence supporting both sides of this issue so it remains unclear whether flavonoids are or are not substrates of ABC transporters.

1.6. Study hypothesis, objectives and significance

Conventional cytotoxic cancer chemotherapy effectively kills tumor cells, but it does so with little selectivity which often results in collateral damage to normal, healthy organs and tissues [127]. Therefore various strategies to increase specificity of chemotherapies for tumors (e.g. targeted delivery, molecular-targeted therapies) or to decrease toxicity to non-tumor tissues are underway [184]. Naturally occurring constituents of the human diet such as flavonoids (low molecular weight polyphenols ubiquitous in plants) are of particular interest as sources of compounds with anticancer activity that have the potential to decrease toxic side effects in normal cells [117]. Flavonoids have demonstrated good

potential as anticancer agents by their antiproliferative activity against human tumor cell lines both *in vitro* [86,159] and as xenografts in immunocompromised mice [37,114].

In this study, I investigated the antiproliferative activity of two citrus flavonoids, tangeretin and nobiletin, in human breast and colon cancer cells. While these compounds are among the best flavonoids derived from citrus at inhibiting cancer cell proliferation [144,178], a well characterized activity, there was still much to be determined about their cellular and molecular effects. At the outset of this thesis, there was no common mechanism of action to show that the antiproliferative activity of these flavonoids were mediated by cellular effects A and B, which resulted from modulation of molecules C,D, and E. As cell cycle and apoptosis effects were reported for both tangeretin and nobiletin in some cell lines [116,166,211,312,317], we hypothesized that in human breast and colon cancer cells: 1) tangeretin and nobiletin inhibit proliferation by inducing cell cycle arrest and/or apoptosis through the induction/repression of cell cycle and cell death regulatory genes, and 2) resistance to these compounds is mediated via altered expression of these genes. This investigation of the cellular and molecular determinants of inhibition of proliferation by tangeretin and nobiletin in human cancer cells of different origin was approached in two ways: 1) by assessing their effect on the physiological processes, cell cycle and cell death, and on the molecular regulators of those processes in cell lines susceptible to inhibition of proliferation, and 2) by developing and characterizing cell lines less susceptible to inhibition of proliferation by these flavonoids to assess changes that may result in decreased or abrogation of their effect.

The goal of this work is to provide information on the cellular and molecular events mediated by tangeretin and nobiletin in human cancer cells, thereby increasing the understanding of their anticancer mechanism of action. This improved understanding will allow us to rationally select targets and formulate strategies for their potential use in cancer chemotherapy, likely in combination with other drugs for the maximization of treatment effects.

Chapter 2
MATERIALS AND METHODS

2.1. Reagents

Tangeretin and nobiletin were generously supplied by John Manthey of Agricultural Research Service, USDA (Winter Haven, FL). Propidium iodide (PI), cycloheximide, sucrose, spermine tetrahydrochloride (spermine), trypsin, trypsin inhibitor, and nonidet P40 (NP 40) were obtained from Sigma Chemicals (St Louis, MO). Dimethyl sulfoxide (DMSO) and trisodium citrate were obtained from BDH (Toronto, ON). Tris(hydroxymethyl)-aminomethane hydrochloride (Tris) was obtained from Bioshop (Burlington, ON). Ribonuclease A (RNase A) was obtained from Roche Diagnostics (Laval, QC). Annexin V-FITC antibody was obtained from BD Biosciences Pharmingen (Mississauga, ON). Cell culture media and supplements were obtained from Invitrogen (Burlington, ON). All other reagents and plasticware were obtained from commercial sources.

2.2. Cell lines and culturing conditions

MDA-MB-435, MCF-7 (human ductal breast carcinoma and adenocarcinoma, respectively) and HT-29 (human colorectal adenocarcinoma) cell lines (American Type Culture Collection, Manassas, VA) were grown in α-MEM media plus nucleosides containing 10% fetal bovine serum (growth medium) and maintained at 37°C, in a humidified atmosphere of 5% CO_2 in air.

2.3. Proliferation assay

Cells were plated in 25 cm^2 tissue culture flasks at $1x10^5$ cells per flask and allowed to attach overnight. Cells were treated with a range of concentrations of tangeretin, nobiletin, DMSO or media control for 4 d. Final DMSO concentrations did not exceed 0.27% (v/v). After 4 d, cells were trypsinized and replicate flasks counted using a Beckman Coulter Z1 Particle Counter (Miami, FL). Cell numbers are expressed as a percent of vehicle control.

2.4. Recovery of proliferation assay

Cells were plated in 6-well tissue culture plates at $1.25x10^4$ cells per well and allowed to attach overnight. Tangeretin (54 μM), nobiletin (100 μM for MDA-MB-

435, and 60 μM for MCF-7 and HT-29 cells), or DMSO control were added to cells and incubated for 4 d. On day 4, treatment and control media were replaced with fresh growth medium. Cells were incubated and replicate wells were counted on day 4 and each day for an additional 4 d.

2.5. Flow cytometry analysis of cell cycle distribution

2.5.1. Preparation of bare nuclei

Cells were plated in 75 cm^2 tissue culture flasks at 0.6-1x10^6 cells per flask and incubated overnight to allow attachment. Cells were treated with tangeretin (54 μM), nobiletin (100 μM and 200 μM for MDA-MB-435; 60 μM and 200 μM for MCF-7 and HT-29), or DMSO control for 24, 48, and 72 h. Cells were prepared for flow cytometric analysis of DNA content using a modification of a previously published method [289]. Briefly, cells were trypsinized to detach and washed 3x in a solution containing 250 mM sucrose, 5% v/v DMSO, 40 mM trisodium citrate, pH 7.6. After each wash, cells were centrifuged 5 min, 180 x g at room temperature to pellet cells. Plasma membrane and cytoplasmic proteins were stripped by resuspending cells in 250 μl trypsin in a solution containing 1.5 mM spermine, 0.1% v/v NP40, 0.5 mM Tris, 3.4 mM citrate, pH 7.6 (citrate buffer) and incubating for 10 min at room temperature. Trypsin was inactivated by adding 200 μl trypsin inhibitor (408 Units/ml) in citrate buffer containing RNase A and incubating for 10 min at room temperature. Bare, unfixed nuclei were stabilized and stained by adding 200 μl of a solution containing propidium iodide (PI)(0.42 mg/ml) plus spermine (4.8 mM) in citrate buffer and incubating for 10 min at room temperature. Cellular debris was removed using 30-μm cell strainer cap tubes (VWR, Mississauga, ON). Samples were kept on ice in the dark and analyzed on a Beckman Coulter Epics XL-MCL Flow Cytometer (Miami, FL) within 2-3 h of preparation. A minimum of 25,000 events was collected for each sample. DNA histograms were analyzed using the software program, Multicycle from Phoenix Flow Systems (San Diego, CA).

2.5.2. Fixation and staining of whole cells

Cells were plated in 75 cm^2 tissue culture flasks at 1-2x10^6 cells per flask and incubated 1-2 d in growth media to allow attachment and further proliferation. Cells were treated with tangeretin (54 μM), nobiletin (100 μM and 200 μM for MDA-MB-435, and 60 μM and 200 μM for MCF-7 and HT-29), or DMSO control for 96 h. Cells were trypsinized to detach and washed 3x in cold PBS. Cells were centrifuged between each wash to pellet at 180 x g for 5 min, 4°C. Cells were fixed in 66.6% ethanol (ice-cold) for a minimum of 2 h and stained for analysis by flow cytometry or stored at 4°C until use. Fixative was removed from cells and cells were washed with cold PBS then resuspended and stained with PI (50 mg/ml containing RNase H) for a minimum of 30 min. DNA content was analysed by flow cytometry within 2 h of staining.

2.6. Resumption of cell cycling

Cells were plated in 75 cm^2 tissue culture flasks at 1 x 10^4 cells per flask and allowed to attach overnight. Tangeretin (54 μM), nobiletin (100 μM and 200 μM for MDA-MB-435, and 60 μM and 200 μM for MCF-7 and HT-29), or DMSO controls were added to cells and incubated for 4 d. On day 4, treatment and control media were replaced with fresh growth medium, and cells were incubated for an additional 4 d. Cell cycle distribution was determined on day 5 and 8 (1 d and 4 d after flavonoid removal) using the method outlined in section 2.5.1 above.

2.7. Annexin V/PI staining for apoptosis

Cells were plated in 25 cm^2 tissue culture flasks at 1x10^5 cells per flask, incubated overnight, and treated with tangeretin (54 μM), nobiletin (100 μM and 200 μM for MDA-MB-435, and 60 μM and 200 μM for MCF-7 and HT-29), or controls (DMSO, cisplatin, cycloheximide and media) for 48 h and 72 h. At the end of incubation, treatment and control media were collected since they could contain dead or dying cells that had detached from the flasks. Adherent cells were collected by trypsinization and added to the non-adherent population. Cells

were washed 2x with ice cold phosphate buffered saline (PBS, 136 mM NaCl, 2.8 mM KCl, 10 mM Na_2HPO_4, 1.6 mM KH_2PO_4, pH 7.4) and resuspended in binding buffer (140 mM NaCl, 10 mM HEPES, 2.5 mM CaCl, pH 7.4) at a concentration of $1x10^5$ cells per 100 µl. Cells were stained by adding annexin V-FITC (2 µl) and PI (10 µl, 50 µg/ml) for 15 min at room temperature, away from direct light. Cells were diluted to a final volume of 0.5 ml with binding buffer (400 µl). FITC and PI fluorescence were measured by flow cytometry on a Beckman Coulter Epics XL-MCL Flow Cytometer within 1 h of annexin V/PI addition. A minimum of 10,000 events was collected for each sample.

2.8. RNA isolation from cultured cells

Media was aspirated from flasks and 1 ml Tri®Reagent (Sigma, Oakville, ON) was added to lyse cells. Cells were broken apart and evenly suspended by pipetting and transferred to 1.5 ml microfuge tubes (Ultident, St. Laurent, QC). Chloroform (200 µl) was added and tubes were shaken vigorously for 15 s to mix all phases. Samples were incubated at room temperature for 3 min and then centrifuged at 10,800 rpm for 15 min, 4°C to allow phase separation. The upper, aqueous layer was collected (300-400 µl) and transferred to a new microfuge tube. Isopropanol (500 µl) was added to precipitate the RNA and samples were incubated at room temperature for a minimum of 10 min. RNA was pelleted by centrifugation at 10,800 rpm for 10 min, 4°C. Isopropanol was decanted and 75% ethanol (1 ml) was added to wash RNA. Samples were centrifuged at 8600 rpm for 5 min, 4°C and ethanol was decanted. Tubes were inverted to allow drainage of excess ethanol and RNA to air dry for 15-20 min. RNA was dissolved in RNase-free water at 65°C for 10 min and stored at -20°C until use.

2.9. Reverse transcription (RT)

RNA (1 µg) was diluted to 10 µl with RNase-free water. The following reagents were added to RNA for a total reaction volume of 20 µl: 2 µl deoxyribonucleotides (10 mM), 4 µl 5x reverse transcription buffer (250 mM Tris-HCl, 375 mM KCl, 15 mM $MgCl_2$, pH 8.3), 1 µl random hexanucleotide primers

(100 pmol/μl), 1 μl Moloney murine leukaemia virus (MMLV) reverse transcriptase (Units/μl), and 2 μl dithiothreitol (0.1 M) (all RT reagents were purchased from Invitrogen, Mississauga, ON). Tubes were flicked to mix and pulsed to pull volume to the bottom of the tube. RNA was reverse transcribed in an Eppendorf Mastercycler gradient thermal cycler (Eppendorf, Westbury, NY) using the following protocol: 10 min at 25°C, 60 min at 37°C, and 5 min at 95°C. Product was stored at -20°C until use.

2.10. Semi-quantitative RT-PCR

Cells were plated in 25 cm^2 tissue culture flasks at 3.75-7.5x10^5 cells per flask and allowed to attach overnight. Tangeretin (54 μM), nobiletin (100 μM and 200 μM for MDA-MB-435, and 60 μM and 200 μM for MCF-7 and HT-29), or DMSO controls were added to cells and incubated for 6 h and 24 h (MDA-MB-435 and MCF-7), or 6 h and 48 h (HT-29). At the end of incubation, RNA was isolated from cells and reverse transcribed as described in sections 2.8 and 2.9. PCR was performed to determine expression of cyclin D1, D2, D3, cyclin E1, E2, cdk2, cdk4, cdk6, p21, p27, A20 and Bcl-2. Each PCR reaction contained 5 μl 10x buffer, 1 μl deoxyribonucleotides (10 mM), 1.5 μl $MgCl_2$ (conc), 5 μl glycerol (1:1 glycerol:water), 0.5 μl each forward and reverse primer (50 pmol/μl), 35.1 μl dH_2O, 1 μl cDNA and 0.4 μl Taq polymerase (with the exception of GAPDH reactions in which water was substituted for glycerol) for a total volume of 50 μl. Primers were obtained from Invitrogen (Burlington, ON) and sequences and PCR conditions are listed in Table 4. PCR was performed in an Eppendorf Mastercycler gradient thermal cycler (Eppendorf, Westbury, NY) using the following conditions: 94°C, 5 min; (94°C, 1 min; T_a, 1 min; 72°C, 1 min); 72°C, 10 min. Product was stored at -20°C until gel electrophoresis. Note, DNase treatment was not used on RNA so there is a possibility that the RNA used in these RT-PCR reactions was contaminated with genomic DNA. PCR product could have been sequenced to confirm the correct product was amplified however, PCR primers were designed to span introns or bridge an exon-exon junction. When two primers span one or more introns, the amplified product from

Table 4. Semi-quantitative PCR primer sequences and conditions.

Name	Sequence	Size	T_a (°C)	# of cycles	Reference
CCND1	5'CTGGAGCCCGTGAAAAAGAGC3' 5'CTGGAGAGGAAGCGTGTGAGG3'	415	55	27	[270]
CCND2	5'TCATGACTTCATTGAGCA3' 5'GTCGTCCTACTCCTTCAC3'	195	50	30	[74]
CCND3	5'TGTCAGGAGCAGATCGAAGC3' 5'CCTTTAGAAGGCACTAGAGC3'	532	50	30	[83]
CCNE1	5' ATGGTATACTTGCTGCTTCGGCC3' 5'AGAACGTGGAGCAGGCGCGCAACT3'	397	55	25	[270]
CCNE2	5'ATCCAGGCCAAGAAGAGGAAA3' 5'GCACAAGGCAGCAGCAGTC3'	825	60	27	[278]
Cdk2	5'TCCGAGAGATCTCTCTGCTTAAGG3' 5'CGAGTCACCATCTCAGCAAAGATG3'	452	55	25	[270]
Cdk4	5'TCCGAGAGATCTCTCTGCTTAAGG3' 5'AGCTCGGTACCAGAGTGTAACAAC3'	396	50	27	[270]
Cdk6	5'TCTTGCTCCAGTCCAGCTAC3' 5'AGCAATCCTCCACAGCTCTG3'	509	55	28	[83]
p21	5'ACAGCAGAGGAAGACCATGT3' 5'GGTATGTACATGAGGAGGTG3'	319	55	27	[83]
p27	5'AACCTCTTCGGCCCGGTGGACCAC3' 5'GTCTGCTCCACAGAACCGGCATTT3'	471	55	27	[270]
A20	5'GTCTTGCCTATGGTTTACAG3' 5'GGGTAGCTACTTCTGTGTG3'	799	48	30	Koropatnick lab
Bcl-2	5'CCCTCCAGATAGCTCATT3' 5'CTAGACAGACAAGGAAAG3'		50	30	Koropatnick lab
GAPDH	5'TATTGGGCGCCTGGTCACCA3' 5'CCACCTTCTTGATGTCATCA3'	752	55	20	Koropatnick lab

genomic DNA will be bigger than expected. All PCR products were the expected size when resolved by gel electrophoresis.

2.11. Gel electrophoresis of PCR product

PCR product (10 μl) (plus 2 μl orange G dye for tracking) was separated on a 1% agarose gel. Gels were run at 100 V for 25 min in 1x TAE buffer (40 mM Tris-HCl, 20 mM acetic acid, 1mM EDTA). Gels were visualised on an ImageMaster VDS gel documentation system (Amersham Pharmacia Biotech, Piscataway, NJ) and images were captured using LISCAP Capture Utility software (Amersham Pharmacia Biotech, Piscataway, NJ). Band intensities were quantitated using ImageQuant v5.1 (Molecular Dynamics, Sunnyvale, CA) and gene expression was normalized to GAPDH expression.

2.12. Sybr Green I quantitative real-time RT-PCR

Sybr Green quantitative real-time RT-PCR was used to confirm microarray analysis of gene expression. Four genes were selected in total, two genes that were upregulated by tangeretin [TNFα-induced protein 3 (TNFAIP3 or A20) and cAMP responsive element modulator (CREM)] and two that were downregulated [cyclin E2 (CCNE2) and dual specificity phosphatase 6 (DUSP6)] plus a housekeeping gene (18S). To obtain template for the PCR reaction, MDA-MB-435 cells were plated in 25 cm^2 tissue culture flasks at 3.75-7.5x10^5 cells per flask and allowed to attach overnight. Tangeretin (54 μM) or DMSO control were added to cells and incubated for 6 h. RNA was isolated from cells and reverse transcribed as described in sections 2.8 and 2.9. Real-time PCR was performed using pre-optimized QuantiTect® Sybr Green PCR kit and Primer Assays (Qiagen, Mississauga, ON) on a Stratagene Mx3000P Real-time Thermal Cycler (La Jolla, CA). Real-time PCR reactions were assembled and performed following the manufacturer's protocol for two-step RT-PCR with each 25 μl reaction containing 12.5 μl 2x QuantiTect® Sybr Green PCR master mix, 2.5 μl 10x QuantiTect® Primer assay, 8 μl RNase-free water and 2 μl template cDNA.. PCR conditions included an initial step to activate HotStar Taq at 95°C for 15

min, followed by 40 cycles of denaturing at 94°C for 15 s, annealing at 55°C for 30 s, and extension at 72°C for 30 s with Sybr Green fluorescence detection and acquisition. At the end of each PCR run, melting curve analysis was performed from 55°C to 95°C ($0.2°Cs^{-1}$) to detect non-specific PCR products and primer-dimer amplification.

2.13. Analysis of real-time RT-PCR data

MxPro™ QPCR software (Stratagene, La Jolla, CA) was used to analyse real-time RT-PCR data. Standard curves for each gene were generated from cDNA samples that theoretically had the highest expression of the target gene. For example, the CCNE2 standard curve was generated from vehicle control cDNA as tangeretin treatment downregulated CCNE2 in microarray analysis. Standard curves confirmed PCR reactions were optimized and only single products were being amplified (R^2 values between 0.996 and 0.999). Quantification of target gene was relative to an internal standard whereby C_t values from target RNAs were compared to those of an internal reference gene (18S). Results are expressed as a ratio of the target-specific signal to the internal reference.

2.14. Microarray analysis of gene expression

MDA-MB-435 cells were plated in 75 cm^2 tissue culture flasks at $1x10^6$ cells per flask and allowed to attach overnight. Cells were treated with 54 µM tangeretin or DMSO control for 6 h. Following the 6 h incubation, cells were harvested by scraping and total RNA was isolated using an RNeasy kit from Qiagen (Mississauga, ON) following the manufacturer's procedure. RNA was stored at -20°C until use. Gene expression was analyzed using Affymetrix human GeneChip® oligonucleotide arrays, HGU133A (Santa Clara, CA). Probe synthesis, hybridization and array scanning were done at London Regional Genomics Centre (London, ON) according to Affymetrix protocols. At the centre, RNA quality was assessed using an Agilent 2100 Bioanalyzer (Palo Alto, CA) and success of the single species array was predicted by hybridization to Affymetrix Test 3 arrays (multiple species arrays) prior to expression analysis.

For gene expression analysis, cDNA was synthesized from total RNA (20 μg) followed by *in vitro* transcription to produce biotin-labeled cRNA. The cRNA was fragmented and hybridized to the HG-U133A array (contains 22,000 full length genes). Arrays were scanned at 570 nm (emission) and 488 nm (excitation) for detection of signal intensities. Data was exported to GeneSpring GX 7.3 (Agilent Technologies, Palo Alto, CA) for analysis. In total, six arrays were done: three treated and three vehicle controls.

2.15. Microarray data mining

Raw intensity data is minimally processed at LRGC before being delivered to clients. Standard manipulations of raw intensity data at this facility includes use of the RMA algorithm in GeneSpring GX from Agilent Technologies (Palo Alto, CA). This algorithm subtracts the chip background and mismatch intensities from the perfect match intensities, runs a per-chip normalization, and converts raw intensity values to expression values using log-transformation. This data was further analysed using GeneSpring GX 7.3. The default 1-color normalization (per chip: normalized to a median or percentile and per gene: normalized to median) was performed. Basically, GeneSpring divides each raw intensity value by the median intensity of the chip, then each value is further divided by the median value of each gene across samples, resulting in the final normalized value. One-way ANOVA of genes "Present or Marginal" in 1 out of 6 samples was performed to obtain a list of genes significantly different in expression from vehicle control ($P \leq 0.05$). The list of significantly changed tangeretin-responsive genes (1,405) was further analysed by categorizing genes based on biological processes. Biological process gene lists for cell growth, proliferation, cell cycle, apoptosis, signal transduction, transcription and stress were generated at the Affymetrix NetAffx™ Analysis Center website (http://www.affymetrix.com/analysis/index.affx) and were cross-referenced to the list of significantly changed genes.

The list of significantly changed genes was also uploaded to the Ingenuity Pathway Analysis site (https://analysis.ingenuity.com, Ingenuity Systems,

Redwood City, CA) to identify biological networks and pathways affected by tangeretin. This web-based application makes use of the literature-derived Ingenuity Pathways Knowledge Base (IPKB), containing large amounts of individually modelled relationships between genes, proteins, and cellular and molecular processes, to generate significant biological networks and pathways with associated functional analysis. Of the 1405 submitted genes, 1314 were mapped to corresponding gene objects in the IPKB, and 748 and 728 genes, respectively, were considered "focus genes" for network and functional/canonical pathways analyses. Ingenuity software queries the IPKB for interactions between focus genes and all other genes stored in the database and generates a set of networks. Each network is ranked by a score based on a comparison of the number of focus genes participating in a given network or pathway, relative to the total number of occurrences of those genes in all networks or pathways stored in the database. The score of network is displayed as the negative log of the P value, indicating the likelihood of focus genes in a network being found together due to random chance. A score of 3 indicates that there is a 1 in 1000 chance the focus genes are in a network due to random chance therefore, scores ≥ 3 have at least a 99.9% confidence of not being generated by chance alone. IPA then associates networks with functional and canonical pathways in a manner similar to that employed to calculate the score for a network, the difference being that the proportion is calculated for the global set of genes regulated in a pathway over total genes participating in that category.

2.16. Selection of flavonoid/DMSO resistance

MDA-MB-435, MCF-7 and HT-29 cells were plated in 6-well plates at $1x10^5$ cells per well ($5x10^4$ cells/ml) and allowed to attach overnight. Cells were treated with a range of concentrations of tangeretin and nobiletin based on data from proliferation assays (see Table 5 for concentrations). Final DMSO concentrations range from 0.1 to 2.0% (v/v). Cells were visually inspected every 7 d to determine growth. Confluent plates were discarded and treatment media was refreshed on subconfluent plates. This cycle was repeated until visible colonies were formed

Table 5. Concentrations of tangeretin and nobiletin used to select colonies less sensitive to the growth inhibitory effects of tangeretin and nobiletin. Concentrations were selected on the basis of dose-response graphs.

	Concentration (mM)	
Cell Line	***Tangeretin***	***Nobiletin***
MDA-MB-435	0.1, 0.3, 0.4, 0.5	0.01, 0.1, 0.3, 0.5
MCF-7	0.1, 0.2, 0.3, 0.4, 0.5	0.1, 0.2, 0.3
HT-29	0.3, 0.4, 0.5	0.1, 0.2, 0.3, 0.4, 0.5

which took 5-8 weeks. Single colonies were selected and transferred to 25 cm^2 flasks. This was done for 2-10 colonies, depending on extent of colony formation. Colonies were expanded in the same concentration of flavonoid they were selected in, with weekly media changes until flasks were confluent enough for subculturing and banking. Cell populations established in this manner were identified by parental line, flavonoid concentration, and an alphabetical attachment to distinguish between colonies e.g. the population established from MDA-MB-435 cells incubated in 200 μg/ml (0.54 mM) tangeretin, colony number 8, was designated MDA-MB-435TAN200H.

2.17. Colony forming assay

Parental, flavonoid- and DMSO-selected cells were plated in 6-well plates at $5x10^2$ cells per well (100 cells/ml) and allowed to attach overnight. Next day, cells were treated with a range of concentrations of tangeretin (0-67 μM) and nobiletin (0-200 μM) or DMSO control and incubated 10-14 d. Treatment and control media were added to media already on the plates to avoid cells having to recondition media. At the end of incubation, media was removed from cells and cells were washed 2x with room temperature PBS. Cells were covered with 0.5 ml methylene blue staining solution [1% methylene blue (Sigma Chemicals, St Louis, MO), 1% glutaraldehyde (VWR, Mississauga, ON) in 70% ethanol] for 3 min. Excess stain was collected for reuse. Remaining stain was washed off under slow-running, cold tap water. Plates were upended on paper towels to dry. To quantitate colonies, plates were placed upside down on a white surface in a well lit area and each well was counted manually. Counted colonies contained at least 50 cells and satellite colonies were excluded.

2.18. Growth assay

Parental and flavonoid-selected cells were plated in 25 cm^2 tissue culture flasks at $1x10^5$ cells per flask ($2x10^4$ cells/ml) and allowed to grow for 1, 2, 3 and 4 d in flavonoid-free media. At the end of each incubation period, media was removed, cells were washed with PBS, trypsinized and replicate flasks counted

using a Beckman Coulter Z1 particle counter. Mean cell numbers for parental and flavonoid-selected cells were plotted vs. time.

2.19. Microarray analysis of tangeretin-induced parental and tangeretin-resistant MDA-MB-435

MDA-MB-435 parental and tangeretin-selected MDA-MB-435TAN200H cells were plated at $1x10^6$ cells per flask and incubated overnight. Parental MDA-MB-435 cells were treated with DMSO vehicle control and tangeretin-selected TAN200H cells with 0.5 mM tangeretin. Cells were grown to 80-90% confluence and harvested by scraping. RNA was isolated using Trizol® and 20 μg of RNA was used for microarray analysis. Gene expression was analyzed using Affymetrix human GeneChip® oligonucleotide arrays (Santa Clara, CA), specifically the HGU95A array containing 10,000 full length genes. Probe synthesis, hybridization and array scanning were done at the Ottawa Health Research Institute (Ottawa, ON) according to Affymetrix protocols. Data was exported to GeneSpring GX 7.3 (Agilent Technologies, Palo Alto, CA) for analysis. This was a single experiment, consisting of a parental and a tangeretin-selected array.

2.20. Microarray data mining and pathways analysis

Data was analysed using GeneSpring GX 7.3 from Agilent Technologies (Palo Alto, CA). Preprocessing of data and normalizations were performed as stated in Section 2.15. Filtering on fold changes of genes "Present of Marginal" in 1 out of 2 samples was performed to obtain a list of genes 2-fold or greater increased or decreased in tangeretin-selected cells. The list of 2-fold changed tangeretin-responsive genes (817) was further analysed by categorizing genes based on biological processes. Biological process gene lists for cell growth, proliferation, cell cycle, apoptosis, and stress were generated at the Affymetrix NetAffx™ Analysis Center website (http://www.affymetrix.com/analysis/index.affx) and were cross-referenced to the

list of 2-fold up of downregulated genes. Ingenuity Pathways Analysis was done on the list of 2-fold changed genes as described in section 2.15.

2.21. Cross resistance analysis using Alamar Blue™ assay

Parental and resistant cells were plated in 96-well plates at $1.5x10^3$ cells per well in 100 μl ($1.5x10^4$ cells/ml) and allowed to attach overnight. Cells were treated for 4 d with a range of concentrations of common chemotherapy drugs (5-fluorouracil, vincristine sulphate, taxol, and cisplatin). Drugs and controls (at 2x the final concentration) were added in 100 μl of growth medium to 100 μl of media already in the wells. On day 4, 100 μl of media was removed from each well and replaced with 10% Alamar Blue™ in growth medium. Cells were incubated with Alamar Blue™ for 4 h and fluorescence was read on a Wallac 1420 Victor Plate Reader (PerkinElmer, Wellesley, MA). Fluorescence measurements were made by exciting at 530-560 nm and measuring emission at 590 nm. This assay relies on metabolism of a chromogenic substrate to a fluorescent product by mitochondrial enzymes, therefore a more metabolically active cell will have more fluorescence then a less active cell. No cell controls were used for each concentration of drug to rule out any contribution to fluorescence by reduction of Alamar Blue™ by drugs in the growth medium. Average background fluorescence was subtracted from test values and fluorescence was expressed as a percent of control.

2.22. Confirmation of vincristine resistance

Vincristine-selected, parental and multi-drug resistant head and neck squamous cell carcinoma lines (HN-5a, HN-5aV5f and HN-5aV15e) were generously donated by Dr. Peter Ferguson (London Regional Cancer Program, London, ON). These cells overexpress P-glycoprotein as the mechanism of resistance [77]. HN-5aV5f cells are less resistant to vincristine than HN-5aV15e. Vincristine resistance was confirmed by a standard 4 d proliferation assay (see Section 2.3 for details) using media as control.

2.23. Proliferation assay for vincristine-selected cell lines

HN-5a, HN-5aV5f and HN-5aV15e cells were plated in 25 cm^2 flasks at $1x10^5$ cells per flask and incubated overnight to attach. Cells were treated with a range of concentrations of tangeretin, nobiletin or DMSO control for 4 d. Cells were trypsinized and replicate flasks counted on day 0 and day 4 using a Beckman Coulter Z1 Particle Counter. Cell numbers were expressed as a percent of vehicle control.

2.24. Statistical analysis

All results are presented as mean ± SEM. Significant differences between means of three or more data sets were determined by one-way analysis of variance (one-way ANOVA) with post hoc Tukey test. Differences between two data sets were determined by Student's t-test. Differences were considered significant when $P \leq 0.05$.

Chapter 3
RESULTS

I. Antiproliferative activity of tangeretin and nobiletin in breast and colon cancer cells

3.1. Antiproliferative effects

3.1.1. Dose- and time-dependent inhibition of proliferation

Tangeretin and nobiletin inhibited proliferation of MDA-MB-435, MCF-7 and HT-29 human cancer cells in a dose-dependent manner, with 60-95% inhibition of proliferation in treated cells compared to control cells at the highest concentrations (Figure 10, panels A,B). For tangeretin, concentrations that inhibited proliferation 50% (IC_{50}) compared to controls, in MDA-MB-435, MCF-7 and HT-29 cells were 43.5±1.1, 34.9±8.3 and 35.8±5.4 μM, respectively. For nobiletin, these concentrations were 63.9±5.7, 36.8±10.0 and 46.5 ± 9.5 μM, respectively (Table 6). Data shown in Figure 10 are from one of three independent experiments and, as such, do not correspond with IC_{50} values presented in Table 6. This is because table values were calculated as the mean of results from three experiments. To ensure cellular and molecular effects of tangeretin and nobiletin were observable and quantifiable, concentrations that yielded appreciable inhibition of proliferation (approximately 60-75%) were chosen for all subsequent experiments. For tangeretin, this was 54 μM for all three cell lines. For nobiletin, this was 60 μM in MCF-7 and HT-29 cells, and 100 μM in MDA-MB-435 cells. At these concentrations, the effect of tangeretin and nobiletin was evident early on with significant inhibition of proliferation of all cell lines beginning at 12 h and continuing to 4 d (Figure 11).

3.1.2. Inhibition of proliferation in non-transformed normal cells

The effect of tangeretin and nobiletin on the proliferation of normal, non-transformed cells was assessed in human endothelial umbilical vein cells (HUVEC). Tangeretin and nobiletin inhibited proliferation of HUVECs in a dose-dependent manner, with 80-95% inhibition in treated cells compared to control cells at the highest concentrations (Figure 12, panels A,B), similar to the degree of inhibition observed in the cancer cell lines. This was reflected in the IC_{50}

Figure 10. Dose-dependent inhibition of proliferation by tangeretin (A) and nobiletin (B) in MDA-MB-435 (●), MCF-7 (○), and HT-29 (▼) cells. Cells were treated with the indicated concentrations of tangeretin and nobiletin as described in *Materials and Methods*, and cell numbers were determined after 4 d. Mean cell numbers from quadruplicate measurements were expressed as a % of DMSO control ± SEM. Data shown are from one of three independent experiments. Where error bars are not apparent, they are smaller than the symbol.

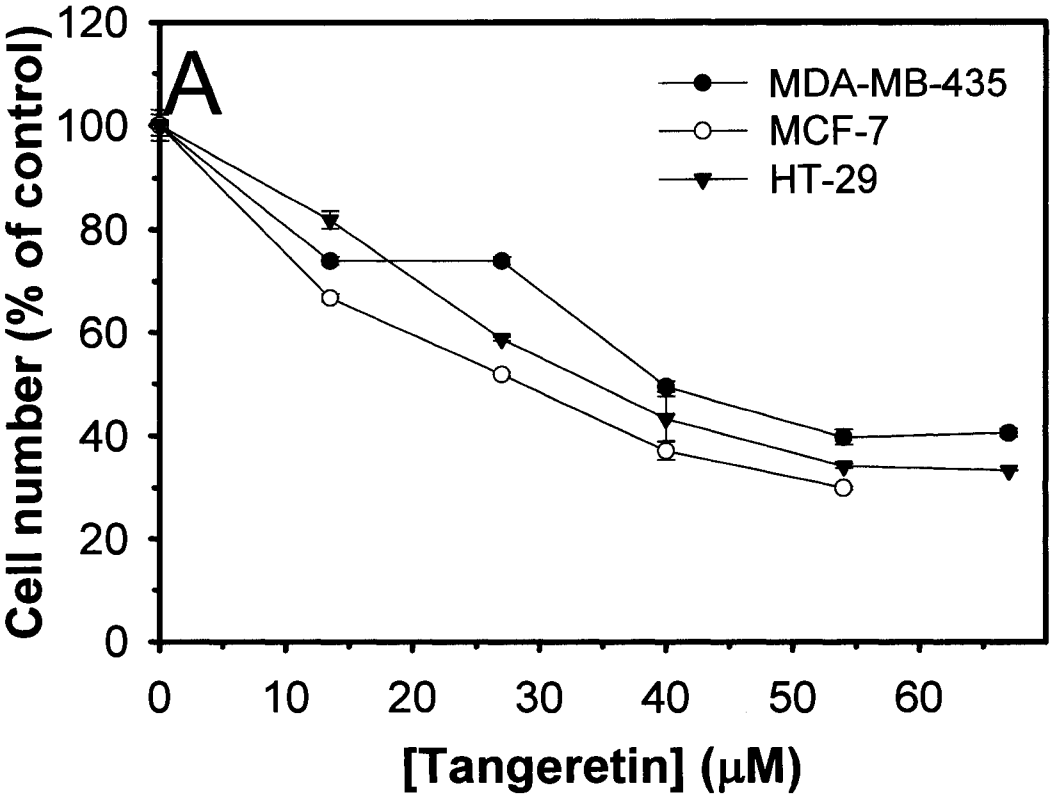
A
MDA-MB-435
MCF-7
HT-29
Cell number (% of control)
120
100
80
60
40
20
0
0
10
20
30
40
50
60
[Tangeretin] (μM)

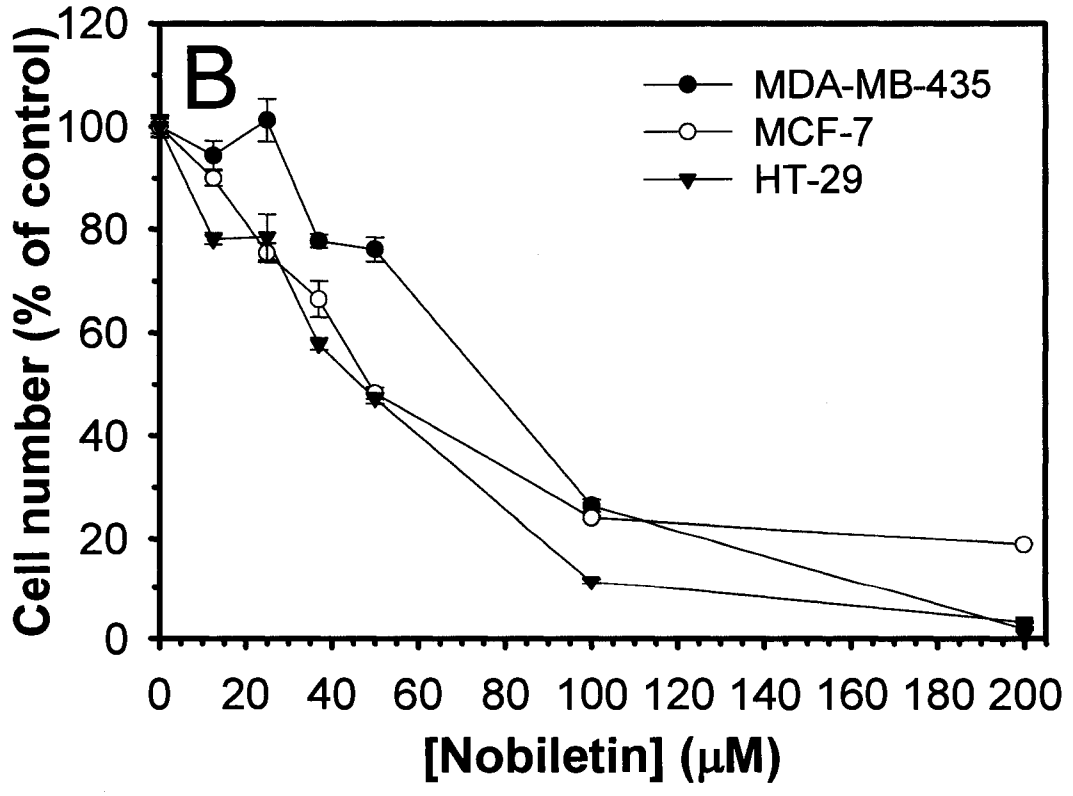
B
MDA-MB-435
MCF-7
HT-29
Cell number (% of control)
120
100
80
60
40
20
0
0
20
40
60
80
100
120
140
160
180
200
[Nobiletin] (μM)

Figure 11. Time-dependent inhibition of proliferation by tangeretin and nobiletin in MDA-MB-435 (A,D), MCF-7 (B,E), and HT-29 (C,F) cells. Cells were treated with tangeretin or vehicle control [A,B,C: DMSO (●) or tangeretin/DMSO 54 μM (○)], and nobiletin or vehicle control [D,E,F: DMSO (■) or nobiletin/DMSO (□)]. MCF-7 and HT-29 cells were treated with 60 μM nobiletin and MDA-MB-435 cells were treated with 100 μM nobiletin. Cell numbers were determined at the time of plating and at 12, 24, 48, 72 and 96 h following the addition of flavonoid. Mean cell numbers ± SEM are representative of three or four independent experiments. *Significantly different from vehicle controls (Student's t-test, $P \leq 0.05$).

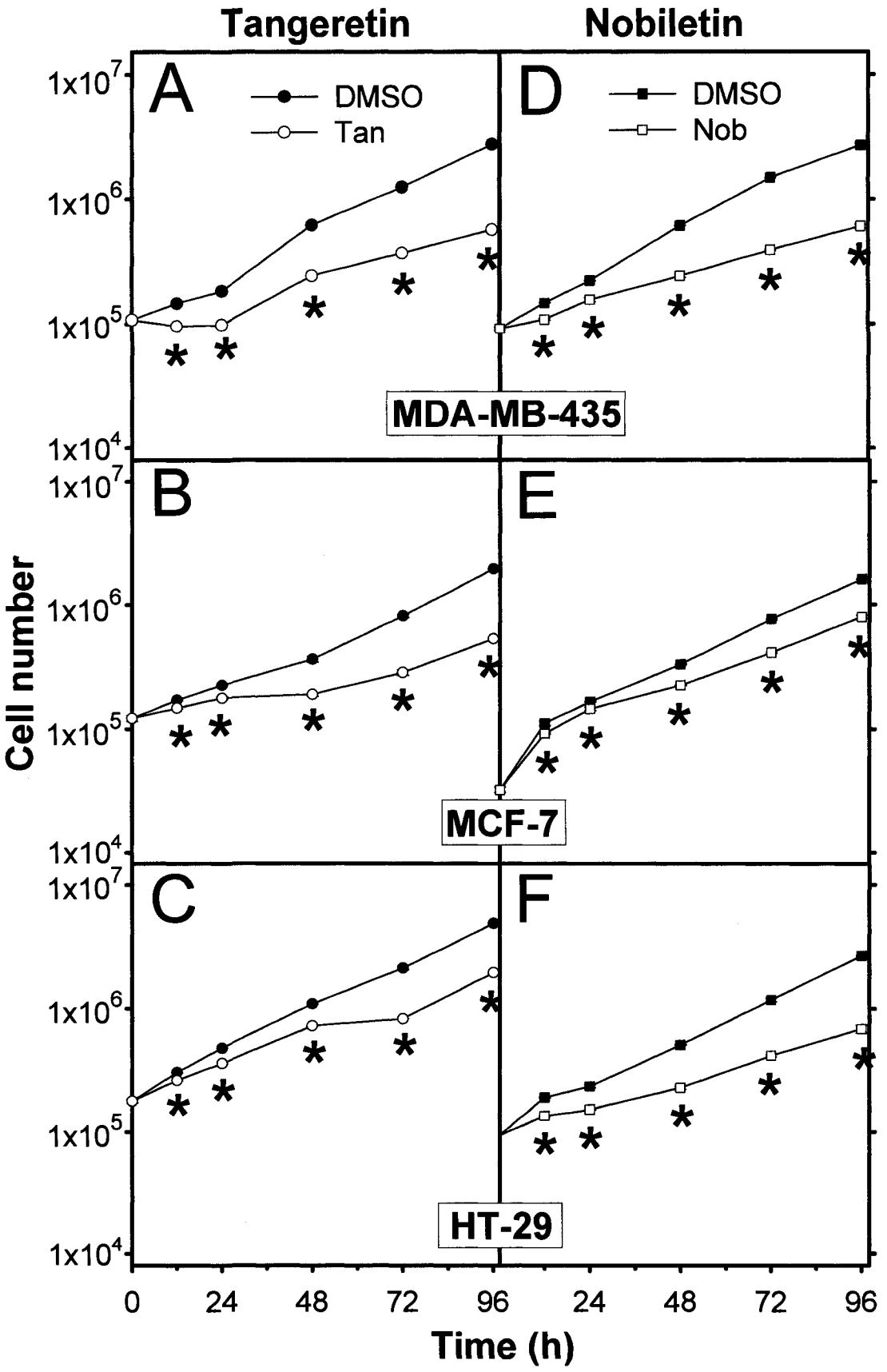
Tangeretin
Nobiletin
A
D
DMSO
Tan
Nob
MDA-MB-435
B
E
MCF-7
C
F
HT-29
Cell number
1x10^7
1x10^6
1x10^5
1x10^4
0
24
48
72
96
Time (h)

Figure 12. Dose-dependent inhibition of proliferation by tangeretin (A) and nobiletin (B) in HUVE cells. Cells were treated with the indicated concentrations of tangeretin and nobiletin as described in *Materials and Methods*, and cell numbers were determined after 4 d. Mean cell numbers from quadruplicate measurements are expressed as a % of numbers of control cells treated with identical concentrations of DMSO vehicle ± SEM. Data presented in this figure were combined from 3 independent experiments.

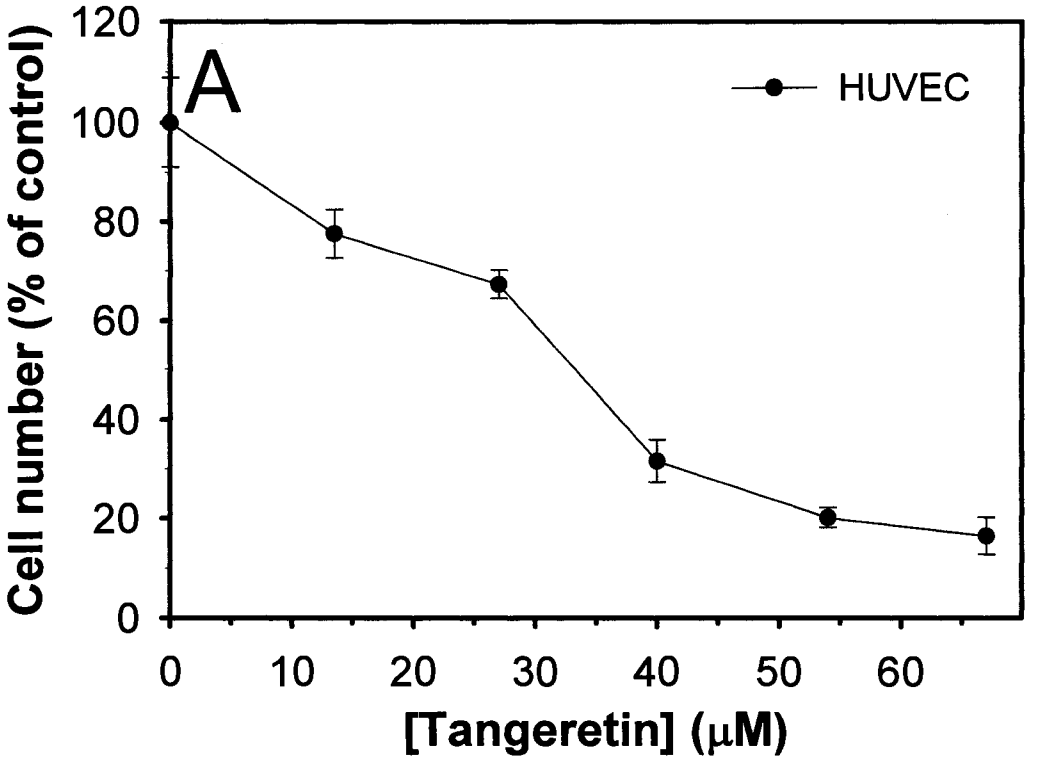
A
HUVEC
Cell number (% of control)
120
100
80
60
40
20
0
0
10
20
30
40
50
60
[Tangeretin] (μM)

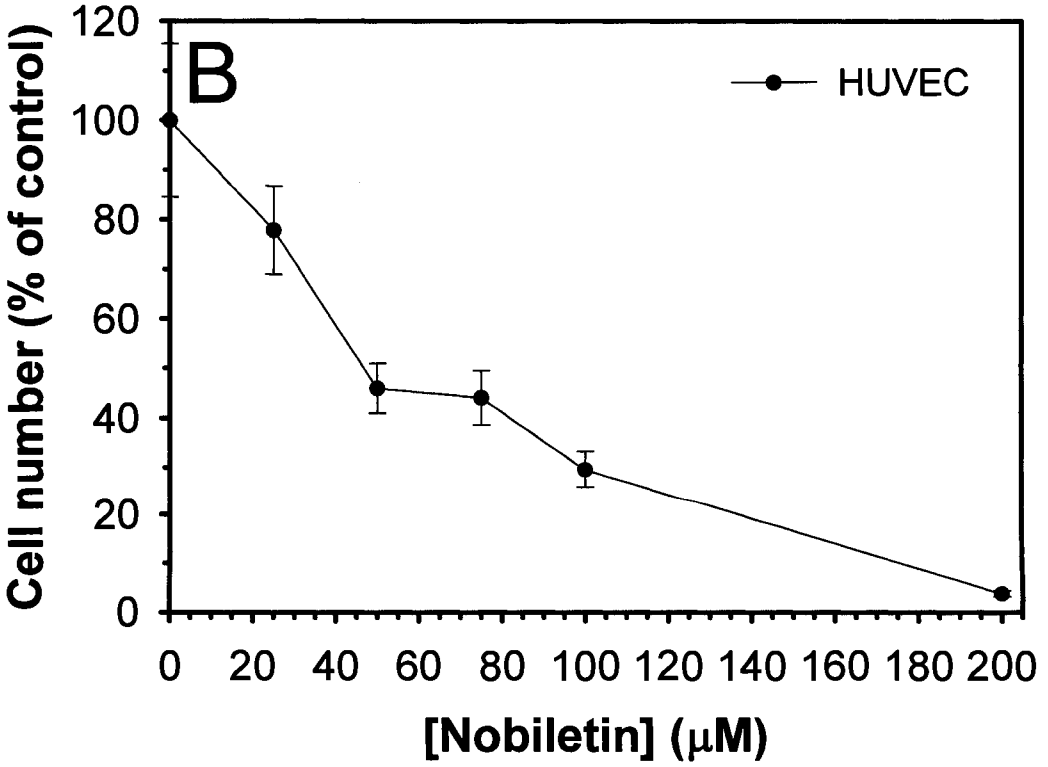
B
HUVEC
Cell number (% of control)
120
100
80
60
40
20
0
0
20
40
60
80
100
120
140
160
180
200
[Nobiletin] (μM)

Table 6. IC_{50} values for tangeretin and nobiletin in MDA-MB-435, MCF-7, HT-29 and HUVE cells. Cells were treated with concentrations of tangeretin and nobiletin as described in *Materials and Methods* for the proliferation assay, and cell numbers were determined after 4 d. Average cell numbers were expressed as a % of DMSO control and plotted against concentration. The concentrations at which proliferation of flavonoid-treated cells were inhibited by 50% compared to vehicle control were taken from three independent dose response curves and are expressed as mean ± SEM. One way ANOVA was performed to assess significance of differences between IC50 values of normal and cancer cells.

	IC50 (μM)	
Cell line	**Tangeretin**	**Nobiletin**
MDA-MB-435	43.5 ± 1.1	63.9 ± 5.7
MCF-7	34.9 ± 8.3	36.8 ± 10.0
HT-29	35.8 ± 5.4	46.5 ± 9.5
HUVEC	37.9 ± 3.8	48.3 ± 13.4

values for tangeretin and nobiletin in HUVECs (37.9±3.8 and 48.3±13.4 μM, respectively) which are comparable to IC_{50} values in the cancer cell lines (see Table 6). IC_{50} values of tangeretin and nobiletin for HUVECs were not significantly different from values for the tested human cancer cell lines.

3.1.3. Recovery of proliferation following removal of tangeretin and nobiletin

To determine whether cells regain their capacity to proliferate following removal of tangeretin or nobiletin, treatment medium was replaced with growth medium following 4 days of exposure to the concentrations of tangeretin or nobiletin indicated in Figure 13. Replacement growth medium contained no tangeretin, nobiletin or DMSO, and proliferation was assessed daily for four days thereafter. From as early as 24 h after media replacement, fold increases for flavonoid-treated MDA-MB-435, MCF-7 and HT-29 cells were comparable to untreated or vehicle-treated controls. By the end of four days, proliferation of tangeretin- and both concentrations of nobiletin-treated cells was similar to or greater than that of control cells for all three cell lines (Figure 13).

3.2. Cellular effects mediating inhibition of proliferation

3.2.1. G1 cell cycle accumulation by tangeretin and nobiletin

The inhibition of proliferation observed in response to tangeretin and nobiletin in MDA-MB-435, MCF-7 and HT-29 cells was assessed for involvement of cell cycle effects. In addition to exposure to relatively low (but nevertheless growth inhibiting) concentrations of tangeretin and nobiletin, a second, higher concentration of nobiletin (200 μM) was included in these experiments to assess dose-dependent effects of this flavonoid on cell cycle. Tangeretin's insolubility precluded assessment of dose-dependent cell cycle effects. Treatment of all three cell lines with tangeretin and nobiletin resulted in significant accumulation of cells in the G1or S phase compared to vehicle controls (see Table 7 for quantification of accumulation). This cell cycle accumulation was significant for tangeretin-treated and all nobiletin-treated MDA-MB-435 and MCF-7 cells by 24 h, continuing to 72 h (Figure 14 and 15, panels A,B). In HT-29 cells, for

Figure 13. Proliferation of MDA-MB-435 (A), MCF-7 (B) and HT-29 (C) cells for 4 d following removal of tangeretin and nobiletin. Cells were treated for 4 d with tangeretin (△), nobiletin (○ and ◊), DMSO vehicle control (■) or growth medium (●). All cells were treated with 54 μM tangeretin, MCF-7 and HT-29 cells were treated with 60 and 200 μM nobiletin and MDA-MB-435 cells were treated with 100 and 200 μM nobiletin. Treatment media was removed and replaced with flavonoid- and DMSO-free growth medium and grown for an additional 4 d. Cell numbers were determined each day following media renewal. Day four cell numbers were considered baseline and cell numbers from subsequent days were expressed as fold increases of this number. Results presented are mean fold increase ± SEM and are representative of 3-6 independent experiments. **Tan**: tangeretin (54 μM), **Nob lo**: nobiletin (60 or 100 μM), **Nob hi**: nobiletin (200 μM)

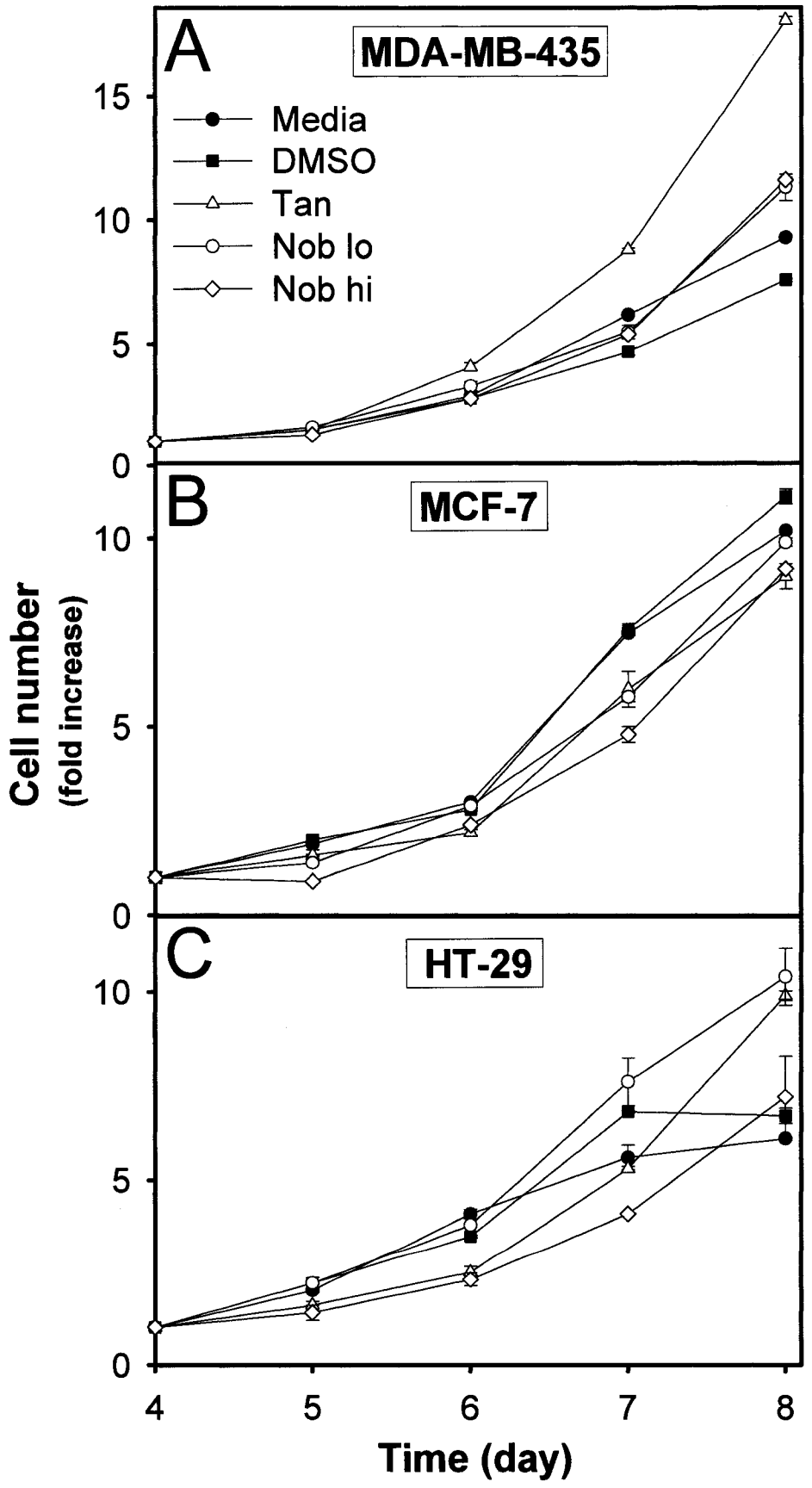
A
MDA-MB-435
Media
DMSO
Tan
Nob lo
Nob hi
B
MCF-7
C
HT-29
Cell number
(fold increase)
Time (day)
0
5
10
15
4
5
6
7
8

Table 7. Increases in % of cells in G1 or S phase induced by tangeretin or nobiletin treatment of MDA-MB-435, MCF-7 and HT-29 cells. Cells were treated for 24, 48 and 72 h with tangeretin (54 μM), nobiletin (24-200 μM) or DMSO control. Cell nuclei were stained with propidium iodide, and DNA content analyzed by flow cytometry. The % total population for vehicle treated cells (in Fig 14 and 15) were subtracted from % total population for tangeretin or nobiletin treated cells to give % increases in G1 or S populations at each time point. All values presented are significantly different than vehicle control by ANOVA.

[a]percent increase in S phase

		% Increase compared to vehicle control		
Cell line	***Flavonoid***	***24h***	***48h***	***72h***
MDA-MB-435	***Tan***	19.2	5.0	6.0
	Nob lo	39.8	20.6	16.1
	Nob hi	22.3	32.9	29.2
MCF-7	***Tan***	20.7	16.5	10.6
	Nob lo	10.6	9.9	8.2
	Nob hi	14.8	42.3	40.3
HT-29	***Tan***	9.5[a]	17.0	22.0
	Nob lo	4.0[a]	9.4	8.0
	Nob hi	31.2	43.7	34.5

tangeretin and the lower concentration of nobiletin (60 μM), G1 accumulation was seen at 48 and 72 h, following a transient accumulation of cells in S phase at 24 h (Figure 14 and 15, panel C). This transient S phase accumulation was not observed at the higher nobiletin concentration (200 μM) at which cells were accumulated in G1 by 24 h, continuing up to 72 h (Figure 15, panel C). Both flavonoids maintained cell cycle accumulation up to 96 h in all three cell lines (data not shown). However, with the exception of tangeretin-treated HT-29 cells, there was no apparent relationship with time as the percentage of cells accumulated in G1/S remained constant over time. With nobiletin, the percentage of cells accumulated was directly proportional to concentration (Figure 15, panels A-C). Data presented in Figures 14 and 15 were replicated in three independent experiments. (Note, a sample DNA histogram is shown in Figure 35, Appendix II.)

3.2.2. Resumption of cell cycling following removal of tangeretin and nobiletin

To determine whether cells regain their capacity to cycle following removal of the flavonoids, treatment medium was replaced with flavonoid-free growth medium and cell cycle distribution was assessed one and four days after media renewal. Tangeretin- and nobiletin-treated MDA-MB-435 and MCF-7 cells returned to normal cycling within a day of flavonoid removal and this was maintained up to four days (Figure 16, panels A,B). Tangeretin-exposed HT-29 cells resumed cell cycling with the fraction of cells in all cell cycle compartments comparable to vehicle-treated controls within a day of flavonoid removal. Nobiletin-treated HT-29 cells, however, did not resume cycling comparable to vehicle-treated controls until four days after media renewal (Figure 16, panel C).

3.2.3. Lack of apoptosis induction by tangeretin and nobiletin at concentrations that significantly suppress proliferation

Involvement of apoptosis or cell death in the inhibition of proliferation induced by tangeretin and nobiletin in MDA-MB-435, MCF-7 and HT-29 was investigated. Cells were treated for 4 days with these flavonoids and apoptotic (annexin V+) and dead (annexin V+/PI+) cells were quantified using flow cytometry. Dead cells

Figure 14. Cell cycle distribution in tangeretin-treated MDA-MB-435 (A), MCF-7 (B) and HT-29 (C) cells. Cells were treated for 24, 48 and 72 h with tangeretin [54 μM (white bars)] or DMSO control (black bars). Cell nuclei were stained with propidium iodide, and DNA content analyzed by flow cytometry. Percent of total cell population values were obtained in triplicate for each time point using Multicycle for Windows software, and are expressed as means ± SEM. The data shown are representative of three independent experiments. *Significantly different from DMSO controls (one-way ANOVA, $P \leq 0.05$). **Tan**: tangeretin (54 μM)

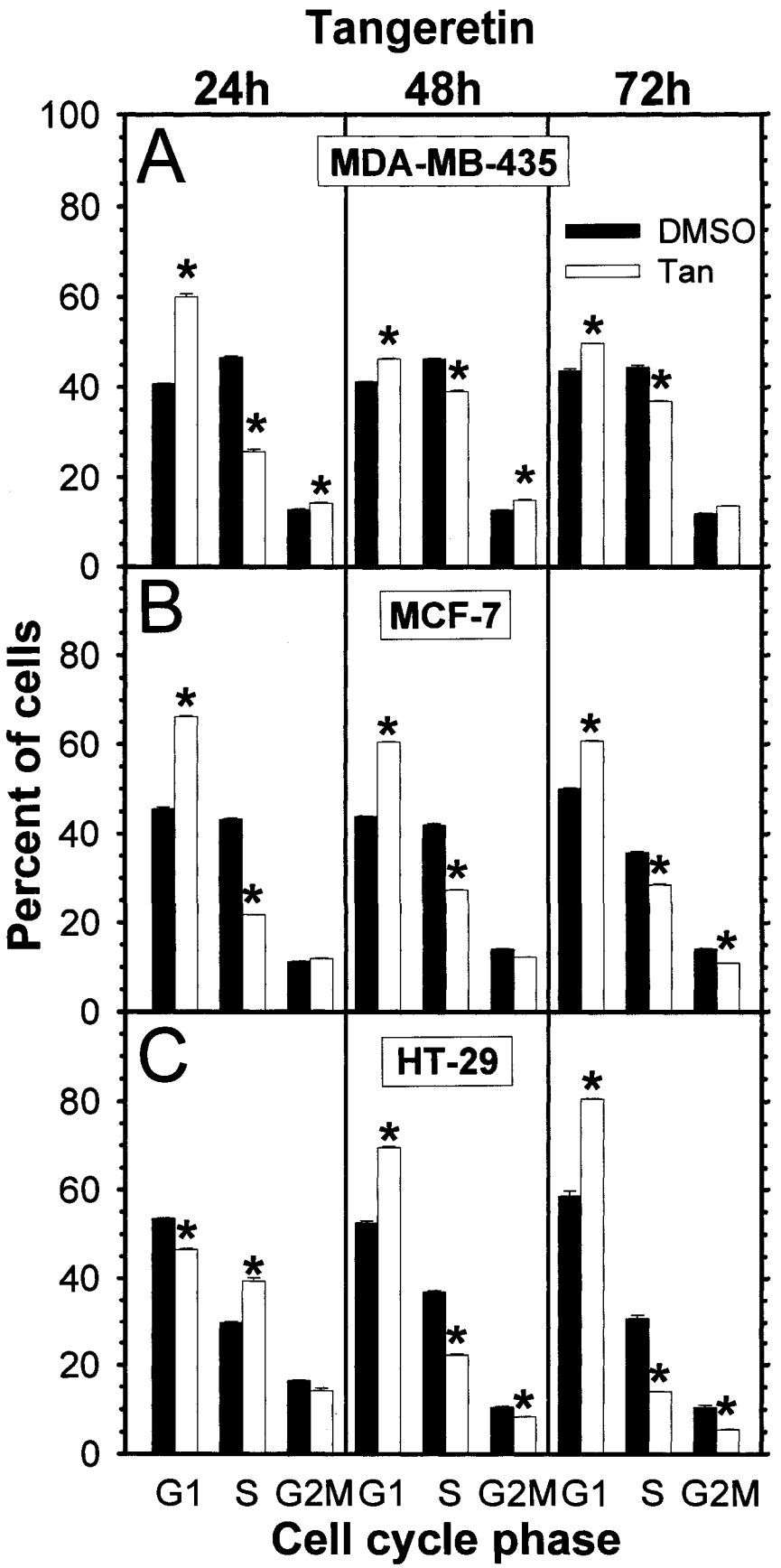
Tangeretin
24h
48h
72h
A
MDA-MB-435
B
MCF-7
C
HT-29
DMSO
Tan
Percent of cells
100
80
60
40
20
0
G1
S
G2M
Cell cycle phase

Figure 15. Cell cycle distribution in nobiletin-treated MDA-MB-435 (A), MCF-7 (B) and HT-29 (C) cells. Cells were treated for 24, 48 and 72 h with nobiletin [A: 100 or 200 μM (white and grey bars, respectively), B,C: 60 or 200 μM (white and grey bars, respectively)] or DMSO control (A,B,C, black bars). Cell nuclei were stained with propidium iodide, and DNA content analyzed by flow cytometry. Percent of total cell population values were obtained in triplicate for each time point using Multicycle for Windows software, and are expressed as means ± SEM. The data shown are representative of three independent experiments. *Significantly different from DMSO controls (one-way ANOVA, $P \leq 0.05$). **Nob lo**: nobiletin (60 or 100 μM), **Nob hi**: nobiletin (200 μM)

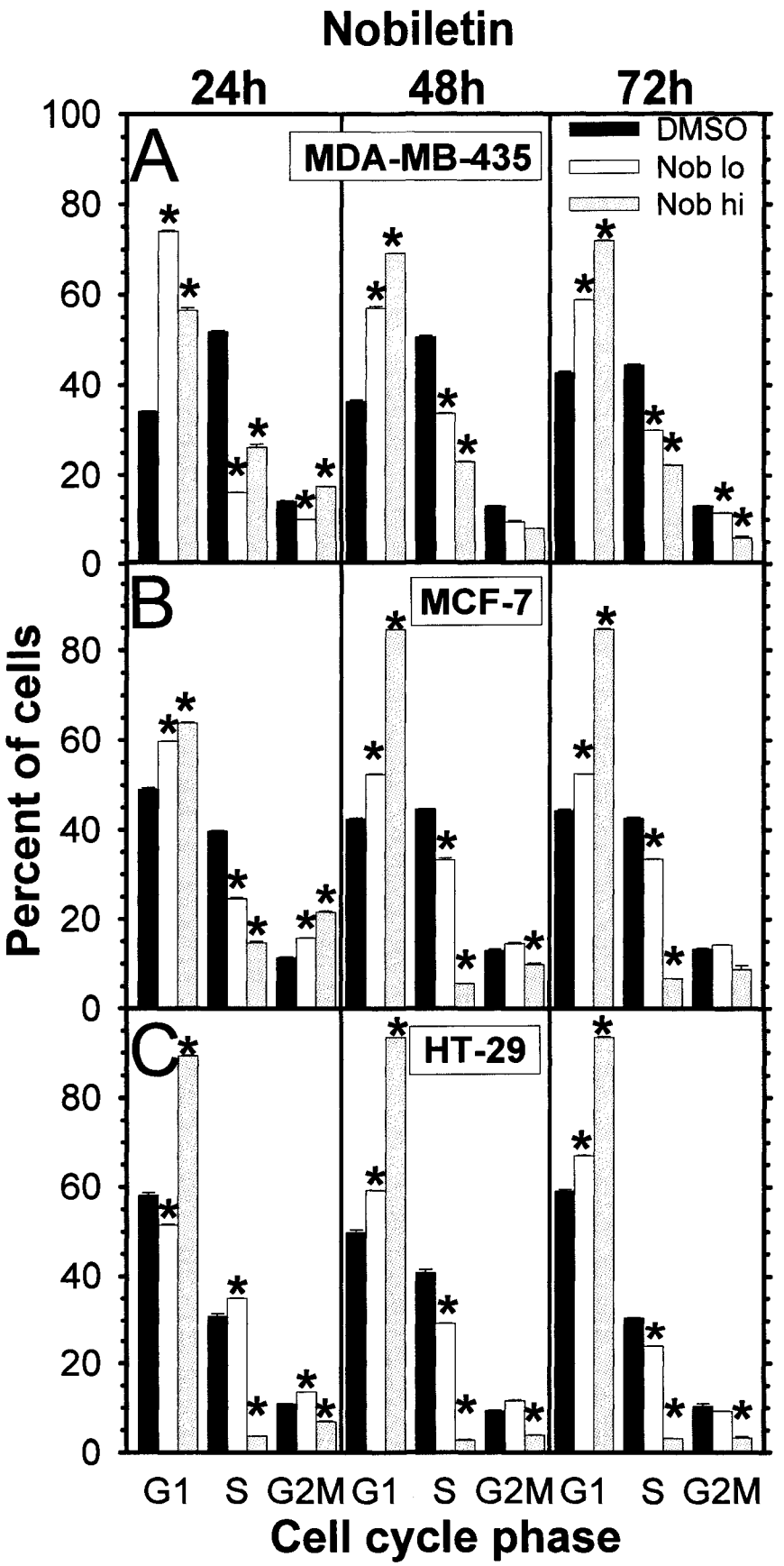
Nobiletin
24h
48h
72h
DMSO
Nob lo
Nob hi
A
MDA-MB-435
B
MCF-7
C
HT-29
Percent of cells
0
20
40
60
80
100
G1
S
G2M
Cell cycle phase

Figure 16. Cell cycle distribution in MDA-MB-435 (A), MCF-7 (B) and HT-29 (C) cells 24 h and 96 h following removal of tangeretin or nobiletin. Cells were treated with tangeretin [A,C: 54 μM (white bars)], nobiletin [A: 100 μM (grey bars), B,C: 60 μM (grey bars)] or DMSO control (A,B,C, black bars) for 4 d. Treatment media was then removed and replaced with growth medium alone, and cells were grown for an additional 4 d. Cell cycle distribution was assessed 24 h and 96 h following media change. Percent of total cell population values were obtained in triplicate for each time point using Multicycle for Windows software, and are expressed as means ± SEM. The data shown were combined from three independent experiments. *Significantly different from DMSO control (one-way ANOVA, $P < 0.05$). **Tan**: tangeretin (54 μM), **Nob**: nobiletin (60 or 100 μM)

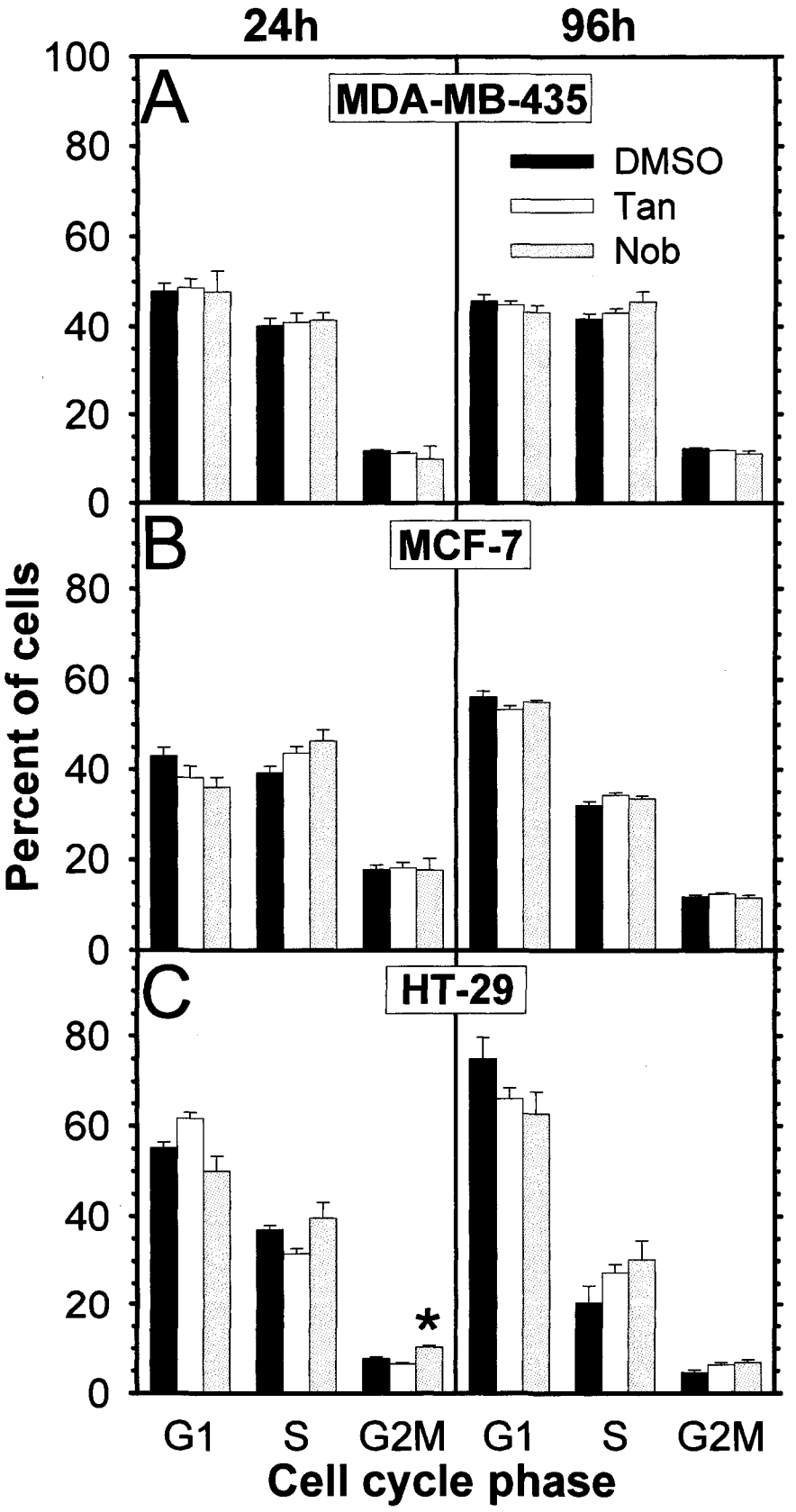
24h
96h
A
MDA-MB-435
DMSO
Tan
Nob
B
MCF-7
C
HT-29
*
Percent of cells
100
80
60
40
20
0
G1
S
G2M
G1
S
G2M
Cell cycle phase

include cells that are in the late stages of apoptosis as well as cells that have died by necrosis. There was no significant increase in apoptotic or dead populations for tangeretin-treated cells compared to vehicle control (Figure 17). There was no significant increase above control in apoptosis or cell death by other means at 48 h or 72 h following treatment of MDA-MB-435, MCF-7 and HT-29 cells with tangeretin at concentrations that were shown to inhibit proliferation by 60-75%. Similar results were obtained for nobiletin-treated MCF-7 and HT-29 cells at 48 h and 72 h, and MDA-MB-435 cells at 48 h (Figure 18) but, there was a significant increase in the percent of dead cells for nobiletin-treated MDA-MB-435 cells at 72 h. However, this increase in the percent of dead cells (although significant compared to dead cells in controls) was not significant when total dead and dying (apoptotic) cell numbers were compared to the same combined number for control cell populations (data not shown). The absence of apoptosis or cell death in MCF-7 and HT-29 cells was not due to an inability to undergo induced cell death since appreciable death was induced by other drugs (Figure 17 and 18).

3.2.3.1. Apoptosis induction at higher concentrations of nobiletin

Cell death was measured in the three cancer cell lines after treatment with a concentration of nobiletin (200 μM) greater than that required to suppress proliferation in the absence of apoptosis. Treatment of cells with higher concentrations of tangeretin was not practical due to insufficient solubility of tangeretin at experimentally acceptable concentrations of DMSO. Apoptotic cells (annexin V+) and dead and dying cells which includes apoptotic cells and cells dead and dying by other means, denoted as total cell death (annexin V+ plus annexin V+/PI+) were quantified by flow cytometry after 24, 48, 72 and 96 h of treatment. There was a significant increase in apoptotic (5-15%) and total dead and dying (5-30%) cells for nobiletin-treated MDA-MB-435, MCF-7 and HT-29 cells compared to vehicle control (Figure 19, 20 and 21). For MCF-7 and HT-29 cells, apoptosis was evident from 48 h to 96 h (Figure 20 and 21, panel A), but

Figure 17. Apoptosis and necrosis in tangeretin-treated MDA-MB-435 (A), MCF-7 (B) and HT-29 (C) cells. Cells were treated for 48 h and 72 h with tangeretin (A,B,C: 54 μM), DMSO vehicle control (all panels), positive control [A,B: cycloheximide (356 μM), C: cisplatin (20 μM)], or untreated control (all panels). Apoptotic and dead cells were assessed as described in *Materials and Methods*. The data shown were combined from two independent experiments.
*Significantly different from untreated controls (one-way ANOVA, $P \leq 0.05$). No significant differences were induced in any cell lines by treatment with tangeretin. **UC**: untreated control, **PC**: positive control [cycloheximide (356 μM) or cisplatin (20 μM)], **VC**: DMSO vehicle control, **Tan**: tangeretin (54 μM).

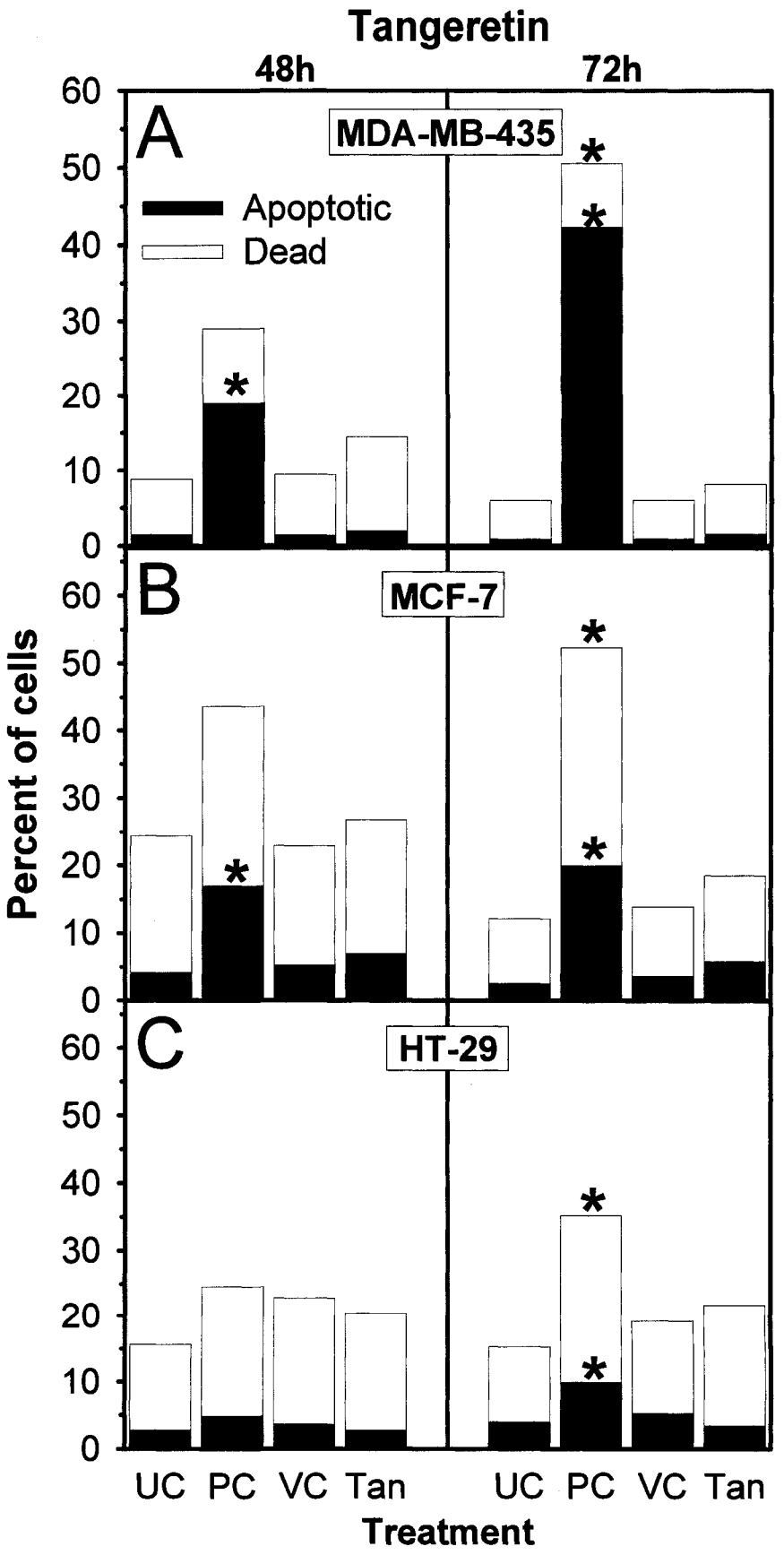
Tangeretin
48h
72h
A
MDA-MB-435
Apoptotic
Dead
B
MCF-7
C
HT-29
Percent of cells
0
10
20
30
40
50
60
UC PC VC Tan UC PC VC Tan
Treatment

Figure 18. Apoptosis and necrosis in nobiletin-treated MDA-MB-435 (A), MCF-7 (B) and HT-29 (C) cells. Cells were treated for 48 h and 72 h with nobiletin (B,C: 60 μM, A: 100 μM), DMSO vehicle control (all panels), positive control [A,B: cycloheximide (356 μM), C: cisplatin (20 μM)], or untreated control (all panels). Apoptotic and dead cells were assessed as described in *Materials and Methods.* The data shown were combined from two independent experiments.
*Significantly different from control (one-way ANOVA, $P \leq 0.05$). **UC**: untreated control, **PC**: positive control [cycloheximide (356 μM) or cisplatin (20 μM)], **VC**: DMSO vehicle control, **Nob**: nobiletin (60 μM or 100 μM).

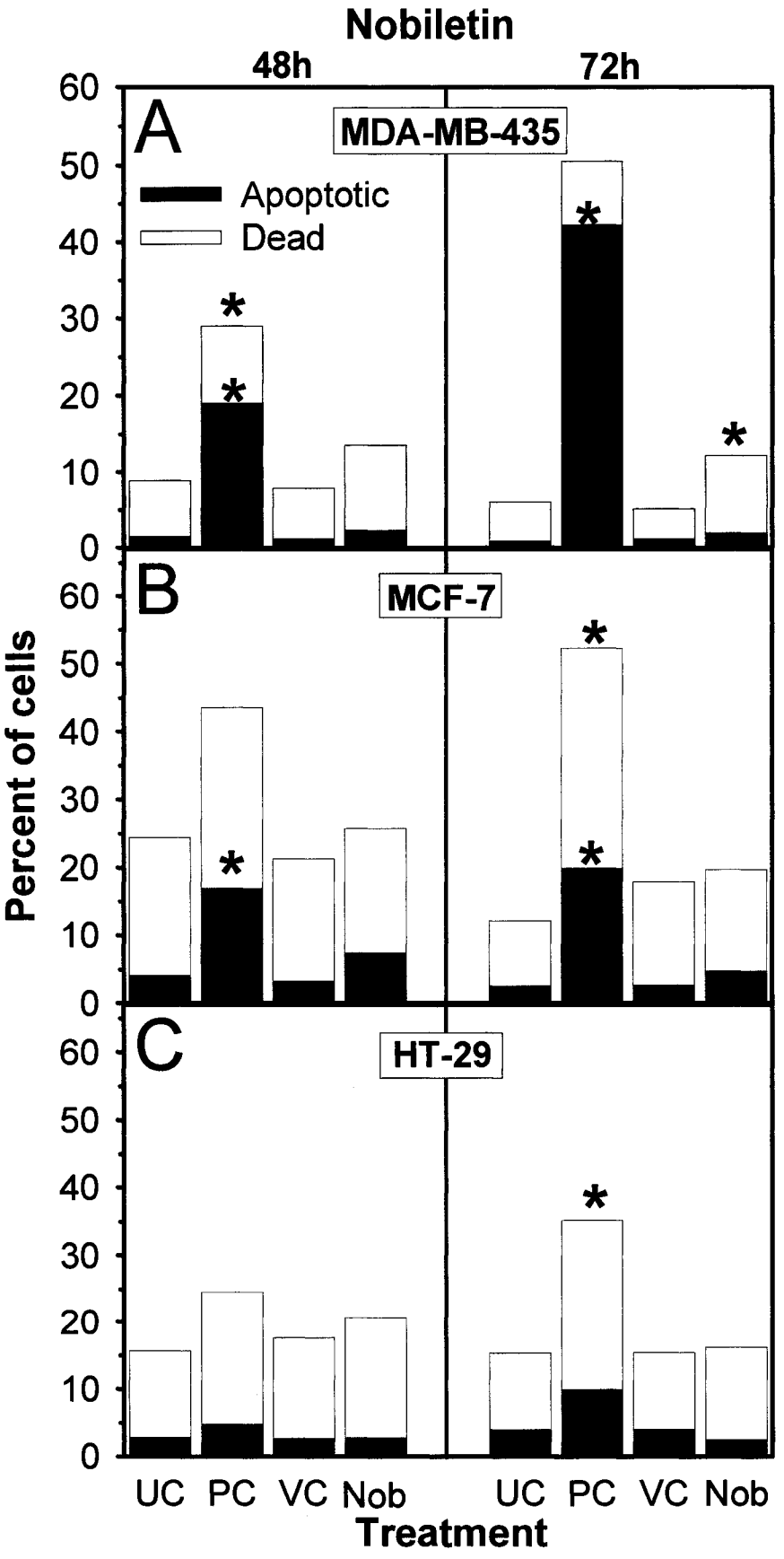
Nobiletin
48h
72h
A
MDA-MB-435
Apoptotic
Dead
B
MCF-7
C
HT-29
Percent of cells
0
10
20
30
40
50
60
UC
PC
VC
Nob
Treatment

Figure 19. Apoptosis and total cell death in MDA-MB-435 cells treated with a high concentration of nobiletin. Cells were treated for 1-4 d with nobiletin (all panels: 200 μM, white bars) or DMSO vehicle control (all panels: black bars). Cells undergoing apoptosis (A) or dead and dying cells (B) were quantified by flow cytometry as described in *Materials and Methods*. Percent of total cells were obtained in triplicate for each time point, and are expressed as means ± SEM. The data shown were combined from three independent experiments. *Significantly different from DMSO vehicle control (one-way ANOVA, $P \leq 0.05$). **Nob**: nobiletin (200 μM).

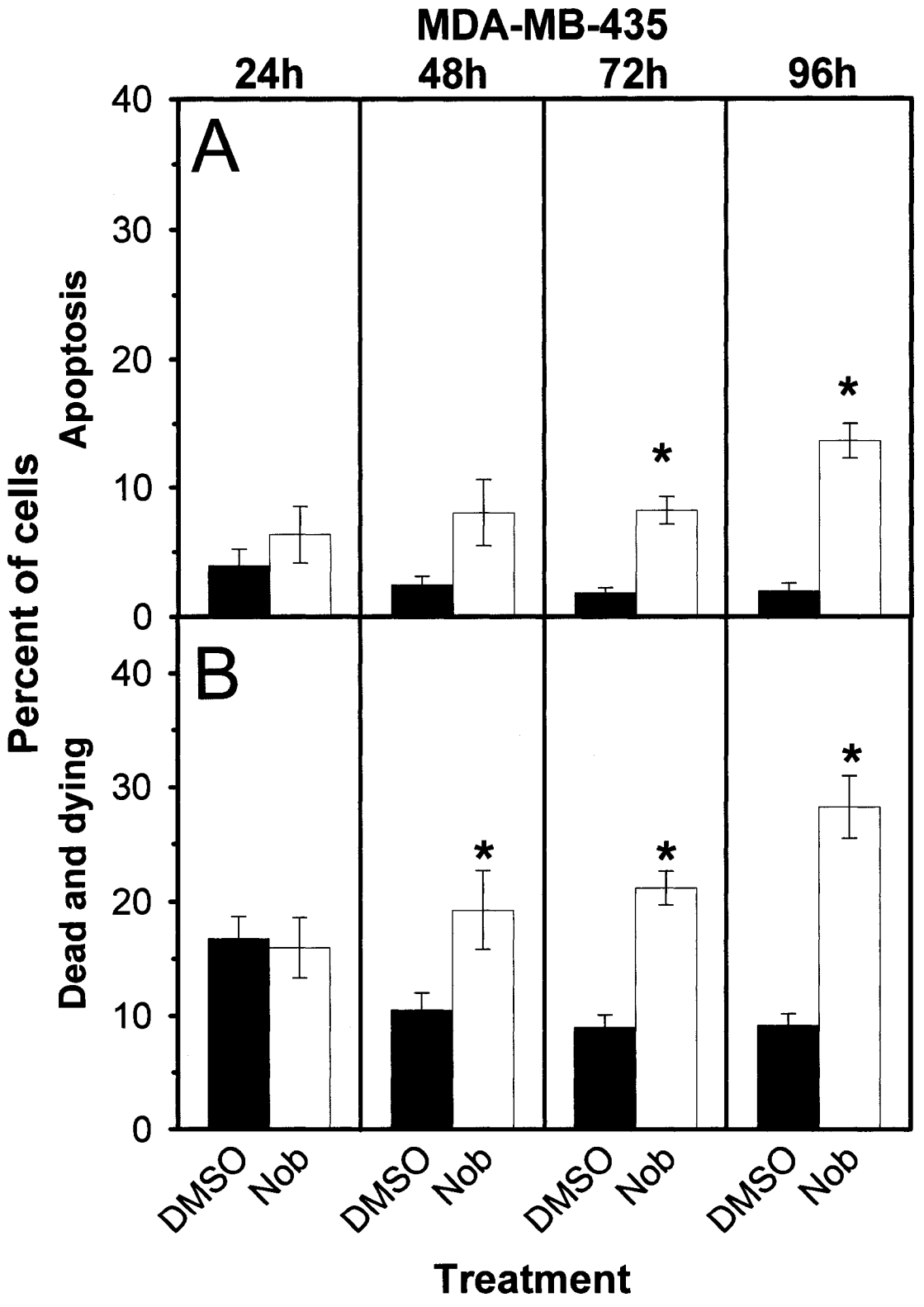
MDA-MB-435
24h
48h
72h
96h
A
B
Percent of cells
Apoptosis
Dead and dying
0
10
20
30
40
*
DMSO
Nob
Treatment

Figure 20. Apoptosis and total cell death in MCF-7 cells treated with a high concentration of nobiletin. Cells were treated for 1-4 d with nobiletin (all panels: 200 μM, white bars) or DMSO vehicle control (all panels: black bars). Cells undergoing apoptosis (A) or dead and dying cells (B) were quantified by flow cytometry as described in *Materials and Methods*. Percent of total cells were obtained in triplicate for each time point, and are expressed as means ± SEM. The data shown were combined from three independent experiments. *Significantly different from DMSO vehicle control (one-way ANOVA, $P \leq 0.05$). **Nob**: nobiletin (200 μM).

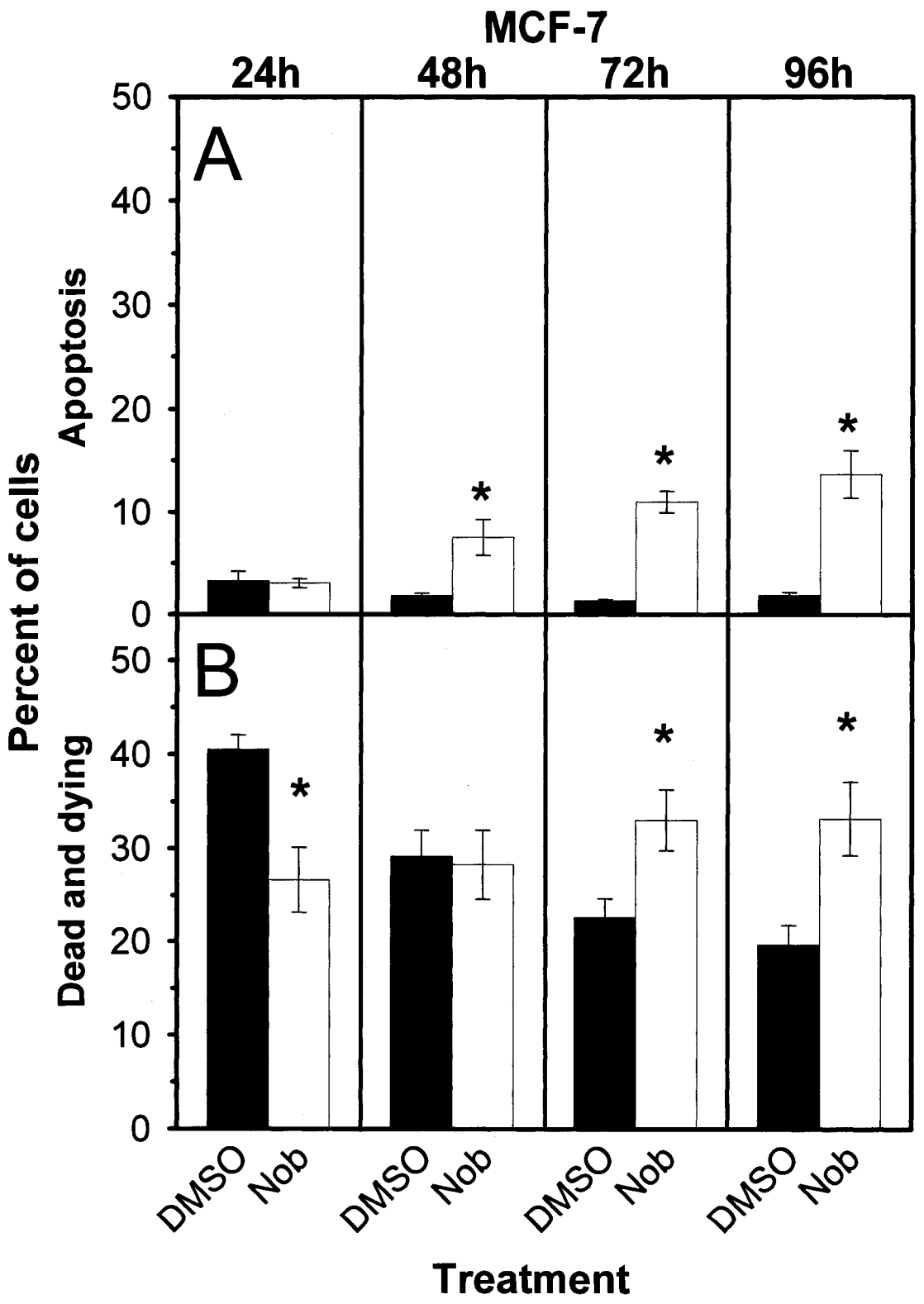
MCF-7
24h
48h
72h
96h
A
B
Apoptosis
Dead and dying
Percent of cells
50
40
30
20
10
0
*
DMSO
Nob
Treatment

Figure 21. Apoptosis and total cell death in HT-29 cells treated with a high concentration of nobiletin. Cells were treated for 1-4 d with nobiletin (all panels: 200 μM, white bars) or DMSO vehicle control (all panels: black bars). Cells undergoing apoptosis (A) or dead and dying cells (B) were quantified by flow cytometry as described in *Materials and Methods*. Percent of total cells were obtained in triplicate for each time point, and are expressed as means ± SEM. The data shown were combined from three independent experiments. *Significantly different from DMSO vehicle control (one-way ANOVA, $P \leq 0.05$). **Nob**: nobiletin (200 μM).

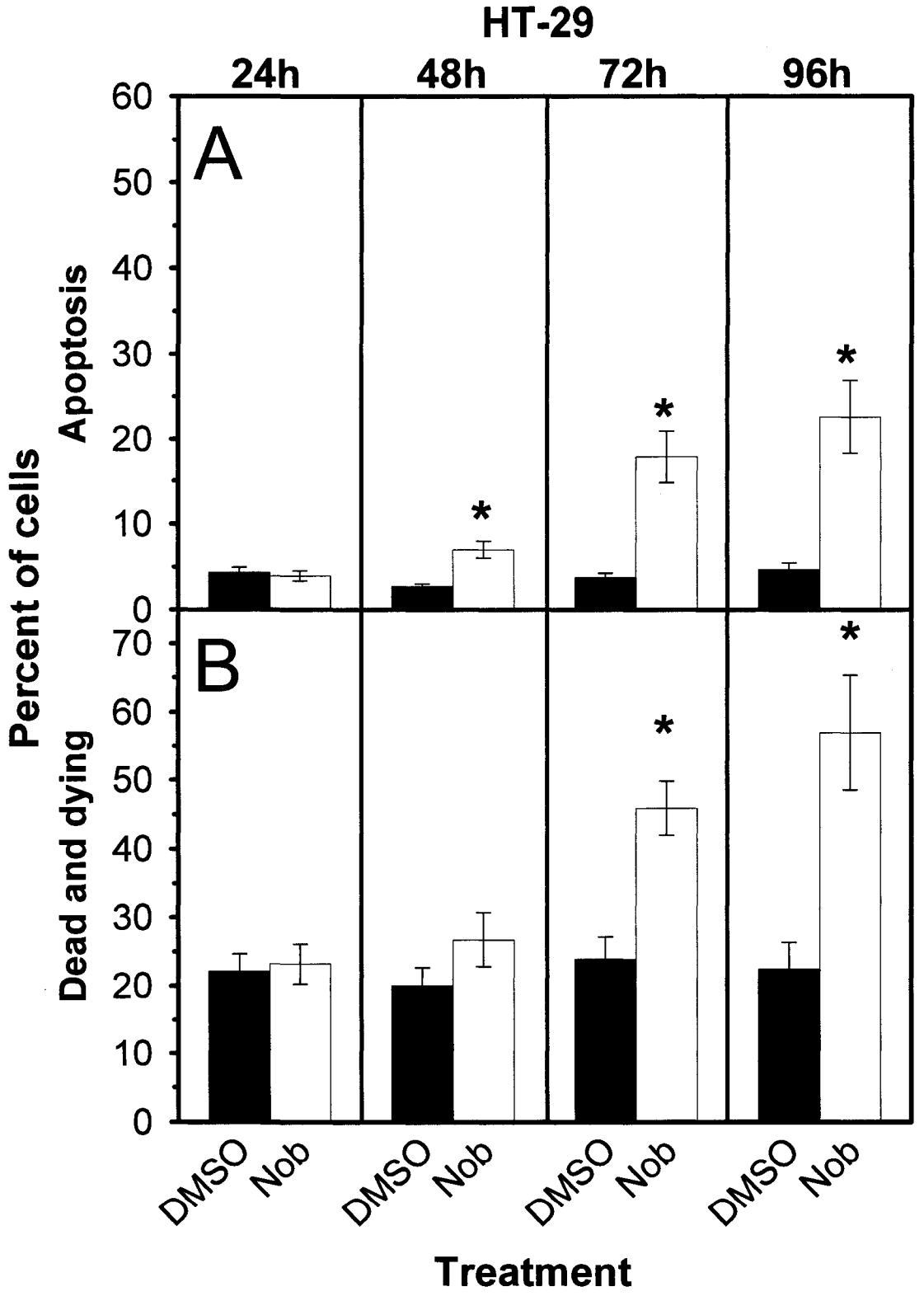
HT-29
24h
48h
72h
96h
A
B
Apoptosis
Dead and dying
Percent of cells
0
10
20
30
40
50
60
70
*
DMSO
Nob
Treatment

for MDA-MB-435 cells, apoptosis appeared later at 72 h continuing to 96 h (Figure 19, panel A). The timing of significant increases in dead and dying populations for the three cell lines was the reverse of apoptosis; total cell death in MCF-7 and HT-29 cells was not significant until 72 h continuing to 96 h, whereas in MDA-MB-435 cells, it was significant from 48 h onwards. Additionally in MCF-7 cells, total cell death in nobiletin-treated cells was significantly decreased at 24 h compared to vehicle control.

3.3. Molecular effects mediating inhibition of proliferation

3.3.1. Analysis of expression of cell cycle and apoptosis regulatory genes by semi-quantitative RT-PCR.

Tangeretin and nobiletin mediate inhibition of proliferation of MDA-MB-435, MCF-7 and HT-29 cells through the accumulation of cells in G1. At higher concentrations of nobiletin (200 μM), apoptosis and cell death were associated with that inhibition, while lower concentrations (60 μM) inhibited proliferation without the involvement of cell death. To investigate the molecular basis of these cell cycle and apoptosis effects, cell cycle (G1-specific) and apoptosis regulatory genes cyclin D1, D2, and D3, cyclin E1, and E2, p21, p27, cdk2, cdk4, cdk6, A20 and Bcl-2 were selected for analysis of increased or decreased levels of mRNA in response to treatment with tangeretin or nobiletin. Genes were selected based on involvement in regulation of G1 progression and apoptosis. Expression was measured in all three cell lines by semi-quantitative RT-PCR at an early time point (6 h) and later (24 or 48 h) when G1 accumulation had occurred. Expression changes (significantly increased or decreased) were observed for five genes in total: cyclin E2, cyclin D2, cdk4, cdk6 and A20 (Table 8). Changes were largely specific to cell lines or flavonoids. In MDA-MB-435 cells, expression of A20 was increased at 24 h in tangeretin-treated cells, and expression of Cdk4 and A20 was increased and Cdk6 was decreased at 6 h in nobiletin-treated cells. In MCF-7 cells, tangeretin increased expression of cyclin D2 at both time points and Cdk4 at 24 h; nobiletin increased Cdk4 expression at 6 h. In HT-29 cells,

Table 8. Expression of cell cycle and apoptosis regulatory genes by semi-quantitative RT-PCR for tangeretin- and nobiletin-treated MDA-MB-435, MCF-7 and HT-29 cells. Cells were treated for 6 h (all cell lines) and 24 h (MDA-MB-435 and MCF-7) or 48 h (HT-29) with tangeretin (54 μM), nobiletin (MDA-MB-435: 100 μM, MCF-7 and HT-29: 60 μM) or DMSO control. Total RNA was isolated, reverse transcribed, and amplified as described in *Materials and Methods*. Gene expression in all samples was normalized to GAPDH expression and normalized values for treated samples were expressed as a ratio of control. The data shown were combined from two independent experiments and are presented as significantly up or down, or unchanged compared to vehicle control. **up**: increased expression, **down**: decreased expression, –: no change in expression

		MDA-MB-435		MCF-7		HT-29	
Gene	***Flavonoid***	***6h***	***24h***	***6h***	***24h***	***6h***	***48h***
CCNE2	Tangeretin	–	–	–	–	–	–
	Nobiletin	–	–	–	–	–	up
CCND2	Tangeretin	–	–	up	up	–	–
	Nobiletin	–	–	–	–	–	–
Cdk4	Tangeretin	–	–	–	up	–	up
	Nobiletin	up	–	up	–	–	up
Cdk6	Tangeretin	–	–	–	–	–	–
	Nobiletin	down	–	–	–	–	–
A20	Tangeretin	–	up	–	–	up	up
	Nobiletin	up	–	–	–	–	–

tangeretin increased A20 expression at both time points and Cdk4 at 48 h; nobiletin increased cyclin E2 and Cdk4 expression at 48 h. The only change common across cell lines was the upregulation of Cdk4 by nobiletin in all three cell lines. It was also upregulated by tangeretin in two of three cell lines.

3.3.2. Global analysis of gene expression by microarray analysis

Selection of genes for semi-quantitative RT-PCR analysis of mRNA expression was based on the observation that tangeretin and nobiletin affected cell cycle and apoptosis, and specifically focused on genes involved in those processes. Microarray analysis allows the assessment of expression of a large number of genes, without prejudice, including those involved in cell cycle and apoptosis among multiple other physiological processes and pathways. The expression of over 22,000 genes was assessed in MDA-MB-435 cells following short-term exposure (6 h) to tangeretin using Affymetrix oligonucleotide arrays.

Array analysis was performed on RNA obtained from three separate experiments. Tangeretin changed the expression of 1,405 genes (Table 27, Appendix I), including 506 that were significantly upregulated, and 899 that were significantly downregulated. Biological process gene lists were compiled from the Affymetrix NetAffx™ website (http://www.affymetrix.com/analysis/index.affx) and used to query the list of genes significantly changed by tangeretin in GeneSpring GX 7.3. The NetAffx™ Analysis Center contains an annotated database of Affymetrix GeneChip genes which can be searched for genes involved in specific biological events. Candidate biological processes of potential importance in mediating the antiproliferative effect of tangeretin were growth, proliferation, cell cycle, apoptosis, signal transduction, transcription, and stress. Table 9 summarizes the numbers of genes increased or decreased in each biological process category and full gene lists for these processes are presented in Tables 10-16.

Querying the list of significantly changed for cell cycle related genes identified 95 genes whose expression was changed by tangeretin (Table 12). Of those genes, 19 were increased in expression and 76 decreased in expression. Among

Table 9. Biological process categorisation of tangeretin-responsive genes in MDA-MB-435 cells. Cells were treated for 6 h with tangeretin (54 μM) or DMSO control. RNA was isolated and human Affymetrix arrays (HGU133A) were used to assess gene expression. GeneSpring GX 7.3 data mining software was used to obtain and categorise lists of genes that were significantly up- or downregulated following short-term tangeretin treatment as described in *Materials and Methods.* Numbers of genes in each biological process category are shown in the table.

Biological process	*Number of genes*		
	Increased	**Decreased**	**Total**
cell growth	5	15	20
proliferation	11	41	52
cell cycle	19	76	95
apoptosis	8	59	67
signal transduction	62	96	156
transcription	3	19	22
stress	4	4	9

Table 10. Cell growth related genes significantly changed in tangeretin-treated MDA-MB-435 cells. Cells were treated for 6 h with tangeretin (54 μM) or DMSO control. RNA was isolated and human Affymetrix arrays (HGU133A) were used to assess gene expression as described in *Materials and Methods*. Gene expression of treated and control samples were normalized to control using GeneSpring GX 7.3 data mining software, and normalized values for treated samples were expressed as a ratio of control ± SEM. Ratios higher than 1 are upregulated, ratios below 1 are downregulated. Statistical analysis operations in GeneSpring was used to obtain lists of genes that were significantly up- or downregulated (one-way ANOVA, $P \leq 0.05$). These lists were cross-referenced to cell growth gene lists obtained from NetAffx to yield cell growth-related genes modulated by tangeretin. The data shown were combined from three independent experiments. The data shown were combined from three independent experiments.

Common ID	Gene name	Ratio to control	SEM
TAO1	thousand and one amino acid protein kinase	1.43	0.15
APBB2	FE65-like protein	1.41	0.09
SOCS2	suppressor of cytokine signaling-2	1.29	0.07
NEDD9	neural precursor cell expressed, developmentally down-regulated 9	1.29	0.05
SLC3A2	solute carrier family 3, 2	1.28	0.05
PPP2CB	protein phosphatase 2, catalytic subunit, β	0.88	0.02
C20orf20	MRG-binding protein	0.81	0.02
NET1	neuroepithelial cell transforming gene 1	0.79	0.03
LOC90410		0.79	0.03
OGFR	opioid growth factor receptor	0.79	0.04
PPP2CA	protein phosphatase 2, catalytic subunit, α	0.77	0.02
MORF4	mortality factor 4	0.76	0.05
CSNK2A1	casein kinase 2, alpha 1 polypeptide	0.74	0.05
GAS41	glioma-amplified sequence-41	0.73	0.02
PML	promyelocytic leukemia protein	0.71	0.05
PPP2R1B	protein phosphatase 2, regulatory subunit A, β	0.71	0.04
MORF4L1	MORF-related gene 15	0.70	0.02
PC-LKC	protocadherin LKC precursor	0.60	0.07
PML	promyelocytic leukemia protein	0.56	0.08
IGFBP5	insulin-like growth factor binding protein 5	0.34	0.09

Table 11. Proliferation related genes significantly changed in tangeretin-treated MDA-MB-435 cells. Cells were treated for 6 h with tangeretin (54 μM) or DMSO control. RNA was isolated and human Affymetrix arrays (HGU133A) were used to assess gene expression as described in *Materials and Methods*. Gene expression of treated and control samples were normalized to control using GeneSpring GX 7.3 data mining software, and normalized values for treated samples were expressed as a ratio of control ± SEM. Ratios higher than 1 are upregulated, ratios below 1 are downregulated. Statistical analysis operations in GeneSpring was used to obtain lists of genes that were significantly up- or downregulated (one-way ANOVA, $P \leq 0.05$). These lists were cross-referenced to proliferation gene lists obtained from NetAffx to yield proliferation-related genes modulated by tangeretin. The data shown were combined from three independent experiments.

Common ID	Gene name	Ratio to control	SEM
MYC	v-myc myelocytomatosis viral oncogene	1.71	0.12
CHRNA10	cholinergic receptor, nicotinic, α polypeptide 10	1.58	0.06
ERBB4	v-erb-a erythroblastic leukemia viral oncogene, 4	1.55	0.06
MET	met proto-oncogene	1.51	0.09
TCFL5	transcription factor-like 5 protein	1.45	0.05
PSPH		1.42	0.10
MET	met proto-oncogene	1.40	0.07
MET	tpr-met fusion protein	1.37	0.11
HGS	hepatocyte growth factor-regulated tyrosine kinase substrate	1.32	0.02
FLJ21148	hypothetical protein FLJ21148	1.23	0.06
LAMC1	laminin, gamma 1 precursor	1.17	0.01
ZFP36L2	butyrate response factor 2	0.90	0.01
S100A11	S100 calcium binding protein A11	0.89	0.02
PTEN	phosphatase and tensin	0.86	0.03
UBE2C	ubiquitin-conjugating enzyme E2C	0.85	0.02
CDK7	cyclin-dependent kinase 7	0.85	0.01
ILK	integrin-linked kinase	0.83	0.03
CDC2L5	cell division cycle 2-like 5	0.83	0.03
CUL3	cullin 3	0.81	0.04
DNAJA2	DnaJ (Hsp40) homolog, subfamily A, 2	0.81	0.03
CDKN3	cyclin-dependent kinase inhibitor 3	0.81	0.03
CDKN1B	cyclin-dependent kinase inhibitor 1B	0.80	0.02
EPHB4	ephrin receptor EphB4 precursor	0.80	0.03
TGFBR2	TGF-betaIIR α	0.80	0.02
PPAP2A	phosphatidic acid phosphatase type 2A	0.80	0.01
PA2G4	proliferation-associated 2G4	0.80	0.01
H41	hypothetical protein H41	0.78	0.02
CUL2	cullin 2	0.78	0.04
DKC1	dyskerin	0.77	0.02
TOB1	transducer of ERBB2, 1	0.77	0.05
EEF1E1	eukaryotic translation elongation factor 1, ε 1	0.77	0.03
CTBP2	zinc finger, RAN-binding domain containing 1	0.77	0.03
CUL3	cullin 3	0.76	0.02
DLG7	discs large homolog 7	0.76	0.04
	similar to Patched protein	0.76	0.05
NBS1	2,4-dienoyl CoA reductase 1 precursor	0.76	0.04
PRKRIR	protein-kinase, interferon-inducible RNA dependent inhibitor, repressor	0.76	0.02
ZFP36L2	butyrate response factor 2	0.75	0.06
H41	hypothetical protein H41	0.75	0.05

Common ID	Gene name	Ratio to control	SEM
CSNK2A1	casein kinase 2, α 1 polypeptide	0.74	0.05
	CDNA FLJ12521 fis, clone NT2RM2001840	0.73	0.03
IL6R	interleukin 6 receptor	0.70	0.04
THY1	Thy-1 cell surface antigen	0.69	0.05
BUB3	budding uninhibited by benzimidazoles 3	0.69	0.06
CDKN2D	cyclin-dependent kinase inhibitor 2D	0.68	0.06
SKP2	S-phase kinase-associated protein 2 (p45)	0.67	0.06
	IMAGE:3085853	0.64	0.02
SKP2	S-phase kinase-associated protein 2	0.63	0.06
TIEG	TGFB inducible early growth response	0.61	0.03
GFER	erv1-like growth factor	0.59	0.04
INSIG1	insulin induced gene 1	0.58	0.03
PURA	purine-rich element binding protein A	0.58	0.07

Table 12. Cell cycle related genes significantly changed in tangeretin-treated MDA-MB-435 cells. Cells were treated for 6 h with tangeretin (54 μM) or DMSO control. RNA was isolated and human Affymetrix arrays (HGU133A) were used to assess gene expression as described in *Materials and Methods*. Gene expression of treated and control samples were normalized to control using GeneSpring GX 7.3 data mining software, and normalized values for treated samples were expressed as a ratio of control ± SEM. Ratios higher than 1 are upregulated, ratios below 1 are downregulated. Statistical analysis operations in GeneSpring was used to obtain lists of genes that were significantly up- or downregulated (one-way ANOVA, $P \leq 0.05$). These lists were cross-referenced to cell cycle gene lists obtained from NetAffx to yield cell cycle-related genes modulated by tangeretin. The data shown were combined from three independent experiments.

Common ID	Gene name	Ratio to control	SEM
CCNL2	cyclin L2	1.72	0.07
MYC	v-myc myelocytomatosis viral oncogene	1.71	0.12
MUTYH	mutY homolog	1.59	0.02
PMS1	postmeiotic segregation increased 1	1.53	0.08
INHA	inhibin alpha subunit precursor	1.49	0.09
PARC	p53-associated parkin-like cytoplasmic protein	1.48	0.06
DUSP1	dual specificity phosphatase 1	1.45	0.15
APBB2	FE65-like protein	1.41	0.09
CCNT2	cyclin T2	1.37	0.02
RAD17	RAD17 homolog isoform 1,2,4	1.32	0.05
NEDD9	neural precursor cell expressed, developmentally down-regulated 9	1.29	0.05
DDX11	Similar to DEAD/H box polypeptide 11	1.28	0.06
BRCA2	breast cancer 2, early onset	1.26	0.05
HDAC6	histone deacetylase 6	1.24	0.08
BPAG1	bullous pemphigoid antigen 1	1.20	0.01
ATR	ataxia telangiectasia and Rad3 related protein	1.20	0.04
GPR21	RAB GTPase activating protein 1	1.18	0.04
PLCB1	phospholipase C, beta 1	1.18	0.01
RAD17	RAD17 homolog isoform 1,2,3,4	1.05	0.01
TCF7L2	transcription factor 7-like 2	0.93	0.02
RBBP6	retinoblastoma-binding protein 6 isoform 1,2,3	0.92	0.02
JAK2	Janus kinase 2	0.90	0.02
SMC4L1	structural maintenance of chromosomes 4-like 1	0.89	0.01
	nuclear transcription factor Y, gamma	0.88	0.03
PPP2CB	protein phosphatase 2, catalytic subunit, β	0.88	0.02
ZWINT	ZW10 interactor	0.88	0.03
NRAS	neuroblastoma RAS viral oncogene homolog	0.88	0.02
CHC1	chromosome condensation 1	0.87	0.02
PTEN	phosphatase and tensin homolog	0.86	0.03
BRMS1	breast cancer metastasis suppressor 1	0.86	0.02
CTCF	CCCTC-binding factor	0.86	0.02
DDX11	DEAD/H box polypeptide 11	0.85	0.00
UBE2C	ubiquitin-conjugating enzyme E2C	0.85	0.02
CDK7	cyclin-dependent kinase 7	0.85	0.01
SART1	squamous cell carcinoma antigen recognized by T cells 1	0.84	0.02
NFYC	nuclear transcription factor Y, γ	0.84	0.04
FH	fumarate hydratase	0.84	0.02
NFYC	nuclear transcription factor Y, γ	0.84	0.02
DLP	Dim1-like protein	0.84	0.05
TFDP2	transcription factor Dp-2	0.83	0.03

Common ID	Gene name	Ratio to control	SEM
STAG2	stromal antigen 2	0.83	0.01
PTMA		0.82	0.04
EIF4G2	eukaryotic translation initiation factor 4 γ, 2	0.82	0.03
NUDC	nuclear distribution gene C homolog	0.81	0.03
CUL3	cullin 3	0.81	0.04
PTMA	prothymosin alpha	0.81	0.04
DNAJA2	DnaJ (Hsp40) homolog, subfamily A, 2	0.81	0.03
CDKN3	cyclin-dependent kinase inhibitor 3	0.81	0.03
CDKN1B	cyclin-dependent kinase inhibitor 1B	0.80	0.02
KPNA2	karyopherin alpha 2	0.80	0.04
PA2G4	proliferation-associated 2G4	0.80	0.01
MAD2L1	MAD2-like 1	0.79	0.03
H2AFX	H2A histone family, member X	0.79	0.03
GAK	cyclin G associated kinase	0.79	0.03
SPIN	spindlin	0.78	0.03
KRAS2	Kirsten rat sarcoma 2 viral oncogene homolog	0.78	0.04
CCNB1	cyclin B1	0.78	0.03
CDC34	cell division cycle 34	0.78	0.03
CUL2	cullin 2	0.78	0.04
DKC1	dyskerin	0.77	0.02
RHOB	ras homolog gene family, B	0.77	0.02
GAS7	growth arrest-specific 7	0.77	0.02
PLK4	protein-serine/threonine kinase	0.77	0.03
PPP2CA	protein phosphatase 2, catalytic subunit, α	0.77	0.02
EEF1E1	eukaryotic translation elongation factor 1 ε 1	0.77	0.03
CUL3	cullin 3	0.76	0.02
DLG7	discs large homolog 7	0.76	0.04
	similar to Patched protein	0.76	0.05
NBS1	2,4-dienoyl CoA reductase 1 precursor	0.76	0.04
GTSE1	G-2 and S-phase expressed 1	0.75	0.05
GAS2L1	growth arrest-specific 2 like 1	0.75	0.01
CDC20	cell division cycle 20	0.75	0.04
CENPE	centromere protein E	0.74	0.05
GAS7	growth arrest-specific 7	0.74	0.04
GTSE1	G-2 and S-phase expressed 1	0.74	0.02
STK6	serine/threonine protein kinase 6	0.73	0.05
GMNN	geminin	0.73	0.04
CSPG6	chondroitin sulfate proteoglycan 6	0.72	0.04
KNTC2	kinetochore associated 2	0.71	0.02
ASPM	abnormal spindle-like, microcephaly associated	0.71	0.01
PML	promyelocytic leukemia protein	0.71	0.05
PPP2R1B	protein phosphatase 2, regulatory subunit A, β	0.71	0.04
HSPC132	HSPC132	0.69	0.01

Common ID	Gene name	Ratio to control	SEM
ATF5	activating transcription factor 5	0.68	0.02
CDKN2D	cyclin-dependent kinase inhibitor 2D	0.68	0.06
SKP2	S-phase kinase-associated protein 2 (p45)	0.67	0.06
CCNE2	cyclin E2	0.65	0.06
CCNE1	cyclin E1	0.65	0.03
SKP2	S-phase kinase-associated protein 2	0.63	0.06
FLJ23311	FLJ23311 protein	0.61	0.05
CDK8	cyclin-dependent kinase 8	0.61	0.02
PML	promyelocytic leukemia protein	0.56	0.08
CCNE2	cyclin E2	0.46	0.02
JAK2	Janus kinase 2	0.43	0.04
DUSP6	dual specificity phosphatase 6	0.34	0.00

Table 13. Apoptosis related genes significantly changed in tangeretin-treated MDA-MB-435 cells. Cells were treated for 6 h with tangeretin (54 μM) or DMSO control. RNA was isolated and human Affymetrix arrays (HGU133A) were used to assess gene expression as described in *Materials and Methods*. Gene expression of treated and control samples were normalized to control using GeneSpring GX 7.3 data mining software, and normalized values for treated samples were expressed as a ratio of control ± SEM. Ratios higher than 1 are upregulated, ratios below 1 are downregulated. Statistical analysis operations in GeneSpring was used to obtain lists of genes that were significantly up- or downregulated (one-way ANOVA, $P \leq 0.05$). These lists were cross-referenced to apoptosis gene lists obtained from NetAffx to yield apoptosis-related genes modulated by tangeretin. The data shown were combined from three independent experiments.

Common ID	Gene Name	Ratio to control	SEM
TNFAIP3	tumor necrosis factor, alpha-induced protein 3	2.88	0.28
TNFAIP3	tumor necrosis factor, alpha-induced protein 3	1.52	0.03
INHA	inhibin alpha subunit precursor	1.49	0.09
TAO1	thousand and one amino acid protein kinase	1.43	0.15
SOCS2	suppressor of cytokine signaling-2	1.29	0.07
PPM1F	protein phosphatase 1F	1.28	0.05
TNFRSF6B	tumor necrosis factor receptor superfamily, 6b	1.24	0.06
ANXA4	annexin IV	1.14	0.04
RTN4	reticulon 4	0.90	0.02
APG5L	APG5 autophagy 5-like	0.89	0.02
	Rho-assoc., coiled-coil cont. protein kinase 1	0.89	0.02
SH3GLB1	SH3-containing protein SH3GLB1	0.88	0.03
VCP	valosin-containing protein	0.88	0.02
PPP2CB	protein phosphatase 2, catalytic subunit, β	0.88	0.02
PDCL3	phosducin-like 3	0.87	0.02
FOXO3A	forkhead box O3A	0.87	0.03
PTEN	phosphatase and tensin homolog	0.86	0.03
SH3GLB1	SH3-containing protein SH3GLB1	0.86	0.01
HMGB1	high-mobility group box 1	0.86	0.02
PRDX2	peroxiredoxin 2	0.86	0.03
DPF2	D4, zinc and double PHD fingers family 2	0.85	0.05
MST4	serine/threonine protein kinase MASK	0.85	0.02
SART1	squamous cell carcinoma antigen recognized by T cells 1	0.84	0.02
BCL2L2	BCL2-like 2 protein	0.84	0.02
RYBP	RING1 and YY1 binding protein	0.84	0.03
NME6	nucleoside diphosphate kinase type 6	0.82	0.04
CUL3	cullin 3	0.81	0.04
APG5L	autophagy 5-like	0.80	0.00
BAD	BCL2-antagonist of cell death protein	0.79	0.02
PHLDA1	pleckstrin homology-like domain, family A, 1	0.78	0.03
CUL2	cullin 2	0.78	0.04
RHOB	ras homolog gene family, member B	0.77	0.02
PPP2CA	protein phosphatase 2, catalytic subunit, α	0.77	0.02
EEF1E1	eukaryotic translation elongation factor 1 ε 1	0.77	0.03
CUL3	cullin 3	0.76	0.02
HMGB1	similar to HMG-1	0.76	0.01
SMNDC1	survival motor neuron domain containing 1	0.76	0.05
SON	SON DNA binding protein	0.75	0.02
CGI-94	comparative gene identification protein	0.75	0.03
TRAF4	TNF receptor-associated factor 4 isoform 1,2	0.74	0.07
SON	SON DNA binding protein	0.73	0.03

Common ID	Gene Name	Ratio to control	SEM
MALT1	mucosa associated lymphoid tissue protein 1	0.73	0.06
	CDNA FLJ12521 fis, clone NT2RM2001840	0.73	0.03
TNFAIP8	tumor necrosis factor, alpha-induced protein 8	0.72	0.06
CASP2	caspase 2	0.72	0.06
BAK1	BCL2-antagonist/killer 1	0.72	0.03
PML	promyelocytic leukemia protein	0.71	0.05
PPP2R1B	protein phosphatase 2, regulatory subunit A, β	0.71	0.04
PHLDA1	pleckstrin homology-like domain, family A, 1	0.71	0.07
SIVA	CD27-binding (Siva) protein isoform 1,2	0.71	0.05
HSPC132	HSPC132	0.69	0.01
THY1	Thy-1 cell surface antigen	0.69	0.05
	CDNA FLJ43274 fis, clone KIDNE2008914	0.68	0.07
SIVA	CD27-binding (Siva) protein isoform 1,2	0.68	0.06
CFLAR	CASP8 and FADD-like apoptosis regulator	0.67	0.02
BAG2	BCL2-associated athanogene 2	0.66	0.02
CASP6	caspase 6	0.65	0.05
APG12L	autophagy 12-like	0.65	0.02
	UI-H-BI4-aor-d-03-0-UI.s1 NCI_CGAP_Sub8	0.64	0.02
TNFRSF6	tumor necrosis factor receptor superfamily, 6	0.63	0.01
CASP6	caspase 6	0.63	0.07
PURA	purine-rich element binding protein A	0.58	0.07
PML	promyelocytic leukemia protein	0.56	0.08
APAF1	apoptotic protease activating factor	0.55	0.03
IER3	immediate early response 3	0.53	0.04
TNFAIP8	tumor necrosis factor, alpha-induced protein 8	0.53	0.05
HSPA1A	heat shock 70kDa protein 1A	0.51	0.04

Table 14. Signal transduction related genes significantly changed in tangeretin-treated MDA-MB-435 cells. Cells were treated for 6 h with tangeretin (54 μM) or DMSO control. RNA was isolated and human Affymetrix arrays (HGU133A) were used to assess gene expression as described in *Materials and Methods*. Gene expression of treated and control samples were normalized to control using GeneSpring GX 7.3 data mining software, and normalized values for treated samples were expressed as a ratio of control ± SEM. Ratios higher than 1 are upregulated, ratios below 1 are downregulated. Statistical analysis operations in GeneSpring was used to obtain lists of genes that were significantly up- or downregulated (one-way ANOVA, $P \leq 0.05$). These lists were cross-referenced to signal transduction gene lists obtained from NetAffx to yield signal transduction-related genes modulated by tangeretin. The data shown were combined from three independent experiments.

Common ID	Gene name	Ratio to control	SEM
CREM	cAMP responsive element modulator	3.36	0.58
NR4A2	nuclear receptor subfamily 4, group A, 2	2.94	0.15
CREM	cAMP responsive element modulator	2.34	0.51
GEM	GTP-binding mitogen-induced T-cell protein	2.17	0.23
SH3BP5	SH3-domain binding protein 5	1.95	0.12
NR4A2	nuclear receptor subfamily 4, group A, 2	1.91	0.18
OGT	O-linked GlcNAc transferase	1.86	0.19
TANK	TRAF interacting protein TANK	1.84	0.07
NR4A2	nuclear receptor subfamily 4, group A, 2	1.83	0.27
GDF15	growth differentiation factor 15	1.82	0.15
RAI3	retinoic acid induced 3	1.76	0.16
ITPR1	inositol 1,4,5-triphosphate receptor, type 1	1.73	0.16
TANK	TRAF interacting protein TANK	1.72	0.09
LTB4R	leukotriene B4 receptor	1.70	0.13
RPS6KA2	ribosomal protein S6 kinase, 2	1.69	0.07
OR12D2	olfactory receptor, family 12, subfamily D, 2	1.64	0.08
PLD1	phospholipase D1, phophatidylcholine-specific	1.63	0.15
OPN3	opsin 3 (encephalopsin, panopsin)	1.61	0.06
DSCR1	Down syndrome critical region gene 1	1.61	0.12
ERBB4	v-erb-a erythroblastic leukemia viral oncogene, 4	1.55	0.06
PDE4D	cAMP-specific phosphodiesterase 4D	1.53	0.12
CREM	cAMP responsive element modulator	1.51	0.18
MET	met proto-oncogene	1.51	0.09
HRMT1L1		1.49	0.11
INHA	inhibin alpha subunit precursor	1.49	0.09
CELSR3	cadherin EGF LAG seven-pass G-type receptor 3	1.48	0.06
NICAL	NEDD9 interacting protein with calponin homology	1.47	0.04
OGT	O-linked GlcNAc transferase	1.45	0.07
GPR126		1.45	0.06
PLD1	phospholipase D1, phophatidylcholine-specific	1.45	0.13
AKAP9	A-kinase anchor protein 9	1.44	0.14
APBB2	FE65-like protein	1.41	0.09
MGC10731	hypothetical protein MGC10731	1.41	0.07
MET	met proto-oncogene	1.40	0.07
MET	tpr-met fusion protein	1.37	0.11
DDR2	discoidin domain receptor family, 2	1.36	0.06
SH3BP5	SH3-domain binding protein 5	1.35	0.11
PDE4D	phosphodiesterase 4D, cAMP-specific	1.35	0.08
RABL2B	RAB, member of RAS oncogene family-like 2B	1.33	0.04

Common ID	Gene name	Ratio to control	SEM
CNR2	cannabinoid receptor 2	1.33	0.04
HGS	HGF-regulated tyrosine kinase substrate	1.32	0.02
DVL3	dishevelled 3	1.32	0.06
ST7	suppression of tumorigenicity	1.31	0.09
SOCS2	suppressor of cytokine signaling-2	1.29	0.07
NEDD9	neural precursor cell expressed, developmentally down-regulated 9	1.29	0.05
CEACAM6		1.28	0.05
ITPK1	inositol 1,3,4-triphosphate 5/6 kinase	1.27	0.02
DSCR1	Down syndrome critical region gene 1	1.27	0.06
RAB5B	RAB5B, member RAS oncogene family	1.26	0.07
LGALS3BP	galectin 3 binding protein	1.25	0.05
SPG7	spastic paraplegia 7	1.24	0.04
PDE8A	phosphodiesterase 8A	1.24	0.03
FLJ21148	hypothetical protein FLJ21148	1.23	0.06
PDE8A	phosphodiesterase 8A	1.22	0.04
IQGAP1	IQ motif cont. GTPase activating protein 1	1.21	0.05
IGF2R	insulin-like growth factor 2 receptor	1.21	0.01
GOLGA5	Golgi autoantigen, golgin subfamily a, 5	1.20	0.03
PLCB1	phospholipase C, β1 (phosphoinositide-specific)	1.18	0.01
ITPR3	inositol 1,4,5-triphosphate receptor, type 3	1.18	0.02
ANXA4	annexin IV	1.14	0.04
TRRAP		1.12	0.03
GNG7	guanine nucleotide binding protein, γ 7	1.11	0.03
TCF7L2	transcription factor 7-like 2 (T-cell specific, HMG-box)	0.93	0.02
MAP2K4	mitogen-activated protein kinase kinase 4	0.93	0.01
GNB1	guanine nucleotide-binding protein, β-1	0.91	0.02
GNB2	guanine nucleotide-binding protein, β-2	0.91	0.01
ARF6	ADP-ribosylation factor 6	0.89	0.01
CRKL	v-crk sarcoma virus CT10 oncogene homolog	0.89	0.02
GNAS	guanine nucleotide binding protein, α stimulating	0.89	0.02
	Rho-associated, coiled-coil containing protein kinase 1	0.89	0.02
FGD1	faciogenital dysplasia protein	0.89	0.01
CSNK1A1	casein kinase 1, α 1	0.89	0.02
S100A11	S100 calcium binding protein A11	0.89	0.02
PPP2R2A	protein phosphatase 2, regulatory subunit, α	0.88	0.02
NRAS	neuroblastoma RAS viral oncogene homolog	0.88	0.02
GNA11	guanine nucleotide binding protein, β 11	0.87	0.03
AKAP8	A-kinase anchor protein 8	0.86	0.04

Common ID	Gene name	Ratio to control	SEM
HMGB1	high-mobility group box 1	0.86	0.02
NCOA3	nuclear receptor coactivator 3	0.85	0.02
CSNK1A1	casein kinase 1, α 1	0.85	0.02
RAB14	RAB14, member RAS oncogene family	0.85	0.03
SPRY2	sprouty 2	0.84	0.03
GRB2	growth factor receptor-bound protein 2	0.83	0.04
OSTF1	osteoclast stimulating factor 1	0.83	0.04
SMAD2	MAD, mothers against decapentaplegic, 2	0.83	0.01
ADORA2B	adenosine A2b receptor	0.82	0.02
MAPK14	MAP kinase	0.82	0.02
RARB	retinoic acid receptor, β	0.82	0.04
	CDNA FLJ38130 fis, clone D6OST2000464	0.82	0.03
CSNK1D	casein kinase 1, δ	0.82	0.04
PPP2R5E	protein phosphatase 2A, regulatory subunit, ε	0.81	0.01
NR2F2	nuclear receptor subfamily 2, group F, 2	0.80	0.02
CREBBP	CREB binding protein	0.80	0.01
CD97	CD97 antigen	0.80	0.01
IFNGR2	interferon gamma receptor 2	0.80	0.01
NET1	neuroepithelial cell transforming gene 1	0.79	0.03
RAB23	Ras-related protein Rab-23	0.79	0.03
GNAI3	guanine nucleotide binding protein, α inhibiting, 3	0.79	0.02
KRAS2	Kirsten rat sarcoma 2 viral oncogene homolog	0.78	0.04
RYK	RYK receptor-like tyrosine kinase precursor	0.78	0.03
DKFZP434E2135		0.78	0.02
RHOB	ras homolog gene family, B	0.77	0.02
RAB5A	RAB5A, member RAS oncogene family	0.77	0.02
FGF13	fibroblast growth factor 13	0.77	0.04
EEF1E1	eukaryotic translation elongation factor 1 ε 1	0.77	0.03
ARHGEF12	Rho guanine nucleotide exchange factor 12	0.77	0.03
RIN3	Ras and Rab interactor 3	0.77	0.04
RAP1B	RAP1B, member of RAS oncogene family	0.76	0.03
SHOC2	soc-2 suppressor of clear homolog	0.76	0.02
PRKACB	protein kinase, cAMP-dependent, catalytic, β	0.76	0.03
HMGB1	similar to nonhistone chromosomal protein HMG-1	0.76	0.01
	similar to Patched protein	0.76	0.05
NBS1	2,4-dienoyl CoA reductase 1 precursor	0.76	0.04
VDR	vitamin D (1,25- dihydroxyvitamin D3) receptor	0.76	0.02
PRKRIR	protein-kinase, interferon-inducible RNA dependent inhibitor, repressor	0.76	0.02
RAB8A	mel transforming oncogene	0.76	0.01
GTSE1	G-2 and S-phase expressed 1	0.75	0.05

Common ID	Gene name	Ratio to control	SEM
RAB35	RAB35, member RAS oncogene family	0.75	0.05
CD2AP	CD2-associated protein	0.75	0.02
PDCL	phosducin-like	0.75	0.04
ANGPT1	angiopoietin 1	0.75	0.06
RPS6KA1	ribosomal protein S6 kinase, 1	0.74	0.05
ITSN1	intersectin 1 (SH3 domain protein)	0.74	0.05
RAP2C	RAP2C, member of RAS oncogene family	0.74	0.03
RAP2C	RAP2C, member of RAS oncogene family	0.74	0.04
GTSE1	G-2 and S-phase expressed 1	0.74	0.02
TRAF4	TNF receptor-associated factor 4	0.74	0.07
RAB22A	RAS-related protein RAB-22A	0.73	0.05
TUBB4	tubulin, beta, 4	0.73	0.03
	CDNA FLJ12521 fis, clone NT2RM2001840	0.73	0.03
TIAM1	T-cell lymphoma invasion and metastasis 1	0.73	0.05
CSPG6	chondroitin sulfate proteoglycan 6	0.72	0.04
TLE3	transducin-like enhancer of split 3	0.72	0.04
PML	promyelocytic leukemia protein	0.71	0.05
NCOA1	nuclear receptor coactivator 1	0.71	0.03
IL6R	interleukin 6 receptor	0.70	0.04
RAGE	renal tumor antigen	0.70	0.06
RAB14	ras-related protein rab-14	0.70	0.03
GNAI3	guanine nucleotide binding protein, α inhibiting, 3	0.69	0.03
TLR1	toll-like receptor 1	0.69	0.02
HSPC132	HSPC132	0.69	0.01
PRKCD	protein kinase C, δ	0.67	0.05
ADM	adrenomedullin	0.67	0.03
VDR	vitamin D (1,25- dihydroxyvitamin D3) receptor	0.65	0.06
RIT1	Ras-like without CAAX 1	0.65	0.03
	IMAGE:3085853	0.64	0.02
TNFRSF6	tumor necrosis factor receptor superfamily, 6	0.63	0.01
AKAP13	Rho GTPase-specific GTP exchange factor	0.61	0.04
FZD7	frizzled 7	0.61	0.05
ROCK2	Rho-associated, coiled-coil containing protein kinase 2	0.61	0.02
ARHGEF3	Rho guanine nucleotide exchange factor 3	0.61	0.03
ARF6	ADP-ribosylation factor 6	0.60	0.02
C12orf2	chromosome 12 open reading frame 2	0.59	0.07
PML	promyelocytic leukemia protein	0.56	0.08
NR2F1	nuclear receptor subfamily 2, group F, 1	0.48	0.04
IGFBP5	insulin-like growth factor binding protein 5	0.34	0.09

Table 15. Transcription related genes significantly changed in tangeretin-treated MDA-MB-435 cells. Cells were treated for 6 h with tangeretin (54 μM) or DMSO control. RNA was isolated and human Affymetrix arrays (HGU133A) were used to assess gene expression as described in *Materials and Methods*. Gene expression of treated and control samples were normalized to control using GeneSpring GX 7.3 data mining software, and normalized values for treated samples were expressed as a ratio of control ± SEM. Ratios higher than 1 are upregulated, ratios below 1 are downregulated. Statistical analysis operations in GeneSpring was used to obtain lists of genes that were significantly up- or downregulated (one-way ANOVA, $P \leq 0.05$). These lists were cross-referenced to transcription gene lists obtained from NetAffx to yield transcription-related genes modulated by tangeretin. The data shown were combined from three independent experiments.

Common ID	Gene name	Ratio to control	SEM
BHLHB2	differentiated embryo chondrocyte expressed gene 1	2.06	0.20
IVNS1ABP	influenza virus NS1A binding protein	1.69	0.16
IVNS1ABP	influenza virus NS1A binding protein	1.54	0.13
SSRP1	structure specific recognition protein 1	0.92	0.00
ILF2	interleukin enhancer binding factor 2	0.90	0.01
CSDA	cold shock domain protein A	0.88	0.03
PPP2CB	protein phosphatase 2, catalytic subunit, β	0.88	0.02
HMGB1	high-mobility group box 1	0.86	0.02
HNRPD	heterogeneous nuclear ribonucleoprotein D	0.85	0.01
RYBP	RING1 and YY1 binding protein	0.84	0.03
SFPQ	splicing factor proline/glutamine rich	0.84	0.02
CHD4	chromodomain helicase DNA binding protein 4	0.83	0.03
PTMA	Prothymosin alpha	0.82	0.04
YY1	YY1 transcription factor	0.82	0.04
SSB	Sjogren syndrome antigen B	0.81	0.01
SSB	Sjogren syndrome antigen B	0.80	0.03
SFPQ	splicing factor proline/glutamine rich	0.76	0.03
ZNF207	zinc finger protein 207	0.74	0.02
CHD4	chromodomain helicase DNA binding protein 4	0.71	0.02
SAFB	scaffold attachment factor B	0.71	0.04
NFE2L2	nuclear factor (erythroid-derived 2)-like 2	0.68	0.01
ADNP	activity-dependent neuroprotector	0.62	0.07

Table 16. Stress related genes significantly changed in tangeretin-treated MDA-MB-435 cells. Cells were treated for 6 h with tangeretin (54 μM) or DMSO control. RNA was isolated and human Affymetrix arrays (HGU133A) were used to assess gene expression as described in *Materials and Methods*. Gene expression of treated and control samples were normalized to control using GeneSpring GX 7.3 data mining software, and normalized values for treated samples were expressed as a ratio of control ± SEM. Ratios higher than 1 are upregulated, ratios below 1 are downregulated. Statistical analysis operations in GeneSpring were used to obtain lists of genes that were significantly up- or downregulated (one-way ANOVA, $P \leq 0.05$). These lists were cross-referenced to stress gene lists obtained from NetAffx to yield stress-related genes modulated by tangeretin. The data shown were combined from three independent experiments.

Common ID	Gene name	Ratio to control	SEM
DUSP1	dual specificity phosphatase 1	1.45	0.15
TAO1	thousand and one amino acid protein kinase	1.43	0.15
HYOU1	hypoxia up-regulated 1 oxygen regulated	1.19	0.01
PDIR	protein disulfide isomerase-related	1.14	0.03
MAPK14	MAP kinase	0.82	0.02
PDLIM1	PDZ and LIM domain 1	0.81	0.02
SUI1	putative translation initiation factor	0.76	0.01
PRKRIR	protein-kinase, interferon-inducible double stranded RNA dependent inhibitor, repressor	0.76	0.02

the upregulated were cyclin L2, cyclin T2, myc oncogene and DUSP1. Downregulated genes included CCNE1, CCNE2, CCNB1, CDK8, SKP2 and DUSP6. There were 67 apoptosis genes with increased (8) or decreased (59) expression (Table 13). Included in the upregulated were A20 and INHA (inhibin alpha). Among the downregulated were APAF1, BAD, CASP2, CASP6, BAG2 and BAK1.

Ingenuity Pathways Analysis (IPA) was used to generate and rank networks of genes responsive to tangeretin exposure in MDA-MB-435 cells (see section 2.15, Materials and Methods). IPA identified 68 networks in total with 7 of these networks having a score of 38, each containing the maximum of 35 focus genes. The predominant functions associated with these seven networks (excluding diseases and developmental processes) were gene expression, cellular function and maintenance, cellular movement, cell death and cell signaling. There were 6 additional networks with scores below 38 but greater than 10. Functions associated with these networks were cell cycle, DNA replication, recombination, amino acid metabolism, tumor morphology, cell signaling, protein synthesis, gene expression and RNA trafficking. The top 8 networks with gene lists and associated functions are shown in Table 17.

IPA takes these functions and ranks them in order of significance. Cellular and molecular pathways predicted to be significantly affected in MDA-MB-435 by tangeretin treatment (Figure 22) were consistent with the functions associated with the individual networks. Cell cycle is ranked number 2 and cell death is ranked number 7 out of 21 pathways.

The 'canonical pathways' feature is used to identify specific metabolic and signaling pathways likely to be modulated by tangeretin. IPA identified 12 significant metabolic and signaling pathways predicted to be affected by tangeretin exposure (Figure 23). Included in this list was hypoxia signaling in the cardiovascular system, apoptosis, MAPK, death receptor and cell cycle (G2/M DNA damage checkpoint) signaling.

Table 17. IPA Network analysis of significantly changed tangeretin-responsive genes in MDA-MB-435 cells. A list of genes significantly changed was obtained using GeneSpring software as described in *Materials and Methods*. Interactions and functional associations between genes on this list was analysed and mapped into networks of similar function using Ingenuity Pathways Analysis. The top scoring networks are shown along with the associated functions and numbers of genes in each network. The higher the score the less chance there is that genes occur together in a network by random chance. Significantly changed genes are shown in bold print.

Network	Genes	Functions	Score	No. of genes
1	**HNRPH1, RPL10, CCNB1, LAMP1, DDX3X, MYC, ANXA4,GADD45GIP1, RPS19, TLE4, ARL6IP, UBE2C, BRD2, NFYC, NFYA, H3F3B, CSDA, JRK, NUCB1, ATPIF1, VPS52, CTCF, PRDX2, CPD, SNRPN, RBMS1, TDE1, METAP2, GAS2L1, NOL5A, RFXANK, H3F3A, DSTN, NFYB, JTV1**	gene expression, cellular development, hematological system development and function	38	35
2	**USP18, TNPO1, PSMA4, TXNIP, TSC2, RUFY1, GTF3C2, CAST, RANBP2, CDKN2D, KPNA2, KPNA1, RNUT1, ZNF148, FNBP3, PSMA5, USP4, FLJ20436, SKP2, NUP50, EXOSC2, HNRPDL, CCNE2, CDKN1B, SKP1A, PSMA2, KPNB1, HNRPD, CDC34, OACT2, IRF3, CDC42EP3, TCOF1, SSB, SMB3**	cellular function and maintenance, nervous system development and function, cardiovascular system development and function	38	35
3	**LMNA, SMARCE1, NEDD9, SMARCA4, NRP2, TRFP, UBE2L3, BRMS1, GBP1, CD47, RCOR1, UBQLN2, TCF12, FLOT1, THRAP5, SPRY2, MICAL1, BRCA2, KRT18, TMPO, CRSP2, TROAP, OGT, LAMA4, CHD4, FADS3, SURB7, PTPN12, ARID4A, SLC3A2, SAP30, ITGB1, LAMC1, MED6, THY1**	gene expression, cellular movement, cardiovascular system development and function	38	35
4	**RAB5A, HMGB1, FUSIP1, RPS6KA1, ETV1, ILF2, EWSR1, NR2C1, HOXB7, DMD, CHML, NCOA1, NR2F1, SSA2, ATF2, CREBBP, GABPA, NCOA3, RARB, YES1, YY1, HLA-C, ILF3, RCN2, VDR, RQCD1, SGCB, EZH2, ITPK1, PTMA, SGCE, SGCD, ASXL1, EED, RYBP**	gene expression, developmental disorders, skeletal and muscular disorders	38	35
5	**GRB2, SSB1, PKD2, WASL, PHLDA1, CLTB, MAX, CD2AP, ADM, PLAG1, KLF3, SOCS2, LMO4, CAV1, ACP1, ITSN1, MET, WSB1, DNMT3B, PLEC1, FAS, JAK2, UBE2I, DIAPH1, PIAS2, TNPO3, CUL2, IFNGR2, TFAP2C, TCEB1, WSB2, CTBP2, ATF5,**	cell death, skeletal and muscular system development and function, organismal	38	35

	SCAMP1, SPTAN1	development		
6	**ARHGEF3, TUBB3, PPP2R2A, PRKCD, CASP2, CSPG6, TUBB2A, P53CSV, PPP2R1B, MYT1, PPP2R3A, MCAM, BAK1, PPP2CA, PPP2CB, CCNE1, PSCD2, NRAS, CUL3, CASP6, TUBA1, TRIB1, TUBB2C, MAP2K4, ARF6, TUBA3, BCL2L2, APAF1, STAG2, RHOB, BAD, ARFGAP1, PLD1, RPS6KA2, TAOK2**	cell death, connective tissue disorders, cancer	38	35
7	**IER3, VCP, GNA11, RAD17, SMAD2, GNB2, ITPR1, GNAS, SOX9, ATR, AKAP9, EIF4ENIF1, GNAI3, LTBP1, PLCB1, SNX1, TOB1, PURA, GNG7, CEBPB, KLF10, FMR1, HDAC6, SP100, FKBP3, PDE4D, EEF1E1, HGS, H2AFX, MRPL11, ZFYVE9, GNB1, BCOR, PML, BRPF1**	cell signaling, cancer, hematological diseases	38	35
8	BUB1B, MAD2L2, **C5ORF18, CDC20, KNTC2**, CDCA1, EPC1, **RAB5B**, ING3, **PELI1, STK6, SAC3D1, C20ORF20, PPP2R5E, SPBC25**, MLLT10, SPBC24, EP400, **C1ORF48, GMNN, KRT10, ZWINT (HZwint-1), ZNF143, MORF4L1**, TACC2, CCND1, **SS18**, POU2F1, MAD2L1, SMARCB1, **BUB3, RAB14, YEATS4, PLK4, FBXO5**	cell cycle, DNA replication, recombination and repair, cancer	17	23

Figure 22. Molecular and cellular functions/events significantly modulated in MDA-MB-435 following short-term treatment with tangeretin from Ingenuity Pathways Analysis. Functions are listed on the x-axis and the y-axis shows the -log(significance score) which is -log of the p value determined by Ingenuity based on the number of genes involved in a pathway and their relative weight in the process. The line represents the threshold of significance. Higher significance scores indicate that there are more genes from the gene list of interest associated with a particular function.

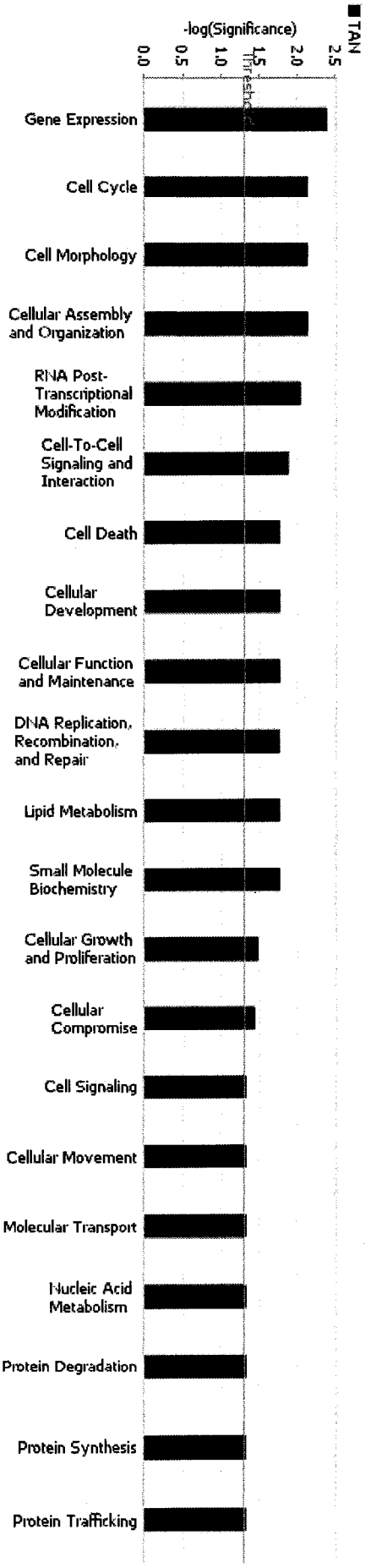
TAN
-log(Significance)
0.0
0.5
1.0
1.5
2.0
2.5
Gene Expression
Cell Cycle
Cell Morphology
Cellular Assembly and Organization
RNA Post-Transcriptional Modification
Cell-To-Cell Signaling and Interaction
Cell Death
Cellular Development
Cellular Function and Maintenance
DNA Replication, Recombination, and Repair
Lipid Metabolism
Small Molecule Biochemistry
Cellular Growth and Proliferation
Cellular Compromise
Cell Signaling
Cellular Movement
Molecular Transport
Nucleic Acid Metabolism
Protein Degradation
Protein Synthesis
Protein Trafficking

Figure 23. Canonical metabolic and signaling pathways significantly modulated in MDA-MB-435 following short-term treatment with tangeretin from Ingenuity Pathways Analysis. Pathways are listed on the x-axis and the y-axis shows the -log(significance score) which is -log of the p value determined by Ingenuity based on the number of genes involved in a pathway and their relative weight in the process. The line represents the threshold of significance. Higher significance scores indicate that there are more genes from the gene list of interest associated with a particular pathway.

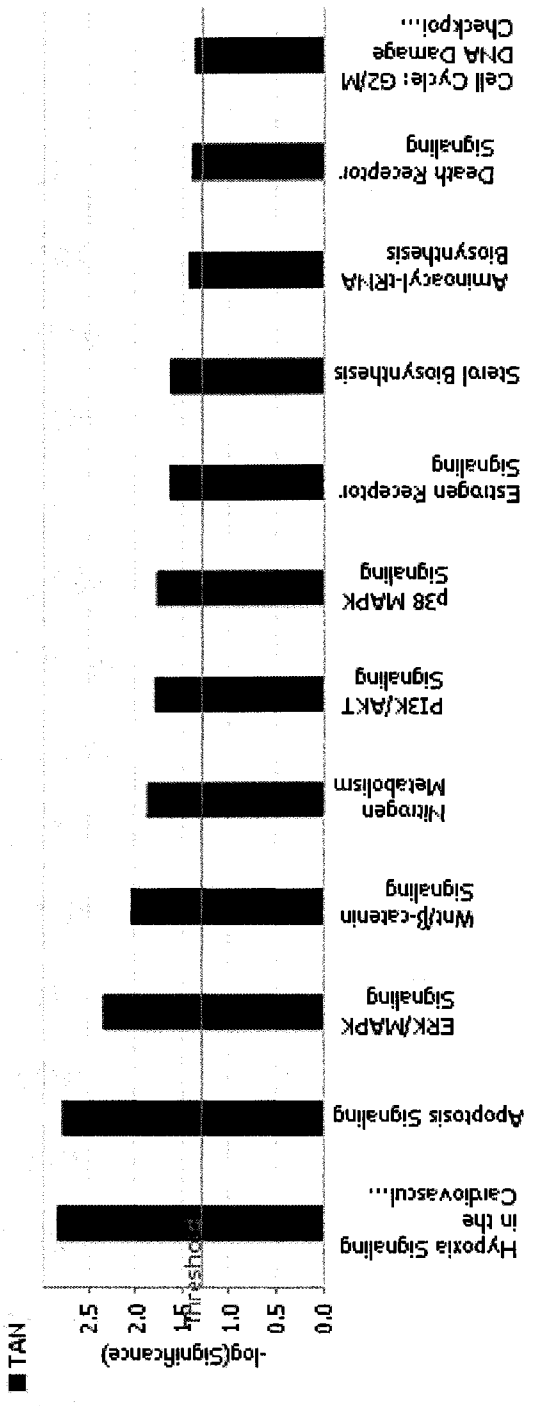
TAN
-log(Significance)
0.0
0.5
1.0
1.5
2.0
2.5
Threshold
Hypoxia Signaling in the Cardiovascul...
Apoptosis Signaling
ERK/MAPK Signaling
Wnt/β-catenin Signaling
Nitrogen Metabolism
PI3K/AKT Signaling
p38 MAPK Signaling
Estrogen Receptor Signaling
Sterol Biosynthesis
Aminoacyl-tRNA Biosynthesis
Death Receptor Signaling
Cell Cycle: G2/M DNA Damage Checkpoi...

3.3.3. Validation of microarray results using Sybr Green real-time RT-PCR

The expression of a small subset of genes whose mRNA levels were significantly increased or decreased by tangeretin as indicated by Affymetrix microarray analysis was confirmed by real-time RT-PCR. Four genes from the list of tangeretin-responsive genes were selected based on the degree of change in expression (at least a 2-fold change in mRNA levels) as well as involvement in cell cycle or apoptosis. They were CCNE2, DUSP6, CREM and TNFAIP3 or A20. CCNE2 and DUSP6 expression were downregulated following tangeretin treatment by 2- and 3-fold, respectively, in both the microarray analysis and real-time RT-PCR (Figure 24). The amount of change and the relationship of this change remained consistent across methods for the two downregulated genes; the downregulation of DUSP6 was greater than that of CCNE2 as indicated by data obtained by either method. Genes whose expressions were upregulated by tangeretin in the microarray analysis (CREM and A20), were also found to be upregulated using real-time RT-PCR (Figure 24). The expressions of CREM and A20 were increased 3.2- and 2.7-fold, respectively, when assayed by microarray analysis and 0.7 and 1.9, respectively, when assayed by real-time RT-PCR.

Figure 24. Confirmation of microarray data using real-time RT-PCR. The expression of four genes (CREM, A20, CCNE2 and DUSP6, respectively plus 18S as an internal control), whose expression was up- or down-regulated in the microarray analysis (A), was verified by real-time RT-PCR (B). For panel B, MDA-MB-435 cells were treated with tangeretin (54 μM) for 6 h. Total RNA was isolated, reverse transcribed and gene expression was quantified by Sybr Green real-time PCR as described in *Materials and Methods*. Gene expression was normalized to 18S and normalized values were expressed as fold change compared to vehicle control. Data shown are from a single experiment.

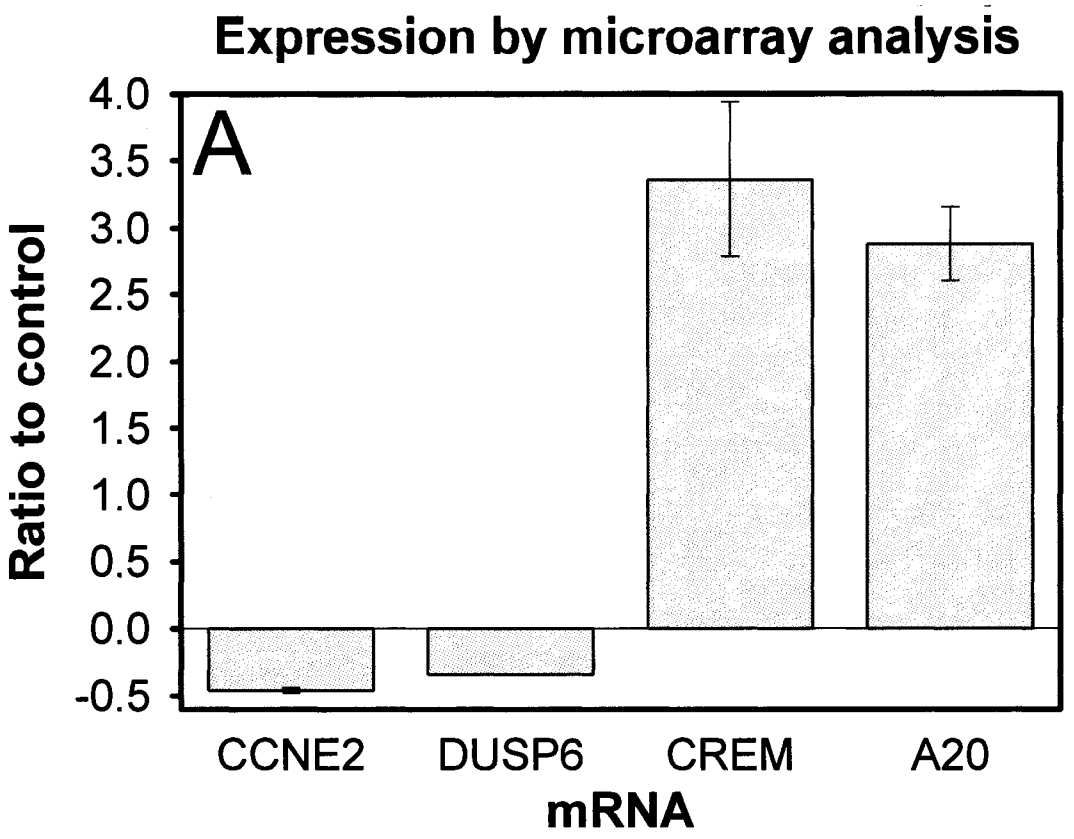
Expression by microarray analysis
A
Ratio to control
4.0
3.5
3.0
2.5
2.0
1.5
1.0
0.5
0.0
-0.5
CCNE2
DUSP6
CREM
A20
mRNA

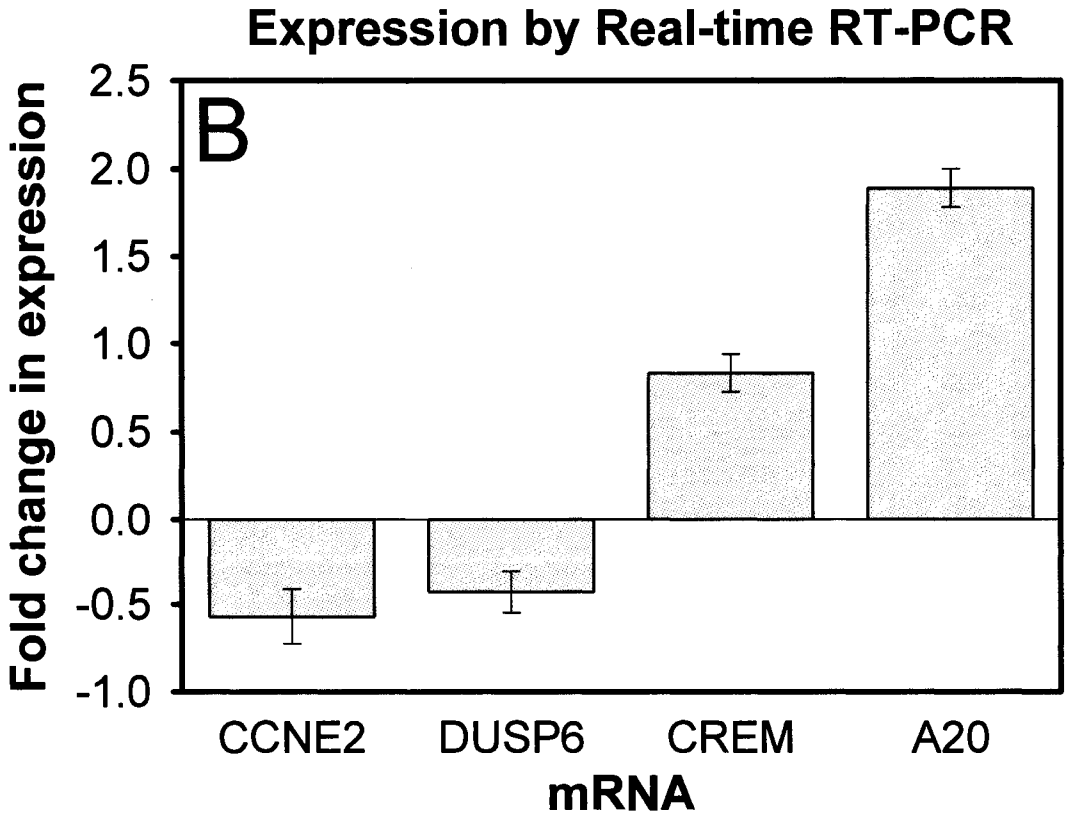
Expression by Real-time RT-PCR
B
Fold change in expression
2.5
2.0
1.5
1.0
0.5
0.0
-0.5
-1.0
CCNE2
DUSP6
CREM
A20
mRNA

II. Flavonoid resistance: tangeretin-resistant MDA-MB-435 breast cancer cells as a model

3.4. Comparison of characteristics of resistant clones to parental

3.4.1. Selection of flavonoid resistant populations

Assessing the characteristics of tangeretin- and nobiletin-resistant populations, and determining the effects of flavonoids on these cells was another approach to this investigation of the mechanisms mediating the antiproliferative effect of tangeretin and nobiletin on cancer cells. Establishing populations of tangeretin- and nobiletin-resistant cells was required, as there are few reports of flavonoid-resistant cell lines, particularly cell lines resistant to non-synthetic, naturally-occurring flavonoids. Populations of MDA-MB-435, MCF-7 and HT-29 cells with decreased sensitivity to the antiproliferative effects of tangeretin and nobiletin were selected using a dose escalation scheme. This involved growing cells under a range of concentrations of these flavonoids, until achieving a concentration that permitted survival and proliferation of only a sector of the starting population. This did not involve a stepwise selection of colonies at lower concentrations and re-selection of those colonies at increasingly higher concentrations. Instead, cells were seeded at densities that accommodated growth to a continuous monolayer (if concentrations permitted) or as discrete colonies following the die-off of a portion of the population. Colonies for all three cell lines were successfully selected following nobiletin treatment, but only MDA-MB-435 cells yielded selectable colonies following tangeretin treatment (Table 18). The whole process from cell plating to colony selection took 5-8 weeks.

Selection of populations that were potentially less sensitive to the growth inhibitory effects of tangeretin and nobiletin occurred at concentrations much higher than what was routinely used in the present study. Solubility was an issue for both compounds and required final DMSO concentrations of 0.1-2.0% v/v. In spite of the presence of DMSO, some precipitation of flavonoid did occur but this did not appear to affect the concentration-dependent reduction in colony

Table 18. Concentrations at which tangeretin- and nobiletin-resistant MDA-MB-435, MCF-7 and HT-29 cells were selected. Cells were treated for 4-6 weeks with high concentrations of tangeretin or nobiletin, as described in *Materials and Methods*, to select populations of cells less sensitive to their antiproliferative effects. Concentrations at which colony formation occurred and persisted are shown in the table and are from a single experiment. **NC**: no colonies selected

Cell line	Tangeretin (mM)	Nobiletin (mM)
MDA-MB-435	0.54	0.75
MCF-7	NC	0.19
HT-29	NC	0.22

formation. Attempts were made to repeat selection of MDA-MB-435 colonies following long-term treatment with high concentrations of tangeretin but with lower concentrations of DMSO. The vehicle (DMSO) was applied at a final concentration of 2% to solubilize the selecting concentration of tangeretin (0.54 mM) in the first successful attempt at colony formation and selection, however, in subsequent attempts, DMSO concentrations were lowered to 0.5%. Under these new conditions, colony formation failed to occur therefore, 2% DMSO without tangeretin was used instead and colonies of MDA-MB-435 cells were successfully isolated. Only a single (successful) attempt was made to select populations of MDA-MB-435, MCF-7, and HT-29 cells less sensitive to nobiletin. Tangeretin- and DMSO-selected populations of MDA-MB-435 cells are the focus of the remaining experiments, with a lesser focus on the nobiletin-selected MDA-MB-435 cells.

3.4.2. Tangeretin resistance

MDA-MB-435 parental and a tangeretin-selected population (MDA-MB-435TAN200H) were grown at low density in a range of concentrations of tangeretin to assess their capacity to survive and proliferate as colonies. The fraction of cells surviving, as indicated by the number of cells able to survive and proliferate as colonies, was significantly higher for the tangeretin-selected cells, beginning at 27 μM and continuing to 67 μM (Figure 25). These cells were less sensitive than parental cells to the growth inhibitory effect of tangeretin.

3.4.3. DMSO-selected tangeretin resistance

The colony forming ability of a DMSO-selected line (MDA-MB-435DMSO2A), when exposed to tangeretin, was compared to that of the tangeretin-selected MDA-MB-435TAN200H line. DMSO2A cells were significantly more capable of surviving and proliferating when treated with tangeretin (12.5-67 μM) compared to the tangeretin-selected line (Figure 26) and by inference, the MDA-MB-435 parental line. DMSO-selected cells were less sensitive to the growth inhibitory effects of tangeretin than tangeretin-selected cells.

Figure 25. Colony forming ability of tangeretin-treated MDA-MB-435 and MDA-MB-435TAN200H cells. MDA-MB-435 parental (black bars) and MDA-MB-435TAN200H tangeretin-selected (white bars) cells were treated for 10-14 d with a range of concentrations of tangeretin (0-67 μM) or DMSO control, and colonies were quantified as described in *Materials and Methods*. Colony numbers were obtained in triplicate for each concentration, and are expressed as a fraction of cells surviving (compared to vehicle control). The data shown were combined from three independent experiments. *Significantly different from parental cells (one-way ANOVA, $P \leq 0.05$).

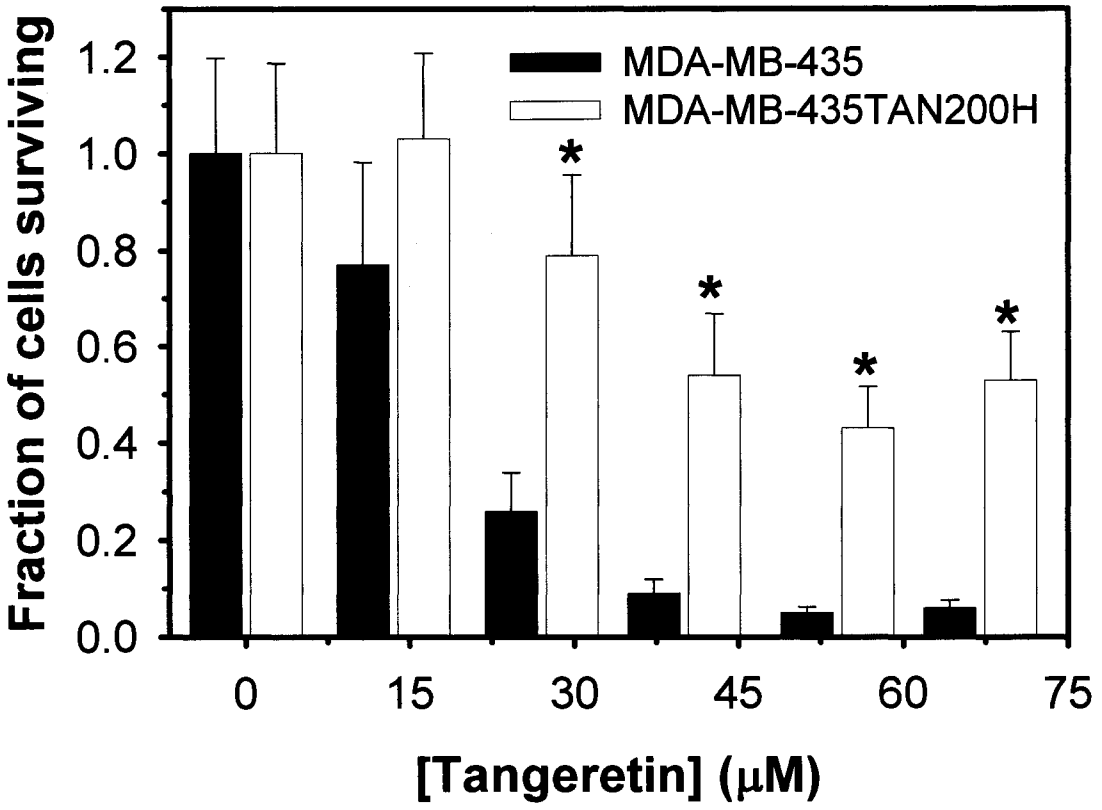
Fraction of cells surviving
1.2
1.0
0.8
0.6
0.4
0.2
0.0
MDA-MB-435
MDA-MB-435TAN200H
*
*
*
*
0
15
30
45
60
75
[Tangeretin] (μM)

Figure 26. Colony forming ability of tangeretin-treated MDA-MB-435TAN200H and MDA-MB-435DMSO2A cells. MDA-MB-435TAN200H (tangeretin-selected, black bars) and MDA-MB-435DMSO2A (DMSO-selected, white bars) cells were treated for 10-14 d with a range of concentrations of tangeretin (0-67 μM) or DMSO control, and colonies were quantified as described in *Materials and Methods*. Colony numbers were obtained in triplicate for each concentration, and are expressed as a fraction of cells surviving (compared to vehicle control). The data shown were combined from two independent experiments. *Significantly different from MDA-MB-435TAN200H cells (one-way ANOVA, $P \leq 0.05$).

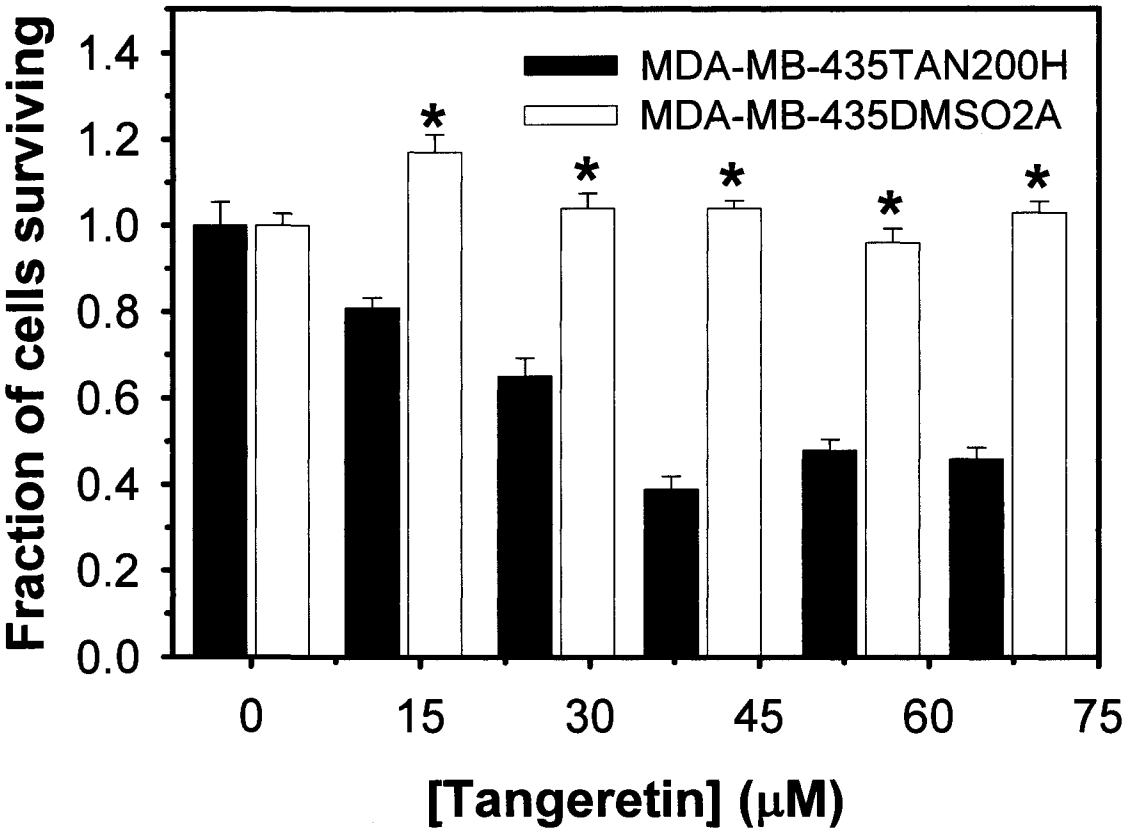
Fraction of cells surviving
1.4
1.2
1.0
0.8
0.6
0.4
0.2
0.0
MDA-MB-435TAN200H
MDA-MB-435DMSO2A
*
*
*
*
*
0
15
30
45
60
75
[Tangeretin] (μM)

3.4.4. Nobiletin resistance

Parental MDA-MB-435, two nobiletin-selected (MDA-MB-435NOB300B and M), plus the DMSO-selected (MDA-MB-435DMSO2A) cells were assessed for their ability to survive and proliferate when treated with nobiletin. The fraction of cells surviving was significantly higher for the nobiletin-selected lines treated with 50-100 μM of nobiletin (Figure 27). At the highest concentration of nobiletin, there was no difference in the fraction of cells surviving for either of the nobiletin-selected lines. DMSO-selected cells survived and proliferated similar to parental cells when treated with nobiletin. Nobiletin-selected cells are less sensitive to the growth inhibitory effects of nobiletin than parental cells, and DMSO-selected cells did not have the same increased resistance to nobiletin as they did to tangeretin.

3.4.5. Growth of tangeretin-selected cells in the absence of tangeretin

The growth of parental MDA-MB-435 and 7 tangeretin-selected (MDA-MB-435TAN200B,D,E,F,G,H,M) cell lines was assessed in flavonoid-free medium. The tangeretin-selected lines segregated into two groups, with one group growing as well as parental cells (MDA-MB-435TAN200B,D,F,H) and the other group growing slower than parental cells (MDA-MB-435TAN200E,G,M) (Figure 28). MDA-MB-435TAN200H, the focus of much of the comparative analysis of parental vs. tangeretin-selected cells, sits at the lower boundary of the former group.

Figure 27. Colony forming ability of nobiletin-treated MDA-MB-435, MDA-MB-435DMSO2A, MDA-MB-435NOB300B and MDA-MB-435NOB300M cells. MDA-MB-435 (parental, black bars), MDA-MB-435DMSO2A (DMSO-selected, white bars), MDA-MB-435NOB300B (nobiletin-selected, light grey bars) and MDA-MB-435NOB300M (nobiletin-selected, dark grey bars) cells were treated for 10-14 d with a range of concentrations of nobiletin (0-200 μM) or DMSO control, and colonies were quantified as described in *Materials and Methods*. Colony numbers were obtained in triplicate for each concentration, and are expressed as a fraction of cells surviving (compared to vehicle control). The data shown were combined from two independent experiments. *Significantly different from parental cells (one-way ANOVA, $P \leq 0.05$).

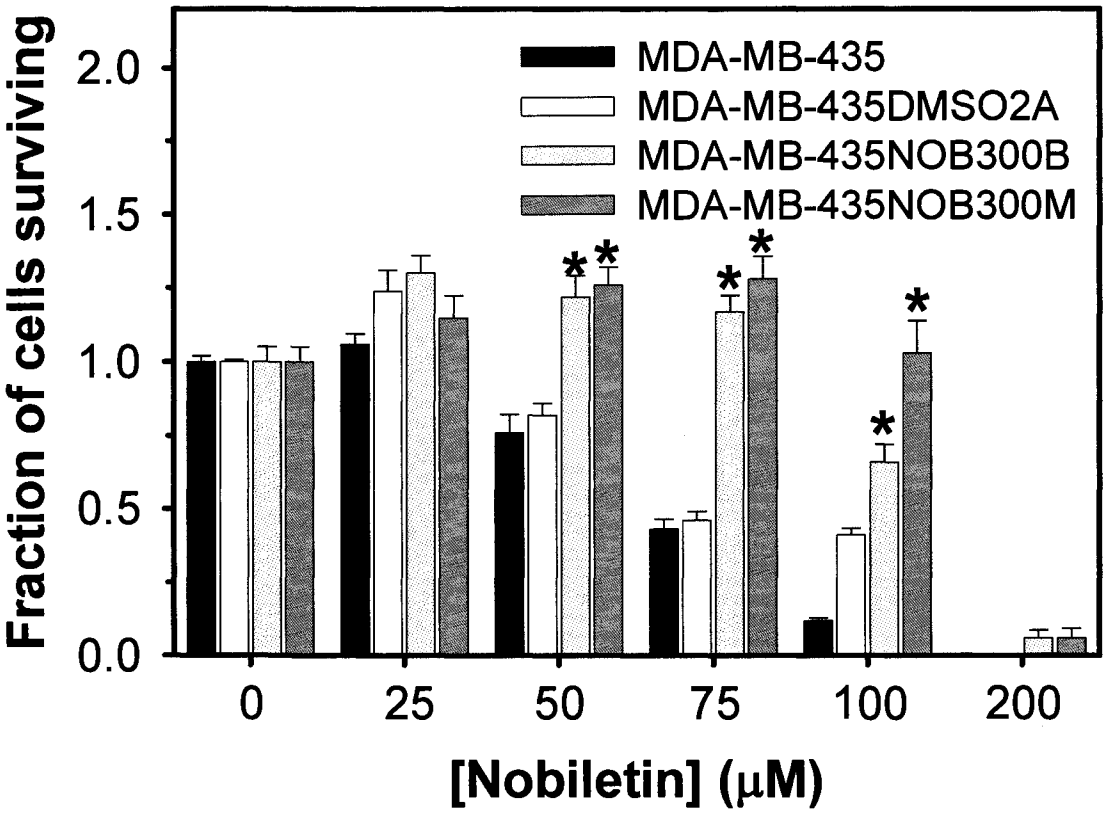
Fraction of cells surviving
2.0
1.5
1.0
0.5
0.0
MDA-MB-435
MDA-MB-435DMSO2A
MDA-MB-435NOB300B
MDA-MB-435NOB300M
*
*
*
*
*
0
25
50
75
100
200
[Nobiletin] (μM)

Figure 28. Growth of MDA-MB-435 parental and tangeretin-selected cells in flavonoid-free growth medium. MDA-MB-435 parental (●) and 7 MDA-MB-435 tangeretin-selected cell lines (TAN200B: ♦, TAN200D: ■, TAN200E: ▲, TAN200F: ◊, TAN200G: ○, TAN200H: ▽, TAN200M: □) were grown in growth medium for 4 d. Cell numbers were determined 24, 48, 72 and 96 h after plating. Cell numbers were obtained in sextuplicate for each time point, and are expressed as means ± SEM. The data shown were combined from 2-3 independent experiments.

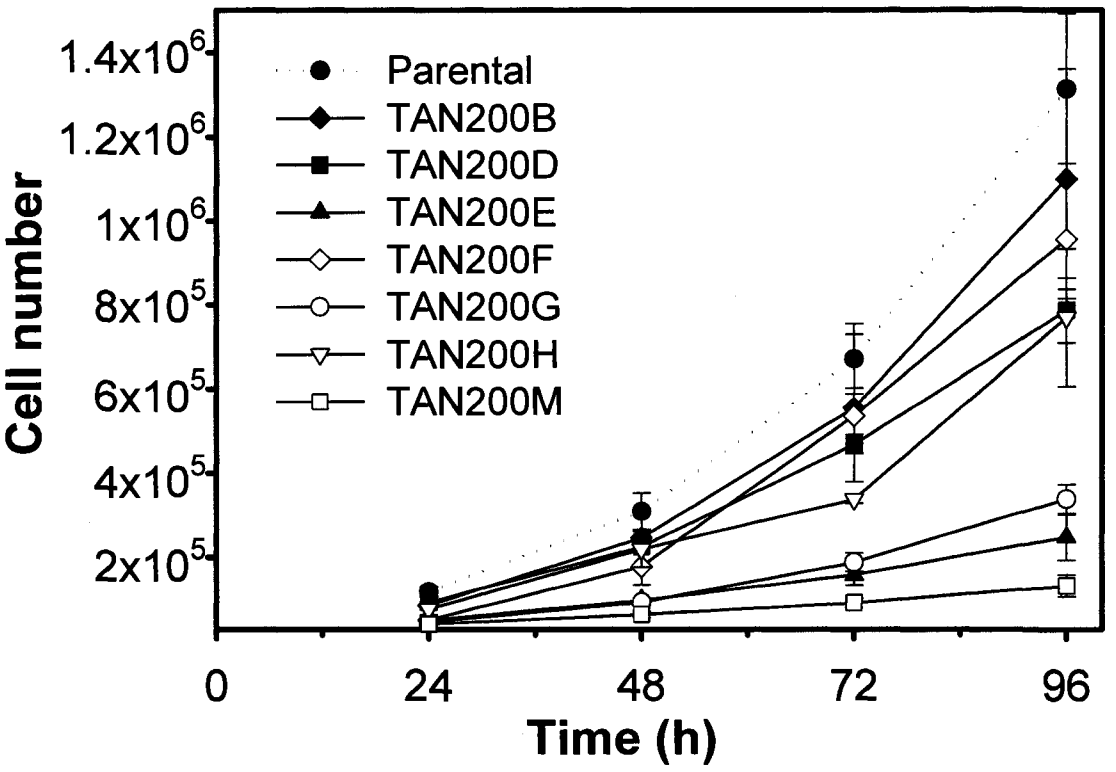
Cell number
1.4x10^6
1.2x10^6
1x10^6
8x10^5
6x10^5
4x10^5
2x10^5
Parental
TAN200B
TAN200D
TAN200E
TAN200F
TAN200G
TAN200H
TAN200M
0
24
48
72
96
Time (h)

Figure 29. Cell cycle distribution in MDA-MB-435TAN200H (A) and MDA-MB-435DMSO2A (B) cells. Cells were treated for 24 h and 96 h with tangeretin [*all panels*: 54 μM (white bars)], nobiletin [*all panels*: 100 μM (grey bars)] or DMSO control (*all panels*, black bars) as described in *Materials and Methods*. Cell cycle distribution was assessed at 24 h and 96 h by flow cytometry. Percent of total cell population values were obtained in triplicate for each time point using Multicycle for Windows software, and are expressed as means ± SEM. The data shown were combined from three independent experiments. *Significantly different from DMSO control (one-way ANOVA, $P < 0.05$). **Tan**: tangeretin (54 μM), **Nob**: nobiletin (100 μM)

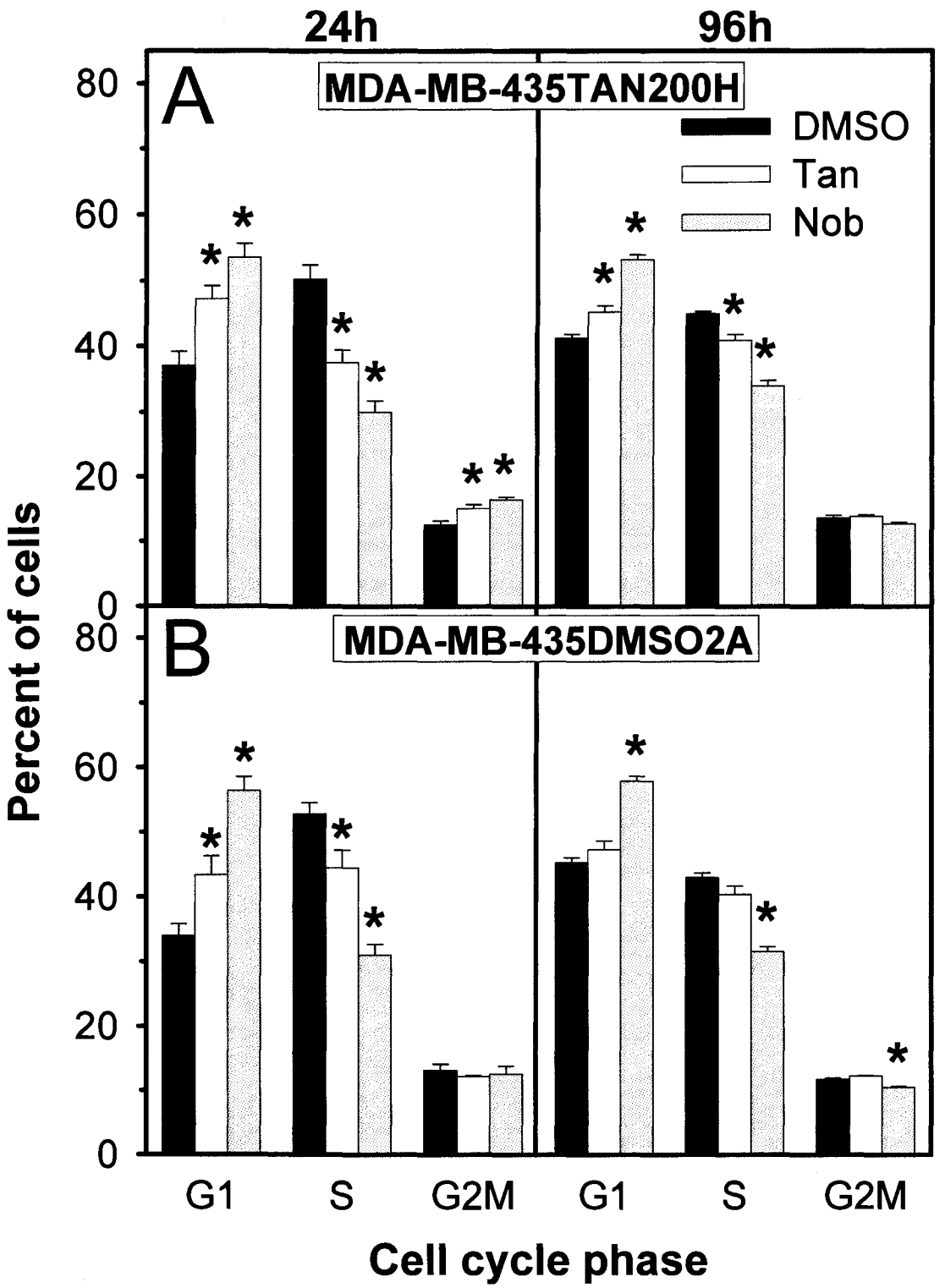
24h
96h
A
MDA-MB-435TAN200H
DMSO
Tan
Nob
B
MDA-MB-435DMSO2A
Percent of cells
0
20
40
60
80
G1
S
G2M
G1
S
G2M
Cell cycle phase

3.4.6. Cell cycle distribution in tangeretin- and DMSO-selected cells

Given that tangeretin- and DMSO-selected cells survived and proliferated better than parental cells when treated with tangeretin, assessing the effect of flavonoids on cell cycle distribution may provide important information on the biological basis of this decreased sensitivity to tangeretin. Tangeretin and nobiletin significantly increased the percentage of cells in G1, accompanied by a decrease in S phase, in both MDA-MB-435TAN200H and MDA-MB-435DMSO2A cells at 24 h (Figure 29). For the tangeretin-selected TAN200H cells, the G1 increase was also accompanied by a significant increase in the percentage of cells in G2/M at the 24 h but not 96 h time point. G1 accumulation with S phase depletion continued to 96 h for this cell line (Figure 29, panel A). In DMSO-selected DMSO2A cells, G1 accumulation continued to 96 h for nobiletin but was abrogated in tangeretin-treated cells (Figure 29, panel B).

3.4.7. Microarray analysis of gene expression in a tangeretin-resistant line

The expression of 10,000 genes was assessed in MDA-MB-435 parental and MDA-MB-435TAN200H tangeretin-selected cells treated with DMSO or tangeretin, respectively, in a single experiment. Tangeretin altered the expression of 817 genes by two-fold or greater, 423 upregulated and 394 downregulated (Table 28, Appendix I). Biological process gene lists were compiled from the Affymetrix NetAffx™ website and used to query the list of genes changed by tangeretin in tangeretin-selected cells. Table 19 summarizes the numbers of genes increased or decreased in each biological process category and full lists can be found in Tables 20-24. In two of five categories (cell cycle and proliferation), more genes were upregulated than downregulated in response to tangeretin. In parental MDA-MB-435 cells treated with tangeretin, the reverse was the case; both cell cycle and proliferation categories had more genes downregulated than upregulated (Table 9).

Categorisation of the list of 2-fold changed for cell cycle related genes identified 88 genes whose expression was changed by tangeretin (Table 22). Of

Table 19. Biological process categorization of tangeretin-responsive genes in tangeretin-selected MDA-MB-435TAN200H cells. TAN200H cells were treated with tangeretin (0.54 mM) and MDA-MB-435 parental cells with DMSO vehicle control in a single experiment. RNA was isolated and human Affymetrix arrays (HGU95A) were used to assess gene expression. GeneSpring GX 7.3 software was used to obtain and categorise lists of genes that were 2-fold up- or downregulated following tangeretin treatment as described in *Materials and Methods.* Numbers of genes in each biological process category are shown in the table.

	Number of genes		
Biological process	**Increased**	**Decreased**	**Total**
cell growth	6	9	15
proliferation	30	25	55
cell cycle	57	31	88
apoptosis	13	34	47
stress	2	8	10

Table 20. Cell growth related genes 2-fold increased or decreased in tangeretin-treated MDA-MB-435TAN200H cells. TAN200H cells were treated with tangeretin (0.54 mM) and MDA-MB-435 parental cells with DMSO vehicle control. RNA was isolated and human Affymetrix arrays (HGU95A) were used to assess gene expression as described in *Materials and Methods*. Using GeneSpring GX 7.3 data mining software, gene expression of treated and control samples were normalized to control, and normalized values for treated samples were expressed as fold change. Lists of genes 2-fold up- or downregulated following tangeretin treatment were obtained. These lists were cross-referenced to cell growth gene lists obtained from NetAffx to yield growth-related genes modulated by tangeretin. The data shown is from a single analysis.

Common ID	Gene name	Fold change
CYR61	cysteine-rich, angiogenic inducer, 61	3.01
IGFBP1	insulin-like growth factor binding protein 1	2.66
NEDD9	neural precursor cell expressed, developmentally down-regulated 9	2.61
SIPA1	signal-induced proliferation-associated prot. 1	2.47
CDC2L1		2.12
ING3		2.11
IFNG	interferon, gamma	-2.04
CSNK2A1	casein kinase II alpha 1	-2.13
LTBP4	latent transforming growth factor beta binding protein 4	-2.18
SLC3A2	solute carrier family 3, 2	-2.20
CSNK2A1	casein kinase II alpha 1	-2.27
TGFB2		-2.73
TP53	tumor protein p53	-3.08
FHL1	four and a half LIM domains 1	-3.62
DCBLD2	endothelial and smooth muscle cell-derived neuropilin-like protein	-3.97

Table 21. Proliferation related genes 2-fold increased or decreased in tangeretin-treated MDA-MB-435TAN200H cells. TAN200H cells were treated with tangeretin (0.54 mM) and MDA-MB-435 parental cells with DMSO vehicle control. RNA was isolated and human Affymetrix arrays (HGU95A) were used to assess gene expression as described in *Materials and Methods*. Using GeneSpring GX 7.3 data mining software, gene expression of treated and control samples were normalized to control, and normalized values for treated samples were expressed as fold change. Lists of genes 2-fold up- or downregulated following tangeretin treatment were obtained. These lists were cross-referenced to proliferation gene lists obtained from NetAffx to yield proliferation-related genes modulated by tangeretin. The data shown is from a single analysis.

Common ID	Gene name	Fold change
NCK2		8.57
CDC25A	cell division cycle 25A	5.86
IL7	interleukin 7 precursor	4.73
INSIG1	insulin induced gene 1	4.47
DLG1	synapse-associated protein 97	3.97
MAPRE2	microtubule-assoc protein, RP/EB family, 2	3.62
CDK2	cyclin-dependent kinase 2	3.56
DAB2	disabled homolog 2	3.48
IL8	interleukin 8 precursor	3.26
CSE1L	CSE1 chromosome segregation 1-like protein	3.15
NRD1		3.13
CYR61	cysteine-rich, angiogenic inducer, 61	3.01
BTG3	B-cell translocation gene 3	2.95
CDC6	CDC6 homolog	2.88
CDC7	CDC7 cell division cycle 7	2.80
IL8	interleukin 8 precursor	2.71
MET	met proto-oncogene precursor	2.58
CDC25C	cell division cycle 25C protein	2.57
		2.54
SIPA1	signal-induced proliferation-assoc protein 1	2.47
MKI67	antigen identified by monoclonal Ab Ki-67	2.47
KIF2C	kinesin family member 2C	2.41
DTYMK	deoxythymidylate kinase (thymidylate kinase)	2.41
CDK2	cyclin-dependent kinase 2	2.41
CDKN2C	cyclin-dependent kinase inhibitor 2C	2.32
CENPF	centromere protein F	2.30
PCNA	proliferating cell nuclear antigen	2.24
PCNA	proliferating cell nuclear antigen	2.18
CDC2L1		2.12
BRCA1	breast cancer 1	2.10
BUB1	budding uninhibited by benzimidazoles 1 homolog	2.10
SPP1	secreted phosphoprotein 1	-2.08
CSNK2A1	casein kinase II alpha 1	-2.13
PPAP2A	phosphatidic acid phosphatase type 2A	-2.27
CSNK2A1	casein kinase II alpha 1	-2.27
SPP1	secreted phosphoprotein 1	-2.39
CDKN2A	cyclin-dependent kinase inhibitor 2A	-2.51
MIA		-2.52
CUL2	cullin 2	-2.57
TNFSF9	tumor necrosis factor superfamily, 9	-2.67
TGFB2	T	-2.73
VEGF	vascular endothelial growth factor	-2.85

Common ID	Gene name	Fold change
PIM2	pim-2 oncogene	-2.87
TACSTD2	tumor-associated calcium signal transducer 2 precursor	-2.91
VEGF	vascular endothelial growth factor	-2.98
TP53	tumor protein p53	-3.08
WARS	tryptophanyl-tRNA synthetase	-3.31
BIN1	bridging integrator 1	-3.50
VEGF	vascular endothelial growth factor	-3.57
CD74	cell surface glycoprotein	-3.64
PTN	pleiotrophin	-3.69
TIMP1	tissue inhibitor of metalloproteinase 1 precursor	-4.08
IFITM1	interferon induced transmembrane protein 1	-5.81
BST2	bone marrow stromal cell antigen 2	-6.94
ELF4	E74-like factor 4	-9.01
AZGP1	alpha-2-glycoprotein 1, zinc	-27.25

Table 22. Cell cycle related genes 2-fold increased or decreased in tangeretin-treated MDA-MB-435TAN200H cells. TAN200H cells were treated with tangeretin (0.54 mM) and MDA-MB-435 parental cells with DMSO vehicle control. RNA was isolated and human Affymetrix arrays (HGU95A) were used to assess gene expression as described in *Materials and Methods*. Using GeneSpring GX 7.3 data mining software, gene expression of treated and control samples were normalized to control, and normalized values for treated samples were expressed as fold change. Lists of genes 2-fold up- or downregulated following tangeretin treatment were obtained. These lists were cross-referenced to cell cycle gene lists obtained from NetAffx to yield cell cycle-related genes modulated by tangeretin. The data shown is from a single analysis.

Common ID	Gene name	Fold Change
AXL	AXL receptor tyrosine kinase	7.94
CDC25A	cell division cycle 25A	5.86
DUSP1	dual specificity phosphatase 1	5.71
PTP4A1	protein tyrosine phosphatase type IVA, 1	4.32
DLG1	synapse-associated protein 97	3.97
MAPRE2	microtubule-assoc protein, RP/EB family, 2	3.62
DLEU2	deleted in lymphocytic □eukaemia, 2	3.62
CDK2	cyclin-dependent kinase 2	3.56
RBBP6	retinoblastoma-binding protein 6	3.42
CDC45L	CDC45-like	3.26
IL8	interleukin 8 precursor	3.26
CCNE2	cyclin E2	2.97
BTG3	B-cell translocation gene 3	2.95
CDC6	CDC6 homolog	2.88
CDC7	CDC7 cell division cycle 7	2.80
MAP2K6	mitogen-activated protein kinase kinase 6	2.73
IL8	interleukin 8 precursor	2.71
PLK4	polo-like kinase 4	2.70
RBL2		2.62
NEDD9	neural prec cell expressed, dev. Down-reg 9	2.61
CDC25C	cell division cycle 25C protein	2.57
SMC4L1	SMC4 struct. Maint. Of chromosomes 4-like 1	2.57
PLK4	polo-like kinase 4	2.54
PTP4A1	protein tyrosine phosphatase type IVA, 1	2.53
SIPA1	signal-induced proliferation-assoc protein 1	2.47
MKI67	antigen identified by monoclonal Ab Ki-67	2.47
MCM6	minichromosome maintenance protein 6	2.42
CCNT1	cyclin T1	2.41
DTYMK	deoxythymidylate kinase (thymidylate kinase)	2.41
CDK2	cyclin-dependent kinase 2	2.41
BARD1	BRCA1 associated RING domain 1	2.33
CDKN2C	cyclin-dependent kinase inhibitor 2C	2.32
CENPF	centromere protein F (350/400kD)	2.30
PCNA	proliferating cell nuclear antigen	2.24
PNN	pinin, desmosome associated protein	2.22
LIG1	DNA ligase I	2.22
MSH2	mutS homolog 2	2.20
MCM7	minichromosome maintenance protein 7	2.18
PCNA	proliferating cell nuclear antigen	2.18
AURKB	aurora kinase B	2.18
MSH2	mutS homolog 2	2.16
PPP3CB	protein phosphatase 3, catalytic subunit, beta	2.15
CDC2	cell division cycle 2 protein	2.13

Common ID	Gene name	Fold Change
ZWINT	ZW10 interactor	2.13
CDC2L1		2.12
DHCR24	24-dehydrocholesterol reductase	2.11
BRCA1	breast cancer 1	2.10
BUB1	budding uninhib. by benzimidazoles 1 homolog	2.10
MYBL2	MYB-related protein B	2.08
PMS1	postmeiotic segregation 1	2.07
CDC2	cell division cycle 2 protein	2.05
CCNA2	cyclin A	2.05
KIF23	kinesin family member 23	2.04
CDC20	cell division cycle 20	2.04
MAPK6	mitogen-activated protein kinase 6	2.03
MAD2L1	Mad2	2.01
UBB	ubiquitin	2.00
E2F5	E2F transcription factor 5	-2.00
PCTK1	PCTAIRE protein kinase 1	-2.03
EXT2	exostosin 2	-2.03
F2R	coagulation factor II receptor precursor	-2.05
HK2		-2.08
TERF1	telomeric repeat binding factor 1	-2.08
PPP3CB	protein phosphatase 3, catalytic subunit, beta	-2.09
HMG20B	high-mobility group 20B	-2.14
PPP1R13B	protein phosphatase 1, regulatory subunit 13B	-2.23
DUSP4	dual specificity phosphatase 4	-2.27
GPR21	RAB GTPase activating protein 1	-2.45
CDKN2A	cyclin-dependent kinase inhibitor 2A	-2.51
CUL2	cullin 2	-2.57
HDAC5		-2.62
TGFB2		-2.73
VEGF	vascular endothelial growth factor	-2.85
CCND1	cyclin D1	-2.93
VEGF	vascular endothelial growth factor	-2.98
PPP1R15A	protein phosphatase 1, regulatory subunit 15A	-3.01
TP53	tumor protein p53	-3.08
PCTK1	PCTAIRE protein kinase 1	-3.11
CCNG2	cyclin G2	-3.19
BIN1	bridging integrator 1	-3.50
VEGF	vascular endothelial growth factor	-3.57
PTN	pleiotrophin	-3.69
KATNA1		-3.91
E2F5	E2F transcription factor 5	-4.57
PCTK2	PCTAIRE protein kinase 2	-4.67
IFITM1	interferon induced transmembrane protein	-5.81
DDIT3	TLS-CHOP	-6.29
HTATIP2	HIV-1 Tat interactive protein 2, 30kDa	-9.09

Table 23. Apoptosis related genes 2-fold increased or decreased in tangeretin-treated MDA-MB-435TAN200H cells. TAN200H cells were treated with tangeretin (0.54 mM) and MDA-MB-435 parental cells with DMSO vehicle control. RNA was isolated and human Affymetrix arrays (HGU95A) were used to assess gene expression as described in *Materials and Methods*. Using GeneSpring GX 7.3 data mining software, gene expression of treated and control samples were normalized to control, and normalized values for treated samples were expressed as fold change. Lists of genes 2-fold up- or downregulated following tangeretin treatment were obtained. These lists were cross-referenced to apoptosis gene lists obtained from NetAffx to yield apoptosis-related genes modulated by tangeretin. The data shown is from a single analysis.

Common ID	Gene name	Fold change
IL7	interleukin 7 precursor	4.73
TNFAIP3	tumor necrosis factor, alpha-induced protein 3	3.50
HIP1	huntingtin interacting protein 1	3.22
CSE1L	CSE1 chromosome segregation 1-like protein	3.15
SIPA1	signal-induced proliferation-assoc protein 1	2.47
BARD1	BRCA1 associated RING domain 1	2.33
API5	apoptosis inhibitor 5	2.30
CDC2L1		2.12
DHCR24	24-dehydrocholesterol reductase	2.11
BRCA1	breast cancer 1	2.10
MYBL2	MYB-related protein B	2.08
SON	SON DNA-binding protein	2.07
UBE4B	ubiquitination factor E4B	2.04
ANXA1	annexin I	-2.04
F2R	coagulation factor II receptor precursor	-2.05
SPP1	secreted phosphoprotein 1	-2.08
PPP1R13B	protein phosphatase 1, regulatory subunit 13B	-2.23
PSEN1	presenilin 1	-2.29
STK4	serine/threonine kinase 4	-2.33
TNF	tumor necrosis factor alpha	-2.39
SPP1	secreted phosphoprotein 1	-2.39
CDKN2A	cyclin-dependent kinase inhibitor 2A	-2.51
CUL2	cullin 2	-2.57
TOSO	regulator of Fas-induced apoptosis	-2.64
TNFSF9	tumor necrosis factor superfamily, 9	-2.67
TGFB2		-2.73
IKBKG	inhibitor of kappa light polypeptide, kinase γ	-2.74
TRA1	tumor rejection antigen 1	-2.74
ARHGEF6	Rac/Cdc42 guanine nucl. exchange factor 6	-2.76
TRAF3	TNF receptor-associated factor 3	-2.78
VEGF	vascular endothelial growth factor	-2.85
HSPA5	heat shock 70kDa protein 5	-2.98
VEGF	vascular endothelial growth factor	-2.98
PPP1R15A	protein phosphatase 1, regulatory subunit 15A	-3.01
TP53	tumor protein p53	-3.08
CALR	calreticulin precursor	-3.31
PRKCZ	protein kinase C, zeta	-3.41
GULP1	engulfment adaptor PTB domain containing 1	-3.44
BCAP31	B-cell receptor-associated protein 31	-3.53
VEGF	vascular endothelial growth factor	-3.57
CD74	cell surface glycoprotein	-3.64
IER3	immediate early response 3	-3.69
PHLDA1	pleckstrin homology-like domain, family A, 1	-4.44

Common ID	Gene name	Fold change
CALR		-5.26
TNFRSF21	tumor necrosis factor receptor superfamily, 21	-6.02
HTATIP2	HIV-1 Tat interactive protein 2	-9.09
BCL2A1	BCL2-related protein A1	-9.52

Table 24. Stress related genes 2-fold increased or decreased in tangeretin-treated MDA-MB-435TAN200H cells. TAN200H cells were treated with tangeretin (0.54 mM) and MDA-MB-435 parental cells with DMSO vehicle control. RNA was isolated and human Affymetrix arrays (HGU95A) were used to assess gene expression as described in *Materials and Methods*. Using GeneSpring GX 7.3 data mining software, gene expression of treated and control samples were normalized to control, and normalized values for treated samples were expressed as fold change. Lists of genes 2-fold up- or downregulated following tangeretin treatment were obtained. These lists were cross-referenced to stress gene lists obtained from NetAffx to yield stress-related genes modulated by tangeretin. The data shown is from a single analysis.

Common ID	Gene name	Fold change
DUSP1	dual specificity phosphatase 1	5.71
DHCR24	24-dehydrocholesterol reductase	2.11
GSR	glutathione reductase	-2.03
ATF4		-2.39
GSTT1	glutathione S-transferase theta 1	-2.72
VEGF	vascular endothelial growth factor	-2.85
VEGF	vascular endothelial growth factor	-2.98
VEGF	vascular endothelial growth factor	-3.57
PDLIM1	PDZ and LIM domain 1 (elfin)	-3.64
HYOU1	oxygen regulated protein precursor	-3.85

those genes, 57 were increased in expression and 31 decreased in expression. Among the upregulated were CCNE2, CCNA2, CCNT2, CDC2, CDK2 and DUSP1. Downregulated genes included CCND1, CCNG2, E2F5 and DUSP4. There were 47 apoptosis genes with increased (13) or decreased (34) expression (Table 23). Included in the upregulated were A20 and API5. Among the downregulated were BCL2A1, IER and TNFα.

Ingenuity Pathways Analysis (IPA) was used to generate and rank networks of genes responsive to tangeretin exposure in tangeretin-selected MDA-MB-435TAN200H cells. IPA identified 43 networks in total with six of those networks having a score of 44, each containing the maximum of 35 focus genes (Table 25). The predominant functions associated with these six networks (excluding diseases and developmental processes) were lipid metabolism, molecular transport, cell-to-cell signaling and interaction, cellular growth and proliferation, cell death, cell cycle, DNA replication and recombination. There were 15 additional networks with scores below 44 but greater than 10. Functions associated with these networks were cell cycle, cellular assembly and organization, gene expression, tissue and cell morphology, cell signaling, cellular growth and proliferation, drug metabolism, molecular transport, cell death and amino acid metabolism.

IPA takes these functions and ranks them in order of significance. Cellular and molecular pathways predicted to be significantly affected by tangeretin treatment (Figure 30) were consistent with the functions associated with the individual networks. There were 22 pathways in total and cell cycle and cell death ranked number 1 and 3, respectively.

Canonical pathways analysis differs from functional pathways analysis because it identifies specific metabolic and signaling pathways likely to be modulated by tangeretin exposure. IPA canonical pathways analysis identified 9 significant metabolic and signaling pathways predicted to be affected by tangeretin exposure (Figure 31). Included in this list was G1/S checkpoint

Table 25. IPA Network analysis of genes 2-fold increased or decreased in tangeretin-treated MDA-MB-435TAN200H cells. GeneSpring data mining software was used to obtain lists of genes that were 2-fold up- or downregulated following tangeretin treatment.as described in *Materials and Methods*. Interactions and functional associations between genes on this list was analysed and mapped into networks of similar function using Ingenuity Pathways Analysis. The top scoring networks are shown along with the associated functions and numbers of genes in each network. The higher the score the less chance there is that genes occur together in a network by random chance. Significantly changed genes are shown in bold print.

Network	Genes	Functions	Score	No. of genes
1	**IFITM1, TNFSF9, CBS, TNFRSF21, ZNF330, HRSP12, ASAH1, ADORA2B, TM4SF1, SFI1, GSTT1, ST6GAL1, SERPINB8, EFNB2, ZNF267, BTG3, ALCAM, UGCG, PRSS23, COL16A1, RPS6KA4, DAF, HLA-F, SLC1A3, MMP16, CUL2, SEMA3C, RAPGEF5, FOXF2, SUPT4H1, TNF, BST2, SERPINB1, PPAP2A, EPHB3**	lipid metabolism, small molecule biochemistry, molecular transport	44	35
2	**TYRP1, SMG1, IDI1, HLA-DMB, PHLDA1, CENTD1, NDP52, WARS, KLRC2, PIM2, HLA-DRB5, HSPA5, CTSD, NCAM1, CALR, HLA-DMA, HLA-E, IGBP1, RIS1, CD74, ANKS1, PDE4B, HYOU1, KLRC3, VLDLR, HLA-DRA, IFNGR2, TYR, EIF4EBP1, MLANA, IFNG, HLA-DPB1, SPTB, AZGP1, SILV**	immune response, cell-to-cell signaling and interaction, immune and lymphatic system development and function	44	35
3	**TYMS, BACH1, DHFR, EPHA2, PTP4A1, HMMR, ING3, HCAP-D3, TXNRD1, GART, NDRG1, PPP1R15A, RAD23A, WDHD1, ZNF148, NQO1, ATF3, BARD1, PTRF, BUB1, LTBP1, BTBD2, PPP1R13B, TP53, PLK2, RBBP6, SMC4L1, EGR3, FUBP1, MKI67, ERCC6, RAD54L, SON, VRK1, THBS2**	cancer, reproductive system disease, cellular growth and proliferation	44	35
4	**TGFB2, HSPG2, PNN, SMAD6, HERPUD1, CDC20, CDC2, ACAT2, ETV4, POLD3, TIMP1, CDC6, DKK1, SOX9, NMB, PCNA, SMAD5, CD44, CCNA2, MET, ANXA1, GDF15, BGLAP, C5ORF13, SPP1, DNMT1, MAD2L1, AXL, SPRY1, ANK3, JUN, SMURF2, PRIM1, TIAM1, PSEN1**	cell death, cancer, cell cycle	44	35
5	**CDKN2A, CDC25C, RPL5, RBL2, PBX1, NPAT, SDC4, HTATIP2, PDLIM3, ARHGEF12, TRA1, SNTB2, PTN, TMPO, ITGA2, CITED2, DAB2, DUSP4, F2R, ZNF124, PTPRZ1, VEGF, SLBP, ITGB3, SERPINA3, NASP, CYR61, MMP1, DUSP1, KIFC1, TFPI, GPRC5A, ITGA1, ID1, PLTP**	cellular movement, cardiovascular system development and function, cancer	44	35
6	**MRE11A, RPA1, CDC45L, PIK3R1, MCM7, LIG1, ID2, CDC7,**	cell cycle, DNA	38	35

Network	Genes	Functions	Score	No. of genes
	CCNT1, MCM6, PRKCZ, PIK3C3, PKN1, CDKN2C, BRCA1, RECQL, DDIT3, MCM4, ELF4, MARCKS, RFC5, CCND1, CCNE2, RFC2, SF3B1, CDK2, NCK2, IRS1, PTPRF, MSH2, HDAC5, MSC, E2F5, UBE2A, MYBL2	replication, recombination and repair, connective tissue development and function		

Figure 30. Molecular and cellular functions/events significantly modulated in MDA-MB-435TAN200H in response to tangeretin from Ingenuity Pathways Analysis. Functions are listed on the x-axis and the y-axis shows the -log(significance score) which is -log of the p value determined by Ingenuity based on the number of genes involved in a pathway and their relative weight in the process. The line represents the threshold of significance. Higher significance scores indicate that there are more genes from the gene list of interest associated with a particular function or event.

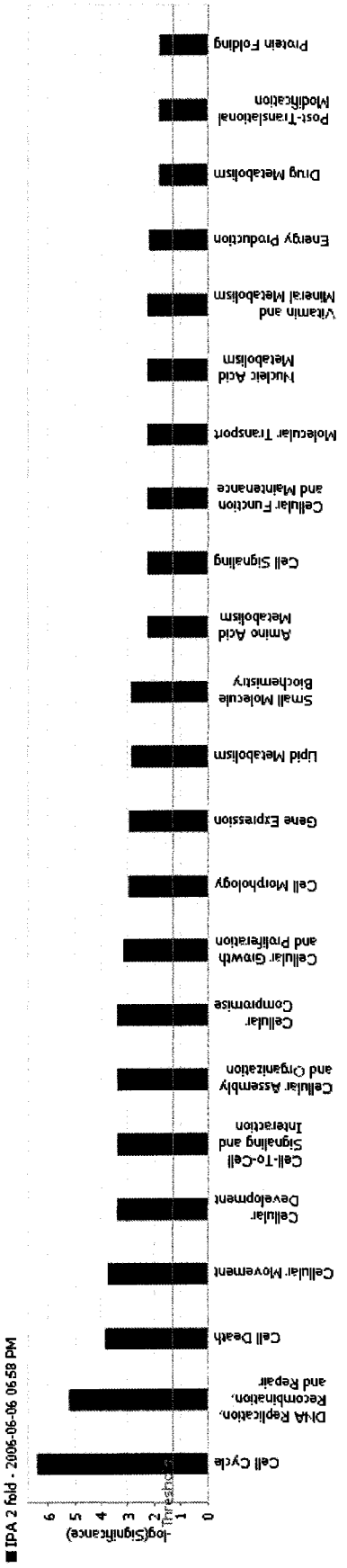
IPA 2 fold - 2006-06-06 06:58 PM
-log(Significance)
6
5
4
3
2
1
0
threshold
Cell Cycle
DNA Replication, Recombination, and Repair
Cell Death
Cellular Movement
Cellular Development
Cell-To-Cell Signaling and Interaction
Cellular Assembly and Organization
Cellular Compromise
Cellular Growth and Proliferation
Cell Morphology
Gene Expression
Lipid Metabolism
Small Molecule Biochemistry
Amino Acid Metabolism
Cell Signaling
Cellular Function and Maintenance
Molecular Transport
Nucleic Acid Metabolism
Vitamin and Mineral Metabolism
Energy Production
Drug Metabolism
Post-Translational Modification
Protein Folding

Figure 31. Canonical metabolic and signaling pathways significantly modulated in MDA-MB-435TAN200H in response to tangeretin from Ingenuity Pathways Analysis. Pathways are listed on the x-axis and the y-axis shows the -log(significance score) which is -log of the p value determined by Ingenuity based on the number of genes involved in a pathway and their relative weight in the process. The line represents the threshold of significance. Higher significance scores indicate that there are more genes from the gene list of interest associated with a particular pathway.

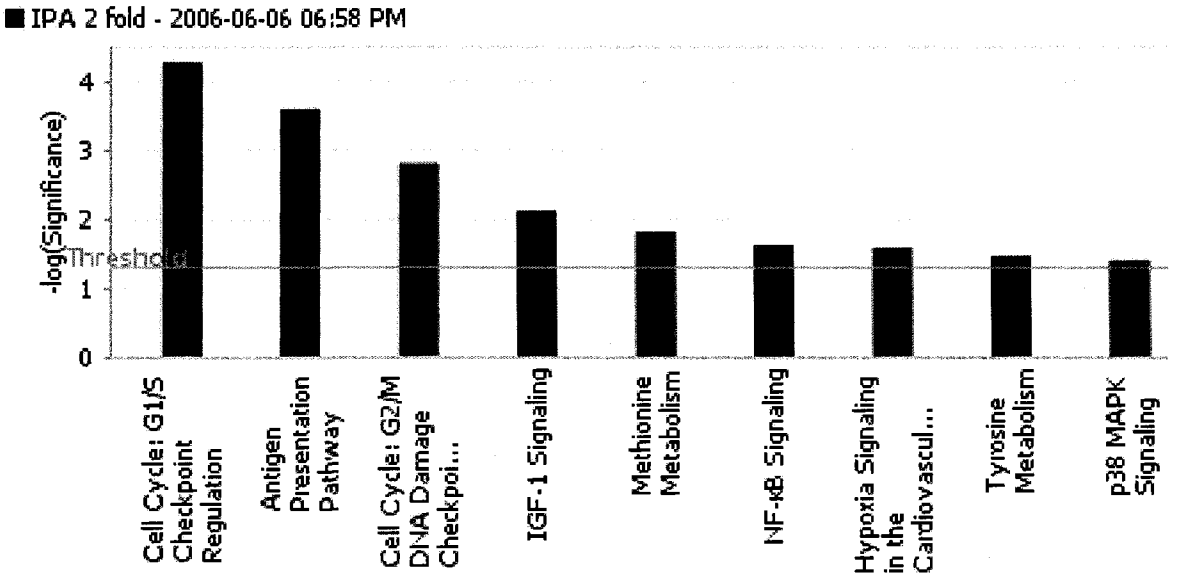
IPA 2 fold - 2006-06-06 06:58 PM
-log(Significance)
0
1
2
3
4
Threshold
Cell Cycle: G1/S Checkpoint Regulation
Antigen Presentation Pathway
Cell Cycle: G2/M DNA Damage Checkpoi...
IGF-1 Signaling
Methionine Metabolism
NF-κB Signaling
Hypoxia Signaling in the Cardiovascul...
Tyrosine Metabolism
p38 MAPK Signaling

regulation, G2/M DNA damage checkpoint signaling, MAPK signaling and hypoxia signaling in the cardiovascular system. Also included on this list were inflammation-related pathways, namely antigen presentation, IGF-1 signaling and NF-kB signaling pathways. The expression of genes involved in these pathways include IL7, TNFAIP3, IL8 and IGFBP1 which were upregulated, and HLA-F, TNFα, IL13R, HLA-DMB, CX3CL1, TNFSF9, TGFB2, TRAF3, IRAK1, HLA-E, IFNγ2, and HLA-DRA which were downregulated.

3.5. Investigating the mechanism of tangeretin-resistance

3.5.1. Cross resistance to chemotherapy drugs

Four common chemotherapy drugs (5-fluorouracil, cisplatin, vincristine sulphate, and taxol) with different mechanisms of action were selected to assess antiproliferative effects on tangeretin-selected cells. The response of these cells to the chemotherapy drugs provides clues to the mechanism by which they decrease their susceptibility to tangeretin. All four drugs decreased metabolic activity in all tangeretin-selected cells in a dose-dependent manner similar to parental MDA-MB-435 cells (Figure 32). In a comparison of IC_{50} values, there was no single drug to which tangeretin-selected cells were all less or more sensitive to. Four of the seven tangeretin-selected lines had decreased sensitivity to one or two chemotherapy drugs (Table 26): TAN200D was less sensitive to vincristine and taxol, TAN200F had decreased sensitivity to taxol, TAN200H had decreased sensitivity to vincrisitine, and TAN200M was less sensitive to 5-fluorouracil. None of the tangeretin-selected cells MDA-MB-435TAN200B,D,F,H showed decreased sensitivity to taxol.

3.5.2. P-glycoprotein overexpression and resistance to flavonoids

Parental and vincristine-resistant head and neck cancer cells overexpressing P-gp were used to assess whether this drug efflux transporter plays a role in decreased sensitivity to the antiproliferative effect of tangeretin and nobiletin. Vincristine decreased proliferation in a dose-dependent manner in both parental and vincristine-selected head and neck cancer cells, however, proliferation was

significantly higher in vincristine-selected cells (Figure 33), confirming resistance to vincristine. Tangeretin and nobiletin inhibited proliferation of both the low and moderately vincristine-resistant cells, as well or even more effectively than parental cells (Figure 34). P-glycoprotein overexpression did not decrease the antiproliferative effect of tangeretin.

Figure 32. Dose response of MDA-MB-435 parental and tangeretin-selected cells to chemotherapy drugs. MDA-MB-435 parental (●) and 7 MDA-MB-435 tangeretin-selected cell lines (TAN200B: ♦, TAN200D: ■, TAN200E: ▲, TAN200F: ◊, TAN200G: ○, TAN200H: ▽, TAN200M: □) were treated for 4 d with 5-fluorouracil (A: 0-10 μM) or cisplatin (B: 0-8 μM). Metabolic activity was quantified using the alamarBlue™ assay as described in *Materials and Methods*. Fluorescence was baseline adjusted and is expressed as a percent of control ± SEM. The data shown were combined from 2-3 independent experiments.

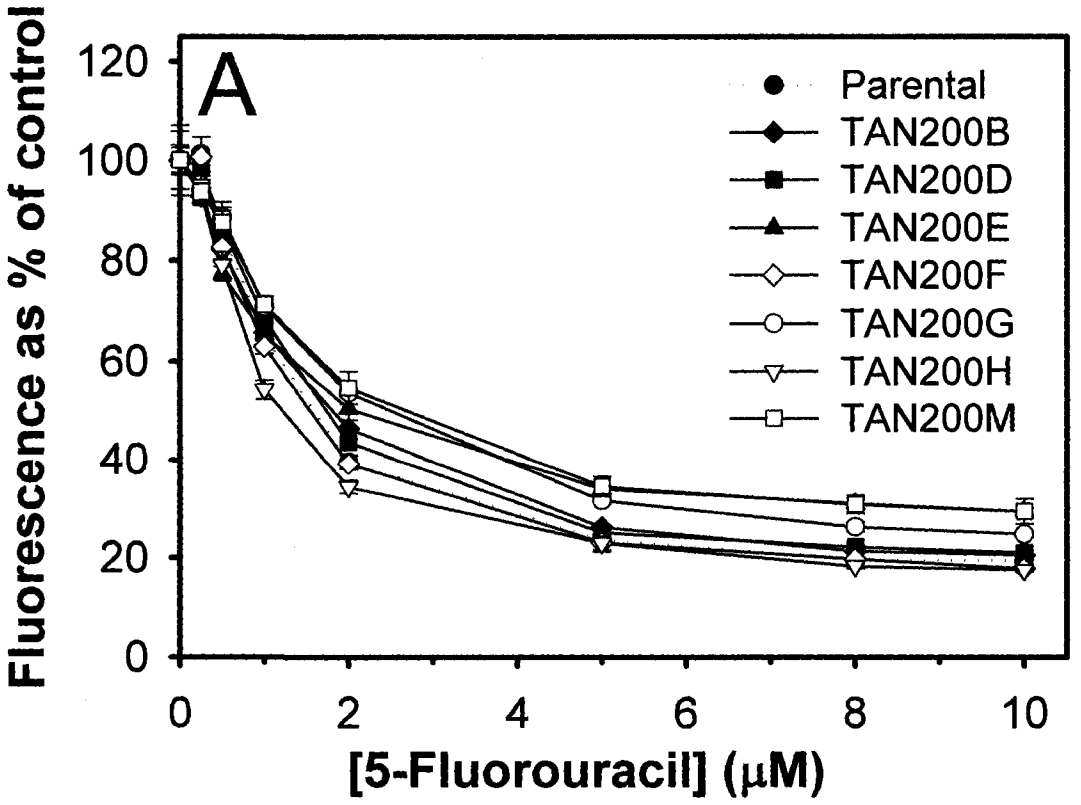
A
Parental
TAN200B
TAN200D
TAN200E
TAN200F
TAN200G
TAN200H
TAN200M
Fluorescence as % of control
120
100
80
60
40
20
0
0
2
4
6
8
10
[5-Fluorouracil] (μM)

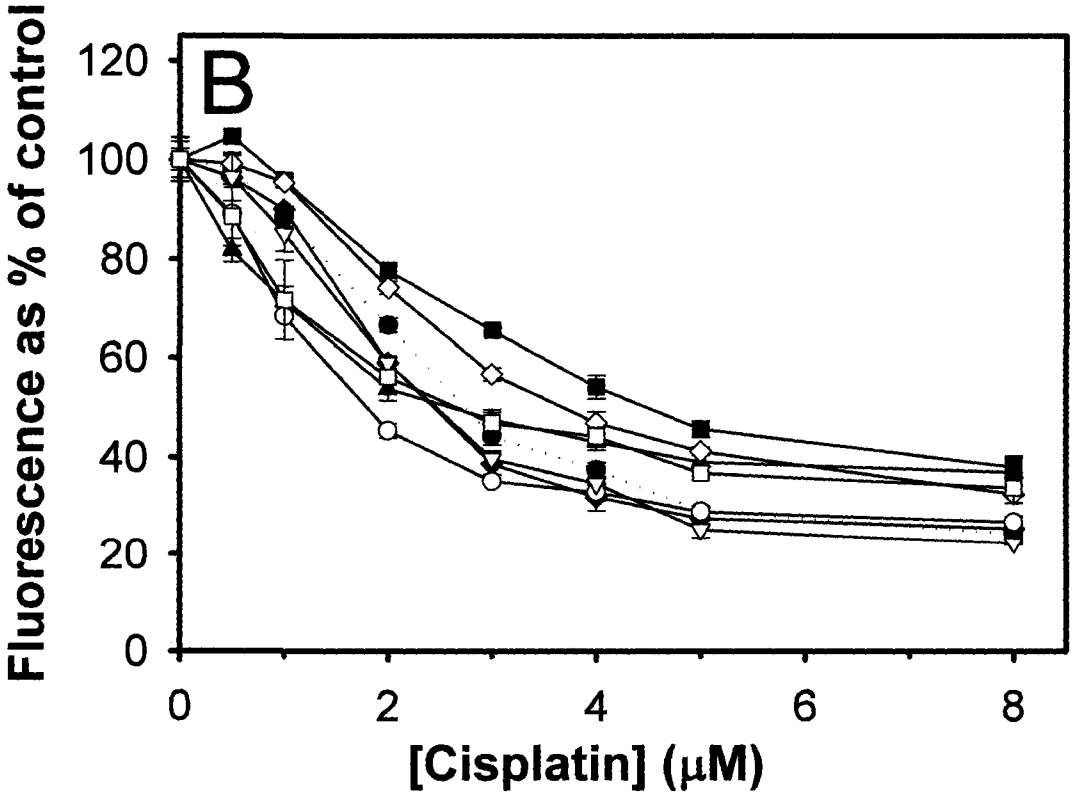
B
Fluorescence as % of control
120
100
80
60
40
20
0
0
2
4
6
8
[Cisplatin] (μM)

Figure 32 con't. Dose response of MDA-MB-435 parental and tangeretin-selected cells to chemotherapy drugs. MDA-MB-435 parental (●) and 7 MDA-MB-435 tangeretin-selected cell lines (TAN200B: ♦, TAN200D: ■, TAN200E: ▲, TAN200F: ◊, TAN200G: ○, TAN200H: ▽, TAN200M: □) were treated for 4 d with vincristine sulphate (C: 0-2.5 nM) or taxol (D: 0-8 nM). Metabolic activity was quantified using the alamarBlue™ assay as described in *Materials and Methods*. Fluorescence was baseline adjusted and is expressed as a percent of control ± SEM. The data shown were combined from 2-3 independent experiments.

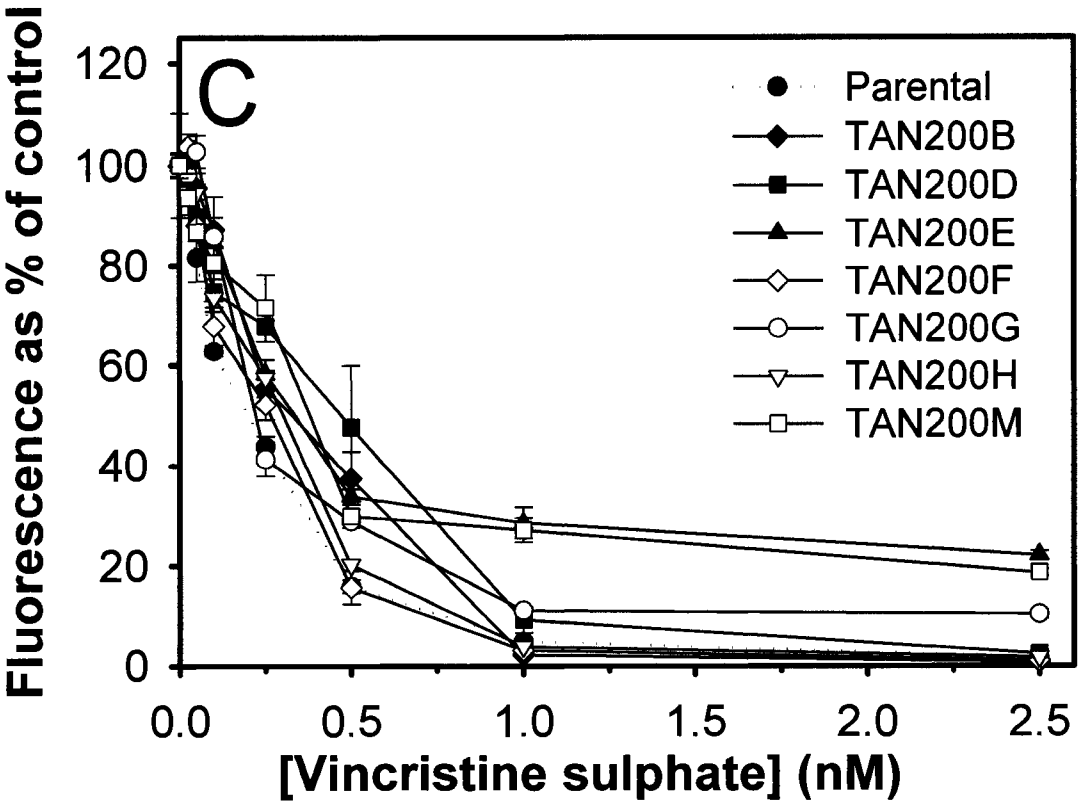
C
Parental
TAN200B
TAN200D
TAN200E
TAN200F
TAN200G
TAN200H
TAN200M
Fluorescence as % of control
120
100
80
60
40
20
0
0.0
0.5
1.0
1.5
2.0
2.5
[Vincristine sulphate] (nM)

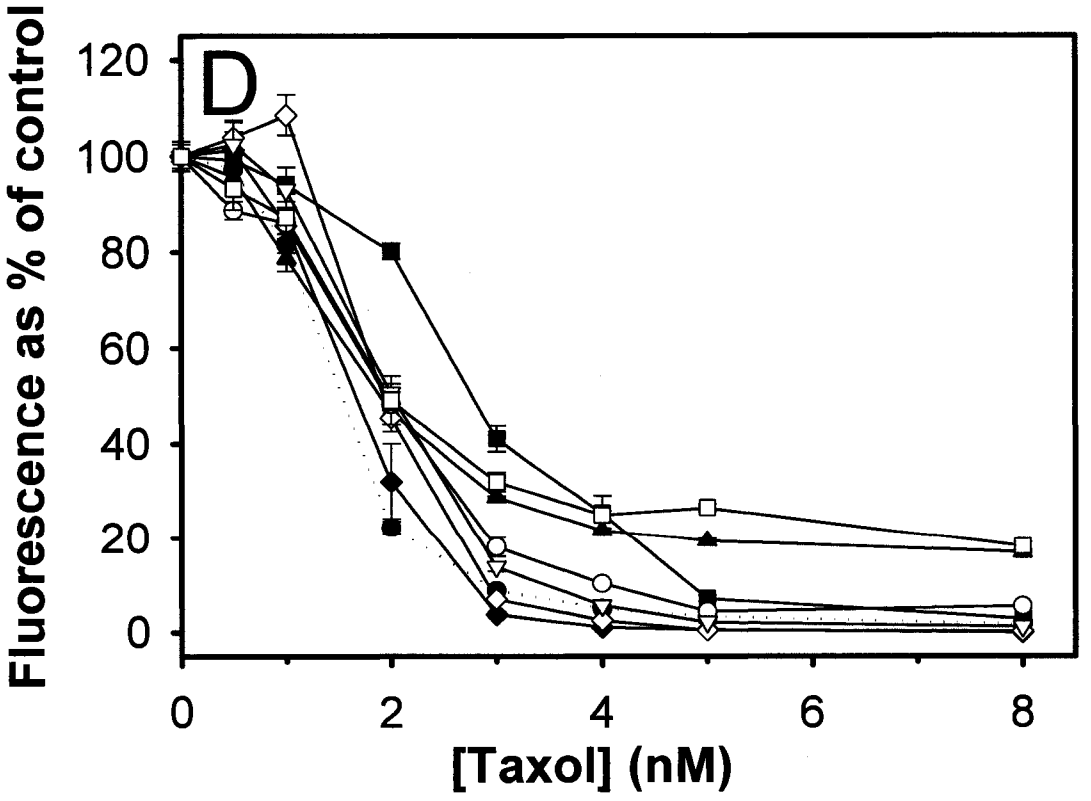
D
Fluorescence as % of control
120
100
80
60
40
20
0
0
2
4
6
8
[Taxol] (nM)

Table 26. IC_{50} values for cancer chemotherapy drugs in MDA-MB-435 parental and tangeretin-selected cells. The concentrations at which proliferation of 5-fluorouracil-, cisplatin-, vincristine- and taxol-treated cells were inhibited by 50% compared to untreated control were taken from 2-3 independent dose response curves and are expressed as mean ± SEM. [a]Significantly different from parental cells (one-way ANOVA, $P \leq 0.05$).

Cell Line	Cheomotherapeutic Drug			
	5-Fluorouracil (μM)	**Cisplatin (μM)**	**Vincristine sulphate (nM)**	**Taxol (nM)**
MDA-MB-435	1.75±0.16	2.52±0.12	0.26±0.04	2.52±0.12
Tan200B	1.68±0.08	2.70±0.30	0.33±0.00	2.70±0.30
Tan200D	1.63±0.06	4.55±0.10	0.42±0.04[a]	4.55±0.10[a]
Tan200E	2.60±0.60	2.65±0.15	0.42±0.09	2.65±0.15
Tan200F	1.50±0.06	4.08±0.19	0.29±0.01	4.08±0.19[a]
Tan200G	1.87±0.19	1.58±0.18	0.26±0.05	1.58±0.18
Tan200H	1.35±0.13	3.20±0.38	0.30±0.00[a]	3.20±0.38
Tan200M	4.33±1.58[a]	2.50±0.20	0.53±0.15	2.50±0.20

Figure 33. Confirmation of vincristine resistance for the head and neck cell lines. HN-5a (●), HN-5aV5f (○), and HN-5aV15e (▼) cells were treated with a range of concentrations of vincristine sulphate for 4 d and cell numbers were determined as described in *Materials and Methods*. Mean cell numbers from quadruplicate measurements are expressed as a percent of control ± SEM. The data shown were combined from three independent experiments. *Significantly different from the parental cell line (one-way ANOVA, $P \leq 0.05$).

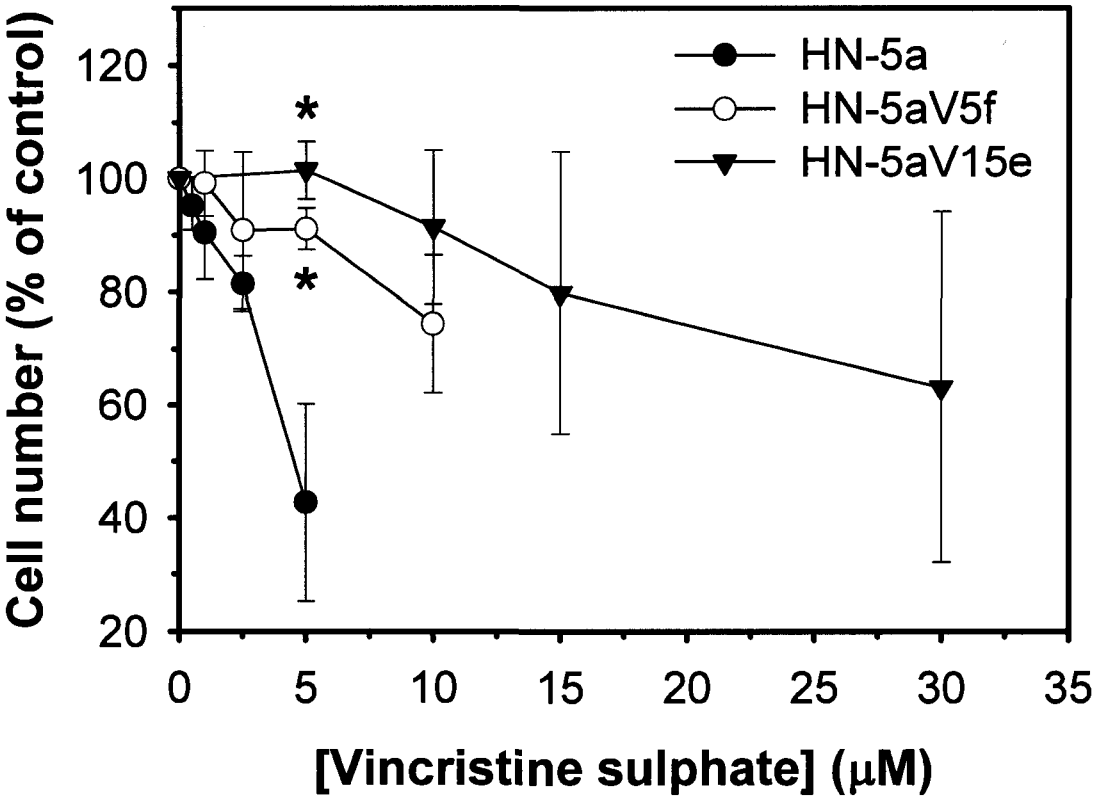
Cell number (% of control)
120
100
80
60
40
20
0
5
10
15
20
25
30
35
[Vincristine sulphate] (μM)
HN-5a
HN-5aV5f
HN-5aV15e
*
*

Figure 34. Dose-dependent inhibition of proliferation by tangeretin and nobiletin in HN-5a (A), HN-5aV5f (B) and HN-5aV15e (C) cells. Cells were treated for 4 d with tangeretin (○), nobiletin (▼) or DMSO vehicle control (●), and cell numbers were determined as described in *Materials and Methods*. Mean cell numbers from quadruplicate measurements are expressed as a percent of control ± SEM. The data shown were combined from three independent experiments. Where error bars are not apparent, they are smaller than the symbol. *Significantly different from DMSO vehicle control (one-way ANOVA, $P \leq 0.05$). Tan: tangeretin (0-50 μg/ml or 0-134 μM), Nob: nobiletin (0-50 μg/ml or 0-124 μM).

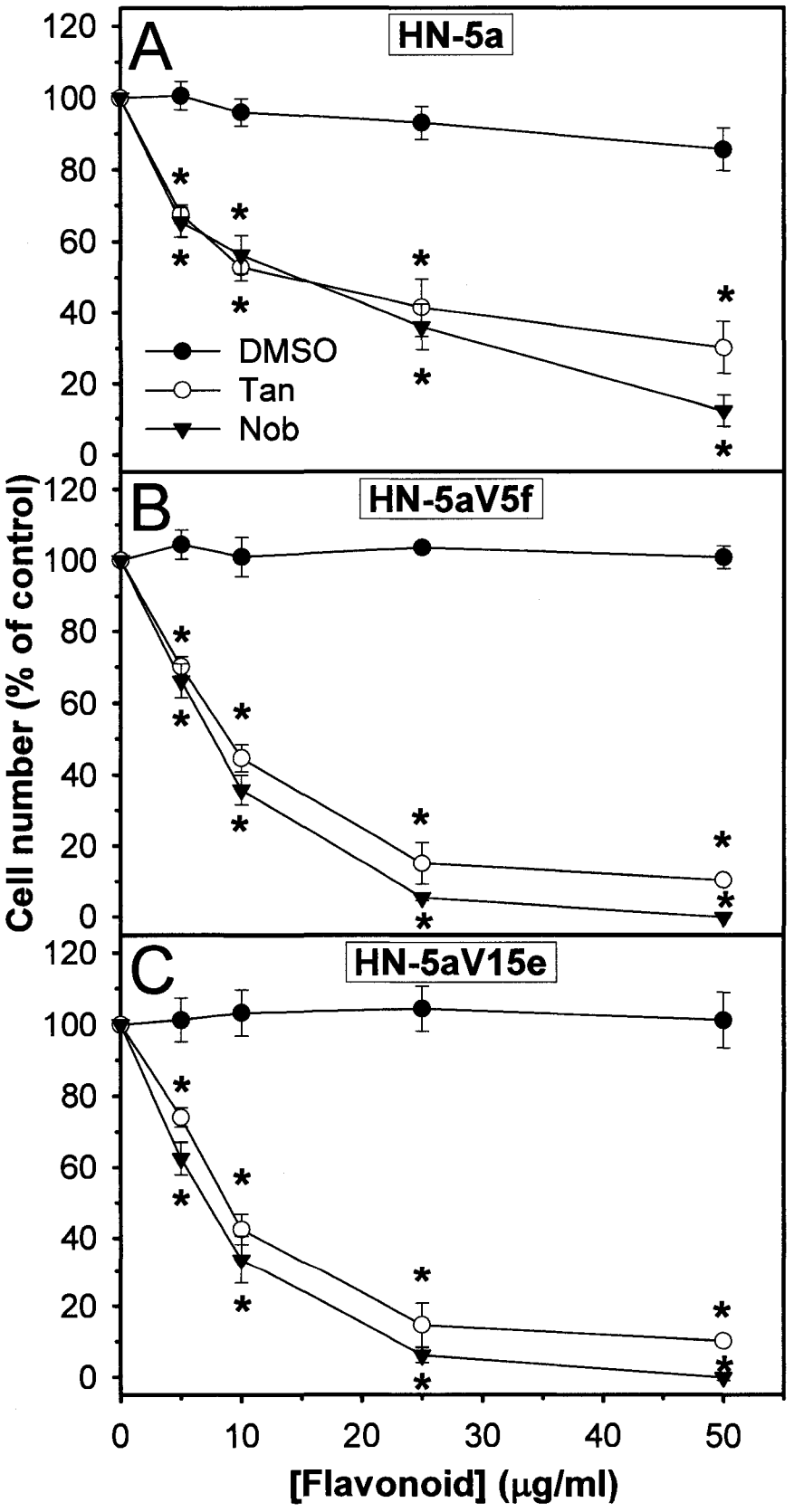
A
HN-5a
B
HN-5aV5f
C
HN-5aV15e
DMSO
Tan
Nob
Cell number (% of control)
[Flavonoid] (μg/ml)
0
20
40
60
80
100
120
0
10
20
30
40
50

Chapter 4
DISCUSSION

4.1. Tangeretin and nobiletin susceptible cell lines

4.1.1. Tangeretin and nobiletin inhibit proliferation of cancer cells

The antiproliferative effect of tangeretin and nobiletin was investigated in two breast cancer cell lines (MDA-MB-435 and MCF-7) and a colon cancer cell line (HT-29). Cell lines of varied tissue origins were selected to assess the universality of the antiproliferative mechanism of action. Structurally, tangeretin and nobiletin differ only in the presence of an extra methoxy group (in nobiletin). Studying them in tandem has the added benefit of highlighting common cellular and molecular effects.

Both tangeretin and nobiletin effectively inhibited proliferation of human breast and colon cancer cell lines in a dose- and time-dependent manner. Tangeretin (with IC_{50} values lower than those for nobiletin in all three cancer cell lines) inhibited proliferaction more effectively than nobiletin. This is consistent with a study by Manthey *et al.* who reported lower IC_{50} values for tangeretin compared with nobiletin in six cancer cell lines including the ones utilized in this study (MDA-MB-435, MCF-7 and HT-29) [178]. The greater efficacy of tangeretin is also documented in studies utilizing colorectal cancer [211], lung cancer, melanoma, leukemia and gastric cancer cell lines [144]. The IC_{50} values for tangeretin and nobiletin obtained in the Manthey study in MDA-MB-435, MCF-7 and HT-29 cells were lower than obtained in the present study (for tangeretin: 0.34-1.6 μM vs. 34.9-43.5 μM, respectively; and for nobiletin: 1.2-4.7 μM vs. 36.8-63.9 μM, respectively) suggesting slightly greater antiproliferative effects. The difference in potency could be due to differences in the purity of compounds (i.e. the presence of minor constituents), and/or differences in growth conditions used to maintain cell lines. Other published IC_{50} values for tangeretin and nobiletin, from different cell lines, are closer to the values obtained in this study (37.5 and 66.2 μM, respectively [211]; and 6.5-12 μM and 8.3-22 μM, respectively [144]).

Although tangeretin is a more effective inhibitor of proliferation, there was no significant difference between tangeretin and nobiletin in the time required to observe antiproliferative effects. Both exerted growth inhibitory effects on MDA-MB-435, MCF-7 and HT-29 cells within 12 h of administration, continuing up to 4 days. Similar results were reported for the inhibition of proliferation of colorectal cancer cells by tangeretin beginning 12 h after treatment and lasting up to 48 h [211]. Other studies typically did not assess inhibition of proliferation at earlier time points, but did establish inhibition of proliferation at 24 h [116,317], 48 h [178,312], 72 h [207,308], and up to 7 days [138] following addition of tangeretin or nobiletin to cells.

4.1.2. Tangeretin and nobiletin inhibit proliferation of normal cells

Non-transformed human umbilical vein endothelial cells (HUVEC) were utilized to assess whether the antiproliferative effect of tangeretin and nobiletin is specific to cancer cells. The IC_{50} values for tangeretin and nobiletin in this normal, non-tumorigenic cell line were not significantly different from those in the tumor cell lines indicating that, in this study, the antiproliferative effects of tangeretin and nobiletin were not specific to cancer cells. This contrasts with findings from a study by Kawaii *et al.* who determined the antiproliferative activity of a panel of 28 citrus flavonoids in four human and mouse cancer cell lines (melanoma, leukemia, lung, and gastric cancer), and two non-transformed lines (human foreskin keratinocytes (HFK) and HUVE cells) [144]. The antiproliferative activity of 7 flavonoids (including tangeretin and nobiletin) toward the normal cell lines were found to be 10% of that of the antiproliferative activity toward all tumor cell lines, demonstrating weak antiproliferative activity toward normal cells. Another study found tangeretin, nobiletin, quercetin and taxifolin exerted a weak growth inhibitory effect against normal human embryonic fibroblast-like cells compared to cancer cells [137]. Cancer specific antiproliferative effects are demonstrated by other flavonoids. Wogonin, a hydroxyy-methoxy-flavone inhibited proliferation of human monocytic leukemia (THP-1) and osteogenic sarcoma (HOS) cells but not human fetal lung normal diploid cells (TIG-1) [115]. Differential growth inhibition was observed for epigallocatechin gallate between

virally transformed fibroblasts (WI38VA), colorectal cancer cells (Caco-2), breast cancer cells (Hs578T), and their respective normal counterparts [46]. This evidence from *in vitro* studies suggests the proliferation of normal, non-transformed cells is less affected than cancer cells by treatment with flavonoids, including tangeretin and nobiletin.

More convincing evidence of the selectivity of flavonoids for tumors comes from studies using whole animal human xenograft models showing an antiproliferative effect on tumors but a lack of toxic effects in non-diseased, normal organs and tissues. Dietary feeding of silibinin, a flavanone from milk thistle, significantly inhibited the growth of prostate cancer tumors in nude mice without any apparent signs of toxicity to non-tumor tissues over 60 d [255]. Furthermore, in a safety study of oral tangeretin in mice with daily intakes equivalent to 0.28 g in humans (equivalent to 40 μM *in vitro* exposure, assuming equal dilution throughout the body), no signs of liver, kidney or pancreas toxicity were found (assessed by biochemical measurements) following four weeks of tangeretin consumption [284]. There was no anticancer component to this study, however, it does show that tangeretin is not toxic to non-diseased organs at concentrations known to have inhibitory effects on tumor cells. Overall, literature evidence supports a decreased antiproliferative effect of flavonoids on normal, non-tumor cells and tissues, contrary to findings from the present study.

However, it is not unexpected that tangeretin and nobiletin inhibited the proliferation of HUVECs as well as cancer cells in the present study. HUVECs are endothelial cells which are dependent upon vascular endothelial growth factor (VEGF) for growth and differentiation [167]. VEGF is an important mitogen in angiogenesis and vasculature development [36] and flavonoids have been reported to inhibit VEGF production resulting in anti-angiogenic effects and inhibition of proliferation *in vitro* and *in vivo* [131,151,238,245,256]. Thus, in the present study, tangeretin and nobiletin could be exerting an anti-angiogenic effect, contributing to the overall antiproliferative effect on HUVECs.

4.1.3. Inhibition of proliferation is mediated by effects on cell cycle and apoptosis

Tangeretin- and nobiletin-treated MDA-MB-435, MCF-7 and HT-29 cells were investigated for changes in cell cycle distribution. Tangeretin (54 μM) induced significant accumulation (10-20%) of cells in the G1 or S phase of the cell cycle in all three cell lines within 24 h of administration. Although cell line specific differences in cell cycle distribution were observed in response to tangeretin. For example, HT-29 cells accumulated in S rather than G1 after 24 h, whereas both breast cancer cell lines accumulated in G1 rather than S phase. This accumulation of HT-29 cells in S phase was transient and G1 accumulation (and S phase depletion) ensued at 48 and 72 h of tangeretin exposure in all three lines. Nobiletin had a similar effect, at concentrations ranging from 60-200 μM, with the same HT-29-specific transient S-phase accumulation and G1 depletion at 24 h, at the lowest concentration (60 μM) of nobiletin. The early accumulation of HT-29 cells in S phase disappears with longer treatment periods and is not observed at higher concentrations of nobiletin. Induction of G1 accumulation by tangeretin and nobiletin in this study is consistent with previous reports of G1 arrest induced by tangeretin in COLO 205 human colorectal tumor cells [211] and nobiletin in TMK-1 gastric tumor cells [312].

Tangeretin and nobiletin have also been reported to induce G2/M phase accumulation in HL-60 promyelocytic leukemia [116] and in HepG2 hepatocellular cancer [207] cell lines, respectively. This effect was not evident in the breast and colon cancer cell lines assessed in this study. All concentrations of tangeretin or nobiletin had no consistent effect on the percentage of cells in G2/M. The occurrence of G1 or S or G2/M accumulation in response to tangeretin or nobiletin treatment appears to be a cell line specific phenomenon in which the outcome can be influenced by the degree of change in expression of cell cycle regulatory molecules. For example, Ohnishi *et al.* found nobiletin downregulated the expression of both cyclin E2 and cyclin B1 (G1- and G2/M-type cyclins, respectively), resulting in G2/M arrest in HepG2 cells [207]. Yet, in

the present study, tangeretin downregulated the expression of the same two cyclins in MDA-MB-435 cells, and in this instance it resulted in G1 arrest. The different response could be due to a higher downregulation of cyclin B1 compared to cyclin E2 in the former case, and more downregulation of cyclin E2 in the latter. While both flavonoids decreased expression of the same molecular targets, availability and tolerance to modulation of those targets in each cell line potentially accounts for the different cell cycle distribution.

Concentration of flavonoid is another factor influencing the cell cycle phase in which cells accumulate. For example, treatment of nasopharyngeal cancer cells with quercetin induced accumulation in G2/M at a lower concentration (14.8 μM) and in G1 at a higher concentration (52.1 μM) [208]. In contrast, silibinin induced accumulation in G1 at lower concentrations (50 and 75 μg/ml) and in both G1 and G2/M phases at a higher concentration (100 μg/ml) [2]. In the present study transient S-phase accumulation was observed in HT-29 cells treated with the lower concentration of nobiletin (60 μM) followed by G1 accumulation at later time points and a higher concentration (200 μM). The lower concentration of nobiletin may downregulate the expression of G1/S regulatory molecules sufficient to induce S phase accumulation but insufficient for G1 phase accumulation. At higher concentrations, or over time with accumulation of nobiletin within these cells, G1 regulatory molecules may have been downregulated enough to induce G1 phase accumulation. This suggests that the amount of flavonoid available to affect changes may influence the degree of change in expression of cell cycle regulatory molecules and thus where cells accumulate in the cell cycle.

In addition to cell cycle arrest, both flavonoids were reported to induce apoptosis *in vitro*. Nobiletin has been reported to induce apoptosis in human TMK-1 gastric [312], HepG2 hepatocellular [207] and Colo 320 colorectal [317] cancer cell lines. Tangeretin has been reported to induce apoptosis in HL-60 leukemia cells [116] which have been suggested to be particularly susceptible to damage and death [66]. Further reports of tangeretin effects on apoptotic events

are sparse, likely due to its hydrophobic nature which limits its solubility in water to concentrations of 50-60 μM or less, a feature shared, to a lesser degree, by nobiletin. In the present study, neither flavonoid induced apoptosis in any of the tumor cell lines at the lower of the two concentrations tested. However, nobiletin did induce cell death in MDA-MB-435 cells (at 100 μM), and both apoptosis and cell death in all three cell lines at the highest concentration (200 μM). Nobiletin-induced cell death in MDA-MB-435 cells at 100 μM was not statistically significant when apoptotic and dead populations were combined for a total measure of dead and dying cells. The occurrence of apoptosis at the higher concentration of nobiletin in all three cell lines is consistent with the concentrations of nobiletin reported to induce apoptosis in gastric, hepatocellular and colorectal cancer cells [207,312,317], with the exception of one qualitative report of apoptosis in a gastric tumor cell line after treatment with 60 μM nobiletin [312], the lowest concentration used in the present study. These results suggest that at concentrations that have profound inhibitory effects on proliferation of MDA-MB-435, MCF-7 and HT-29 cells, apoptosis was not required for significant inhibition of proliferation by tangeretin and nobiletin, even though nobiletin was capable of inducing cell death or apoptosis at high concentrations.

The effect of tangeretin in the three cell lines can be classified as cytostatic (i.e. the ability to inhibit proliferation without inducing damage likely to delay or suppress growth and/or survival). Tangeretin induced G1 cell cycle accumulation without inducing apoptosis. The classification of nobiletin was not so clear. Nobiletin induced cell cycle accumulation at lower concentrations, and cell cycle accumulation with apoptosis at higher concentrations. Nobiletin had a concentration-dependent cytostatic and/or cytotoxic effect in all three cell lines. The EGFR inhibitor, Iressa (gefitinib, ZD1839), had a similar concentration-dependent cytostatic/cytotoxic effect in ovarian, breast and colon cancer cell lines [52] and is widely regarded as a cytostatic agent [149]. The classification of the effects of tangeretin and nobiletin as cytostatic or cytotoxic is useful in light of their potential as cancer chemotherapies. However, determining the reversibility of antiproliferative effects of these compounds on cancer cells was pursued to

add further depth to these classifications. Four day growth-inhibited cells were removed from tangeretin or nobiletin treatment to flavonoid- and DMSO-free growth media, and proliferation was assessed for an additional four days. When flavonoid-treated (54-100 μM), growth-inhibited cells were re-cultured in flavonoid-free medium, cells recovered their ability to proliferate and regained cell cycle distribution comparable to controls within one day of flavonoid removal. Resumption of proliferation and cell cycling was assessed at 24 h intervals starting one day after flavonoid removal, continuing to 4 days. Therefore, it is not possible to determine whether cells recovered earlier than one day after flavonoid removal. These data support the observation of a cytostatic effect for both flavonoids when administered at lower concentrations. With a cytostatic effect on tumors, cellular proliferation can be reduced or halted while cell viability remains intact. Inhibition of proliferation of tumor cells without inducing cell death could potentially reduce cytotoxicity to normal, non-tumor host cells, particularly if those normal tissues are low- or non-proliferating. Normal tissues with high rates of proliferation (e.g. intestinal epithelial crypt cells and hepatic and hematopoietic precursor cells) could conceivably be affected by these compounds, but there is evidence to support the selectivity of these flavonoids against tumor cells (see Section 4.1.1).

Although a high concentration of nobiletin (200 μM) induced both cell cycle accumulation and apoptosis (a cytotoxic response) in all three cell lines, these cells were still able to recover and proliferate comparable to control when re-cultured in flavonoid-free media. This is in contrast to findings for the PKC inhibitor UCN-01 [219]; when re-cultured in drug-free media, glioma cells only resumed proliferation following short-term exposures (6-24 h) to UCN-01. Longer periods of exposure to UCN-01 severely compromised recovery of proliferative activity in the glioma cells. The recovery of cells treated with high levels of nobiletin suggests that the surviving cells were not permanently or irreversibly damaged. Further, if the antiproliferative effects of flavonoids are tumor-specific as suggested by the literature, then apoptotic effects at higher concentration are desirable; however, if flavonoids do have an effect on non-tumor tissues, a lower

concentration cytostatic response would still be achievable and effective. Regardless of the type of effect (cytostatic or cytotoxic), cells treated with tangeretin or nobiletin, at all concentrations tested in this study, were able to quickly recover and proliferate following flavonoid removal.

The resumption of baseline proliferative and cycling capabilities by tumor cells following flavonoid removal implies that continuous exposure to these flavonoids is required for sustained inhibition of tumor proliferation. Cytostatic small molecule ERK inhibitors are faced with similar challenges [155]. However, they have been effectively combined with cytotoxic agents to improve anticancer efficacy. As anticancer therapies, flavonoids could be used in a similar way (combination therapy) to maximize anticancer effect. The implication of reversible antiproliferative effects for non-tumor tissues potentially affected by flavonoids is that they would be expected to recover and regain function after the cessation of treatment.

4.1.4. Molecular determinants of tangeretin and nobiletin induced cell cycle accumulation and apoptosis

Initially, a "top-down" approach was adopted to investigate the anticancer mechanism(s) of tangeretin and nobiletin. At the cellular level, inhibition of cancer cell proliferation by these flavonoids was mediated by induction of cell cycle accumulation and/or cell death. This led to an investigation of the molecular basis for the observed effects on cell cycle and apoptosis. The expression of a panel of cell cycle and apoptosis regulatory genes was evaluated using semi-quantitative RT-PCR following exposure to tangeretin and nobiletin. The results of these analyses were found to be inconsistent after numerous repeats (4-6), so a "bottom-up" approach was adopted. In this approach, a global analysis of gene expression without focus on specific classes of genes was performed using microarray technology. Three separate array analyses were performed using RNA from three separate experiments. Results from these analyses were validated by a single real-time RT-PCR experiment using RNA from a fourth experiment, different from those utilized for microarray analysis. Findings from

the bottom-up approach will be discussed including a brief discussion of findings from the top-down (semi-quantitative) approach.

The semi-quantitative analysis of gene expression (using conventional RT-PCR) in MDA-MB-435, MCF-7 and HT-29 cells following exposure to tangeretin and nobiletin was employed to determine expression changes in a panel of cell cycle and apoptosis regulatory genes. Changes in these genes could explain the observed effects of these compounds on cell cycle and apoptosis. Additionally, global analysis of expression of over 22,000 genes, including cell cycle and apoptosis regulatory genes, was performed using oligonucleotide array analysis in MDA-MB-435 cells following short-term exposure to tangeretin alone. Quantitative real-time RT-PCR analysis was utilized on a small subset of genes to validate microarray results. Results from the semi-quantitative analysis of gene expression in MDA-MB-435, MCF-7 and HT-29 cells following exposure to tangeretin and nobiletin were inconsistent among individual repeats within the experiment. They were also inconsistent with results from microarray and real-time RT-PCR analysis. For example, CCNE2 expression in MDA-MB-435 following tangeretin treatment was found to be unchanged using semi-quantitative RT-PCR but was downregulated when assessed by both microarray analysis and quantitative real-time RT-PCR. For RT-PCR to be quantitative, measurements must be made during the exponential phase of the amplification reaction which does not last very long [222]. The exponential phase eventually plateaus into a saturated phase where products may approach similar levels regardless of initial copy numbers. The limitation of conventional RT-PCR is due to the relative insensitivity of the detection method namely, gel electrophoresis with ethidium bromide staining, whereby product often has to be amplified to the saturation phase to be detectable, making this technique at best qualitative. This limitation in the detection method of conventional RT-PCR products is potentially the reason inconsistent results were obtained for the expression of cell cycle and apoptosis regulatory genes in the three cell lines following flavonoid treatment. Those results were reported, however microarray data will be used for the

purposes of defining a molecular basis for the antiproliferative activity of the flavonoids.

To study gene expression, microarray analysis offers several advantages over other methods of determining RNA expression such as northern blots, and RNase protection assays. It is fast, sensitive and most importantly, it allows the determination of expression of a vast number of genes in a single experiment [313]. It is not necessary to know what genes or mechanisms are important beforehand because arrays offer a broader, more complete and less biased view of cellular response. Some disadvantages include cost which limits access to the technique, and a lack of rigorous standards for data collection, analysis and validation [231]. In the present study, Affymetrix oligonucleotide arrays were used to assess changes in gene expression following short-term exposure to tangeretin. Due to the costliness of oligonucleotide arrays, microarray analysis (three separate repeats) was only performed for one cell line (MDA-MB-435) exposed to one flavonoid (tangeretin) at a single time point (6 h). Tangeretin was selected for these experiments due to the more potent antiproliferative effect on tumor cells (compared to nobiletin), and the 6 h time point was chosen to allow assessment of immediate early responders to tangeretin exposure. A vast amount of data was generated and presented in its entirety (see Appendix I). However, only gene expression changes consistent with the observed cell cycle and apoptosis effects of tangeretin in MDA-MB-435 cells were explored. Any changes discussed are specific to this cell line and these conditions.

To briefly re-cap cell cycle regulation, cell cycle progression is controlled by the activity of cyclin-dependent kinases and their regulatory subunits, called cyclins [165]. Progression through the early stages of G1 is controlled by Cdk4 and Cdk6 which associate with D-type cyclins. Cyclin D-Cdk complexes phosphorylate Rb leading to the expression of Cyclin E-Cdk2 complexes mid to late G1 and is required for progression to S phase and DNA synthesis [248] (Figure 6). Negative regulation of cyclin/Cdk complexes occurs through two families of Cdk inhibitors called INK4 (Cdk4 and Cdk6 inhibitors: p15, p16, p18 and p19) and CIP/KIP (Cdk2 inhibitors: p21 and p27). G1 accumulation is

associated with downregulation of cyclins and Cdks [234], upregulation of Cdk inhibitors [45], and downregulation of components of the ubiquitin degradation system [35,249].

Tangeretin induced accumulation of cells in the G1 phase of the cell cycle, resulting in significant inhibition of proliferation of MDA-MB-435 cells. Microarray analysis, following short-term exposure of MDA-MB-435 cells to tangeretin, revealed gene expression changes consistent with accumulation in G1, including downregulated expression of G1-specific cyclins CCNE1 and CCNE2, as well as components of the SCF complex (CDC34, CUL3, UBE2C and SKP2) involved in ubiquitin mediated degradation of cyclins, Cdks and CKIs. Downregulation of these SCF components results in decreased ubiquitination of Cdks, cyclins and CKIs and thus stabilization of protein levels. For example, Vitamin D3 induced G1 arrest by downregulating levels of cyclin E and associated kinase activity resulting in decreased phosphorylation of p27 which led to decreased interaction of p27 with Skp2 and thus, decreased degradation [169]. Vitamin D3 also decreased the expression of Skp2 resulting in p27 stabilization. In another study, Rb was found to repress Skp2 expression resulting in the stabilization of p27, allowing the inactivation of cyclin-Cdk complexes and subsequent G1 arrest [130]. Some expression changes appeared to counteract G1 accumulation, such as the downregulation of mRNA expression of Cdk inhibitors CDKN1B (p27) and CDKN2D (p19). Shibahara *et al.* reported both increased and unchanged p27 mRNA levels in conjunction with increased levels of protein, depending on the cell line [249]. Since neither protein levels nor activity were assessed in this study, it is impossible to say whether these changes at the mRNA level translate to changes at the protein level. However, as mentioned above, downregulation of SCF components could result in the stabilization of these CKIs. Exposure to tangeretin decreased expression of cyclins E1 and E2, and ubiquitin ligase components in MDA-MB-435 cells leading to accumulation in the G1 phase of the cell cycle which ultimately resulted in the inhibition of proliferation observed in these cells.

The antiproliferative activity of tangeretin could also involve induction of cell death or apoptosis as discussed in the introduction. Apoptosis or programmed cell death can be triggered through an intrinsic (mitochondrial) or extrinsic (death receptor) pathway [132] (Figure 7). Apoptosis *via* the intrinsic pathway requires neutralization of anti-apoptotic Bcl-2 family members (including Bcl-2, Bcl-2l2 or Bcl-w, Bcl-x_L, Mcl-1) through association with pro-apoptotic BH3-only family members (such as Puma, Noxa, Bmf, Bik, Bok, Bid, Bad, Bim), and permeabilization of the mitochondrial membrane by other pro-apoptotic Bcl-2 family members (such as Bax, Bak), leading to cytochrome c release and assembly of the apoptosome which is involved in caspase activation [44,90]. Caspases are the initiators and effectors for apoptosis induced *via* the intrinsic or extrinsic pathway [76]. Homeostasis is maintained by balanced expression of pro- and anti-apoptotic members of the Bcl-2 family [215].

The antiproliferative activity of tangeretin in MDA-MB-435 cells did not involve induction of apoptosis or cell death. Gene expression changes consistent with the lack of induction of apoptosis by tangeretin included downregulation of the pro-apoptotic BAK1 and BAD, initiator caspase 2 and executioner caspase 6, and a component of the apoptosome, APAF1. Also consistent with the lack of apoptosis was the upregulation of TNFAIP3 (A20) which is an anti-apoptotic protein [186]. Several other anti-apoptotic genes (e.g. BCL-2L2 or BCL-w, BAG2 and HSP70) were downregulated, instead of upregulated which would be more consistent with the absence of apoptosis. However, it has been reported that loss of Bcl-w expression did not sensitize granulocytes to apoptosis induced by cytokine withdrawal or cytotoxic stress [288], suggesting a redundancy in its function as an anti-apoptotic protein. Thus, downregulation of Bcl-w does not necessarily shift the balance towards apoptosis as other anti-apoptotic Bcl-2 family members could be compensating for Bcl-w. Upregulation of Hsp70 increases the ability of cells to cope with increased concentrations of unfolded or denatured proteins in stress-induced apoptosis [203]. The decrease in Hsp70 mRNA expression suggests that such conditions were not in effect in the present study, thereby eliminating the need to upregulate Hsp70. Bag2 is a negative

regulator of heat shock proteins and not much is known about its involvement in apoptosis. Overall, the expression changes observed by microarray analysis for apoptosis-related genes in response to tangeretin were consistent with a lack of apoptosis, strengthening the observation that tangeretin did not induce apoptosis in MDA-MB-435 cells.

4.1.5. Physiological relevance of concentrations used

A common concern with *in vitro* studies of dietary compounds is the relevance of concentrations of compounds used in tissue culture to concentrations achievable in the body. The concentrations of flavonoids utilized in this study were comparable to the levels achievable *in vivo*, attained through consumption of concentrated flavonoid supplements by rodents. For example, in hamsters fed a 1% tangeretin, tangeretin/nobiletin or polymethoxylated flavone diet, total tangeretin and tangeretin metabolites reached levels equivalent to 16-67 μM intact tangeretin in the liver and 21 μM in serum, following 35 d of feeding [160]. Since the liver is responsible for the majority of flavonoid metabolism (see section 1.2.5), it is within expectation to find higher concentrations there, as well as in circulation en route to and from the liver (in serum). Cells in tissue culture are not exposed to as many different metabolites as they would be in the body. However, *in vivo* it is important that measurement of metabolites be included because there is increasing evidence that metabolites may contribute to the bioactivity of flavonoids (see section 1.2.5). The concentration of tangeretin used in the current study (54 μM) is within the range reported by Kurowska *et al.* [160] and inhibited human tumor cell growth by 60-75%. Little information on relevant *in vivo* concentrations of nobiletin has been reported. However, the nobiletin concentrations utilized for this study (60-100 μM) were selected to yield similar inhibition of growth of human tumor cell lines as those of tangeretin (the highest concentration of nobiletin, 200 μM, was selected to determine dose dependency of the cellular effects examined). For tangeretin (and likely nobiletin as well due to the structural similarity), exposure to levels achievable *in vivo* inhibited growth of human tumor cell lines originating from two tissue types (breast and colon).

4.2. Flavonoid resistance

4.2.1. Flavonoid or DMSO selected

Flavonoids exist as minor constituents of the human diet but due to their anticancer activity they may have potential use in cancer chemotherapy. It is thus essential to increase knowledge about their potential and possible limitations as therapeutic agents. A common limitation to the success of many therapeutic agents is resistance (acquired or inherent). Therefore, efforts were made to develop flavonoid-resistant populations, first, to determine if this were possible, and second, to use resistant populations to study anticancer mechanisms of tangeretin and nobiletin, hypothesizing that cellular and molecular changes would be the reverse of those observed in flavonoid-susceptible lines.

The procedure used to select flavonoid-resistant populations is a modification of a previously published method used in the Koropatnick lab to select carboplatin- [78] and 5-FUdR-resistant [79] cells. Cells were exposed to continuous (not incrementally increased) concentrations of flavonoids for up to 8 weeks. Concentrations were increased until arrival at a concentration where a small population of cells survived and proliferated as colonies (new cells were used for each new concentration). Selecting flavonoid-resistant populations in this manner may have limited the degree of resistance that was attainable. That is, it may have been possible to obtain more highly-resistant cells had the same batch of cells been used from start to finish, with incremental increases in the concentration of flavonoid on those cells, allowing the cells to become acclimatized to each concentration. It is possible that there might have been more cells that survived 100 μM nobiletin, for instance, if they were exposed sequentially to 5 μM, 10 μM, 30 μM, and so on, up to 100 μM, as opposed to 100 μM outright. On the other hand, utilizing such a rigorous selecting condition from the outset could have yielded a more hardy population of cells that are able to withstand the more potent anticancer activity of flavonoids at higher concentrations.

Selection of flavonoid-resistant populations was successful for nobiletin for all three cell lines but only for one cell line exposed to tangeretin (MDA-MB-435). The tangeretin-resistant MDA-MB-435 cell line was the first to be selected, therefore a repeat selection of this cell line was attempted first. Efforts to repeat selection of tangeretin-resistant MDA-MB-435 cells with the same concentration of tangeretin using a lower DMSO concentration were unsuccessful (i.e., there was no colony formation). In the initial experiment to select for tangeretin resistance the final percentage of DMSO used for the selecting concentration of tangeretin was 2%. Repeating the experiment with 2% DMSO alone (in the absence of tangeretin) successfully yielded colonies for selection. The use of 2% DMSO in the initial experiment evolved to accommodate the high concentrations of flavonoid that were used in the selection process. Concentrations of DMSO in the range of 1% or greater were reported to have biological effects (including G1 cell cycle arrest, induction of differentiation, and intracellular electrical uncoupling) on cells [84,237]. With the concentration of DMSO being 2% in the development of tangeretin resistance, it is likely DMSO had some biological effects on the subpopulations selected in the above experiment. Concentrations of DMSO lower than 1% do not have effects significantly different than media controls. It is important to note that DMSO effects were only a concern for tangeretin- and DMSO-selected cells. DMSO concentrations were kept below 1% (they were, in fact, 0.6% or lower) during selection for nobiletin-resistance (nobiletin is more soluble than tangeretin), so DMSO effects do not appear to be a factor in nobiletin selection.

Using colony forming assays, tangeretin-, nobiletin- and DMSO-selected cells were found to be less sensitive or more resistant to inhibition of proliferation by tangeretin and nobiletin. Flavonoid- and DMSO-selected cell lines survived, established and expanded colonies better than parental cells when exposed to a range of concentrations of tangeretin or nobiletin. The DMSO-selected line was better at colony formation (i.e. formed more colonies) in tangeretin than its tangeretin-selected counterpart, suggesting a higher degree of resistance to the effects of tangeretin. However, there were no significant differences in the

number of colonies for DMSO-selected cells treated with nobiletin compared to parental cells treated with nobiletin. This suggests the resistance of the DMSO-selected line is specific to tangeretin which is an interesting finding as tangeretin was not a selecting factor. It appears that DMSO selected for or induced changes which made the cells less susceptible to the effects of tangeretin, but not nobiletin. Regardless of the selecting pressure and resultant evolutionary changes, both tangeretin- and DMSO-selected cells exhibited resistance to tangeretin.

The selection of flavonoid-resistant populations is a novel finding. The only evidence in literature on resistance to flavonoids is of flavopiridol (a semi-synthetic flavonoid) resistance. Flavopiridol resistance was demonstrated in breast cancer cells and acute leukemia patients [200,224]. Flavonoids, however, are better known for their ability to restore sensitivity to chemotherapy drugs (vincristine and daunorubicin) by inhibiting P-gp activity in cells that overexpress P-gp as a method of resistance [105,282]. This study is the first report of cell populations selected for their decreased sensitivity to naturally-occurring flavonoids. Having a resistant population of cells in conjunction with the originating parental lines allows a parallel study of the cellular and molecular basis of the antiproliferative activity of tangeretin and nobiletin in sensitive parental populations, as well as the cellular and molecular basis of decreased antiproliferative activity in resistant populations.

The development of tumor cell populations resistant to naturally occurring flavonoids has implications for the potential use of these compounds as anticancer agents. It establishes that development of flavonoid resistance by tumor cells is possible following long-term treatment with high concentrations of flavonoids. It is important to determine this information for any potential chemotherapy so that strategies can be put in place to avoid or decrease the likelihood of treatment resistance to flavonoids occurring.

4.2.2. Investigating mechanisms of tangeretin resistance

The investigation of tangeretin resistance mechanisms was approached in two ways: 1) assessing the antiproliferative effect of some common cancer chemotherapy drugs (5-FU, cisplatin, vincristine and taxol), with known mechanisms of resistance, on tangeretin-resistant populations. Common mechanisms of resistance for these drugs include: alterations in TS for 5-FU [218], increased DNA excision repair and decreased intracellular drug levels for cisplatin [141], P-gp overexpression for vincristine [229], and alterations in tubulin and microtubules for taxol [236] (see Luqmani 2005 [174] for a more in-depth review of drug resistance mechanisms in cancer). Cross resistance of tangeretin-resistant lines to any of these drugs would suggest the possible involvement of mechanisms of resistance common to that drug in resistance or decreased response to tangeretin. 2) Assessing the antiproliferative effect of tangeretin and nobiletin on cell lines overexpressing the drug efflux transporter P-gp. While the antiproliferative effects of the flavonoids on cells expressing the majority of the resistance mechanisms listed above are not directly testable, their effect on P-gp overexpressing cells is testable.

The antiproliferative effect of the four chemotherapy drugs (5-FU, cisplatin, vincristine and taxol) were assessed in tangeretin-selected tangeretin-resistant MDA-MB-435 cells to determine if there was a decreased response or resistance to these drugs. There were no consistent trends in cross resistance of the 7 tangeretin-selected populations to the chemotherapy drugs. Two populations had decreased sensitivity to taxol, two to vincristine and one to 5-FU. None of the tangeretin-selected cells were cross-resistant to cisplatin. Four of the five occurrences of cross resistance were towards taxol and vincristine. Resistance to both these drugs can be mediated through upregulation of the P-gp drug efflux transporter [162]. Therefore, upregulation of P-gp expression is a potential mechanism for decreased sensitivity of tangeretin-selected MDA-MB-435 cells to tangeretin.

The involvement of P-gp overexpression in decreased sensitivity to tangeretin was investigated using vincristine-selected, P-gp overexpressing head and neck cancer cell lines [77]. Vincristine-selected cells were just as sensitive to the antiproliferative effects of tangeretin and nobiletin as parental head and neck cells. The proliferation of all three cell lines was significantly inhibited by all concentrations of tangeretin and nobiletin (0-50 μg/ml). Although IC_{50} values were not determined, both vincristine resistant lines appear to be more sensitive to the effects of tangeretin and nobiletin. This data indicates that overexpression of P-gp did not confer resistance to tangeretin or nobiletin to head and neck cancer cells. Tangeretin-resistant cell lines do not appear to share any of the mechanisms of treatment resistance common to the panel of cancer drugs tested in this study.

4.2.3. Growth characteristics of tangeretin-resistant lines

The growth characteristics of tangeretin-resistant cell populations was assessed in the absence of flavonoids to determine if there were changes in growth rate compared to parental cells. None of the tangeretin-selected lines proliferated at a faster rate than the parental MDA-MB-435 cells. The more extensively tested line, MDA-MB-435TAN200H, grew similar to but not as well as parental. This is consistent with reports of decreased proliferation in cisplatin-, carboplatin- and taxol-resistant ovarian cancer cell lines compared to parental [169] suggesting decreased proliferation as a possible mechanism or contributor to drug resistance. In another study, increased proliferation was associated with increased sensitivity of leukemia cells to several chemotherapy drugs *in vitro* [134] implying a relationship between decreased proliferation and resistance to chemotherapy. The decreased proliferative activity observed for the tangeretin-resistant lines could play a role in resistance to tangeretin.

4.2.4. Cell cycle effects of tangeretin in resistant cells

Changes at the cellular level were assessed in tangeretin-resistant cell lines to determine contribution to the observed resistance to tangeretin. Cell cycle changes in response to tangeretin and nobiletin exposure were investigated in

tangeretin and DMSO-selected cells. Cell cycle effects were investigated because it was the only cellular mechanism found to mediate inhibition of proliferation by tangeretin in parental MDA-MB-435 cells. The effects of nobiletin exposure on the cell cycle of tangeretin-resistant cells were explored as well, to determine if cell cycle changes (if any) were specific to tangeretin. Any changes in the cell cycle response of the resistant lines to these flavonoids could mean that it (cell cycle) is a process crucial for the antiproliferative effect of these compounds, thus making it a suitable target for escaping the antiproliferative effect.

Exposure of parental MDA-MB-435 cells to tangeretin and nobiletin resulted in G1 accumulation by 24 h, extending up to 96 h. Exposure of tangeretin-selected MDA-MB-435TAN200H cells to these flavonoids also resulted in significant accumulation in G1 at 24 and 96 h. However, there was also significant accumulation in G2/M at 24 h (but not 96 h). Both flavonoids induced this transient G2/M accumulation indicating a lack of specificity for tangeretin. The DMSO-selected cells, MDA-MB-435DMSO2A, accumulated in G1 after treatment with either flavonoid for 24 h and remained accumulated until 96 h for nobiletin but not tangeretin. There was an abrogation of tangeretin-induced cell cycle accumulation in this tangeretin-resistant, DMSO-selected line but not for the tangeretin-selected line or parental MDA-MB-435 cells. However, the abrogation of cell cycle accumulation in tangeretin-selected cells may simply require more time to develop than the 96 h used in these analyses. Given that induction of cell cycle accumulation is a primary mechanism of inhibition of proliferation by tangeretin, it is not surprising that abrogation of cell cycle accumulation mediates the resistance of DMSO-selected cells to the effects of tangeretin.

Disappearance of the cell cycle effects of tangeretin in DMSO-selected cells suggests that tangeretin initially had access to molecular targets, allowing it to mediate cell cycle effects. However, within 2-4 days, targets became unavailable or inaccessible, eradicating the effect on cell cycle. Tangeretin could have induced changes in gene expression, protein expression or protein activity that

eventually led to escape from tangeretin-induced cell cycle accumulation. The former possibility is explored in the following section.

4.2.5. Tangeretin resistance and gene expression changes

To determine the molecular response of tangeretin-resistant cells to tangeretin exposure, global analysis of expression of over 10,000 genes was performed using (Affymetrix) oligonucleotide arrays on tangeretin-selected MDA-MB-435TAN200H cells following short-term exposure to tangeretin. The objective of using tangeretin-induction was to identify gene expression changes induced by tangeretin in resistant cells, and compare it to expression changes induced by tangeretin in parental cells to explain any differences in cellular effects. This identifies genes immediately responsive to tangeretin and potentially responsible for decreasing the effect of tangeretin in resistant cells. However, this experiment was designed with another objective in mind (to determine gene expression changes in the resistant line in the absence of tangeretin compared to gene expression in non-induced parental cells), and instead of using tangeretin-induced parental cells as a control, DMSO-treated parental MDA-MB-435 cells were used. Admittedly, the design of this microarray experiment makes it difficult to distinguish between genes acutely induced by tangeretin, and those constitutively over or underexpressed as a result of chronic exposure to tangeretin. Despite this design flaw, any gene whose expression was found to be changed is a potential mediator of resistance to tangeretin.

Due to the high cost of array analysis, gene expression was assessed in MDA-MB-435 parental and MDA-MB-435TAN200H tangeretin-selected cells treated with DMSO and tangeretin, respectively, in a single experiment. Findings from this single experiment should be considered preliminary. Two-fold changes in expression were chosen arbitrarily as the cut-off for significantly increased or decreased gene expression. It should be noted that selecting significantly changed genes using the fold change method biases data towards genes with lower levels of expression, as it is easier to observe 2-fold differences in a gene that has low expression compared to one with high expression [196].

Tangeretin induced accumulation of tangeretin-resistant MDA-MB-435 cells in G1 and G2/M phases of the cell cycle at 24 h, and in G1 at 96 h compared to G1 accumulation at all time points for parental cells. Microarray analysis of parental cells following short-term exposure to tangeretin found gene expression changes in cell cycle regulators consistent with accumulation in G1. Tangeretin also induced gene expression changes consistent with G1 (but not G2/M) accumulation in tangeretin-resistant cells. For example the G1 cyclin, cyclin D1, was downregulated which is associated with G1 accumulation [248]. As for the lack of expression changes typical of G2/M accumulation, array analysis was performed on cells exposed to tangeretin for 6 h, well in advance of G2/M accumulation at 24 h, so it is possible that changes in expression of G2/M regulatory genes had not occurred yet or had occurred but were not detectable at that time point. There were expression changes inconsistent with cell cycle accumulation such as the upregulation of other cell cycle regulatory cyclins and cdks (e.g. G1/S specific cyclin E2 and CDK2, and G2/M specific cyclin A2, and CDC2), and downregulation of the transcriptional repressor, E2F5. Increased expression of cyclin/Cdk pairs is associated with cell cycle progression [165,286], however, these cells eventually accumulate in G1 and G2/M by 24 h which is inconsistent with progression. These expression changes are suggestive of attempts to counteract molecular effects that lead to cell cycle accumulation, thereby mediating resistance through lessening or reversal of cell cycle effects, although it should be noted that reversal of cell cycle accumulation was not observed (up to 4 days) in these tangeretin-selected cells.

Ingenuity Pathways Analysis (IPA) was used to predict pathways responsive to tangeretin exposure in tangeretin-selected MDA-MB-435TAN200H cells. G1/S checkpoint regulation and G2/M DNA damage checkpoint signaling were identified as pathways induced by tangeretin exposure in tangeretin-resistant cells. This is consistent with G1 and G2/M phase accumulation observed for these cells. Also included on this list were inflammation-related pathways, namely antigen presentation, IGF-1 signaling and NF-kB signaling pathways which was linked to changes in the expression of immunomodulating genes. This

was not observed for parental MDA-MB-435 cells induced with tangeretin and it is a surprising finding. It is something that requires confirmation with more repeats of this gene expression analysis using appropriate controls before any conclusions can be made.

4.3. Conclusions

The present study demonstrated that the flavonoids, tangeretin and nobiletin, reduced proliferation of human tumor cell lines of disparate origin. This reduction in proliferation involved cell cycle effects that resulted in accumulation of cells in the G1/S cell cycle compartment, and, only at higher concentrations, induction of cell death/apoptosis. The rapid recovery and growth of cells after exposure to flavonoids was indistinguishable from the growth of control cells, suggesting that tangeretin and nobiletin have a non-toxic, reversible effect on cellular proliferation at lower concentrations, and that non-toxic effect is separable from death induced at very high concentrations. The ability of these compounds to inhibit growth in the absence of toxicity suggests that they interact selectively with mediators of cell cycle events, and that interactions promoting toxicity are excluded. Tangeretin induced selective changes in the expression of genes mediating cell cycle events, particularly in advance of accumulation of cells in G1/S and this may be the case for nobiletin as well. These and other compounds that inhibit proliferation of human cancers without inducing irreversible toxicity may be advantageous in treating human tumors by restricting proliferation in a manner unlikely to permanently harm normal, non-tumor host cells. In addition, we show for the first time, the selection of populations resistant to non-synthetic flavonoids which exhibit specific resistance to flavonoids.

4.4. Future studies

This body of work attempts to define the cellular events (and the molecular changes that mediate them) that ensue following exposure of cells to tangeretin and nobiletin. The goal is to provide insight into what happens to a cell from the time it is exposed to tangeretin or nobiletin, to events that occur in the plasma

membrane, in the nucleus, and subsequent cellular events. The approach was to establish cellular mechanism(s) and subsequently determine the molecular basis of those mechanism(s). There is still much work to be done to expand on the data presented here and to determine events leading up to gene expression changes and subsequent biological effects.

4.4.1. Gene expression analysis

Tangeretin and nobiletin have a common cellular mechanism in the three cell lines used in the present study but, does this translate into commonalities in gene expression? The tangeretin-induced MDA-MB-435 microarray analysis data provides a good starting point for further analysis of tangeretin- and nobiletin-induced gene expression changes in other cancer cell lines. Microarray analyses can be done to assess expression changes specific to each flavonoid in each cell line. Genes modulated by both compounds in all three cell lines would be strong candidates for further investigation as primary targets of these flavonoids.

4.4.2. Further characterization of flavonoid resistance

The main focus of the experiments characterizing flavonoid resistance were the tangeretin-selected populations. Establishing and characterizing nobiletin resistance is equally as important. Determining more about cross-resistance, cell cycle effects, apoptosis and gene expression in these populations could shed more light on the mechanism(s) of resistance in the tangeretin-selected populations. Ultimately, differences in cellular effects and gene expression between the flavonoid-resistant and parental cells would be indicative of cellular and molecular pathways central to the antiproliferative effect of tangeretin and nobiletin.

4.4.3. Intracellular localization studies

A pivotal experiment would be the determination of the exact subcellular locale of tangeretin and nobiletin once they gain access to the cell. Knowing the cellular distribution of tangeretin and nobiletin would aid in the distinction of molecular events resulting from direct interactions and those which are

secondary to these interactions (downstream effects). There have been a few studies utilizing the intrinsic fluorescence of certain flavonoids (e.g. quercetin) to determine binding to proteins [102]. This would be a useful property for a subcellular localization study. However, tangeretin and nobiletin are not among the flavonoids that have intrinsic fluorescence (these compounds tend to be highly hydroxylated) and the best way to study their localization would be through the use of fluorescent labels to detect them *in situ*. This was not possible until recently with the development of 3-hydroxyflavone fluorescent compounds designed to study structural changes in lipid membranes [152]. The method used by these researchers to synthesize 3-hydroxyflavone fluorescent probes could be adapted to fluorescently label tangeretin and nobiletin allowing the *in situ* study of their locale in cells.

4.4.4. Signaling pathways upstream of cell cycle and apoptosis effects

Pathways analysis of flavonoid modulated gene expression in combination with literature evidence of signaling pathways influenced by these flavonoids provides the starting point for these studies. The MAPK signaling pathway is a strong candidate as a primary signaling event upstream of cell cycle and apoptosis effects leading to inhibition of proliferation by tangeretin and nobiletin. MAPK signaling pathways function in the control of gene expression, cellular proliferation and programmed cell death [41]. Both ERK and p38 pathways were identified as pathways significantly affected by tangeretin in the IPA analysis of gene expression. Tangeretin was reported to inhibit phosphorylation of ERK1/2 [281] and nobiletin inhibited the phosphorylation of MEK1/2 [188]. Therefore, modulation of MAPK signaling could be an important determinant of the cellular effects of tangeretin and nobiletin and deserves further investigation.

4.4.5. In vivo xenograft model

Surprisingly, to date, tangeretin and nobiletin have not been adequately tested for anti-tumorigenic activity against human xenograft tumor models *in vivo*. Although there have been studies done using crude fractions containing tangeretin and nobiletin (Guthrie unpublished), no studies using purified

compounds have been performed. The three cell lines used in this study have all been determined to be tumorigenic in mouse xenograft models [70,109,125] and *in vivo* bioavailability studies have been done for tangeretin [160] and nobiletin. The next step is to determine whether the antiproliferative effects on human tumor cells observed *in vitro* translate to an effect *in vivo*.

4.5. Implications for the use of flavonoids in the prevention and treatment of human cancers

Caution must be taken in the interpretation of the results and conclusions in this thesis with regard to potential use of tangeretin and nobiletin to prevent and treat human cancers.

4.5.1. Potential use of tangeretin and nobiletin to decrease risk of developing cancers in humans

The concept of a dietary component providing protection from developing cancer is attractive to many. In light of the findings of this thesis, it would not be outside the realm of possibility to conclude that increased consumption of foods containing these or other flavonoids would translate to decreased cancer risk. Here are a few things that must be considered before coming to this conclusion. Processing, storage and interactions with fungicides and pesticides on foods [201] may result in the compounds the body is eventually exposed to being quite different from the original compounds. This is likely to have profound effects on the activity of these compounds. Also, only approximately 5-10% of the flavonoids consumed are absorbed by the body through the GI tract [53]. Therefore, the likelihood of these compounds reaching pre-tumor or tumor cells at an effective concentration is low. Finally, a recent study found grapefruit intake was significantly associated with an increased risk of breast cancer for subjects in the highest category of intake [190]. Thus, consumption of fruits and vegetables under certain circumstances may be harmful to human health. The use of flavonoids such as tangeretin and nobiletin without complete understanding of considerations of this type (and complete understanding is not yet available) is premature.

4.5.2. Potential use of tangeretin and nobiletin to treat cancers in humans

The inhibition of cancer cell proliferation without killing is potentially advantageous for use of tangeretin and nobiletin as cancer therapies. This would, in theory, decrease toxicity to normal tissues whose growth would be inhibited while maintaining the ability to recover and resume growth upon removal of these compounds. Due to this cytostatic activity, tangeretin and nobiletin are likely to be more effective in combination with other drugs [155]. This would require careful consideration of how they might interact or interfere with the activity of the other drug. For instance, tangeretin and nobiletin would antagonize the activity of a drug that requires a high rate of proliferation for effect. Another consideration would be determining the optimal time during treatment to use these compounds. On the basis of results from this study, these flavonoids could conceivably be effective when used alternately with existing therapeutic anticancer drugs. The evidence that resistance to some chemotherapeutic drugs does not lead to cross-resistance to tangeretin or nobiletin suggests that they could likely be effective against tumors initially treated with these drugs. These possibilities should be fully explored before considering tangeretin and nobiletin for use in the treatment of human cancers. While the work presented here shows promise for the therapeutic use of these compounds in human cancer, there remains much to be done.

REFERENCES

1. **Adlercreutz, H.C., Goldin, B.R., Gorbach, S.L., Hockerstedt, K.A., Watanabe, S., Hamalainen, E.K., Markkanen, M.H., Makela, T.H., Wahala, K.T., Hase, T.A., Fotsis, T.** (1995) Soybean phytoestrogen intake and cancer risk. *The Journal of Nutrition*, 125, S757-770.
2. **Agarwal, C., Singh, R.P., Dhanalakshmi, S., Tyagi, A.K., Tecklenburg, M., Sclafani, R.A. and Agarwal, R.** (2003) Silibinin upregulates the expression of cyclin-dependent kinase inhibitors and causes cell cycle arrest and apoptosis in human colon carcinoma HT-29 cells. *Oncogene*, 22, 8271-8282.
3. **Agullo, G., Gamet-Payrastre, L., Manenti, S., Viala, C., Remesy, C., Chap, H. and Payrastre, B.** (1997) Relationship between flavonoid structure and inhibition of phosphatidylinositol 3-kinase: a comparison with tyrosine kinase and protein kinase C inhibition. *Biochem Pharmacol*, 53, 1649-1657.
4. **Aherne, S.A. and O'Brien, N.M.** (2002) Dietary flavonols: chemistry, food content, and metabolism. *Nutrition*, 18, 75-81.
5. **Aklilu, M., Kindler, H.L., Donehower, R.C., Mani, S. and Vokes, E.E.** (2003) Phase II study of flavopiridol in patients with advanced colorectal cancer. *Ann Oncol*, 14, 1270-1273.
6. **Ambudkar, S.V., Dey, S., Hrycyna, C.A., Ramachandra, M., Pastan, I. and Gottesman, M.M.** (1999) Biochemical, cellular, and pharmacological aspects of the multidrug transporter. *Annu Rev Pharmacol Toxicol*, 39, 361-398.
7. **Arguello, F., Alexander, M., Sterry, J.A., Tudor, G., Smith, E.M., Kalavar, N.T., Greene, J.F., Jr., Koss, W., Morgan, C.D., Stinson, S.F., Siford, T.J., Alvord, W.G., Klabansky, R.L. and Sausville, E.A.** (1998) Flavopiridol induces apoptosis of normal lymphoid cells, causes immunosuppression, and has potent antitumor activity In vivo against human leukemia and lymphoma xenografts. *Blood*, 91, 2482-2490.
8. **Arts, I.C., Hollman, P.C., Bueno De Mesquita, H.B., Feskens, E.J. and Kromhout, D.** (2001) Dietary catechins and epithelial cancer incidence: the Zutphen elderly study. *Int J Cancer*, 92, 298-302.
9. **Arts, I.C., Jacobs, D.R., Jr., Gross, M., Harnack, L.J. and Folsom, A.R.** (2002) Dietary catechins and cancer incidence among postmenopausal women: the Iowa Women's Health Study (United States). *Cancer Causes Control*, 13, 373-382.
10. **Athar, M.** (2002) Oxidative stress and experimental carcinogenesis. *Indian J Exp Biol*, 40, 656-667.
11. **Aviram, M., Dornfeld, L., Kaplan, M., Coleman, R., Gaitini, D., Nitecki, S., Hofman, A., Rosenblat, M., Volkova, N., Presser, D., Attias, J., Hayek, T. and Fuhrman, B.** (2002) Pomegranate juice flavonoids inhibit low-density lipoprotein oxidation and cardiovascular diseases: studies in atherosclerotic mice and in humans. *Drugs Exp Clin Res*, 28, 49-62.
12. **Aziz, A.A., Edwards, C.A., Lean, M.E. and Crozier, A.** (1998) Absorption and excretion of conjugated flavonols, including quercetin-4'-O-beta-

glucoside and isorhamnetin-4'-O-beta-glucoside by human volunteers after the consumption of onions. *Free Radic Res*, 29, 257-269.

13. **Backman, J.T., Maenpaa, J., Belle, D.J., Wrighton, S.A., Kivisto, K.T. and Neuvonen, P.J.** (2000) Lack of correlation between in vitro and in vivo studies on the effects of tangeretin and tangerine juice on midazolam hydroxylation. *Clin Pharmacol Ther*, 67, 382-390.
14. **Baier, W.E.** (1955) CHEMISTRY OF BIOFLAVONOIDS. *Annals of the New York Academy of Sciences*, 61, 639-645.
15. **Barrett, S.C.** (1987) Mimicry in plants. *Scientific American*, 76-83.
16. **Barz, W., Bless, W., Borger-Papendorf, G., Gunia, W., Mackenbrock, U., Meier, D., Otto, C. and Super, E.** (1990) Phytoalexins as part of induced defence reactions in plants: their elicitation, function and metabolism. *Ciba Found Symp*, 154, 140-153; discussion 153-146.
17. **Bateson, W., Saunders, E.R., Punnett, R.C.** (1905) Further experiments on inheritance in sweet peas and stocks. *Proc R Soc*, LXXVII, 236-238.
18. **Beecher, G.R.** (2003) Overview of dietary flavonoids: nomenclature, occurrence and intake. *J Nutr*, 133, 3248S-3254S.
19. **Bibby, M.C. and Double, J.A.** (1993) Flavone acetic acid--from laboratory to clinic and back. *Anticancer Drugs*, 4, 3-17.
20. **Bible, K.C., Boerner, S.A., Kirkland, K., Anderl, K.L., Bartelt, D., Jr., Svingen, P.A., Kottke, T.J., Lee, Y.K., Eckdahl, S., Stalboerger, P.G., Jenkins, R.B. and Kaufmann, S.H.** (2000) Characterization of an ovarian carcinoma cell line resistant to cisplatin and flavopiridol. *Clin Cancer Res*, 6, 661-670.
21. **Bible, K.C., Lensing, J.L., Nelson, S.A., Lee, Y.K., Reid, J.M., Ames, M.M., Isham, C.R., Piens, J., Rubin, S.L., Rubin, J., Kaufmann, S.H., Atherton, P.J., Sloan, J.A., Daiss, M.K., Adjei, A.A. and Erlichman, C.** (2005) Phase 1 trial of flavopiridol combined with cisplatin or carboplatin in patients with advanced malignancies with the assessment of pharmacokinetic and pharmacodynamic end points. *Clin Cancer Res*, 11, 5935-5941.
22. **Bidgood, J.** (1905) Floral colours and pigments. *J R Hort Soc*, XXIX, 463-480.
23. **Blagosklonny, M.V.** (2004) Flavopiridol, an inhibitor of transcription: implications, problems and solutions. *Cell Cycle*, 3, 1537-1542.
24. **Block, G., Patterson, B. and Subar, A.** (1992) Fruit, vegetables, and cancer prevention: a review of the epidemiological evidence. *Nutr Cancer*, 18, 1-29.
25. **Bohm, B.A.** (1998) *Introduction to flavonoids*. Harwood academic publishers, Amsterdam, The Netherlands.
26. **Bohmont, C., Aaronson, L.M., Mann, K. and Pardini, R.S.** (1987) Inhibition of mitochondrial NADH oxidase, succinoxidase, and ATPase by naturally occurring flavonoids. *J Nat Prod*, 50, 427-433.
27. **Borris, R.P.** (1996) Natural products research: perspectives from a major pharmaceutical company. *J Ethnopharmacol*, 51, 29-38.

28. **Boyle, R.** (1664) *Experiments and considerations touching colours*, London.
29. **Bracke, M.E., Depypere, H.T., Boterberg, T., Van Marck, V.L., Vennekens, K.M., Vanluchene, E., Nuytinck, M., Serreyn, R. and Mareel, M.M.** (1999) Influence of tangeretin on tamoxifen's therapeutic benefit in mammary cancer. *J Natl Cancer Inst*, 91, 354-359.
30. **Bravo, L.** (1998) Polyphenols: chemistry, dietary sources, metabolism, and nutritional significance. *Nutr Rev*, 56, 317-333.
31. **Breinholt, V.M., Rasmussen, S.E., Brosen, K. and Friedberg, T.H.** (2003) In vitro metabolism of genistein and tangeretin by human and murine cytochrome P450s. *Pharmacol Toxicol*, 93, 14-22.
32. **Bremer, E., van Dam, G., Kroesen, B.J., de Leij, L. and Helfrich, W.** (2006) Targeted induction of apoptosis for cancer therapy: current progress and prospects. *Trends Mol Med*, 12, 382-393.
33. **Brueggemeier, R.W.** (2001) Aromatase, aromatase inhibitors, and breast cancer. *Am J Ther*, 8, 333-344.
34. **Burdette-Radoux, S., Tozer, R.G., Lohmann, R.C., Quirt, I., Ernst, D.S., Walsh, W., Wainman, N., Colevas, A.D. and Eisenhauer, E.A.** (2004) Phase II trial of flavopiridol, a cyclin dependent kinase inhibitor, in untreated metastatic malignant melanoma. *Invest New Drugs*, 22, 315-322.
35. **Butz, N., Ruetz, S., Natt, F., Hall, J., Weiler, J., Mestan, J., Ducarre, M., Grossenbacher, R., Hauser, P., Kempf, D. and Hofmann, F.** (2005) The human ubiquitin-conjugating enzyme Cdc34 controls cellular proliferation through regulation of p27Kip1 protein levels. *Exp Cell Res*, 303, 482-493.
36. **Byrne, A.M., Bouchier-Hayes, D.J. and Harmey, J.H.** (2005) Angiogenic and cell survival functions of vascular endothelial growth factor (VEGF). *J Cell Mol Med*, 9, 777-794.
37. **Caltagirone, S., Rossi, C., Poggi, A., Ranelletti, F.O., Natali, P.G., Brunetti, M., Aiello, F.B. and Piantelli, M.** (2000) Flavonoids apigenin and quercetin inhibit melanoma growth and metastatic potential. *Int J Cancer*, 87, 595-600.
38. **Carlson, B.A., Dubay, M.M., Sausville, E.A., Brizuela, L. and Worland, P.J.** (1996) Flavopiridol induces G1 arrest with inhibition of cyclin-dependent kinase (CDK) 2 and CDK4 in human breast carcinoma cells. *Cancer Res*, 56, 2973-2978.
39. **Casagrande, F. and Darbon, J.M.** (2001) Effects of structurally related flavonoids on cell cycle progression of human melanoma cells: regulation of cyclin-dependent kinases CDK2 and CDK1. *Biochem Pharmacol*, 61, 1205-1215.
40. **Casley-Smith, J.R., Casley-Smith, J.R.** (1986) *High-protein oedemas and the benzo-gamma-pyrones*. Lippincott, Sydney.
41. **Chang, L. and Karin, M.** (2001) Mammalian MAP kinase signalling cascades. *Nature*, 410, 37-40.
42. **Chang, W.S., Lee, Y.J., Lu, F.J. and Chiang, H.C.** (1993) Inhibitory effects of flavonoids on xanthine oxidase. *Anticancer Res*, 13, 2165-2170.

43. **Chen, C.L., Levine, A., Rao, A., O'Neill, K., Messinger, Y., Myers, D.E., Goldman, F., Hurvitz, C., Casper, J.T. and Uckun, F.M.** (1999) Clinical pharmacokinetics of the CD19 receptor-directed tyrosine kinase inhibitor B43-Genistein in patients with B-lineage lymphoid malignancies. *J Clin Pharmacol*, 39, 1248-1255.
44. **Chen, L., Willis, S.N., Wei, A., Smith, B.J., Fletcher, J.I., Hinds, M.G., Colman, P.M., Day, C.L., Adams, J.M. and Huang, D.C.** (2005) Differential targeting of prosurvival Bcl-2 proteins by their BH3-only ligands allows complementary apoptotic function. *Mol Cell*, 17, 393-403.
45. **Chen, Q. and Catharine Ross, A.** (2004) Retinoic acid regulates cell cycle progression and cell differentiation in human monocytic THP-1 cells. *Exp Cell Res*, 297, 68-81.
46. **Chen, Z.P., Schell, J.B., Ho, C.T. and Chen, K.Y.** (1998) Green tea epigallocatechin gallate shows a pronounced growth inhibitory effect on cancerous cells but not on their normal counterparts. *Cancer Lett*, 129, 173-179.
47. **Cheng, S.Y., Shaw, N.S., Tsai, K.S. and Chen, C.Y.** (2004) The hypoglycemic effects of soy isoflavones on postmenopausal women. *J Womens Health (Larchmt)*, 13, 1080-1086.
48. **Chow, H.H., Cai, Y., Hakim, I.A., Crowell, J.A., Shahi, F., Brooks, C.A., Dorr, R.T., Hara, Y. and Alberts, D.S.** (2003) Pharmacokinetics and safety of green tea polyphenols after multiple-dose administration of epigallocatechin gallate and polyphenon E in healthy individuals. *Clin Cancer Res*, 9, 3312-3319.
49. **Chow, H.H., Hakim, I.A., Vining, D.R., Crowell, J.A., Ranger-Moore, J., Chew, W.M., Celaya, C.A., Rodney, S.R., Hara, Y. and Alberts, D.S.** (2005) Effects of dosing condition on the oral bioavailability of green tea catechins after single-dose administration of Polyphenon E in healthy individuals. *Clin Cancer Res*, 11, 4627-4633.
50. **Chowdhury, A.R., Sharma, S., Mandal, S., Goswami, A., Mukhopadhyay, S. and Majumder, H.K.** (2002) Luteolin, an emerging anti-cancer flavonoid, poisons eukaryotic DNA topoisomerase I. *Biochem J*, 366, 653-661.
51. **Chung, S.Y., Sung, M.K., Kim, N.H., Jang, J.O., Go, E.J. and Lee, H.J.** (2005) Inhibition of P-glycoprotein by natural products in human breast cancer cells. *Arch Pharm Res*, 28, 823-828.
52. **Ciardiello, F., Caputo, R., Bianco, R., Damiano, V., Pomatico, G., De Placido, S., Bianco, A.R. and Tortora, G.** (2000) Antitumor effect and potentiation of cytotoxic drugs activity in human cancer cells by ZD-1839 (Iressa), an epidermal growth factor receptor-selective tyrosine kinase inhibitor. *Clin Cancer Res*, 6, 2053-2063.
53. **Clifford, M.N.** (2004) Diet-derived phenols in plasma and tissues and their implications for health. *Planta Med*, 70, 1103-1114.
54. **Collins-Burow, B.M., Burow, M.E., Duong, B.N. and McLachlan, J.A.** (2000) Estrogenic and antiestrogenic activities of flavonoid

phytochemicals through estrogen receptor binding-dependent and -independent mechanisms. *Nutr Cancer*, 38, 229-244.

55. **Conney, A.H.** (2003) Enzyme induction and dietary chemicals as approaches to cancer chemoprevention: the Seventh DeWitt S. Goodman Lecture. *Cancer Res*, 63, 7005-7031.
56. **Constantinou, A. and Huberman, E.** (1995) Genistein as an inducer of tumor cell differentiation: possible mechanisms of action. *Proc Soc Exp Biol Med*, 208, 109-115.
57. **Cotelle, N., Bernier, J.L., Catteau, J.P., Pommery, J., Wallet, J.C. and Gaydou, E.M.** (1996) Antioxidant properties of hydroxy-flavones. *Free Radic Biol Med*, 20, 35-43.
58. **Critchfield, J.W., Welsh, C.J., Phang, J.M. and Yeh, G.C.** (1994) Modulation of adriamycin accumulation and efflux by flavonoids in HCT-15 colon cells. Activation of P-glycoprotein as a putative mechanism. *Biochem Pharmacol*, 48, 1437-1445.
59. **Cummings, J. and Smyth, J.F.** (1989) Flavone 8-acetic acid: our current understanding of its mechanism of action in solid tumours. *Cancer Chemother Pharmacol*, 24, 269-272.
60. **Cushman, M. and Nagarathnam, D.** (1991) Cytotoxicities of some flavonoid analogues. *J Nat Prod*, 54, 1656-1660.
61. **Das, S. and Rosazza, J.P.** (2006) Microbial and enzymatic transformations of flavonoids. *J Nat Prod*, 69, 499-508.
62. **Day, A.J., Canada, F.J., Diaz, J.C., Kroon, P.A., McLauchlan, R., Faulds, C.B., Plumb, G.W., Morgan, M.R. and Williamson, G.** (2000) Dietary flavonoid and isoflavone glycosides are hydrolysed by the lactase site of lactase phlorizin hydrolase. *FEBS Lett*, 468, 166-170.
63. **de Koninck, L.** (1835) *Ann Chem Pharm*, 15, 258.
64. **de Laire, G., Tiemann, F.** (1893) *Chem Ber*, 26, 2010.
65. **De Stefani, E., Ronco, A., Mendilaharsu, M. and Deneo-Pellegrini, H.** (1999) Diet and risk of cancer of the upper aerodigestive tract--II. Nutrients. *Oral Oncol*, 35, 22-26.
66. **Demidenko, Z.N., Vivo, C., Halicka, H.D., Li, C.J., Bhalla, K., Broude, E.V. and Blagosklonny, M.V.** (2005) Pharmacological induction of Hsp70 protects apoptosis-prone cells from doxorubicin: comparison with caspase-inhibitor- and cycle-arrest-mediated cytoprotection. *Cell Death Differ*.
67. **Depeint, F., Gee, J.M., Williamson, G. and Johnson, I.T.** (2002) Evidence for consistent patterns between flavonoid structures and cellular activities. *Proc Nutr Soc*, 61, 97-103.
68. **Di Pietro, A., Conseil, G., Perez-Victoria, J.M., Dayan, G., Baubichon-Cortay, H., Trompier, D., Steinfels, E., Jault, J.M., de Wet, H., Maitrejean, M., Comte, G., Boumendjel, A., Mariotte, A.M., Dumontet, C., McIntosh, D.B., Goffeau, A., Castanys, S., Gamarro, F. and Barron, D.** (2002) Modulation by flavonoids of cell multidrug resistance mediated by P-glycoprotein and related ABC transporters. *Cell Mol Life Sci*, 59, 307-322.

69. **Di Pietro, A., Dayan, G., Conseil, G., Steinfels, E., Krell, T., Trompier, D., Baubichon-Cortay, H. and Jault, J.** (1999) P-glycoprotein-mediated resistance to chemotherapy in cancer cells: using recombinant cytosolic domains to establish structure-function relationships. *Braz J Med Biol Res*, 32, 925-939.
70. **Divisova, J., Kuiatse, I., Lazard, Z., Weiss, H., Vreeland, F., Hadsell, D.L., Schiff, R., Osborne, C.K. and Lee, A.V.** (2006) The growth hormone receptor antagonist pegvisomant blocks both mammary gland development and MCF-7 breast cancer xenograft growth. *Breast Cancer Res Treat*.
71. **Dixon, R.A., Paiva, N.L.** (1995) Stress-induced phenylpropanoid metabolism. *Plant Cell*, 7, 1085-1097.
72. **Donovan, J.L., Bell, J.R., Kasim-Karakas, S., German, J.B., Walzem, R.L., Hansen, R.J. and Waterhouse, A.L.** (1999) Catechin is present as metabolites in human plasma after consumption of red wine. *J Nutr*, 129, 1662-1668.
73. **Doyle, L.A. and Ross, D.D.** (2003) Multidrug resistance mediated by the breast cancer resistance protein BCRP (ABCG2). *Oncogene*, 22, 7340-7358.
74. **Ebert, M.P., Hernberg, S., Fei, G., Sokolowski, A., Schulz, H.U., Lippert, H. and Malfertheiner, P.** (2001) Induction and expression of cyclin D3 in human pancreatic cancer. *J Cancer Res Clin Oncol*, 127, 449-454.
75. **Elangovan, V., Sekar, N. and Govindasamy, S.** (1994) Chemopreventive potential of dietary bioflavonoids against 20-methylcholanthrene-induced tumorigenesis. *Cancer Lett*, 87, 107-113.
76. **Fan, T.J., Han, L.H., Cong, R.S. and Liang, J.** (2005) Caspase family proteases and apoptosis. *Acta Biochim Biophys Sin (Shanghai)*, 37, 719-727.
77. **Ferguson, P.J., Chin-yee, I., Keeney, M** (1992) Absence of P-glycoprotein (Pgp) overexpression in low-level vincristine-resistant human squamous carcinoma cells. *Proceedings: Annual meeting of the American Association for Cancer Research*. Waverly Press, vol. 33, pp. 458.
78. **Ferguson, P.J., Currie, C. and Vincent, M.D.** (1999) Enhancement of platinum-drug cytotoxicity in a human head and neck squamous cell carcinoma line and its platinum-resistant variant by liposomal amphotericin B and phospholipase A2-II. *Drug Metab Dispos*, 27, 1399-1405.
79. **Ferguson, P.J., DeMoor, J.M., Vincent, M.D. and Koropatnick, J.** (2001) Antisense-induced down-regulation of thymidylate synthase and enhanced cytotoxicity of 5-FUdR in 5-FUdR-resistant HeLa cells. *Br J Pharmacol*, 134, 1437-1446.
80. **Ferriola, P.C., Cody, V. and Middleton, E., Jr.** (1989) Protein kinase C inhibition by plant flavonoids. Kinetic mechanisms and structure-activity relationships. *Biochem Pharmacol*, 38, 1617-1624.
81. **Ferry, D.R., Smith, A., Malkhandi, J., Fyfe, D.W., deTakats, P.G., Anderson, D., Baker, J. and Kerr, D.J.** (1996) Phase I clinical trial of the

flavonoid quercetin: pharmacokinetics and evidence for in vivo tyrosine kinase inhibition. *Clin Cancer Res*, 2, 659-668.

82. **Filhol, E.** (1854) Observations sur les matieres colorantes des fleurs. *CR Acad Sci* 39, 194-198.
83. **Fink, J.R. and LeBien, T.W.** (2001) Novel expression of cyclin-dependent kinase inhibitors in human B-cell precursors. *Exp Hematol*, 29, 490-498.
84. **Fiore, M., Zanier, R. and Degrassi, F.** (2002) Reversible G(1) arrest by dimethyl sulfoxide as a new method to synchronize Chinese hamster cells. *Mutagenesis*, 17, 419-424.
85. **Fischer, L., Mahoney, C., Jeffcoat, A.R., Koch, M.A., Thomas, B.E., Valentine, J.L., Stinchcombe, T., Boan, J., Crowell, J.A. and Zeisel, S.H.** (2004) Clinical characteristics and pharmacokinetics of purified soy isoflavones: multiple-dose administration to men with prostate neoplasia. *Nutr Cancer*, 48, 160-170.
86. **Fotsis, T., Pepper, M.S., Aktas, E., Breit, S., Rasku, S., Adlercreutz, H., Wahala, K., Montesano, R. and Schweigerer, L.** (1997) Flavonoids, dietary-derived inhibitors of cell proliferation and in vitro angiogenesis. *Cancer Res*, 57, 2916-2921.
87. **Fuhr, U.** (1998) Drug interactions with grapefruit juice. Extent, probable mechanism and clinical relevance. *Drug Saf*, 18, 251-272.
88. **Galati, G. and O'Brien, P.J.** (2004) Potential toxicity of flavonoids and other dietary phenolics: significance for their chemopreventive and anticancer properties. *Free Radic Biol Med*, 37, 287-303.
89. **Garcia, R., Gonzalez, C.A., Agudo, A. and Riboli, E.** (1999) High intake of specific carotenoids and flavonoids does not reduce the risk of bladder cancer. *Nutr Cancer*, 35, 212-214.
90. **Garrido, C., Gurbuxani, S., Ravagnan, L. and Kroemer, G.** (2001) Heat shock proteins: endogenous modulators of apoptotic cell death. *Biochem Biophys Res Commun*, 286, 433-442.
91. **Geissman, T.A., Heaton, C.D.** (1944) Anthochlor pigments V: The pigments of *Coreopsis grandiflora* Nutt II *J Amer Chem Soc*, 66, 486-487.
92. **Gil, B., Sanz, M.J., Terencio, M.C., Ferrandiz, M.L., Bustos, G., Paya, M., Gunasegaran, R. and Alcaraz, M.J.** (1994) Effects of flavonoids on Naja naja and human recombinant synovial phospholipases A2 and inflammatory responses in mice. *Life Sci*, 54, PL333-338.
93. **Gitz, D.C., Liu, L.,McClure, J.W.** (1998) Phenolic metabolism, growth and UV-B tolerance in phenylalanine ammonia lyase inhibited red cabbage seedlings. *Phytochemistry*, 49, 377-386.
94. **Gottesman, M.M., Fojo, T. and Bates, S.E.** (2002) Multidrug resistance in cancer: role of ATP-dependent transporters. *Nat Rev Cancer*, 2, 48-58.
95. **Gouni-Berthold, I. and Sachinidis, A.** (2004) Molecular mechanisms explaining the preventive effects of catechins on the development of proliferative diseases. *Curr Pharm Des*, 10, 1261-1271.
96. **Grant, S. and Roberts, J.D.** (2003) The use of cyclin-dependent kinase inhibitors alone or in combination with established cytotoxic drugs in cancer chemotherapy. *Drug Resist Updat*, 6, 15-26.

97. **Grayer, R., Harborne, J.** (1994) A survey of antifungal compounds from higher plants 1982-1993. *Phytochemistry*, 37, 19-42.
98. **Grew, N.** (1682) The anatomy of plants, with an idea of a philosophical history of plants. *Royal Society*, London.
99. **Griffiths, L.A.** (1982) *Mammalian metabolism of flavonoids*. Chapman and Hall, London.
100. **Guglielmone, H.A., Agnese, A.M., Nunez Montoya, S.C. and Cabrera, J.L.** (2002) Anticoagulant effect and action mechanism of sulphated flavonoids from Flaveria bidentis. *Thromb Res*, 105, 183-188.
101. **Gupta, O.P., Sing, S., Bani, S., Sharma, N., Malhotra, S., Gupta, B.D., Banerjee, S.K. and Handa, S.S.** (2000) Anti-inflammatory and anti-arthritic activities of silymarin acting through inhibition of 5-lipoxygenase. *Phytomedicine*, 7, 21-24.
102. **Gutzeit, H.O., Henker, Y., Kind, B. and Franz, A.** (2004) Specific interactions of quercetin and other flavonoids with target proteins are revealed by elicited fluorescence. *Biochem Biophys Res Commun*, 318, 490-495.
103. **Hackett, A.M.** (1986) *The metabolism of flavonoid compounds in mammals*. Liss, A.R., New York.
104. **Hackett, A.M., Griffiths, L.A., Broillet, A. and Wermeille, M.** (1983) The metabolism and excretion of (+)-[14C]cyanidanol-3 in man following oral administration. *Xenobiotica*, 13, 279-286.
105. **Hadjeri, M., Barbier, M., Ronot, X., Mariotte, A.M., Boumendjel, A. and Boutonnat, J.** (2003) Modulation of P-glycoprotein-mediated multidrug resistance by flavonoid derivatives and analogues. *J Med Chem*, 46, 2125-2131.
106. **Haghiac, M. and Walle, T.** (2005) Quercetin induces necrosis and apoptosis in SCC-9 oral cancer cells. *Nutr Cancer*, 53, 220-231.
107. **Halliwell, B.** (1999) Antioxidant defence mechanisms: from the beginning to the end (of the beginning). *Free Radic Res*, 31, 261-272.
108. **Harborne, J.B. and Williams, C.A.** (2000) Advances in flavonoid research since 1992. *Phytochemistry*, 55, 481-504.
109. **Harris, S.M., Mistry, P., Freathy, C., Brown, J.L. and Charlton, P.A.** (2005) Antitumour activity of XR5944 in vitro and in vivo in combination with 5-fluorouracil and irinotecan in colon cancer cell lines. *Br J Cancer*, 92, 722-728.
110. **Hauns, B., Haring, B., Kohler, S., Mross, K., Robben-Bathe, P. and Unger, C.** (1999) Phase II study with 5-fluorouracil and ginkgo biloba extract (GBE 761 ONC) in patients with pancreatic cancer. *Arzneimittelforschung*, 49, 1030-1034.
111. **Hauns, B., Haring, B., Kohler, S., Mross, K. and Unger, C.** (2001) Phase II study of combined 5-fluorouracil/ Ginkgo biloba extract (GBE 761 ONC) therapy in 5-fluorouracil pretreated patients with advanced colorectal cancer. *Phytother Res*, 15, 34-38.
112. **Havlin, K.A., Kuhn, J.G., Craig, J.B., Boldt, D.H., Weiss, G.R., Koeller, J., Harman, G., Schwartz, R., Clark, G.N. and Von Hoff, D.D.** (1991)

Phase I clinical and pharmacokinetic trial of flavone acetic acid. *J Natl Cancer Inst*, 83, 124-128.

113. **Havsteen, B.H.** (2002) The biochemistry and medical significance of the flavonoids. *Pharmacol Ther*, 96, 67-202.
114. **Hayashi, A., Gillen, A.C. and Lott, J.R.** (2000) Effects of daily oral administration of quercetin chalcone and modified citrus pectin on implanted colon-25 tumor growth in Balb-c mice. *Altern Med Rev*, 5, 546-552.
115. **Himeji, M., Ohtsuki, T., Fukazawa, H., Tanaka, M., Yazaki, S.I., Ui, S., Nishio, K., Yamamoto, H., Tasaka, K. and Mimura, A.** (2006) Difference of growth-inhibitory effect of Scutellaria baicalensis-producing flavonoid wogonin among human cancer cells and normal diploid cell. *Cancer Lett.*
116. **Hirano, T., Abe, K., Gotoh, M. and Oka, K.** (1995) Citrus flavone tangeretin inhibits leukaemic HL-60 cell growth partially through induction of apoptosis with less cytotoxicity on normal lymphocytes. *Br J Cancer*, 72, 1380-1388.
117. **Hirano, T., Gotoh, M. and Oka, K.** (1994) Natural flavonoids and lignans are potent cytostatic agents against human leukemic HL-60 cells. *Life Sci*, 55, 1061-1069.
118. **Hodnick, W.F., Duval, D.L. and Pardini, R.S.** (1994) Inhibition of mitochondrial respiration and cyanide-stimulated generation of reactive oxygen species by selected flavonoids. *Biochem Pharmacol*, 47, 573-580.
119. **Hofmann, J.** (2004) Protein kinase C isozymes as potential targets for anticancer therapy. *Curr Cancer Drug Targets*, 4, 125-146.
120. **Hollman, P.C., de Vries, J.H., van Leeuwen, S.D., Mengelers, M.J. and Katan, M.B.** (1995) Absorption of dietary quercetin glycosides and quercetin in healthy ileostomy volunteers. *Am J Clin Nutr*, 62, 1276-1282.
121. **Hollman, P.C., van Trijp, J.M., Buysman, M.N., van der Gaag, M.S., Mengelers, M.J., de Vries, J.H. and Katan, M.B.** (1997) Relative bioavailability of the antioxidant flavonoid quercetin from various foods in man. *FEBS Lett*, 418, 152-156.
122. **Hollman, P.C.H., Katan, M. B.** (1997) *Absorption, metabolism, and bioavailability of flavonoids*. Marcel Dekker, New York.
123. **Horinaka, M., Yoshida, T., Shiraishi, T., Nakata, S., Wakada, M., Nakanishi, R., Nishino, H., Matsui, H. and Sakai, T.** (2005) Luteolin induces apoptosis via death receptor 5 upregulation in human malignant tumor cells. *Oncogene*, 24, 7180-7189.
124. **Hoult, J.R., Moroney, M.A. and Paya, M.** (1994) Actions of flavonoids and coumarins on lipoxygenase and cyclooxygenase. *Methods Enzymol*, 234, 443-454.
125. **Huang, X., Bennett, M. and Thorpe, P.E.** (2005) A monoclonal antibody that binds anionic phospholipids on tumor blood vessels enhances the antitumor effect of docetaxel on human breast tumors in mice. *Cancer Res*, 65, 4408-4416.
126. **Imai, Y., Tsukahara, S., Asada, S. and Sugimoto, Y.** (2004) Phytoestrogens/flavonoids reverse breast cancer resistance

protein/ABCG2-mediated multidrug resistance. *Cancer Res*, 64, 4346-4352.

127. **Jaracz, S., Chen, J., Kuznetsova, L.V. and Ojima, I.** (2005) Recent advances in tumor-targeting anticancer drug conjugates. *Bioorg Med Chem*, 13, 5043-5054.
128. **Jatoi, A., Ellison, N., Burch, P.A., Sloan, J.A., Dakhil, S.R., Novotny, P., Tan, W., Fitch, T.R., Rowland, K.M., Young, C.Y. and Flynn, P.J.** (2003) A phase II trial of green tea in the treatment of patients with androgen independent metastatic prostate carcinoma. *Cancer*, 97, 1442-1446.
129. **Jeong, H.J., Shin, Y.G., Kim, I.H. and Pezzuto, J.M.** (1999) Inhibition of aromatase activity by flavonoids. *Arch Pharm Res*, 22, 309-312.
130. **Ji, P. and Zhu, L.** (2005) Using kinetic studies to uncover new Rb functions in inhibiting cell cycle progression. *Cell Cycle*, 4, 373-375.
131. **Jiang, C., Agarwal, R. and Lu, J.** (2000) Anti-angiogenic potential of a cancer chemopreventive flavonoid antioxidant, silymarin: inhibition of key attributes of vascular endothelial cells and angiogenic cytokine secretion by cancer epithelial cells. *Biochem Biophys Res Commun*, 276, 371-378.
132. **Jin, Z. and El-Deiry, W.S.** (2005) Overview of cell death signaling pathways. *Cancer Biol Ther*, 4, 139-163.
133. **Juzwiak, S., Wojcicki, J., Mokrzycki, K., Marchlewicz, M., Bialecka, M., Wenda-Rozewicka, L., Gawronska-Szklarz, B. and Drozdzik, M.** (2005) Effect of quercetin on experimental hyperlipidemia and atherosclerosis in rabbits. *Pharmacol Rep*, 57, 604-609.
134. **Kaaijk, P., Kaspers, G.J., Van Wering, E.R., Broekema, G.J., Loonen, A.H., Hahlen, K., Schmiegelow, K., Janka-Schaub, G.E., Henze, G., Creutzig, U. and Veerman, A.J.** (2003) Cell proliferation is related to in vitro drug resistance in childhood acute leukaemia. *Br J Cancer*, 88, 775-781.
135. **Kametaka, T., Perkin, A.G.** (1910) Cathamine I. *J Chem Soc*, 97, 1415-1427.
136. **Kanadaswami, C., Lee, L.T., Lee, P.P., Hwang, J.J., Ke, F.C., Huang, Y.T. and Lee, M.T.** (2005) The antitumor activities of flavonoids. *In Vivo*, 19, 895-909.
137. **Kandaswami, C., Perkins, E., Drzewiecki, G., Soloniuk, D.S. and Middleton, E., Jr.** (1992) Differential inhibition of proliferation of human squamous cell carcinoma, gliosarcoma and embryonic fibroblast-like lung cells in culture by plant flavonoids. *Anticancer Drugs*, 3, 525-530.
138. **Kandaswami, C., Perkins, E., Soloniuk, D.S., Drzewiecki, G. and Middleton, E., Jr.** (1991) Antiproliferative effects of citrus flavonoids on a human squamous cell carcinoma in vitro. *Cancer Lett*, 56, 147-152.
139. **Karakaya, S.** (2004) Bioavailability of phenolic compounds. *Crit Rev Food Sci Nutr*, 44, 453-464.
140. **Karp, J.E., Passaniti, A., Gojo, I., Kaufmann, S., Bible, K., Garimella, T.S., Greer, J., Briel, J., Smith, B.D., Gore, S.D., Tidwell, M.L., Ross, D.D., Wright, J.J., Colevas, A.D. and Bauer, K.S.** (2005) Phase I and

pharmacokinetic study of flavopiridol followed by 1-beta-D-arabinofuranosylcytosine and mitoxantrone in relapsed and refractory adult acute leukemias. *Clin Cancer Res*, 11, 8403-8412.

141. **Kartalou, M. and Essigmann, J.M.** (2001) Mechanisms of resistance to cisplatin. *Mutat Res*, 478, 23-43.
142. **Kaul, T.N., Middleton, E., Jr. and Ogra, P.L.** (1985) Antiviral effect of flavonoids on human viruses. *J Med Virol*, 15, 71-79.
143. **Kaur, G., Stetler-Stevenson, M., Sebers, S., Worland, P., Sedlacek, H., Myers, C., Czech, J., Naik, R. and Sausville, E.** (1992) Growth inhibition with reversible cell cycle arrest of carcinoma cells by flavone L86-8275. *J Natl Cancer Inst*, 84, 1736-1740.
144. **Kawaii, S., Tomono, Y., Katase, E., Ogawa, K. and Yano, M.** (1999) Antiproliferative activity of flavonoids on several cancer cell lines. *Biosci Biotechnol Biochem*, 63, 896-899.
145. **Keppler, D., Leier, I., Jedlitschky, G. and Konig, J.** (1998) ATP-dependent transport of glutathione S-conjugates by the multidrug resistance protein MRP1 and its apical isoform MRP2. *Chem Biol Interact*, 111-112, 153-161.
146. **Kern, M., Tjaden, Z., Ngiewih, Y., Puppel, N., Will, F., Dietrich, H., Pahlke, G. and Marko, D.** (2005) Inhibitors of the epidermal growth factor receptor in apple juice extract. *Mol Nutr Food Res*, 49, 317-328.
147. **Key, T.J., Schatzkin, A., Willett, W.C., Allen, N.E., Spencer, E.A. and Travis, R.C.** (2004) Diet, nutrition and the prevention of cancer. *Public Health Nutr*, 7, 187-200.
148. **Kimata, M., Inagaki, N. and Nagai, H.** (2000) Effects of luteolin and other flavonoids on IgE-mediated allergic reactions. *Planta Med*, 66, 25-29.
149. **Kindler, H.L.** (2004) Moving beyond chemotherapy: novel cytostatic agents for malignant mesothelioma. *Lung Cancer*, 45 Suppl 1, S125-127.
150. **Kioka, N., Hosokawa, N., Komano, T., Hirayoshi, K., Nagata, K. and Ueda, K.** (1992) Quercetin, a bioflavonoid, inhibits the increase of human multidrug resistance gene (MDR1) expression caused by arsenite. *FEBS Lett*, 301, 307-309.
151. **Kiriakidis, S., Hogemeier, O., Starcke, S., Dombrowski, F., Hahne, J.C., Pepper, M., Jha, H.C. and Wernert, N.** (2005) Novel tempeh (fermented soyabean) isoflavones inhibit in vivo angiogenesis in the chicken chorioallantoic membrane assay. *Br J Nutr*, 93, 317-323.
152. **Klymchenko, A.S., Duportail, G., Ozturk, T., Pivovarenko, V.G., Mely, Y. and Demchenko, A.P.** (2002) Novel two-band ratiometric fluorescence probes with different location and orientation in phospholipid membranes. *Chem Biol*, 9, 1199-1208.
153. **Knekt, P., Jarvinen, R., Seppanen, R., Hellovaara, M., Teppo, L., Pukkala, E. and Aromaa, A.** (1997) Dietary flavonoids and the risk of lung cancer and other malignant neoplasms. *Am J Epidemiol*, 146, 223-230.

154. **Knekt, P., Kumpulainen, J., Jarvinen, R., Rissanen, H., Heliovaara, M., Reunanen, A., Hakulinen, T. and Aromaa, A.** (2002) Flavonoid intake and risk of chronic diseases. *Am J Clin Nutr*, 76, 560-568.
155. **Kohno, M. and Pouyssegur, J.** (2006) Targeting the ERK signaling pathway in cancer therapy. *Ann Med*, 38, 200-211.
156. **Kong, A.N., Yu, R., Chen, C., Mandlekar, S. and Primiano, T.** (2000) Signal transduction events elicited by natural products: role of MAPK and caspase pathways in homeostatic response and induction of apoptosis. *Arch Pharm Res*, 23, 1-16.
157. **Kouroukis, C.T., Belch, A., Crump, M., Eisenhauer, E., Gascoyne, R.D., Meyer, R., Lohmann, R., Lopez, P., Powers, J., Turner, R. and Connors, J.M.** (2003) Flavopiridol in untreated or relapsed mantle-cell lymphoma: results of a phase II study of the National Cancer Institute of Canada Clinical Trials Group. *J Clin Oncol*, 21, 1740-1745.
158. **Kuhnau, J.** (1976) The flavonoids. A class of semi-essential food components: their role in human nutrition. *World Rev Nutr Diet*, 24, 117-191.
159. **Kuntz, S., Wenzel, U. and Daniel, H.** (1999) Comparative analysis of the effects of flavonoids on proliferation, cytotoxicity, and apoptosis in human colon cancer cell lines. *Eur J Nutr*, 38, 133-142.
160. **Kurowska, E.M. and Manthey, J.A.** (2004) Hypolipidemic effects and absorption of citrus polymethoxylated flavones in hamsters with diet-induced hypercholesterolemia. *J Agric Food Chem*, 52, 2879-2886.
161. **Laughton, M.J., Evans, P.J., Moroney, M.A., Hoult, J.R. and Halliwell, B.** (1991) Inhibition of mammalian 5-lipoxygenase and cyclo-oxygenase by flavonoids and phenolic dietary additives. Relationship to antioxidant activity and to iron ion-reducing ability. *Biochem Pharmacol*, 42, 1673-1681.
162. **Lautier, D., Canitrot, Y., Deeley, R.G. and Cole, S.P.** (1996) Multidrug resistance mediated by the multidrug resistance protein (MRP) gene. *Biochem Pharmacol*, 52, 967-977.
163. **Le Marchand, L., Murphy, S.P., Hankin, J.H., Wilkens, L.R. and Kolonel, L.N.** (2000) Intake of flavonoids and lung cancer. *J Natl Cancer Inst*, 92, 154-160.
164. **Lebreton, P.J.** (1828) *Pharm Chim Paris*, 14, 377.
165. **Lee, M.H. and Yang, H.Y.** (2003) Regulators of G1 cyclin-dependent kinases and cancers. *Cancer Metastasis Rev*, 22, 435-449.
166. **Lee, W.R., Shen, S.C., Lin, H.Y., Hou, W.C., Yang, L.L. and Chen, Y.C.** (2002) Wogonin and fisetin induce apoptosis in human promyeloleukemic cells, accompanied by a decrease of reactive oxygen species, and activation of caspase 3 and Ca(2+)-dependent endonuclease. *Biochem Pharmacol*, 63, 225-236.
167. **Leung, D.W., Cachianes, G., Kuang, W.J., Goeddel, D.V. and Ferrara, N.** (1989) Vascular endothelial growth factor is a secreted angiogenic mitogen. *Science*, 246, 1306-1309.

168. **Li, B.Q., Fu, T., Dongyan, Y., Mikovits, J.A., Ruscetti, F.W. and Wang, J.M.** (2000) Flavonoid baicalin inhibits HIV-1 infection at the level of viral entry. *Biochem Biophys Res Commun*, 276, 534-538.
169. **Li, P., Li, C., Zhao, X., Zhang, X., Nicosia, S.V. and Bai, W.** (2004) p27(Kip1) stabilization and G(1) arrest by 1,25-dihydroxyvitamin D(3) in ovarian cancer cells mediated through down-regulation of cyclin E/cyclin-dependent kinase 2 and Skp1-Cullin-F-box protein/Skp2 ubiquitin ligase. *J Biol Chem*, 279, 25260-25267.
170. **Liao, S., Umekita, Y., Guo, J., Kokontis, J.M. and Hiipakka, R.A.** (1995) Growth inhibition and regression of human prostate and breast tumors in athymic mice by tea epigallocatechin gallate. *Cancer Lett*, 96, 239-243.
171. **Liu, G., Gandara, D.R., Lara, P.N., Jr., Raghavan, D., Doroshow, J.H., Twardowski, P., Kantoff, P., Oh, W., Kim, K. and Wilding, G.** (2004) A Phase II trial of flavopiridol (NSC #649890) in patients with previously untreated metastatic androgen-independent prostate cancer. *Clin Cancer Res*, 10, 924-928.
172. **Lopez-Lazaro, M.** (2002) Flavonoids as anticancer agents: structure-activity relationship study. *Curr Med Chem Anticancer Agents*, 2, 691-714.
173. **Lu, X., Jung, J., Cho, H.J., Lim do, Y., Lee, H.S., Chun, H.S., Kwon, D.Y. and Park, J.H.** (2005) Fisetin inhibits the activities of cyclin-dependent kinases leading to cell cycle arrest in HT-29 human colon cancer cells. *J Nutr*, 135, 2884-2890.
174. **Luqmani, Y.A.** (2005) Mechanisms of drug resistance in cancer chemotherapy. *Med Princ Pract*, 14 Suppl 1, 35-48.
175. **Manach, C. and Donovan, J.L.** (2004) Pharmacokinetics and metabolism of dietary flavonoids in humans. *Free Radic Res*, 38, 771-785.
176. **Manach, C., Morand, C., Texier, O., Favier, M.L., Agullo, G., Demigne, C., Regerat, F. and Remesy, C.** (1995) Quercetin metabolites in plasma of rats fed diets containing rutin or quercetin. *J Nutr*, 125, 1911-1922.
177. **Manach, C., Scalbert, A., Morand, C., Remesy, C. and Jimenez, L.** (2004) Polyphenols: food sources and bioavailability. *Am J Clin Nutr*, 79, 727-747.
178. **Manthey, J.A. and Guthrie, N.** (2002) Antiproliferative activities of citrus flavonoids against six human cancer cell lines. *J Agric Food Chem*, 50, 5837-5843.
179. **Marquart, L.** (1835) *Die farben der bluthen, Eine chemisch-physiologische abhandlung*, Bonn.
180. **Martens, S. and Mithofer, A.** (2005) Flavones and flavone synthases. *Phytochemistry*, 66, 2399-2407.
181. **Martin, S.S., Townsend, C.E., Lenscen, A.W.** (1994) Induced isoflavonoids in diverse populations of *Astragalus cicer*. *Biochemical Systematics and Ecology*, 22, 657-661.
182. **Matsukawa, Y., Marui, N., Sakai, T., Satomi, Y., Yoshida, M., Matsumoto, K., Nishino, H. and Aoike, A.** (1993) Genistein arrests cell cycle progression at G2-M. *Cancer Res*, 53, 1328-1331.

183. **Mead, J. and McNair, N.** (2006) Antiparasitic activity of flavonoids and isoflavones against Cryptosporidium parvum and Encephalitozoon intestinalis. *FEMS Microbiol Lett*, 259, 153-157.
184. **Mencher, S.K. and Wang, L.G.** (2005) Promiscuous drugs compared to selective drugs (promiscuity can be a virtue). *BMC Clin Pharmacol*, 5, 3.
185. **Mertens-Talcott, S.U., De Castro, W.V., Manthey, J.A., Derendorf, H. and Butterweck, V.** (2007) Polymethoxylated flavones and other phenolic derivates from citrus in their inhibitory effects on P-glycoprotein-mediated transport of talinolol in Caco-2 cells. *J Agric Food Chem*, 55, 2563-2568.
186. **Miao, H.S., Yu, L.Y., Hui, G.Z. and Guo, L.H.** (2005) Antiapoptotic effect both in vivo and in vitro of A20 gene when transfected into rat hippocampal neurons. *Acta Pharmacol Sin*, 26, 33-38.
187. **Middleton, E., Jr.** (1998) Effect of plant flavonoids on immune and inflammatory cell function. *Adv Exp Med Biol*, 439, 175-182.
188. **Miyata, Y., Sato, T., Yano, M. and Ito, A.** (2004) Activation of protein kinase C betaII/epsilon-c-Jun NH2-terminal kinase pathway and inhibition of mitogen-activated protein/extracellular signal-regulated kinase 1/2 phosphorylation in antitumor invasive activity induced by the polymethoxy flavonoid, nobiletin. *Mol Cancer Ther*, 3, 839-847.
189. **Mo, Y., Nagel, C. and Taylor, L.P.** (1992) Biochemical complementation of chalcone synthase mutants defines a role for flavonols in functional pollen. *Proc Natl Acad Sci U S A*, 89, 7213-7217.
190. **Monroe, K.R., Murphy, S.P., Kolonel, L.N. and Pike, M.C.** (2007) Prospective study of grapefruit intake and risk of breast cancer in postmenopausal women: the Multiethnic Cohort Study. *Br J Cancer*, 97, 440-445.
191. **Moon, Y.J., Wang, X. and Morris, M.E.** (2006) Dietary flavonoids: Effects on xenobiotic and carcinogen metabolism. *Toxicol In Vitro*, 20, 187-210.
192. **Morot, F.S.** (1849) Recherches sur la coloration des vegetaux. *Ann Sci Nat (Bot.) (Paris)*, xiii, 160-235.
193. **Mulholland, P.J., Ferry, D.R., Anderson, D., Hussain, S.A., Young, A.M., Cook, J.E., Hodgkin, E., Seymour, L.W. and Kerr, D.J.** (2001) Pre-clinical and clinical study of QC12, a water-soluble, pro-drug of quercetin. *Ann Oncol*, 12, 245-248.
194. **Murakami, A., Nakamura, Y., Torikai, K., Tanaka, T., Koshiba, T., Koshimizu, K., Kuwahara, S., Takahashi, Y., Ogawa, K., Yano, M., Tokuda, H., Nishino, H., Mimaki, Y., Sashida, Y., Kitanaka, S. and Ohigashi, H.** (2000) Inhibitory effect of citrus nobiletin on phorbol ester-induced skin inflammation, oxidative stress, and tumor promotion in mice. *Cancer Res*, 60, 5059-5066.
195. **Murkies, A.L., Wilcox, G. and Davis, S.R.** (1998) Clinical review 92: Phytoestrogens. *J Clin Endocrinol Metab*, 83, 297-303.
196. **Mutch, D.M., Berger, A., Mansourian, R., Rytz, A. and Roberts, M.A.** (2001) Microarray data analysis: a practical approach for selecting differentially expressed genes. *Genome Biol*, 2, PREPRINT0009.

197. **Mutoh, M., Takahashi, M., Fukuda, K., Komatsu, H., Enya, T., Matsushima-Hibiya, Y., Mutoh, H., Sugimura, T. and Wakabayashi, K.** (2000) Suppression by flavonoids of cyclooxygenase-2 promoter-dependent transcriptional activity in colon cancer cells: structure-activity relationship. *Jpn J Cancer Res*, 91, 686-691.

198. **Nakahara, K., Kawabata, S., Ono, H., Ogura, K., Tanaka, T., Ooshima, T. and Hamada, S.** (1993) Inhibitory effect of oolong tea polyphenols on glycosyltransferases of mutans Streptococci. *Appl Environ Microbiol*, 59, 968-973.

199. **Nakai, N., Fujii, Y., Kobashi, K. and Nomura, K.** (1985) Aldose reductase inhibitors: flavonoids, alkaloids, acetophenones, benzophenones, and spirohydantoins of chroman. *Arch Biochem Biophys*, 239, 491-496.

200. **Nakanishi, T., Karp, J.E., Tan, M., Doyle, L.A., Peters, T., Yang, W., Wei, D. and Ross, D.D.** (2003) Quantitative analysis of breast cancer resistance protein and cellular resistance to flavopiridol in acute leukemia patients. *Clin Cancer Res*, 9, 3320-3328.

201. **Navarro, S., Perez, G., Navarro, G., Mena, L. and Vela, N.** (2007) Influence of fungicide residues on the primary fermentation of young lager beer. *J Agric Food Chem*, 55, 1295-1300.

202. **Nikaido, T., Ohmoto, T., Kinoshita, T., Sankawa, U., Delle Monache, F., Botta, B., Tomimori, T., Miyaichi, Y., Shirataki, Y., Yokoe, I. and et al.** (1989) Inhibition of adenosine 3',5'-cyclic monophosphate phosphodiesterase by flavonoids. III. *Chem Pharm Bull (Tokyo)*, 37, 1392-1395.

203. **Nollen, E.A., Brunsting, J.F., Roelofsen, H., Weber, L.A. and Kampinga, H.H.** (1999) In vivo chaperone activity of heat shock protein 70 and thermotolerance. *Mol Cell Biol*, 19, 2069-2079.

204. **O'Brate, A. and Giannakakou, P.** (2003) The importance of p53 location: nuclear or cytoplasmic zip code? *Drug Resist Updat*, 6, 313-322.

205. **O'Dwyer, P.J., Shoemaker, D., Zaharko, D.S., Grieshaber, C., Plowman, J., Corbett, T., Valeriote, F., King, S.A., Cradock, J., Hoth, D.F. and et al.** (1987) Flavone acetic acid (LM 975, NSC 347512). A novel antitumor agent. *Cancer Chemother Pharmacol*, 19, 6-10.

206. **Ofer, M., Wolffram, S., Koggel, A., Spahn-Langguth, H. and Langguth, P.** (2005) Modulation of drug transport by selected flavonoids: Involvement of P-gp and OCT? *Eur J Pharm Sci*, 25, 263-271.

207. **Ohnishi, H., Asamoto, M., Tujimura, K., Hokaiwado, N., Takahashi, S., Ogawa, K., Kuribayashi, M., Ogiso, T., Okuyama, H. and Shirai, T.** (2004) Inhibition of cell proliferation by nobiletin, a dietary phytochemical, associated with apoptosis and characteristic gene expression, but lack of effect on early rat hepatocarcinogenesis in vivo. *Cancer Sci*, 95, 936-942.

208. **Ong, C.S., Tran, E., Nguyen, T.T., Ong, C.K., Lee, S.K., Lee, J.J., Ng, C.P., Leong, C. and Huynh, H.** (2004) Quercetin-induced growth inhibition and cell death in nasopharyngeal carcinoma cells are associated

with increase in Bad and hypophosphorylated retinoblastoma expressions. *Oncol Rep*, 11, 727-733.

209. **Ono, K., Nakane, H., Fukushima, M., Chermann, J.C. and Barre-Sinoussi, F.** (1990) Differential inhibitory effects of various flavonoids on the activities of reverse transcriptase and cellular DNA and RNA polymerases. *Eur J Biochem*, 190, 469-476.
210. **Ormrod, D.P., Landry, L.G., Conklin, P.L.** (1995) Short term UV-B radiation and ozone exposure effects on aromatic secondary metabolite accumulation of flavonoid-deficient Arabidopsis mutants. *Physiologia Plantarum*, 93, 602-610.
211. **Pan, M.H., Chen, W.J., Lin-Shiau, S.Y., Ho, C.T. and Lin, J.K.** (2002) Tangeretin induces cell-cycle G1 arrest through inhibiting cyclin-dependent kinases 2 and 4 activities as well as elevating Cdk inhibitors p21 and p27 in human colorectal carcinoma cells. *Carcinogenesis*, 23, 1677-1684.
212. **Patel, V., Senderowicz, A.M., Pinto, D., Jr., Igishi, T., Raffeld, M., Quintanilla-Martinez, L., Ensley, J.F., Sausville, E.A. and Gutkind, J.S.** (1998) Flavopiridol, a novel cyclin-dependent kinase inhibitor, suppresses the growth of head and neck squamous cell carcinomas by inducing apoptosis. *J Clin Invest*, 102, 1674-1681.
213. **Peterson, G. and Barnes, S.** (1993) Genistein and biochanin A inhibit the growth of human prostate cancer cells but not epidermal growth factor receptor tyrosine autophosphorylation. *Prostate*, 22, 335-345.
214. **Petri, N., Tannergren, C., Holst, B., Mellon, F.A., Bao, Y., Plumb, G.W., Bacon, J., O'Leary, K.A., Kroon, P.A., Knutson, L., Forsell, P., Eriksson, T., Lennernas, H. and Williamson, G.** (2003) Absorption/metabolism of sulforaphane and quercetin, and regulation of phase II enzymes, in human jejunum in vivo. *Drug Metab Dispos*, 31, 805-813.
215. **Petros, A.M., Olejniczak, E.T. and Fesik, S.W.** (2004) Structural biology of the Bcl-2 family of proteins. *Biochim Biophys Acta*, 1644, 83-94.
216. **Pfeffer, U., Ferrari, N., Morini, M., Benelli, R., Noonan, D.M. and Albini, A.** (2003) Antiangiogenic activity of chemopreventive drugs. *Int J Biol Markers*, 18, 70-74.
217. **Pietta, P.G.** (2000) Flavonoids as antioxidants. *J Nat Prod*, 63, 1035-1042.
218. **Pinedo, H.M. and Peters, G.F.** (1988) Fluorouracil: biochemistry and pharmacology. *J Clin Oncol*, 6, 1653-1664.
219. **Pollack, I.F., Kawecki, S. and Lazo, J.S.** (1996) Blocking of glioma proliferation in vitro and in vivo and potentiating the effects of BCNU and cisplatin: UCN-01, a selective protein kinase C inhibitor. *J Neurosurg*, 84, 1024-1032.
220. **Pommier, Y., Sordet, O., Antony, S., Hayward, R.L. and Kohn, K.W.** (2004) Apoptosis defects and chemotherapy resistance: molecular interaction maps and networks. *Oncogene*, 23, 2934-2949.

221. **Qian, F., Wei, D., Zhang, Q. and Yang, S.** (2005) Modulation of P-glycoprotein function and reversal of multidrug resistance by (-)-epigallocatechin gallate in human cancer cells. *Biomed Pharmacother*, 59, 64-69.
222. **Reue, K.** (1998) mRNA quantitation techniques: considerations for experimental design and application. *J Nutr*, 128, 2038-2044.
223. **Riboli, E. and Norat, T.** (2003) Epidemiologic evidence of the protective effect of fruit and vegetables on cancer risk. *Am J Clin Nutr*, 78, 559S-569S.
224. **Robey, R.W., Medina-Perez, W.Y., Nishiyama, K., Lahusen, T., Miyake, K., Litman, T., Senderowicz, A.M., Ross, D.D. and Bates, S.E.** (2001) Overexpression of the ATP-binding cassette half-transporter, ABCG2 (Mxr/BCrp/ABCP1), in flavopiridol-resistant human breast cancer cells. *Clin Cancer Res*, 7, 145-152.
225. **Rodriguez, J., Yanez, J., Vicente, V., Alcaraz, M., Benavente-Garcia, O., Castillo, J., Lorente, J. and Lozano, J.A.** (2002) Effects of several flavonoids on the growth of B16F10 and SK-MEL-1 melanoma cell lines: relationship between structure and activity. *Melanoma Res*, 12, 99-107.
226. **Rooprai, H.K., Kandanearatchi, A., Maidment, S.L., Christidou, M., Trillo-Pazos, G., Dexter, D.T., Rucklidge, G.J., Widmer, W. and Pilkington, G.J.** (2001) Evaluation of the effects of swainsonine, captopril, tangeretin and nobiletin on the biological behaviour of brain tumour cells in vitro. *Neuropathol Appl Neurobiol*, 27, 29-39.
227. **Ross, J.A. and Kasum, C.M.** (2002) Dietary flavonoids: bioavailability, metabolic effects, and safety. *Annu Rev Nutr*, 22, 19-34.
228. **Rowley, D.C., Hansen, M.S., Rhodes, D., Sotriffer, C.A., Ni, H., McCammon, J.A., Bushman, F.D. and Fenical, W.** (2002) Thalassiolins A-C: new marine-derived inhibitors of HIV cDNA integrase. *Bioorg Med Chem*, 10, 3619-3625.
229. **Rumjanek, V.M., Trindade, G.S., Wagner-Souza, K., de-Oliveira, M.C., Marques-Santos, L.F., Maia, R.C. and Capella, M.A.** (2001) Multidrug resistance in tumour cells: characterization of the multidrug resistant cell line K562-Lucena 1. *An Acad Bras Cienc*, 73, 57-69.
230. **Rump, A.F., Schussler, M., Acar, D., Cordes, A., Ratke, R., Theisohn, M., Rosen, R., Klaus, W. and Fricke, U.** (1995) Effects of different inotropes with antioxidant properties on acute regional myocardial ischemia in isolated rabbit hearts. *Gen Pharmacol*, 26, 603-611.
231. **Russo, G., Zegar, C. and Giordano, A.** (2003) Advantages and limitations of microarray technology in human cancer. *Oncogene*, 22, 6497-6507.
232. **Rusznyak, S., Szent-Gyorgyi, A.** (1936) Vitamin P: flavanols as vitamins. *Nature*, 137, 27.
233. **Sakagami, H., Jiang, Y., Kusama, K., Atsumi, T., Ueha, T., Toguchi, M., Iwakura, I., Satoh, K., Fukai, T. and Nomura, T.** (2000) Induction of apoptosis by flavones, flavonols (3-hydroxyflavones) and isoprenoid-

substituted flavonoids in human oral tumor cell lines. *Anticancer Res*, 20, 271-277.

234. **Salatino, M., Labriola, L., Schillaci, R., Charreau, E.H. and Elizalde, P.V.** (2001) Mechanisms of cell cycle arrest in response to TGF-beta in progestin-dependent and -independent growth of mammary tumors. *Exp Cell Res*, 265, 152-166.
235. **Salgado, E. and Green, D.M.** (1956) Action of bioflavonoids on inflammation. *J Appl Physiol*, 8, 647-650.
236. **Sangrajrang, S. and Fellous, A.** (2000) Taxol resistance. *Chemotherapy*, 46, 327-334.
237. **Santos, N.C., Figueira-Coelho, J., Martins-Silva, J. and Saldanha, C.** (2003) Multidisciplinary utilization of dimethyl sulfoxide: pharmacological, cellular, and molecular aspects. *Biochem Pharmacol*, 65, 1035-1041.
238. **Sartippour, M.R., Shao, Z.M., Heber, D., Beatty, P., Zhang, L., Liu, C., Ellis, L., Liu, W., Go, V.L. and Brooks, M.N.** (2002) Green tea inhibits vascular endothelial growth factor (VEGF) induction in human breast cancer cells. *J Nutr*, 132, 2307-2311.
239. **Scalbert, A. and Williamson, G.** (2000) Dietary intake and bioavailability of polyphenols. *J Nutr*, 130, 2073S-2085S.
240. **Schwartz, G.K., Ilson, D., Saltz, L., O'Reilly, E., Tong, W., Maslak, P., Werner, J., Perkins, P., Stoltz, M. and Kelsen, D.** (2001) Phase II study of the cyclin-dependent kinase inhibitor flavopiridol administered to patients with advanced gastric carcinoma. *J Clin Oncol*, 19, 1985-1992.
241. **Senderowicz, A.M.** (1999) Flavopiridol: the first cyclin-dependent kinase inhibitor in human clinical trials. *Invest New Drugs*, 17, 313-320.
242. **Senderowicz, A.M., Headlee, D., Stinson, S.F., Lush, R.M., Kalil, N., Villalba, L., Hill, K., Steinberg, S.M., Figg, W.D., Tompkins, A., Arbuck, S.G. and Sausville, E.A.** (1998) Phase I trial of continuous infusion flavopiridol, a novel cyclin-dependent kinase inhibitor, in patients with refractory neoplasms. *J Clin Oncol*, 16, 2986-2999.
243. **Senderowicz, A.M. and Sausville, E.A.** (2000) Preclinical and clinical development of cyclin-dependent kinase modulators. *J Natl Cancer Inst*, 92, 376-387.
244. **Shah, M.A., Kortmansky, J., Motwani, M., Drobnjak, M., Gonen, M., Yi, S., Weyerbacher, A., Cordon-Cardo, C., Lefkowitz, R., Brenner, B., O'Reilly, E., Saltz, L., Tong, W., Kelsen, D.P. and Schwartz, G.K.** (2005) A phase I clinical trial of the sequential combination of irinotecan followed by flavopiridol. *Clin Cancer Res*, 11, 3836-3845.
245. **Shao, Z.M., Wu, J., Shen, Z.Z. and Barsky, S.H.** (1998) Genistein exerts multiple suppressive effects on human breast carcinoma cells. *Cancer Res*, 58, 4851-4857.
246. **Shapiro, A.B. and Ling, V.** (1997) Effect of quercetin on Hoechst 33342 transport by purified and reconstituted P-glycoprotein. *Biochem Pharmacol*, 53, 587-596.
247. **Shapiro, G.I., Supko, J.G., Patterson, A., Lynch, C., Lucca, J., Zacarola, P.F., Muzikansky, A., Wright, J.J., Lynch, T.J., Jr. and**

Rollins, B.J. (2001) A phase II trial of the cyclin-dependent kinase inhibitor flavopiridol in patients with previously untreated stage IV non-small cell lung cancer. *Clin Cancer Res*, 7, 1590-1599.

248. **Sherr, C.J.** (1995) D-type cyclins. *Trends Biochem Sci*, 20, 187-190.
249. **Shibahara, T., Onishi, T., Franco, O.E., Arima, K. and Sugimura, Y.** (2005) Down-regulation of Skp2 is correlated with p27-associated cell cycle arrest induced by phenylacetate in human prostate cancer cells. *Anticancer Res*, 25, 1881-1888.
250. **Shukla, S. and Gupta, S.** (2004) Molecular mechanisms for apigenin-induced cell-cycle arrest and apoptosis of hormone refractory human prostate carcinoma DU145 cells. *Mol Carcinog*, 39, 114-126.
251. **Siegenthaler, P., Kaye, S.B., Monfardini, S. and Renard, J.** (1992) Phase II trial with Flavone Acetic Acid (NSC.347512, LM975) in patients with non-small cell lung cancer. *Ann Oncol*, 3, 169-170.
252. **Siess, M.H., Le Bon, A.M., Canivenc-Lavier, M.C. and Suschetet, M.** (2000) Mechanisms involved in the chemoprevention of flavonoids. *Biofactors*, 12, 193-199.
253. **Siess, M.H., Leclerc, J., Canivenc-Lavier, M.C., Rat, P. and Suschetet, M.** (1995) Heterogenous effects of natural flavonoids on monooxygenase activities in human and rat liver microsomes. *Toxicol Appl Pharmacol*, 130, 73-78.
254. **Singh, R.P. and Agarwal, R.** (2006) Natural flavonoids targeting deregulated cell cycle progression in cancer cells. *Curr Drug Targets*, 7, 345-354.
255. **Singh, R.P., Dhanalakshmi, S., Tyagi, A.K., Chan, D.C., Agarwal, C. and Agarwal, R.** (2002) Dietary feeding of silibinin inhibits advance human prostate carcinoma growth in athymic nude mice and increases plasma insulin-like growth factor-binding protein-3 levels. *Cancer Res*, 62, 3063-3069.
256. **Singh, R.P., Sharma, G., Dhanalakshmi, S., Agarwal, C. and Agarwal, R.** (2003) Suppression of advanced human prostate tumor growth in athymic mice by silibinin feeding is associated with reduced cell proliferation, increased apoptosis, and inhibition of angiogenesis. *Cancer Epidemiol Biomarkers Prev*, 12, 933-939.
257. **Singhal, R.L., Yeh, Y.A., Praja, N., Olah, E., Sledge, G.W., Jr. and Weber, G.** (1995) Quercetin down-regulates signal transduction in human breast carcinoma cells. *Biochem Biophys Res Commun*, 208, 425-431.
258. **Smith, V., Raynaud, F., Workman, P. and Kelland, L.R.** (2001) Characterization of a human colorectal carcinoma cell line with acquired resistance to flavopiridol. *Mol Pharmacol*, 60, 885-893.
259. **So, F.V., Guthrie, N., Chambers, A.F., Moussa, M. and Carroll, K.K.** (1996) Inhibition of human breast cancer cell proliferation and delay of mammary tumorigenesis by flavonoids and citrus juices. *Nutr Cancer*, 26, 167-181.

260. **Spencer, J.P., Kuhnle, G.G., Williams, R.J. and Rice-Evans, C.** (2003) Intracellular metabolism and bioactivity of quercetin and its in vivo metabolites. *Biochem J*, 372, 173-181.
261. **Spencer, J.P., Rice-Evans, C. and Williams, R.J.** (2003) Modulation of pro-survival Akt/protein kinase B and ERK1/2 signaling cascades by quercetin and its in vivo metabolites underlie their action on neuronal viability. *J Biol Chem*, 278, 34783-34793.
262. **Stadler, W.M., Vogelzang, N.J., Amato, R., Sosman, J., Taber, D., Liebowitz, D. and Vokes, E.E.** (2000) Flavopiridol, a novel cyclin-dependent kinase inhibitor, in metastatic renal cancer: a University of Chicago Phase II Consortium study. *J Clin Oncol*, 18, 371-375.
263. **Stafford, H.A.** (1990) *Flavonoid metabolism*. CRC Press, Boca Raton.
264. **Stafford, H.A.** (1997) Roles of flavonoids in symbiotic and defense functions in legume roots *The Botanical Review*, 63, 27-40.
265. **Sugiyama, S., Umehara, K., Kuroyanagi, M., Ueno, A. and Taki, T.** (1993) Studies on the differentiation inducers of myeloid leukemic cells from Citrus species. *Chem Pharm Bull (Tokyo)*, 41, 714-719.
266. **Surh, Y.J.** (2003) Cancer chemoprevention with dietary phytochemicals. *Nat Rev Cancer*, 3, 768-780.
267. **Suzuki, R., Kohno, H., Murakami, A., Koshimizu, K., Ohigashi, H., Yano, M., Tokuda, H., Nishino, H. and Tanaka, T.** (2004) Citrus nobiletin inhibits azoxymethane-induced large bowel carcinogenesis in rats. *Biofactors*, 22, 111-114.
268. **Szent-Gyorgyi, A.** (1936) *Nature*, 138, 1057.
269. **Takanaga, H., Ohnishi, A., Yamada, S., Matsuo, H., Morimoto, S., Shoyama, Y., Ohtani, H. and Sawada, Y.** (2000) Polymethoxylated flavones in orange juice are inhibitors of P-glycoprotein but not cytochrome P450 3A4. *J Pharmacol Exp Ther*, 293, 230-236.
270. **Takano, Y., Kato, Y., van Diest, P.J., Masuda, M., Mitomi, H. and Okayasu, I.** (2000) Cyclin D2 overexpression and lack of p27 correlate positively and cyclin E inversely with a poor prognosis in gastric cancer cases. *Am J Pathol*, 156, 585-594.
271. **Takimoto, C.H., Glover, K., Huang, X., Hayes, S.A., Gallot, L., Quinn, M., Jovanovic, B.D., Shapiro, A., Hernandez, L., Goetz, A., Llorens, V., Lieberman, R., Crowell, J.A., Poisson, B.A. and Bergan, R.C.** (2003) Phase I pharmacokinetic and pharmacodynamic analysis of unconjugated soy isoflavones administered to individuals with cancer. *Cancer Epidemiol Biomarkers Prev*, 12, 1213-1221.
272. **Tanaka, T., Makita, H., Kawabata, K., Mori, H., Kakumoto, M., Satoh, K., Hara, A., Sumida, T., Tanaka, T. and Ogawa, H.** (1997) Chemoprevention of azoxymethane-induced rat colon carcinogenesis by the naturally occurring flavonoids, diosmin and hesperidin. *Carcinogenesis*, 18, 957-965.
273. **Terao, J., Piskula, M. and Yao, Q.** (1994) Protective effect of epicatechin, epicatechin gallate, and quercetin on lipid peroxidation in phospholipid bilayers. *Arch Biochem Biophys*, 308, 278-284.

274. **Theoharides, T.C., Alexandrakis, M., Kempuraj, D. and Lytinas, M.** (2001) Anti-inflammatory actions of flavonoids and structural requirements for new design. *Int J Immunopathol Pharmacol*, 14, 119-127.
275. **Toker, A. and Cantley, L.C.** (1997) Signalling through the lipid products of phosphoinositide-3-OH kinase. *Nature*, 387, 673-676.
276. **Tzeng, S.H., Ko, W.C., Ko, F.N. and Teng, C.M.** (1991) Inhibition of platelet aggregation by some flavonoids. *Thromb Res*, 64, 91-100.
277. **Uckun, F.M., Messinger, Y., Chen, C.L., O'Neill, K., Myers, D.E., Goldman, F., Hurvitz, C., Casper, J.T. and Levine, A.** (1999) Treatment of therapy-refractory B-lineage acute lymphoblastic leukemia with an apoptosis-inducing CD19-directed tyrosine kinase inhibitor. *Clin Cancer Res*, 5, 3906-3913.
278. **Ullmannova, V., Stockbauer, P., Hradcova, M., Soucek, J. and Haskovec, C.** (2003) Relationship between cyclin D1 and p21(Waf1/Cip1) during differentiation of human myeloid leukemia cell lines. *Leuk Res*, 27, 1115-1123.
279. **Vaidyanathan, J.B. and Walle, T.** (2003) Cellular uptake and efflux of the tea flavonoid (-)epicatechin-3-gallate in the human intestinal cell line Caco-2. *J Pharmacol Exp Ther*, 307, 745-752.
280. **van der Meer, I.M., Stam, M.E., van Tunen, A.J., Mol, J.N. and Stuitje, A.R.** (1992) Antisense inhibition of flavonoid biosynthesis in petunia anthers results in male sterility. *Plant Cell*, 4, 253-262.
281. **Van Slambrouck, S., Parmar, V.S., Sharma, S.K., De Bondt, B., Fore, F., Coopman, P., Vanhoecke, B.W., Boterberg, T., Depypere, H.T., Leclercq, G. and Bracke, M.E.** (2005) Tangeretin inhibits extracellular-signal-regulated kinase (ERK) phosphorylation. *FEBS Lett*, 579, 1665-1669.
282. **van Zanden, J.J., de Mul, A., Wortelboer, H.M., Usta, M., van Bladeren, P.J., Rietjens, I.M. and Cnubben, N.H.** (2005) Reversal of in vitro cellular MRP1 and MRP2 mediated vincristine resistance by the flavonoid myricetin. *Biochem Pharmacol*, 69, 1657-1665.
283. **Vanhaesebroeck, B., Leevers, S.J., Panayotou, G. and Waterfield, M.D.** (1997) Phosphoinositide 3-kinases: A conserved family of signal transducers. *Trends in Biochemical Sciences*, 22, 267-272.
284. **Vanhoecke, B.W., Delporte, F., Van Braeckel, E., Heyerick, A., Depypere, H.T., Nuytinck, M., De Keukeleire, D. and Bracke, M.E.** (2005) A safety study of oral tangeretin and xanthohumol administration to laboratory mice. *In Vivo*, 19, 103-107.
285. **Varghese, L., Agarwal, C., Tyagi, A., Singh, R.P. and Agarwal, R.** (2005) Silibinin efficacy against human hepatocellular carcinoma. *Clin Cancer Res*, 11, 8441-8448.
286. **Vermeulen, K., Van Bockstaele, D.R. and Berneman, Z.N.** (2003) The cell cycle: a review of regulation, deregulation and therapeutic targets in cancer. *Cell Prolif*, 36, 131-149.
287. **Vickery, H.B., Nelson, E.M., Almquist, H.J. and Elvehjem, C.A.** (1950) Term "vitamin P" recommended to be discontinued. *Science*, 112, 628.

288. **Villunger, A., Scott, C., Bouillet, P. and Strasser, A.** (2003) Essential role for the BH3-only protein Bim but redundant roles for Bax, Bcl-2, and Bcl-w in the control of granulocyte survival. *Blood*, 101, 2393-2400.
289. **Vindelov, L.L., Christensen, I.J. and Nissen, N.I.** (1983) A detergent-trypsin method for the preparation of nuclei for flow cytometric DNA analysis. *Cytometry*, 3, 323-327.
290. **von Kostanecki, S., Tambor, J.** (1895) Ueber die Constitution des Fisetins *Berichte der Deutschen Chemischen Gesellschaft* 28, 2302-2309.
291. **Walker, E.H., Pacold, M.E., Perisic, O., Stephens, L., Hawkins, P.T., Wymann, M.P. and Williams, R.L.** (2000) Structural determinants of phosphoinositide 3-kinase inhibition by wortmannin, LY294002, quercetin, myricetin, and staurosporine. *Mol Cell*, 6, 909-919.
292. **Walle, T.** (2007) Methoxylated flavones, a superior cancer chemopreventive flavonoid subclass? *Semin Cancer Biol*, 17, 354-362.
293. **Walle, T., Otake, Y., Walle, U.K. and Wilson, F.A.** (2000) Quercetin glucosides are completely hydrolyzed in ileostomy patients before absorption. *J Nutr*, 130, 2658-2661.
294. **Walle, U.K. and Walle, T.** (2002) Induction of human UDP-glucuronosyltransferase UGT1A1 by flavonoids-structural requirements. *Drug Metab Dispos*, 30, 564-569.
295. **Wang, C. and Kurzer, M.S.** (1997) Phytoestrogen concentration determines effects on DNA synthesis in human breast cancer cells. *Nutr Cancer*, 28, 236-247.
296. **Wang, H.K.** (2000) The therapeutic potential of flavonoids. *Expert Opin Investig Drugs*, 9, 2103-2119.
297. **Weiss, M.R.** (1991) Floral color changes as cues for pollinators. *Nature*, 354, 227-229.
298. **Wenzel, U., Kuntz, S., Brendel, M.D. and Daniel, H.** (2000) Dietary flavone is a potent apoptosis inducer in human colon carcinoma cells. *Cancer Res*, 60, 3823-3831.
299. **Wheldale, M.** (1909) Note on the physiological interpretation of the Mendelian factors for colour in plants. *Rep Evol Com Roy Soc Rpl*, 5, 26-31.
300. **Wheldale Onslow, M.** (1916) *The anthocyanin pigments of plants*. Cambridge University Press, Cambridge.
301. **Whitlock, J.A., Krailo, M., Reid, J.M., Ruben, S.L., Ames, M.M., Owen, W. and Reaman, G.** (2005) Phase I clinical and pharmacokinetic study of flavopiridol in children with refractory solid tumors: a Children's Oncology Group Study. *J Clin Oncol*, 23, 9179-9186.
302. **Wigand, A.** (1862) Einige Satze iiber die physiologische Bedeutung des gerbstoffes und der Pflanzenfarbe. *Bot vtg*, 20, 121-125.
303. **Wilkinson, J.t. and Clapper, M.L.** (1997) Detoxication enzymes and chemoprevention. *Proc Soc Exp Biol Med*, 216, 192-200.
304. **Williams, R.J., Spencer, J.P. and Rice-Evans, C.** (2004) Flavonoids: antioxidants or signalling molecules? *Free Radic Biol Med*, 36, 838-849.

305. **Wilson, M.I., Greenberg, B.M.** (1993) Protection of the D1 photosystem II reaction center protein from degradation in ultraviolet radiation following adaptation of Brassica napus L. to growth in ultraviolet radiation. *Photochem. Photobiol.*, 57, 556-563.
306. **Woo, H.H., Jeong, B.R. and Hawes, M.C.** (2005) Flavonoids: from cell cycle regulation to biotechnology. *Biotechnol Lett*, 27, 365-374.
307. **Wujcik, D.** (2006) EGFR as a target: rationale for therapy. *Semin Oncol Nurs*, 22, 5-9.
308. **Yanez, J., Vicente, V., Alcaraz, M., Castillo, J., Benavente-Garcia, O., Canteras, M. and Teruel, J.A.** (2004) Cytotoxicity and antiproliferative activities of several phenolic compounds against three melanocytes cell lines: relationship between structure and activity. *Nutr Cancer*, 49, 191-199.
309. **Yang, C.S., Landau, J.M., Huang, M.T. and Newmark, H.L.** (2001) Inhibition of carcinogenesis by dietary polyphenolic compounds. *Annu Rev Nutr*, 21, 381-406.
310. **Yao, L.H., Jiang, Y.M., Shi, J., Tomas-Barberan, F.A., Datta, N., Singanusong, R. and Chen, S.S.** (2004) Flavonoids in food and their health benefits. *Plant Foods Hum Nutr*, 59, 113-122.
311. **Yin, F., Giuliano, A.E. and Van Herle, A.J.** (1999) Signal pathways involved in apigenin inhibition of growth and induction of apoptosis of human anaplastic thyroid cancer cells (ARO). *Anticancer Res*, 19, 4297-4303.
312. **Yoshimizu, N., Otani, Y., Saikawa, Y., Kubota, T., Yoshida, M., Furukawa, T., Kumai, K., Kameyama, K., Fujii, M., Yano, M., Sato, T., Ito, A. and Kitajima, M.** (2004) Anti-tumour effects of nobiletin, a citrus flavonoid, on gastric cancer include: antiproliferative effects, induction of apoptosis and cell cycle deregulation. *Aliment Pharmacol Ther*, 20 Suppl 1, 95-101.
313. **Zarrinkar, P.P., Mainquist, J.K., Zamora, M., Stern, D., Welsh, J.B., Sapinoso, L.M., Hampton, G.M. and Lockhart, D.J.** (2001) Arrays of arrays for high-throughput gene expression profiling. *Genome Res*, 11, 1256-1261.
314. **Zhai, S., Dai, R., Friedman, F.K. and Vestal, R.E.** (1998) Comparative inhibition of human cytochromes P450 1A1 and 1A2 by flavonoids. *Drug Metab Dispos*, 26, 989-992.
315. **Zhang, S., Yang, X. and Morris, M.E.** (2004) Flavonoids are inhibitors of breast cancer resistance protein (ABCG2)-mediated transport. *Mol Pharmacol*, 65, 1208-1216.
316. **Zhao, J. and Agarwal, R.** (1999) Tissue distribution of silibinin, the major active constituent of silymarin, in mice and its association with enhancement of phase II enzymes: implications in cancer chemoprevention. *Carcinogenesis*, 20, 2101-2108.
317. **Zheng, Q., Hirose, Y., Yoshimi, N., Murakami, A., Koshimizu, K., Ohigashi, H., Sakata, K., Matsumoto, Y., Sayama, Y. and Mori, H.** (2002) Further investigation of the modifying effect of various

chemopreventive agents on apoptosis and cell proliferation in human colon cancer cells. *J Cancer Res Clin Oncol*, 128, 539-546.

318. **Zi, X., Feyes, D.K. and Agarwal, R.** (1998) Anticarcinogenic effect of a flavonoid antioxidant, silymarin, in human breast cancer cells MDA-MB 468: induction of G1 arrest through an increase in Cip1/p21 concomitant with a decrease in kinase activity of cyclin-dependent kinases and associated cyclins. *Clin Cancer Res*, 4, 1055-1064.

APPENDIX I

Complete gene lists

Table 27. List of genes significantly increased or decreased in expression in tangeretin-treated MDA-MB-435 cells. Cells were treated for 6 h with tangeretin (54 μM) or DMSO control. RNA was isolated and human Affymetrix arrays (HGU133A) were used to assess gene expression as described in *Materials and Methods*. GeneSpring GX 7.3 data mining software was used to obtain lists of genes that were significantly up- or downregulated following short-term tangeretin treatment (one-way ANOVA, $P \leq 0.05$). Gene expression of treated and control samples were normalized to control, and normalized values for treated samples are expressed as a ratio of control ± SEM. Ratios higher than 1 are upregulated, ratios below 1 are downregulated. The data shown were combined from three independent experiments.

Common ID	Gene name	Ratio to control	SEM
JRK		5.15	0.11
CREM		3.36	0.58
NR4A2	nuclear receptor subfamily 4, group A, 2	2.94	0.15
TNFAIP3	TNF alpha-induced protein 3	2.88	0.28
THNSL1	hypothetical protein FLJ22002	2.43	0.23
SLC6A15	solute carrier family 6 (neurotransm. transp.), 15	2.35	0.38
CREM	cAMP responsive element modulator	2.34	0.51
KIAA1199	KIAA1199 protein	2.30	0.38
TTLL1	tubulin tyrosine ligase-like family, 1	2.23	0.35
GEM	GTP-binding mitogen-induced T-cell prot.	2.17	0.23
GOLGIN-67	golgin-67	2.15	0.07
PLA2G6	phospholipase A2, group VI	2.11	0.15
PLA2G6	phospholipase A2, group VI	2.09	0.19
DFNB31	CASK-interacting protein CIP98	2.07	0.16
BHLHB2	diff. embryo chondrocyte expressed gene 1	2.06	0.20
ASB13	ankyrin repeat and SOCS box-cont. prot. 13	2.04	0.13
	cDNA DKFZp686L01105	2.03	0.37
	Clone 24487	2.02	0.17
KIAA0220	KIAA0220-like protein	1.99	0.21
MAN1B1	mannosidase, alpha, class 1B, 1	1.98	0.15
AVPI1	vasopressin-induced protein	1.97	0.21
LOC339047		1.96	0.24
SH3BP5	SH3-domain binding protein 5 (BTK-assoc.)	1.95	0.12
FLJ36166	hypothetical protein FLJ36166	1.93	0.24
NR4A2	nuclear receptor subfamily 4, group A, 2	1.91	0.18
LOC51315	hypothetical protein LOC51315	1.90	0.09
TXNRD3	thioredoxin reductase 3	1.87	0.14
OGT	O-linked GlcNAc transferase	1.86	0.19
FLJ23018	hypothetical protein FLJ23018	1.86	0.09
AMT	aminomethyltransferase	1.85	0.17
TANK	TRAF interacting protein TANK	1.84	0.07
PEPP2	phosphoinositol 3-phosphate-binding prot.-2	1.84	0.32
NR4A2	nuclear receptor subfamily 4, group A, 2	1.83	0.27
	clone TST04054	1.83	0.13
MGC3731	hypothetical protein MGC3731	1.83	0.05
	cDNA clone MAMMA1000264	1.83	0.21
TTC13	tetratricopeptide repeat domain 13	1.83	0.03
GDF15	growth differentiation factor 15	1.82	0.15
EWSR1	Ewing sarcoma breakpoint region 1	1.81	0.22
WBSCR20C	Williams Beuren synd. chromosome reg. 20C	1.80	0.07
SCN11A	sodium channel, voltage-gated, type XI, alpha	1.79	0.09
USP52	ubiquitin specific protease 52	1.79	0.15

Common ID	Gene name	Ratio to control	SEM
TAF1C	(TBP)-associated factor, RNA polymerase I, C	1.78	0.12
AIP1	atrophin-1 interacting protein 1	1.76	0.11
RAI3	retinoic acid induced 3	1.76	0.16
HNRPD	heterogeneous nuclear ribonucleoprotein D	1.75	0.14
LOC161527	golgin-like protein	1.75	0.14
HSRTSBETA	rTS beta protein	1.73	0.10
ITPR1	inositol 1,4,5-triphosphate receptor, type 1	1.73	0.16
SIAT7B	sialyltransferase 7	1.73	0.11
CTH	cystathionase	1.73	0.14
CCNL2	cyclin L2	1.72	0.07
TBC1D3	TBC1 domain family, 3	1.72	0.06
TANK	TRAF interacting protein TANK	1.72	0.09
TEB4	similar to S. cerevisiae SSM4	1.72	0.09
MSH5	mutS homolog 5	1.72	0.11
C10orf77	hypothetical protein FLJ22529	1.71	0.23
SH3YL1	SH3 domain containing, Ysc84-like 1	1.71	0.22
MOCOS	molybdenum cofactor sulfurase	1.71	0.12
MYC	v-myc myelocytomatosis viral oncogene	1.71	0.12
FADS3	fatty acid desaturase 3	1.71	0.24
USP36	ubiquitin specific protease 36	1.70	0.18
LTB4R	leukotriene B4 receptor	1.70	0.13
STYK1	protein kinase STYK1	1.70	0.12
RPS6KA2	ribosomal protein S6 kinase, polypeptide 2	1.69	0.07
NPC1	Niemann-Pick disease, type C1	1.69	0.05
IVNS1ABP	influenza virus NS1A binding protein	1.69	0.16
FLJ32731		1.69	0.03
CLCN5	chloride channel 5	1.68	0.26
NRP2	neuropilin 2	1.67	0.09
DNAJC8	DnaJ (Hsp40) , subfamily C, member 8	1.66	0.18
NT5E	5' nucleotidase, ecto	1.66	0.29
HSA9947	putative ATPase	1.66	0.15
PLSCR4	phospholipid scramblase 4	1.65	0.20
MGC57820	KIAA0393 protein	1.65	0.04
MLH3	mutL homolog 3	1.64	0.15
OR12D2	olfactory receptor, family 12, subfamily D, 2	1.64	0.08
KIAA1002	KIAA1002 protein	1.63	0.10
PLD1	phospholipase D1, phophatidylcholine-specific	1.63	0.15
SLC22A18	tumor supp. subtransferable candidate 5	1.62	0.13
KIAA0767	KIAA0767 protein	1.62	0.04
OPN3	opsin 3 (encephalopsin, panopsin)	1.61	0.06
THBS3	thrombospondin 3 precursor	1.61	0.15
DSCR1	Down syndrome critical region gene 1	1.61	0.12
UGCG	ceramide glucosyltransferase	1.60	0.07
SLC24A1	solute carrier family 24	1.60	0.16

Common ID	Gene name	Ratio to control	SEM
	(sodium/potassium/calcium exchanger), 1		
MUTYH	mutY homolog	1.59	0.02
DKFZp547I014	hypothetical protein DKFZp547I014	1.58	0.09
CRYM	crystallin, mu	1.58	0.08
BEX1	brain expressed, X-linked 1	1.58	0.06
C21orf18	chromosome 21 open reading frame 18	1.58	0.17
CHRNA10	cholinergic rec., nicotinic, α polypeptide 10	1.58	0.06
FLJ23053		1.58	0.09
NRP2	neuropilin 2	1.57	0.09
UBE3B	ubiquitin protein ligase E3B	1.56	0.14
GOLGIN-67	golgin-67	1.56	0.13
RPL17	ribosomal protein L17	1.56	0.14
	interferon	1.55	0.02
ERBB4	v-erb-a erythroblastic leuk. viral oncogene 4	1.55	0.06
ASB1	ankyrin repeat and SOCS box-cont. prot. 1	1.55	0.12
KIAA1196	KIAA1196 protein	1.55	0.08
MCAM	melanoma cell adhesion molecule	1.55	0.09
HLCS	holocarboxylase synthetase	1.55	0.11
PABPN1	poly(A) binding protein, nuclear 1	1.54	0.14
IVNS1ABP	influenza virus NS1A binding protein	1.54	0.13
FLJ12700	hypothetical protein FLJ12700	1.54	0.03
SLC19A2	solute carrier family 19, member 2	1.54	0.10
PEX1		1.54	0.06
NPD014	NPD014 protein	1.54	0.07
CBS	cystathionine-beta-synthase	1.54	0.11
PDE4D	cAMP-specific phosphodiesterase 4D	1.53	0.12
KCTD13	K+ channel tetramerisation domain cont. 13	1.53	0.11
HERPUD1	homocysteine-, ER stress-inducible, ubiquitin-like domain, 1	1.53	0.10
PAQR6	progestin and adipoQ receptor VI	1.53	0.11
PMS1	PMS1 postmeiotic segregation increased 1	1.53	0.08
SLC35E2		1.53	0.10
APBB3	amyloid β precursor prot.-binding, family B, 3	1.52	0.06
TNFAIP3	TNF alpha-induced protein 3	1.52	0.03
LOC55831	30 kDa protein	1.52	0.09
WBSCR20C	Williams Beuren synd. chromosome reg. 20C	1.52	0.09
CREM	cAMP responsive element modulator	1.51	0.18
	breast expressed mRNA from chromosome X.	1.51	0.05
MET	met proto-oncogene	1.51	0.09
PKD2	polycystin 2	1.51	0.16
HKR3	GLI-Kruppel family member HKR3	1.49	0.17
KYNU	kynureninase (L-kynurenine hydrolase)	1.49	0.10
HRMT1L1	cDNA DKFZp566M043	1.49	0.11
CLN2	ceroid-lipofuscinosis, neuronal 2	1.49	0.03

Common ID	Gene name	Ratio to control	SEM
CXorf12	chromosome X open reading frame 12	1.49	0.17
C20orf36	myelin transcription factor 1	1.49	0.11
INHA	inhibin alpha subunit precursor	1.49	0.09
SS18L1	SS18-like protein 1	1.48	0.12
CELSR3	cadherin EGF LAG 7-pass G-type receptor 3	1.48	0.06
PARC	p53-associated parkin-like cytoplasmic prot.	1.48	0.06
FLJ20399	hypothetical protein FLJ20399	1.48	0.09
KIAA0934	KIAA0934 protein	1.48	0.05
FLJ23053		1.48	0.09
DZIP1	DAZ interacting protein 1	1.47	0.07
NICAL	NEDD9 interacting protein with calponin homology and LIM domains	1.47	0.04
ARFGAP1	ADP-ribosylation fact. GTPase activat. prot. 1	1.47	0.06
WBSCR20C	Williams Beuren synd. chromosome reg. 20C	1.46	0.08
C14orf78	chromosome 14 open reading frame 78	1.46	0.06
FLJ23221	hypothetical protein FLJ23221	1.46	0.11
G2	G2 protein	1.46	0.05
	Alu subfamily SX	1.46	0.02
VPS13C	vacuolar protein sorting 13C protein	1.46	0.03
KIAA0657	KIAA0657 protein	1.46	0.10
MSH5	mutS homolog 5	1.46	0.06
FLJ11286	angiopoietin-like 6	1.46	0.08
DUSP1	dual specificity phosphatase 1	1.45	0.15
PLAT	plasminogen activator, tissue type	1.45	0.05
ATP6V0A2	ATPase, H+ transporting, lysosomal V0 subunit a, 2	1.45	0.08
OGT	O-linked GlcNAc transferase	1.45	0.07
CAMSAP1	calmodulin regulated spectrin-assoc. prot. 1	1.45	0.10
GPR126	clone RP1-287G14	1.45	0.06
NEDD4L	ubiquitin-protein ligase NEDD4-like	1.45	0.06
PLD1	phospholipase D1, phophatidylcholine-specific	1.45	0.13
TCFL5	transcription factor-like 5 protein	1.45	0.05
NRP2	neuropilin 2	1.44	0.06
C20orf104		1.44	0.15
GARS	glycyl-tRNA synthetase	1.44	0.07
AKAP9	A-kinase anchor protein 9	1.44	0.14
CROT	carnitine O-octanoyltransferase	1.44	0.12
ANKRD3	ankyrin repeat domain 3	1.44	0.08
NAGLU	N-acetylglucosaminidase, alpha	1.44	0.11
SAMD4	sterile alpha motif domain containing 4	1.44	0.10
CENTG2	Similar to ARF GTPase-activating protein	1.43	0.01
NIPSNAP1	nipsnap homolog 1	1.43	0.12
MASK-BP3	Soares infant brain 1NIB	1.43	0.06
FLJ10038	hypothetical protein FLJ10038	1.43	0.06

Common ID	Gene name	Ratio to control	SEM
AARS	alanyl-tRNA synthetase	1.43	0.09
TAO1	thousand and one amino acid protein kinase	1.43	0.15
KIAA0962	KIAA0962 protein	1.42	0.13
PSPH		1.42	0.10
FKBP9	FK506 binding protein 9	1.42	0.08
CEBPB		1.42	0.06
KCTD7	K channel tetramerisation domain cont. 7	1.41	0.11
APBB2	FE65-like protein	1.41	0.09
ZXDA		1.41	0.06
CTGLF1	ARF GTPase-activating protein	1.41	0.03
STX16	syntaxin 16	1.41	0.03
RPL37A	ribosomal protein L37a	1.41	0.05
DNAL4	dynein, axonemal, light polypeptide 4	1.41	0.05
KIAA0804	KIAA0804 protein	1.41	0.01
FLJ11196	acheron	1.41	0.08
MGC10731	hypothetical protein MGC10731	1.41	0.07
FLJ23191	hypothetical protein FLJ23191	1.41	0.02
NRP2	neuropilin 2	1.41	0.03
KIF3C	kinesin family member 3C	1.40	0.11
IVNS1ABP	influenza virus NS1A binding protein	1.40	0.03
	hypothetical protein DJ328E19.C1.1	1.40	0.04
FLJ11305	hypothetical protein FLJ11305	1.40	0.06
KIAA0556	KIAA0556 protein	1.40	0.03
MET	met proto-oncogene	1.40	0.07
JRK	jerky homolog	1.40	0.05
ZNF36	Gessler Wilms tumor similar to contains Alu repetitive element	1.40	0.05
C8orf2	chromosome 8 open reading frame 2	1.39	0.11
FAM38A	KIAA0233 gene product	1.39	0.05
C20orf44	basic FGF-repressed Zinc binding protein	1.39	0.07
SAMD4	sterile alpha motif domain containing 4	1.38	0.07
EIF2C4	eukaryotic translation initiation factor 2C, 4	1.38	0.11
SCG2	secretogranin II precursor	1.37	0.13
IKBKB	inhibitor of kappa light polypeptide gene enhancer in B-cells, kinase beta	1.37	0.07
	similar to contains Alu repetitive element	1.37	0.05
COG5	component of oligomeric golgi complex 5	1.37	0.06
FLJ10404	hypothetical protein FLJ10404	1.37	0.03
PTER	phosphotriesterase related	1.37	0.02
C6orf111	cDNA clone IMAGE:1521385	1.37	0.04
ENO3	enolase 3	1.37	0.07
MET	tpr-met fusion protein	1.37	0.11
CCNT2	cyclin T2	1.37	0.02
MGC23401	hypothetical protein MGC23401	1.36	0.04

Common ID	Gene name	Ratio to control	SEM
RCOR3	hypothetical protein FLJ10876	1.36	0.04
DDR2	discoidin domain receptor family, 2	1.36	0.06
CLN2	ceroid-lipofuscinosis, neuronal 2	1.36	0.01
SBLF	stoned B-like factor	1.36	0.12
OS-9	cDNA clone IMAGE:2263518	1.35	0.02
SH3BP5	SH3-domain binding protein 5	1.35	0.11
PDE4D	phosphodiesterase 4D, cAMP-specific	1.35	0.08
SLC33A1	acetyl-coenzyme A transporter	1.35	0.06
FLJ22639	hypothetical protein FLJ22639	1.35	0.05
CALM1	calmodulin 1 (phosphorylase kinase, delta)	1.35	0.07
ZNF451	zinc finger protein 451	1.34	0.05
MGC4278		1.34	0.06
MAN2A2	mannosidase, alpha, class 2A, 2	1.34	0.08
APLP2	amyloid beta (A4) precursor-like protein 2	1.34	0.04
FLJ21657	hypothetical protein FLJ21657	1.34	0.02
FLJ12998	hypothetical protein FLJ12998	1.34	0.07
PMS2L2	postmeiotic segregation increased 2-like 2	1.34	0.10
UROS	uroporphyrinogen III synthase	1.34	0.07
PMS2L5	postmeiotic segregation increased 2-like 6	1.34	0.01
NUCB1	nucleobindin 1	1.34	0.10
DOM3Z		1.34	0.08
BBS1	Bardet-Biedl syndrome 1	1.34	0.02
CRYZL1	crystallin, zeta-like 1	1.33	0.02
NLGN1	neuroligin 1	1.33	0.04
NEDD4L	neural precursor cell expressed, developmentally down-regulated 4-like	1.33	0.08
CHC1L	RCC1-like G exchanging factor RLG	1.33	0.03
DNAJB9	DnaJ (Hsp40) homolog, subfamily B, 9	1.33	0.12
CREB3L2	cAMP responsive elem. binding prot. 3-like 2	1.33	0.02
RABL2B	RAB, member of RAS oncogene family-like 2B	1.33	0.04
STX16	syntaxin 16	1.33	0.09
	cDNA clone MAMMA1001745	1.33	0.10
CNR2	cannabinoid receptor 2 (macrophage)	1.33	0.04
ZNF297B		1.33	0.04
FLJ21820	hypothetical protein FLJ21820	1.33	0.04
LOC157567	hypothetical protein LOC157567	1.33	0.07
SPTAN1	spectrin, alpha, non-erythrocytic 1	1.32	0.06
CXorf6	chromosome X open reading frame 6	1.32	0.07
HGS	hepatocyte growth factor-regulated tyrosine kinase substrate	1.32	0.02
RAD17	RAD17 homolog	1.32	0.05
PTPRO	receptor-type protein tyrosine phosphatase O	1.32	0.04
GTPBP2	GTP binding protein 2	1.32	0.04
AHI1	Abelson helper integration site	1.32	0.06

Common ID	Gene name	Ratio to control	SEM
WSB1	WD repeat and SOCS box-containing 1	1.32	0.10
MAFF	clone CTA-447C4	1.32	0.09
LOC129642	hypothetical protein BC016005	1.32	0.09
DVL3	dishevelled 3	1.32	0.06
GMDS	GDP-mannose 4,6-dehydratase	1.32	0.06
ZNF264		1.32	0.07
ST7	suppression of tumorigenicity	1.31	0.09
ITGB3	contains Alu repetitive element	1.31	0.09
KIAA0907		1.31	0.06
SULT1B1	sulfotransferase family, cytosolic, 1B, 1	1.31	0.04
FLJ14001	hypothetical protein FLJ14001	1.31	0.07
TCOF1	Treacher Collins-Franceschetti syndrome 1	1.31	0.10
DHODH	cDNA clone IMAGE:3882661	1.31	0.05
ABCC10	ATP-binding cassette, sub-family C, 10	1.30	0.05
GOLGIN-67	golgin-67	1.30	0.05
TFPI	tissue factor pathway inhibitor	1.30	0.08
STK19	serine/threonine kinase 19	1.30	0.05
COH1	Cohen syndrome 1	1.30	0.02
GLS	glutaminase C	1.30	0.09
KIAA0436	putative L-type neutral amino acid transporter	1.30	0.04
RPL10	ribosomal protein L10	1.30	0.09
ZNF291	zinc finger protein 291	1.30	0.09
COL15A1	alpha 1 type XV collagen precursor	1.29	0.06
KIAA0423	KIAA0423	1.29	0.04
ACADVL	acyl-CoA dehydrogenase, very long chain	1.29	0.05
SOCS2	suppressor of cytokine signaling-2	1.29	0.07
ABCC5	ATP-binding cassette, sub-family C, 5	1.29	0.06
TSAP6	dudulin 2	1.29	0.07
	PRO1693	1.29	0.03
LOC56965	EUROIMAGE 1977056	1.29	0.05
ALDH6A1	aldehyde dehydrogenase 6 family, A1	1.29	0.10
TAPBP	tapasin	1.29	0.01
LYSAL1	lysosomal apyrase-like 1	1.29	0.05
NEDD9	neural precursor cell expressed, developmentally down-regulated 9	1.29	0.05
HEMK	HEMK homolog	1.29	0.08
FLJ12270		1.29	0.04
PPM1F	protein phosphatase 1F	1.28	0.05
PAM	peptidylglycine α-amidating monooxygenase	1.28	0.01
	hypothetical protein DKFZp761N09121	1.28	0.06
SLC3A2	solute carrier family 3 (activators of dibasic and neutral amino acid transport), 2	1.28	0.05
KIF3C	kinesin family member 3C	1.28	0.03
GGCX	gamma-glutamyl carboxylase	1.28	0.06

Common ID	Gene name	Ratio to control	SEM
ZNF331	zinc finger protein 331	1.28	0.05
SURF1	surfeit 1	1.28	0.07
DDX11	Similar to DEAD/H box polypeptide 11	1.28	0.06
C6orf62	chromosome 6 open reading frame 62	1.28	0.06
CEACAM6		1.28	0.05
ILT10	leukocyte immunoglobulin-like receptor, subfamily A, 5	1.28	0.05
PTPRG	protein tyrosine phosphatase, receptor type, G	1.28	0.06
DUSP10	dual specificity phosphatase 10	1.28	0.06
KIAA0962	KIAA0962 protein	1.28	0.04
BMP1	bone morphogenetic protein 1	1.28	0.02
HEXA	hexosaminidase A (alpha polypeptide)	1.28	0.02
PRPF4B	serine/threonine-protein kinase PRP4K	1.28	0.04
KIAA0090	KIAA0090 protein	1.28	0.06
TPCN1	two pore segment channel 1	1.27	0.06
DPAGT1	UDP-N-acetylglucosamine-dolichyl-phosphate N-acetylglucosaminephosphotransferase	1.27	0.01
LTBP1	latent transf. growth fact. β binding prot. 1	1.27	0.01
LPIN2	lipin 2	1.27	0.04
FLJ21940	FLJ21940 protein	1.27	0.07
KIAA0892	KIAA0892	1.27	0.02
SOX17	SRY-box 17	1.27	0.10
SDAD1	SDA1 domain containing 1	1.27	0.03
MGC8902	cDNA clone IMAGE:2960610	1.27	0.01
ITPK1	inositol 1,3,4-triphosphate 5/6 kinase	1.27	0.02
SEL1L	sel-1 suppressor of lin-12-like	1.27	0.05
DSCR1	calcipressin 1	1.27	0.06
TROAP	trophinin associated protein (tastin)	1.26	0.04
KIAA1815		1.26	0.01
LOC376745		1.26	0.07
BRCA2	breast cancer 2, early onset	1.26	0.05
NRCAM	neuronal cell adhesion molecule	1.26	0.02
SSB1	SPRY domain-containing SOCS box protein	1.26	0.04
FLJ14360	hypothetical protein FLJ14360	1.26	0.03
DZIP1	DAZ interacting protein 1	1.26	0.07
	DKFZP434J154 protein; CGI-50 protein	1.26	0.04
SLC7A1	solute carrier family 7 (cationic amino acid transporter, y+ system), 1	1.26	0.03
CTSL	cathepsin L preproprotein	1.26	0.05
FLJ20719	hypothetical protein LOC149013	1.26	0.03
RAB5B	RAB5B, member RAS oncogene family	1.26	0.07
	cDNA clone MDSBZA03	1.26	0.01
C14orf147	chromosome 14 open reading frame 147	1.26	0.06
RUFY1	RUN and FYVE domain-containing 1	1.26	0.06

Common ID	Gene name	Ratio to control	SEM
	DKFZP586B1621 protein	1.25	0.06
CDA08	T-cell immunomodulatory protein	1.25	0.01
TDRKH	tudor and KH domain containing	1.25	0.02
PSCA	prostate stem cell antigen	1.25	0.06
EPRS	glutamyl-prolyl tRNA synthetase	1.25	0.05
HMGA1L4	high mobility group AT-hook 1-like 4	1.25	0.01
FLJ10618	hypothetical protein FLJ10618	1.25	0.02
CPR8	cell cycle progression 8 protein	1.25	0.02
TBX6	T-box 6	1.25	0.07
EIF2AK3	euk. translation initiation factor 2-α kinase 3	1.25	0.05
LRBA	LPS-responsive vesicle trafficking, beach & anchor cont.	1.25	0.06
PLEC1	plectin 1	1.25	0.05
ILF3	interleukin enhancer binding factor 3	1.25	0.06
PTPRM	protein tyrosine phosphatase, receptor type, M	1.25	0.07
LGALS3BP	galectin 3 binding protein	1.25	0.05
LOC286148	hypothetical protein LOC286148	1.25	0.02
RANBP2	RAN binding protein 2	1.24	0.04
SPG7	paraplegin isoform 1	1.24	0.04
ASPH	aspartate beta-hydroxylase	1.24	0.05
TNFRSF6B	TNF receptor superfamily, 6b	1.24	0.06
RUTBC3	RUN and TBC1 domain containing 3	1.24	0.06
DNAJC10	ER-resident protein ERdj5	1.24	0.03
C20orf121		1.24	0.09
CPD	carboxypeptidase D precursor	1.24	0.04
DFNA5	deafness, autosomal dominant 5 protein	1.24	0.05
HDAC6	histone deacetylase 6	1.24	0.08
IKBKB	inhibitor of kappa light polypeptide gene enhancer in B-cells, kinase beta	1.24	0.04
PDE8A	phosphodiesterase 8A	1.24	0.03
CPD	carboxypeptidase D precursor	1.24	0.05
FLJ21148	hypothetical protein FLJ21148	1.23	0.06
CWF19L1	CWF19-like 1, cell cycle control	1.23	0.03
USP4	ubiquitin specific protease, proto-oncogene	1.23	0.05
LOC283820	hypothetical protein LOC283820	1.23	0.03
SPUF	secreted protein of unknown function	1.23	0.06
ATP13A	ATPase type 13A	1.23	0.05
BLP2	BBP-like protein 2	1.23	0.03
TBC1D5	TBC1 domain family, member 5	1.22	0.05
FLJ13119	hypothetical protein FLJ13119	1.22	0.02
MANBA	mannosidase, beta A, lysosomal	1.22	0.07
PDE8A	phosphodiesterase 8A	1.22	0.04
GUSB	glucuronidase, beta	1.22	0.04
THADA		1.22	0.06

Common ID	Gene name	Ratio to control	SEM
KIAA0779	KIAA0779 protein	1.22	0.05
C6orf111	chromosome 6 open reading frame 111	1.22	0.06
DPYD	dihydropyrimidine dehydrogenase	1.22	0.05
ASXL1		1.22	0.07
KIAA0420	KIAA0420 gene product	1.22	0.06
NR2C1	nuclear receptor subfamily 2, group C, 1	1.22	0.05
APLP2	amyloid beta (A4) precursor-like protein 2	1.22	0.06
TFRC	transferrin receptor	1.22	0.05
IQGAP1	IQ motif containing GTPase activating prot. 1	1.21	0.05
TBC1D5	TBC1 domain family, 5	1.21	0.06
GRINL1A	glutamate receptor, ionotropic, N-methyl D-aspartate-like 1A	1.21	0.06
IGF2R	insulin-like growth factor 2 receptor	1.21	0.01
GCS1	mannosyl-oligosaccharide glucosidase	1.21	0.04
CHMP1.5	CHMP1.5 protein	1.21	0.05
APLP2	amyloid beta (A4) precursor-like protein 2	1.21	0.02
CTNS	cystinosis, nephropathic	1.21	0.05
FLJ21820	hypothetical protein FLJ21820	1.21	0.02
TSC2	tuberous sclerosis 2	1.21	0.02
ZFYVE9	MAD homolg interacting protein, receptor activation anchor	1.20	0.06
MRPL24	mitochondrial ribosomal protein L24	1.20	0.04
BPAG1	bullous pemphigoid antigen 1	1.20	0.01
GOLGA5	Golgi autoantigen, golgin subfamily a, 5	1.20	0.03
MGC35048		1.20	0.05
FLOT1	flotillin 1	1.20	0.04
TNPO2	transportin 2 (importin 3, karyopherin beta 2b)	1.20	0.03
PTPRK	protein tyrosine phosphatase, receptor type, K	1.20	0.05
CHKB	choline/ethanolamine kinase	1.20	0.05
CLK2	CDC-like kinase 2	1.20	0.04
ATR	ataxia telangiectasia & Rad3 related protein	1.20	0.04
C1QDC1	C1q domain containing 1	1.20	0.04
TM9SF1	transmembrane 9 superfamily, 1	1.20	0.06
PSAP	prosaposin	1.19	0.01
DNPEP	aspartyl aminopeptidase	1.19	0.05
PEX6	peroxisomal biogenesis factor 6	1.19	0.04
C9orf9	chromosome 9 open reading frame 9	1.19	0.03
UNC84A	unc-84 homolog A	1.19	0.04
KIAA0232	KIAA0232 protein	1.19	0.02
SLC24A1	solute carrier family 24 (sodium/potassium/calcium exchanger), 1	1.19	0.04
KIAA0368	KIAA0368	1.19	0.05
CLSTN1	calsyntenin 1	1.19	0.02
CHPF	chondroitin polymerizing factor	1.19	0.03

Common ID	Gene name	Ratio to control	SEM
HYOU1	oxygen regulated protein precursor	1.19	0.01
RBMS3	RNA binding motif, single stranded interacting protein	1.19	0.05
SCAMP1	secretory carrier membrane protein 1	1.19	0.03
VMP1	hypothetical protein DKFZp566I133	1.18	0.03
PYGL	phosphorylase, glycogen	1.18	0.06
RWDD2		1.18	0.02
GPR21	RAB GTPase activating protein 1	1.18	0.04
TNRC11		1.18	0.04
VPS52	vacuolar protein sorting 52 suppressor of actin mutations 2-like	1.18	0.04
PLCB1	phospholipase C, beta 1	1.18	0.01
GCAT		1.18	0.05
ITPR3	inositol 1,4,5-triphosphate receptor, type 3	1.18	0.02
PLOD2	procollagen-lysine, 2-oxoglutarate 5-dioxygenase 2	1.17	0.04
RSN	restin	1.17	0.04
PMS2L6	postmeiotic segregation increased 2-like 6	1.17	0.02
CUEDC2	CUE domain containing 2	1.17	0.00
LAMP1	lysosomal-associated membrane prot. 1	1.17	0.03
KIAA1940	KIAA1940 protein	1.17	0.03
DNAJB5	DnaJ (Hsp40) homolog, subfamily B, 5	1.17	0.04
LMO4	LIM domain only 4	1.17	0.03
GOSR1	golgi SNAP receptor complex member 1	1.17	0.01
TNIK	Soares infant brain 1NIB	1.17	0.01
LAMC1	laminin, gamma 1 precursor	1.17	0.01
HLA-C	MHC class I, C	1.16	0.03
C21orf33	homolog of zebrafish ES1	1.16	0.01
BET1	BET1 homolog	1.16	0.02
CARS	cysteinyl-tRNA synthetase	1.16	0.02
DNAH17	dynein, axonemal, heavy polypeptide 17	1.16	0.02
POLRMT	mitochondrial DNA-directed RNA polymerase precursor	1.16	0.02
RABGGTB	Rab geranylgeranyltransferase, beta subunit	1.16	0.02
CES2	carboxylesterase 2	1.16	0.02
CHD1L	chromodomain helicase DNA binding protein 1-like	1.16	0.04
BMP1	bone morphogenetic protein 1	1.16	0.01
GNS	glucosamine (N-acetyl)-6-sulfatase	1.16	0.01
TORC3	transducer of regulated CREB 3	1.16	0.04
FLJ10902	hypothetical protein FLJ10902	1.15	0.03
SLC4A4	solute carrier family 4, sodium bicarbonate cotransporter, 4	1.15	0.01
NDUFA1	NADH dehydrogenase (ubiquinone) 1 alpha	1.15	0.03

Common ID	Gene name	Ratio to control	SEM
	subcomplex, 1		
MSH4	mutS homolog 4	1.15	0.02
HDLBP	high density lipoprotein binding protein	1.15	0.02
DDX10	DEAD (Asp-Glu-Ala-Asp) box polypeptide 10	1.15	0.02
PRKCSH	protein kinase C substrate 80K-H	1.15	0.02
APLP2	amyloid beta (A4) precursor-like protein 2	1.15	0.03
PFKL	phosphofructokinase, liver	1.14	0.04
PMS2L2	PMS2 related gene	1.14	0.02
VARS2	valyl-tRNA synthetase 2	1.14	0.02
TFAP4	transcription factor AP-4	1.14	0.04
	contains Alu repetitive element	1.14	0.01
TDE1	tumor differentially expressed protein 1	1.14	0.04
AD-017	glycosyltransferase AD-017	1.14	0.03
	DKFZP564C103 protein	1.14	0.01
ANXA4	annexin A4	1.14	0.04
PPGB	protective protein for beta-galactosidase	1.14	0.02
PDIR	protein disulfide isomerase-related	1.14	0.03
DIAPH2	diaphanous 2	1.14	0.03
PTPRZ1	protein tyrosine phosphatase, receptor-type, Z polypeptide 1	1.14	0.02
HKE2	HLA class II region expressed gene KE2	1.13	0.03
IARS	isoleucine-tRNA synthetase	1.13	0.01
ZNF318	zinc finger protein 318	1.13	0.02
TRIM44	tripartite motif-containing 44	1.13	0.04
FNBP3		1.13	0.03
LAMA4	laminin, alpha 4 precursor	1.12	0.03
CPA4	carboxypeptidase A4	1.12	0.02
CSRP1	cysteine and glycine-rich protein 1	1.12	0.02
MGC3222	hypothetical protein MGC3222	1.12	0.03
TRRAP		1.12	0.03
TM9SF4	transmembrane 9 superfamily protein 4	1.12	0.03
CLTB	clathrin, light polypeptide	1.12	0.03
C2orf28	apoptosis related protein APR-3	1.12	0.03
CPS1	carbamoyl-phosphate synthetase 1, mitocho.	1.11	0.02
GNG7	guanine nucleotide binding protein, gamma 7	1.11	0.03
M-RIP	myosin phosphatase-Rho interacting protein	1.11	0.03
CRSP2	cofactor required for Sp1 transcriptional activation, subunit 2	1.11	0.02
SIRT5	sirtuin 5	1.11	0.03
OSBP	oxysterol binding protein	1.11	0.02
PMS2L2	postmeiotic segregation increased 2-like 9	1.11	0.03
ITGB1	cDNA clone IMAGE:4669168	1.10	0.03
MINPP1	multiple inositol polyphosphate histidine phosphatase, 1	1.10	0.03

Common ID	Gene name	Ratio to control	SEM
P4HB	prolyl 4-hydroxylase, beta subunit	1.10	0.01
SLC30A5	zinc transporter ZTL1	1.09	0.02
GFPT1	glutamine-fructose-6-phosp. transaminase 1	1.09	0.01
SENP6	SUMO-1 specific protease	1.09	0.00
ADP-GK	ATP-dependent glucokinase	1.08	0.01
TM4SF13	tetraspan NET-6transmembrane 4 superfamily, 13	1.08	0.02
RAD17	RAD17 homolog	1.05	0.01
EIF3S1	euk. translation initiation factor 3, subunit 1 α	0.96	0.00
NFIB	nuclear factor I/B	0.95	0.01
B4GALT5	UDP-Gal:betaGlcNAc beta 1,4-galactosyltransferase 5	0.94	0.02
TCF7L2	transcription factor 7-like 2	0.93	0.02
CAST	calpastatin	0.93	0.01
MAP2K4	mitogen-activated protein kinase kinase 4	0.93	0.01
ALDOA	aldolase A	0.93	0.02
DIAPH1	diaphanous 1	0.93	0.02
RBBP6	retinoblastoma-binding protein 6	0.92	0.02
DJ971N18.2		0.92	0.02
SSRP1	structure specific recognition protein 1	0.92	0.00
FLJ20436	hypothetical protein FLJ20436	0.92	0.03
SGPL1	sphingosine-1-phosphate lyase 1	0.92	0.02
GDAP2	ganglioside induced diff. assoc. prot. 2	0.92	0.01
GNB1	guanine nucleotide-binding protein, beta-1	0.91	0.02
ADPRTL2	poly (ADP-ribosyl) transferase-like 2	0.91	0.01
DSTN	destrin (actin depolymerizing factor)	0.91	0.00
RPL29	ribosomal protein L29	0.91	0.00
GNB2	guanine nucleotide-binding protein, beta-2	0.91	0.01
CAV2	caveolin 2	0.91	0.01
MYL6	myosin, light polypeptide 6	0.90	0.02
RTN4	reticulon 4	0.90	0.02
JAK2	Janus kinase 2	0.90	0.02
ZFP36L2	butyrate response factor 2	0.90	0.01
SPR	sepiapterin reductase	0.90	0.02
SMBP	SM-11044 binding protein	0.90	0.02
ILF2	interleukin enhancer binding factor 2	0.90	0.01
YT521	splicing factor YT521-B	0.90	0.02
TBL2	transducin (beta)-like 2	0.90	0.00
SNRPE	small nuclear ribonucleoprotein polypeptide E	0.90	0.03
TOMM20	translocase of outer mitochondrial memb. 20	0.90	0.01
ANXA7	annexin VII	0.90	0.02
ARF6	ADP-ribosylation factor 6	0.89	0.01
APG5L	APG5 autophagy 5-like	0.89	0.02
ATF2		0.89	0.01

Common ID	Gene name	Ratio to control	SEM
CRKL	v-crk sarcoma virus CT10 oncogene homolog	0.89	0.02
GNAS	guanine nucleotide binding protein, alpha stimulating activity polypeptide 1	0.89	0.02
	Rho-associated, coiled-coil cont. prot. kinase 1	0.89	0.02
PAIP1	poly(A) binding protein interacting protein 1	0.89	0.01
RCN2	reticulocalbin 2, EF-hand calcium binding domain	0.89	0.02
FGD1	faciogenital dysplasia protein	0.89	0.01
PTPLB	protein tyrosine phosphatase-like, b	0.89	0.02
RCOR1	REST corepressor	0.89	0.00
TNPO3	transportin 3	0.89	0.01
CSNK1A1	casein kinase 1, alpha 1	0.89	0.02
SP3	Sp3 transcription factor	0.89	0.02
SMC4L1	SMC4 structural maintenance of chromosomes 4-like 1	0.89	0.01
S100A11	S100 calcium binding protein A11	0.89	0.02
SH3GLB1	SH3-containing protein SH3GLB1	0.88	0.03
VCP	valosin-containing protein	0.88	0.02
CD47	CD47 antigen	0.88	0.01
	hypothetical protein LOC340562	0.88	0.03
BRF2	RNA polymerase III transcription initiation fact.	0.88	0.01
STK10	serine/threonine kinase 10	0.88	0.02
HSPH1	heat shock 105kDa/110kDa protein 1	0.88	0.02
TIMM9	translocase of inner mitochondrial membrane 9 homolog	0.88	0.01
GALNT1	UDP-N-acetyl-alpha-D-galactosamine:polypeptide N-acetylgalactosaminyltransferase 1	0.88	0.03
CSDA	cold shock domain protein A	0.88	0.03
	nuclear transcription factor Y, gamma	0.88	0.03
SKP1A		0.88	0.03
PPP2CB	protein phosphatase 2, catalytic subunit, beta	0.88	0.02
H3F3B	H3 histone, family 3B	0.88	0.03
MGAT2	alpha-1,6-mannosyl-glycoprotein beta-1,2-N-acetylglucosaminyltransferase	0.88	0.03
FLJ11021	similar to splicing factor, arginine/serine-rich 4	0.88	0.03
PPP2R2A	alpha isoform of regulatory subunit B55, protein phosphatase 2	0.88	0.02
FKBP3	FK506-binding protein 3	0.88	0.03
ZWINT	ZW10 interactor	0.88	0.03
NRAS	neuroblastoma RAS viral oncogene homolog	0.88	0.02
UBE2I	ubiquitin-conjugating enzyme E2I	0.88	0.02
KIAA0174	KIAA0174 gene product	0.87	0.03
FLJ20297	hypothetical protein FLJ20297	0.87	0.02

Common ID	Gene name	Ratio to control	SEM
KRT10	keratin 10	0.87	0.03
DC8	DKFZP566O1646 protein	0.87	0.02
ADIPOR2	adiponectin receptor 2	0.87	0.02
GNA11	guanine nucleotide binding protein, alpha 11	0.87	0.03
ASF1B	ASF1 anti-silencing function 1 homolog B	0.87	0.03
CHC1	chromosome condensation 1	0.87	0.02
MRPS12	mitochondrial ribosomal protein S12	0.87	0.04
PDCL3	phosducin-like 3	0.87	0.02
RBM25	RNA-binding region (RNP1, RRM) cont. 7	0.87	0.02
JMJD1B	jumonji domain containing 1B	0.87	0.00
DMXL1	Dmx-like 1	0.87	0.02
IRAK4	interleukin-1 receptor-associated kinase 4	0.87	0.03
GAL3ST4	galactose-3-O-sulfotransferase 4	0.87	0.02
SMAP-5	golgi membrane protein SB140	0.87	0.02
FOXO3A	forkhead box O3A	0.87	0.03
PELO	pelota homolog	0.87	0.03
UBQLN2		0.86	0.01
SERPINA4	serine proteinase inhibitor, clade A, 4	0.86	0.01
PTEN	phosphatase and tensin homolog	0.86	0.03
FAM29A	family with sequence similarity 29, A	0.86	0.01
C1orf25	N2,N2-dimethylguanosine tRNA methyltransferase-like	0.86	0.03
PDCD4	programmed cell death 4	0.86	0.01
HMG2L1	high-mobility group protein 2-like 1	0.86	0.02
ZNF148	zinc finger protein 148 (pHZ-52)	0.86	0.03
BRMS1	breast cancer metastasis suppressor 1	0.86	0.02
HNRPA3	heterogeneous nuclear ribonucleoprotein A3	0.86	0.03
RBMS1	RNA binding mot. single-stranded inter. prot. 1	0.86	0.02
HMGN4	high mobility group nucleosomal binding domain 4	0.86	0.03
TRIP13	thyroid hormone receptor interactor 13	0.86	0.01
KPNA1	karyopherin alpha 1	0.86	0.02
SH3GLB1	SH3-containing protein SH3GLB1	0.86	0.01
WTAP	Wilms' tumour 1-associating protein	0.86	0.02
DYRK1A	dual-specificity tyrosine-(Y)-phosphorylation regulated kinase 1A	0.86	0.01
CTCF	CCCTC-binding factor (zinc finger protein)	0.86	0.02
AKAP8	A-kinase anchor protein 8	0.86	0.04
KIAA0355	KIAA0355	0.86	0.01
EML1	echinoderm microtubule assoc. protein like 1	0.86	0.03
HMGB1	high-mobility group box 1	0.86	0.02
AP1G1	adaptor-related protein complex 1, gamma 1	0.86	0.04
NDFIP1	Nedd4 family interacting protein 1	0.86	0.01
PRDX2	peroxiredoxin 2	0.86	0.03

Common ID	Gene name	Ratio to control	SEM
P17.3	neuronal protein 17.3	0.86	0.03
RNF138	ring finger protein 138	0.86	0.00
PGK1	phosphoglycerate kinase 1	0.86	0.02
DDX11	DEAD/H box polypeptide 11	0.85	0.00
CAST	calpastatin	0.85	0.02
HNRPD	heterogeneous nuclear ribonucleoprotein D	0.85	0.01
HRB	HIV-1 Rev binding protein	0.85	0.02
SLC25A10	solute carrier family 25 (mitochondrial carrier; dicarboxylate transporter), 10	0.85	0.00
PSMD14	26S proteasome-associated pad1 homolog	0.85	0.03
NCOA3	nuclear receptor coactivator 3	0.85	0.02
CYP20A1	cytochrome P450, family 20, subfamily A, 1	0.85	0.02
ANP32E	acidic nuclear phosphoprotein 32 family, E	0.85	0.03
KIAA0431	KIAA0431 protein	0.85	0.02
UBE2C	ubiquitin-conjugating enzyme E2C	0.85	0.02
CSNK1A1	casein kinase 1, alpha 1	0.85	0.02
DPF2	D4, zinc and double PHD fingers family 2	0.85	0.05
MST4	serine/threonine protein kinase MASK	0.85	0.02
SPATA6	spermatogenesis associated 6	0.85	0.02
FLJ12671	hypothetical protein FLJ12671	0.85	0.01
HRB2	HIV-1 rev binding protein 2	0.85	0.02
SQLE	squalene monooxygenase	0.85	0.04
EIF3S10	euk. translation initiation factor 3, subunit 10	0.85	0.01
UPF3B	UPF3 regulator of nonsense transcripts B	0.85	0.02
MBNL1	muscleblind-like	0.85	0.02
CDK7	cyclin-dependent kinase 7	0.85	0.01
FEM1C	fem-1 homolog c	0.85	0.04
CLN6	CLN6 protein ceroid-lipofuscinosis, neuronal 6	0.85	0.03
VBP1	von Hippel-Lindau binding protein 1	0.85	0.02
HNRPH1	heterogeneous nuclear ribonucleoprotein H1	0.85	0.04
TFAP2C	transcription factor AP-2 gamma	0.85	0.01
RBMS1	RNA binding mot. single stranded inter. prot. 1	0.85	0.02
PITPNB		0.85	0.01
TFG	TRK-fused gene	0.85	0.02
MPST	3-mercaptopyruvate sulfurtransferase	0.85	0.03
FLJ11021	similar to splicing factor, arginine/serine-rich 4	0.85	0.01
CAP350	centrosome-associated protein 350	0.85	0.03
MRPS31	mitochondrial ribosomal protein S31	0.85	0.04
RAB14	RAB14, member RAS oncogene family	0.85	0.03
ETV1	ets variant gene 1	0.84	0.02
SART1	squamous cell carcinoma antigen recognized by T cells 1	0.84	0.02
KIF22	kinesin family member 22	0.84	0.01
	cDNA clone IMAGE:3009204	0.84	0.03

Common ID	Gene name	Ratio to control	SEM
HPS5	Hermansky-Pudlak syndrome 5	0.84	0.03
CAP350	centrosome-associated protein 350	0.84	0.03
NFYC	nuclear transcription factor Y, gamma	0.84	0.04
BCL2L2	BCL2-like 2 protein	0.84	0.02
RNUT1	RNA, U transporter 1	0.84	0.02
ACP1	acid phosphatase 1	0.84	0.04
FH	fumarate hydratase	0.84	0.02
HNRPUL1	heterogeneous nuclear ribonucleoprotein U-like 1	0.84	0.03
CD84	CD84 antigen (leukocyte antigen)	0.84	0.04
FLJ10036	hypothetical protein FLJ10036	0.84	0.03
SNRPN	small nuclear ribonucleoprotein polypeptide N	0.84	0.01
MEG3	PRO0518	0.84	0.04
MRPL11	mitochondrial ribosomal protein L11	0.84	0.01
ARHGAP11A	similar to human GTPase-activating prot.	0.84	0.02
WAC	WW domain-containing adapter with a coiled-coil region	0.84	0.01
ERCC1	excision repair cross-complementing 1	0.84	0.03
SPRY2	sprouty 2	0.84	0.03
CHPPR		0.84	0.03
FTSJ3	FtsJ homolog 3	0.84	0.02
RYBP	RING1 and YY1 binding protein	0.84	0.03
NFYC	nuclear transcription factor Y, gamma	0.84	0.02
SGCE	sarcoglycan, epsilon	0.84	0.03
CAV1	caveolin 1, caveolae protein, 22kDa	0.84	0.02
ZRF1	zuotin related factor 1	0.84	0.03
CTDSPL	carboxy-terminal domain, RNA polymerase II, polypeptide A, small phosphatase-like	0.84	0.03
DLP	Dim1-like protein	0.84	0.05
SFPQ	splicing factor proline/glutamine rich	0.84	0.02
GTF3C2	general transcription factor IIIC, polypeptide 2	0.84	0.04
HSPC009	HSPC009 protein	0.84	0.04
TRPM2	transient receptor potential cation channel, subfamily M, 2	0.84	0.01
NXT1	NTF2-like export factor 1	0.83	0.02
DNMT3B	DNA cytosine-5 methyltransferase 3 beta	0.83	0.03
KIAA0033	KIAA0033 protein	0.83	0.04
KPNB1	karyopherin (importin) beta 1	0.83	0.02
DHX15	DEAH (Asp-Glu-Ala-His) box polypeptide 15	0.83	0.04
HNRPA2B1	heterogeneous nuclear ribonucleoprotein A2/B1	0.83	0.02
CAV1	caveolin 1	0.83	0.04
GTPBP3		0.83	0.02
GRB2	growth factor receptor-bound protein 2	0.83	0.04
TAS2R14	taste receptor, type 2, member 14	0.83	0.04

Common ID	Gene name	Ratio to control	SEM
CREB3	cAMP responsive element binding protein 3	0.83	0.04
PAQR3	progestin and adipoQ receptor III	0.83	0.04
HNRPD	heterogeneous nuclear ribonucleoprotein D	0.83	0.04
ZDHHC3	zinc finger, DHHC domain containing 3	0.83	0.02
TXNDC9	ATP binding protein assoc. with cell differentiation	0.83	0.00
HRB	HIV-1 Rev binding protein	0.83	0.02
FAH	fumarylacetoacetate hydrolase (fumarylacetoacetase)	0.83	0.03
OSTF1	osteoclast stimulating factor 1	0.83	0.04
TBCE	beta-tubulin cofactor E	0.83	0.01
C10orf26	chromosome 10 open reading frame 26	0.83	0.03
TBCC	beta-tubulin cofactor C	0.83	0.03
CHD4	chromodomain helicase DNA binding prot. 4	0.83	0.03
MGC5242	hypothetical protein MGC5242	0.83	0.01
ILK	integrin-linked kinase	0.83	0.03
DNAPTP6	DNA polymerase-transactivated protein 6	0.83	0.01
SMAD2	mothers against decapentaplegic homolog 2	0.83	0.01
SSA2	Sjogren syndrome antigen A2	0.83	0.01
XTP2	HBxAg transactivated protein 2	0.83	0.03
TFDP2	transcription factor Dp-2	0.83	0.03
PREI3	preimplantation protein 3	0.83	0.02
CDC2L5	cell division cycle 2-like 5	0.83	0.03
ATP6V0B	ATPase, H+ transporting, lysosomal 21kD, V0 subunit c	0.83	0.01
YAP1		0.83	0.01
RPL36	ribosomal protein L36	0.83	0.04
HSPH1	heat shock 105kD	0.83	0.03
DLGAP4	disks large-associated protein 4	0.83	0.04
FLJ21919	FLJ21919 protein	0.83	0.04
STAG2	stromal antigen 2	0.83	0.01
FLJ20274	synonym: hmel2	0.82	0.04
FDFT1	farnesyl-diphosphate farnesyltransferase 1	0.82	0.03
ADORA2B	adenosine A2b receptor	0.82	0.02
USP46	ubiquitin specific protease 46	0.82	0.01
HMOX1	heme oxygenase (decyclizing) 1	0.82	0.04
GCSH	glycine cleavage system protein H	0.82	0.05
MAPK14	p38 mitogen activated protein kinase	0.82	0.02
LOC91966	hypothetical protein LOC91966	0.82	0.02
PAI-RBP1	PAI-1 mRNA-binding protein	0.82	0.03
ENTPD8	ectonucleoside triphosphate diphosphohydrolase 8	0.82	0.02
AP2S1	adaptor-related protein complex 2, sigma 1	0.82	0.03
PLEKHJ1	pleckstrin homology domain cont., family J, 1	0.82	0.02

Common ID	Gene name	Ratio to control	SEM
PTMA		0.82	0.04
TPARL	TPA regulated locus	0.82	0.01
ARPC2	actin related protein 2/3 complex subunit 2	0.82	0.04
DGCR14	DiGeorge syndrome critical region prot. 14	0.82	0.04
TLOC1	translocation protein 1	0.82	0.04
RARB	retinoic acid receptor, beta	0.82	0.04
LOC51668	HSPCO34 protein	0.82	0.05
SERF1A	small EDRK-rich factor 1B, centromeric	0.82	0.05
	CDNA FLJ38130 fis, clone D6OST2000464	0.82	0.03
CSNK1D	casein kinase 1	0.82	0.04
EIF4G2	eukaryotic translation initiation factor 4 gamma, 2	0.82	0.03
AMMECR1	Alport syndrome, mental retardation, midface hypoplasia & elliptocytosis chromosomal region, gene 1	0.82	0.01
NUP50	nucleoporin 50kDa	0.82	0.03
NME6	nucleoside diphosphate kinase type 6	0.82	0.04
PPP1R2		0.82	0.04
SYT1	synaptotagmin I	0.82	0.02
SRRM1	Ser/Arg-related nuclear matrix protein	0.82	0.05
ETHE1	ETHE1 protein ethylmalonic encephalopathy 1	0.82	0.02
HNRPH3	heterogeneous nuclear ribonucleoprotein H3	0.82	0.03
MAP4K4	MAP kinase kinase kinase kinase 4	0.82	0.00
YY1	YY1 transcription factor	0.82	0.04
HSPA8	heat shock 70kDa protein 8	0.81	0.04
PEO1	twinkle progressive external ophthalmoplegia 1	0.81	0.03
KIAA0186		0.81	0.02
C2orf8	chromosome 2 open reading frame 8	0.81	0.04
TOR3A	torsin family 3, member A	0.81	0.01
AFURS1	ATPase family homolog up-regulated in senescence cells	0.81	0.02
CENPA	centromere protein A	0.81	0.01
MRPS7	mitochondrial ribosomal protein S7	0.81	0.04
LSS	lanosterol synthase	0.81	0.04
JTV1	JTV1	0.81	0.02
CGI-141	CGI-141 protein	0.81	0.03
NUDC	nuclear distribution gene C homolog	0.81	0.03
HIF1AN	hypoxia-inducible factor 1, alpha subunit inhibitor	0.81	0.03
SSB	Sjogren syndrome antigen B	0.81	0.01
PDLIM1	PDZ and LIM domain 1 (elfin)	0.81	0.02
TEAD4	TEA domain family member 4	0.81	0.00
VAMP5	vesicle-associated membrane protein 5	0.81	0.02
M96	putative DNA binding protein	0.81	0.05

Common ID	Gene name	Ratio to control	SEM
CUL3	cullin 3	0.81	0.04
SLC2A6	solute carrier family 2 (facilitated glucose transporter), 6	0.81	0.05
SNX1	sorting nexin 1	0.81	0.03
NPAT	nuclear protein, ataxia-telangiectasia	0.81	0.02
POP1	processing of precursor 1	0.81	0.04
HSPC111	hypothetical protein HSPC111	0.81	0.03
C18orf1	chromosome 18 open reading frame 1	0.81	0.03
PPP2R5E	epsilon isoform of regulatory subunit B56, protein phosphatase 2A	0.81	0.01
RNF153	hypothetical protein FLJ20445	0.81	0.01
LEREPO4	erythropoietin 4 immediate early response	0.81	0.01
DNAJD1	DNAJ domain-containing	0.81	0.03
PTMA	prothymosin alpha	0.81	0.04
LASP1	LIM and SH3 protein 1	0.81	0.05
C20orf20	MRG-binding protein	0.81	0.02
LEREPO4	likely ortholog of mouse immediate early response, erythropoietin 4	0.81	0.05
DNAJA2	DnaJ (Hsp40) homolog, subfamily A, 2	0.81	0.03
SEPHS1	selenophosphate synthetase	0.81	0.02
PSMA2	proteasome alpha 2 subunit	0.81	0.01
CDKN3	cyclin-dependent kinase inhibitor 3	0.81	0.03
UBE2D1	ubiquitin-conjugating enzyme E2D 1	0.81	0.01
MO25	MO25 protein	0.81	0.04
KIAA0241	KIAA0241 protein	0.81	0.04
SYNCRIP	synaptotagmin binding, cytoplasmic RNA interacting prot.	0.81	0.03
HNRPF	heterogeneous nuclear ribonucleoprotein F	0.81	0.04
LRRFIP2	leucine rich repeat interacting protein 2	0.81	0.05
PSMA5	proteasome alpha 5 subunit	0.81	0.03
PSMB3	proteasome beta 3 subunit	0.81	0.03
SELT	selenoprotein T	0.81	0.02
FLJ21908	hypothetical protein FLJ21908	0.80	0.04
NR2F2	nuclear receptor subfamily 2, group F, 2	0.80	0.02
FLJ14668	hypothetical protein FLJ14668	0.80	0.01
CREBBP	CREB binding protein	0.80	0.01
SUI1	putative translation initiation factor	0.80	0.02
TUBB2	Tubulin beta-2 chain	0.80	0.04
PIP5K2A	phosphatidylinositol-4-phosphate 5-kinase type II α	0.80	0.02
DDX48	DEAD (Asp-Glu-Ala-Asp) box polypeptide 48	0.80	0.02
APG5L	APG5 autophagy 5-like	0.80	0.00
DDX56	DEAD (Asp-Glu-Ala-Asp) box polypeptide 56	0.80	0.04
CDKN1B	cyclin-dependent kinase inhibitor 1B	0.80	0.02

Common ID	Gene name	Ratio to control	SEM
KRT18	keratin 18	0.80	0.01
NXT2	nuclear transport factor 2-like export factor 2	0.80	0.04
BRD4	bromodomain containing 4	0.80	0.01
CD97	CD97 antigen	0.80	0.01
RBM7	RNA binding motif protein 7	0.80	0.01
EPHB4	ephrin receptor EphB4 precursor	0.80	0.03
EIF4ENIF1	eukaryotic translation init. fact. 4E nuclear import fact. 1	0.80	0.04
C2orf25	hypothetical protein CL25022	0.80	0.03
NUDT4	nudix (nucleoside diphosphate linked moiety X)-type motif 4	0.80	0.04
FLJ22729	hypothetical protein FLJ22729	0.80	0.02
MIZ1	Msx-interacting-zinc finger protein 1	0.80	0.04
TMPO	thymopoietin	0.80	0.02
CGI-115	CGI-115 protein	0.80	0.02
TGFBR2	TGF-betaIIR alpha	0.80	0.02
KPNA2	karyopherin alpha 2	0.80	0.04
PC326	PC326 protein	0.80	0.03
SSB	Sjogren syndrome antigen B	0.80	0.03
PPAP2A	phosphatidic acid phosphatase type 2A	0.80	0.01
TAF5	upreg. during skeletal muscle growth 5	0.80	0.03
NS3TP1	HCV NS3-transactivated protein 1	0.80	0.04
KPNB1	karyopherin (importin) beta 1	0.80	0.03
TCF12	transcription factor 12	0.80	0.04
PA2G4	proliferation-associated 2G4	0.80	0.01
IFNGR2	interferon gamma receptor 2	0.80	0.01
H3F3A	H3 histone, family 3A	0.79	0.02
AASDHPPT	aminoadipate-semialdehyde dehydrogenase-phosphopantetheinyl transferase	0.79	0.02
NET1	neuroepithelial cell transforming gene 1	0.79	0.03
TNFSF5IP1	TNF superfamily, member 5-induced protein 1	0.79	0.01
DP1	polyposis locus protein 1	0.79	0.04
FMR1	fragile X mental retardation 1	0.79	0.05
MGC34132	unnamed protein product	0.79	0.01
KIAA1449	WD repeat endosomal protein	0.79	0.03
FBXO21	F-box only protein 21	0.79	0.04
MAD2L1	MAD2-like 1	0.79	0.03
H3F3B	H3 histone, family 3B	0.79	0.04
UBE2D2	ubiquitin-conjugating enzyme E2D 2	0.79	0.06
PSMA4	proteasome alpha 4 subunit	0.79	0.05
LUC7L2	LUC7-like 2	0.79	0.04
hSyn	brain synembryn	0.79	0.02
CDCA8	cell division cycle associated 8	0.79	0.02
NUMB	numb homolog	0.79	0.04

Common ID	Gene name	Ratio to control	SEM
LOC90410		0.79	0.03
BAD	BCL2-antagonist of cell death protein	0.79	0.02
PHACTR4	hypothetical protein FLJ13171	0.79	0.01
SDF2L1	stromal cell-derived factor 2-like 1	0.79	0.05
CSNK1G1	casein kinase 1, gamma 1	0.79	0.03
SC5DL	sterol-C5-desaturase-like	0.79	0.00
MPZL1	myelin protein zero-like 1	0.79	0.03
GMFB	glia maturation factor, beta	0.79	0.03
U2AF1	U2 small nuclear RNA auxillary factor 1	0.79	0.02
H2AFX	H2A histone family, member X	0.79	0.03
KIF22		0.79	0.06
USP49	Trf-proximal ubiquitin specific protease 49	0.79	0.03
TJP2	tight junction protein 2	0.79	0.02
RAB23	Ras-related protein Rab-23	0.79	0.03
YES1	viral oncogene yes-1 homolog 1	0.79	0.01
TRIM38	tripartite motif-containing 38	0.79	0.02
FLJ12671	hypothetical protein FLJ12671	0.79	0.05
RPP30	ribonuclease P (30kD)	0.79	0.05
FOXF2	forkhead box F2	0.79	0.01
OGFR	opioid growth factor receptor	0.79	0.04
TERE1	transitional epithelia response protein	0.79	0.03
FAM3C	predicted osteoblast protein	0.79	0.02
HT021	HT021	0.79	0.02
GNAI3	guanine nucleotide binding prot., alpha inhibiting activity, 3	0.79	0.02
ETV1	ets variant gene 1	0.79	0.02
GAK	cyclin G associated kinase	0.79	0.03
KPNB1	karyopherin (importin) beta 1	0.79	0.04
RBM22	hypothetical protein FLJ10290	0.79	0.04
MRPS17	mitochondrial ribosomal protein S17	0.79	0.03
AB026190	Kelch motif containing protein	0.79	0.05
PHLDA1	pleckstrin homology-like domain, family A, 1	0.78	0.03
GADD45GIP1	papillomavirus L2 interacting nuclear protein 1	0.78	0.04
PEG10	paternally expressed 10	0.78	0.05
GPKOW	T54 protein	0.78	0.04
	cDNA DKFZp434C2331	0.78	0.05
H41	hypothetical protein H41	0.78	0.02
CRK7	CDC2-related protein kinase 7	0.78	0.03
SPIN	spindlin	0.78	0.03
PPAP2C	phosphatidic acid phosphatase type 2C	0.78	0.02
SUI1	putative translation initiation factor	0.78	0.01
KRAS2	Kirsten rat sarcoma 2 viral oncogene homolog	0.78	0.04
ZNF161	zinc finger protein 161	0.78	0.03
ARID5B	AT rich interactive domain 5B	0.78	0.01

Common ID	Gene name	Ratio to control	SEM
RIOK3	RIO kinase 3	0.78	0.01
CCNB1	cyclin B1	0.78	0.03
EHD4	hepatocellular carcinoma-associated prot.	0.78	0.04
RYK	receptor-like tyrosine kinase precursor	0.78	0.03
PLEKHC1	pleckstrin homology domain containing, family C, 1	0.78	0.02
POLR2D	DNA directed RNA polymerase II, D	0.78	0.02
BCAS2	breast carcinoma amplified sequence 2	0.78	0.04
KRT10	keratin 10	0.78	0.04
FLJ23476	ischemia/reperfusion inducible protein	0.78	0.03
CDC34	cell division cycle 34	0.78	0.03
C16orf34	chromosome 16 open reading frame 34	0.78	0.01
PPIF	peptidylprolyl isomerase F precursor	0.78	0.04
XRCC4	X-ray repair cross complementing prot. 4	0.78	0.03
MDS031	hematopoietic stem/progenitor cells protein	0.78	0.03
CUL2	cullin 2	0.78	0.04
DENR	density-regulated protein	0.78	0.03
LOC93081	hypothetical protein BC015148	0.78	0.04
FLJ11259	hypothetical protein FLJ11259	0.78	0.03
HOXB7	homeo box B7	0.78	0.03
NDUFS8	NADH-coenzyme Q reductase	0.78	0.04
LOC51035	unknown protein LOC51035	0.78	0.04
DNAJA1	DnaJ (Hsp40) homolog, subfamily A, 1	0.78	0.06
ZNF161		0.78	0.05
UBE2B	ubiquitin-conjugating enzyme E2B	0.78	0.04
DDX23	DEAD (Asp-Glu-Ala-Asp) box polypeptide 23	0.78	0.04
IMP-3	IGF-II mRNA-binding protein 3	0.78	0.05
FLJ23047	hypothetical protein FLJ23047	0.78	0.02
DKC1	dyskerin	0.77	0.02
HIP2	huntingtin interacting protein 2	0.77	0.01
FLJ10747	hypothetical protein FLJ10747	0.77	0.07
TOB1	transducer of ERBB2, 1	0.77	0.05
SNRPA1	u2 small nuclear ribonucleoprotein polypeptide A'	0.77	0.02
RHOB	ras homolog gene family, member B	0.77	0.02
GAS7	growth arrest-specific 7	0.77	0.02
PLK4	protein-serine/threonine kinase	0.77	0.03
MRPS12	mitochondrial ribosomal protein S12	0.77	0.02
CDYL	chromodomain protein, Y chromosome-like	0.77	0.06
MTAP	5'-methylthioadenosine phosphorylase	0.77	0.05
NSDHL	NAD(P) dependent steroid dehydrogenase-like	0.77	0.03
TMEM14A	transmembrane protein 14A	0.77	0.02
SUMO2	SMT3 suppressor of mif two 3 homolog 2	0.77	0.02
TUBB2	tubulin, beta, 2	0.77	0.03

Common ID	Gene name	Ratio to control	SEM
RAB5A	RAB5A, member RAS oncogene family	0.77	0.02
PPP2CA	protein phosphatase 2, catalytic subunit, alpha	0.77	0.02
HNRPM	heterogeneous nuclear ribonucleoprotein M	0.77	0.05
C5orf6	putative nuclear protein	0.77	0.02
PTK9	twinfilin	0.77	0.01
SGCB	sarcoglycan, beta	0.77	0.02
FGF13	fibroblast growth factor 13	0.77	0.04
EEF1E1	eukaryotic translation elongation fact. 1 epsilon 1	0.77	0.03
AB026190	Kelch motif containing protein	0.77	0.03
THRAP5	thyroid hormone receptor assoc. prot. 5	0.77	0.03
CYB561	cytochrome b-561	0.77	0.05
EXOSC2	ribosomal RNA processing 4	0.77	0.05
SFRS10	splicing factor, arginine/serine-rich 10	0.77	0.04
CTBP2	zinc finger, RAN-binding domain cont. 1	0.77	0.03
ARHGEF12	Rho guanine nucleotide exchange factor 12	0.77	0.03
BRIX	BRIX	0.77	0.06
ORC1L	origin recognition complex, subunit 1	0.77	0.02
RIN3	Ras and Rab interactor 3	0.77	0.04
ATF2	activating transcription factor 2	0.76	0.04
CYP51A1	lanosterol 14-alpha demethylase	0.76	0.01
CHORDC1	cysteine and histidine-rich domain-cont., 1	0.76	0.03
RKHD2	hypothetical protein LOC51320	0.76	0.02
CUL3	cullin 3	0.76	0.02
RAP1B	RAP1B, member of RAS oncogene family	0.76	0.03
PDLIM3	PDZ and LIM domain 3	0.76	0.02
ENTH	enthoprotin	0.76	0.00
RPS19	ribosomal protein S19	0.76	0.04
CGI-48	CGI-48 protein	0.76	0.05
NUDT4	nudix type motif 4	0.76	0.02
RAE1	RNA export 1	0.76	0.05
SHOC2	soc-2 suppressor of clear homolog	0.76	0.02
HNRPDL	heterogeneous nuclear ribonucleoprotein D-like	0.76	0.05
PRKACB	protein kinase, cAMP-dependent, catalytic, beta	0.76	0.03
MORF4	mortality factor 4	0.76	0.05
LOC339287	cancer susceptibility candidate 3	0.76	0.01
MBNL1	muscleblind-like 1 isoform a	0.76	0.04
HMGB1	similar to nonhistone chromosomal prot. HMG-1	0.76	0.01
FLJ20533	hypothetical protein FLJ20533	0.76	0.00
FIP1L1	FIP1-like 1	0.76	0.06
DLG7	discs large homolog 7	0.76	0.04
MMP24	matrix metalloproteinase 24	0.76	0.05
	similar to Patched protein	0.76	0.05
DDX3X	602536568F1 NIH_MGC_59 Homo sapiens	0.76	0.03

Common ID	Gene name	Ratio to control	SEM
	cDNA clone IMAGE:4655296 5', mRNA sequence.		
HOXB7	homeo box B7	0.76	0.03
CGI-100		0.76	0.01
CHN1		0.76	0.03
PREI3	preimplantation protein 3	0.76	0.03
SUI1	putative translation initiation factor	0.76	0.01
FLJ11773	hypothetical protein FLJ11773	0.76	0.04
NBS1	2,4-dienoyl CoA reductase 1 precursor	0.76	0.04
TOPORS	topoisomerase I binding, arginine/serine-rich	0.76	0.03
MTAP	5'-methylthioadenosine phosphorylase	0.76	0.02
SMNDC1	survival motor neuron domain cont. 1	0.76	0.05
ATPIF1	ATPase inhibitory factor 1	0.76	0.04
SFPQ	splicing factor proline/glutamine rich	0.76	0.03
FLJ13912	hypothetical protein FLJ13912	0.76	0.04
CALM1	calmodulin 1	0.76	0.03
NEK7	NIMA-related kinase 7	0.76	0.02
7h3	hypothetical protein FLJ13511	0.76	0.02
VDR	vitamin D receptor	0.76	0.02
KIAA0276	KIAA0276 protein	0.76	0.03
TXNDC9	ATP binding protein assoc. with cell differentiation	0.76	0.01
PRKRIR	protein-kinase, interferon-inducible	0.76	0.02
PRRX1	paired mesoderm homeobox 1	0.76	0.02
RAB8A	mel transforming oncogene	0.76	0.01
FLJ11292	hypothetical protein FLJ11292	0.76	0.03
	heat shock protein	0.76	0.05
NRF1	nuclear respiratory factor 1	0.76	0.02
MBNL1	muscleblind-like (Drosophila)	0.76	0.02
ZNF200	zinc finger protein 200	0.75	0.03
OAZ2	ornithine decarboxylase antizyme 2	0.75	0.05
THAP1	THAP domain cont., apoptosis assoc. protein 1	0.75	0.04
ZFP36L2	butyrate response factor 2	0.75	0.06
GTSE1	G-2 and S-phase expressed 1	0.75	0.05
SON	SON DNA binding protein	0.75	0.02
NFYA		0.75	0.02
EZH2	enhancer of zeste 2	0.75	0.02
DPH2L2	diphthamide biosynthesis-like protein 2	0.75	0.02
SYNCRIP	synaptotagmin binding, cytoplasmic RNA interacting prot.	0.75	0.03
RAB35	RAB35, member RAS oncogene family	0.75	0.05
USP7	ubiquitin specific protease 7	0.75	0.04
SMARCE1	SWI/SNF-related matrix-assoc. actin-dependent reg. of chromatin e1	0.75	0.01

Common ID	Gene name	Ratio to control	SEM
PELI1	pellino protein	0.75	0.02
CD2AP	CD2-associated protein	0.75	0.02
PTPN12	prot. tyrosine phosphatase, non-receptor type 12	0.75	0.03
PPP2R3A	protein phosphatase 2, regulatory subunit B", alpha	0.75	0.03
NFYA	nuclear transcription factor Y, alpha	0.75	0.03
WTAP	Wilms' tumour 1-associating protein	0.75	0.06
GAS2L1	growth arrest-specific 2 like 1	0.75	0.01
INSIG2	insulin induced protein 2	0.75	0.05
MED6	mediator of RNA polymerase II transcription, 6	0.75	0.05
KIAA0483	KIAA0483 protein	0.75	0.06
TNPO1	transportin 1	0.75	0.05
UBE2L3	ubiquitin-conjugating enzyme E2L 3	0.75	0.04
CGI-94	comparative gene identification transcript 94	0.75	0.03
GOLPH3	golgi phosphoprotein 3	0.75	0.02
RBM14	RNA binding motif protein 14	0.75	0.05
CYB5-M	cytochrome b5 outer mitochondrial membrane precursor	0.75	0.01
BRPF1	bromodomain-containing protein	0.75	0.02
H41	hypothetical protein H41	0.75	0.05
MRPL19	mitochondrial ribosomal protein L19	0.75	0.02
RNMT	RNA methyltransferase	0.75	0.05
ME1		0.75	0.07
PDCL	phosducin-like	0.75	0.04
NUP50	nucleoporin 50kDa	0.75	0.05
CDC20	cell division cycle 20	0.75	0.04
TBPL1	TBP-like 1	0.75	0.03
C1D	nuclear DNA-binding protein	0.75	0.01
METAP2	methionyl aminopeptidase 2	0.75	0.05
MEF2C	myocyte enhancer factor 2C	0.75	0.02
C19orf13	chromosome 19 open reading frame 13	0.75	0.05
GALNACT-2		0.75	0.05
TUBB	tubulin, beta polypeptide	0.75	0.02
BRD2	bromodomain containing protein 2	0.75	0.04
LMNA	lamin A/C	0.75	0.03
ANGPT1	angiopoietin 1	0.75	0.06
FUSIP1	FUS interacting protein 1	0.75	0.02
EPB41L2	erythrocyte membrane prot. band 4.1-like 2	0.75	0.04
FLJ10652	hypothetical protein FLJ10652	0.74	0.05
FLJ11526	hypothetical protein FLJ11526	0.74	0.02
KRT10	keratin 10	0.74	0.03
POLR1D	RNA polymerase I	0.74	0.02
CENPE	centromere protein E	0.74	0.05

Common ID	Gene name	Ratio to control	SEM
ARH	LDL receptor adaptor protein	0.74	0.06
BRD2	bromodomain containing protein 2	0.74	0.04
GAS7	growth arrest-specific 7	0.74	0.04
EHD1	EH-domain containing 1	0.74	0.06
CSNK2A1	casein kinase 2, alpha 1 polypeptide	0.74	0.05
NR0B1	adrenal hypoplasia protein	0.74	0.06
ACLY	ATP citrate lyase	0.74	0.01
H3F3A	H3 histone, family 3A	0.74	0.03
TMPO	thymopoietin	0.74	0.02
RPS6KA1	ribosomal protein S6 kinase, polypeptide 1	0.74	0.05
ITSN1	intersectin 1 (SH3 domain protein)	0.74	0.05
RAP2C	RAP2C, member of RAS oncogene family	0.74	0.03
SNRPA1	small nuclear ribonucleoprotein polypeptide A'	0.74	0.06
PNRC2	proline-rich nuclear receptor coactivator 2	0.74	0.01
SS18L2	synovial sarcoma translocation gene on chromosome 18-like 2	0.74	0.05
DMN	desmuslin	0.74	0.03
ZNF207	zinc finger protein 207	0.74	0.02
LOC56902	putatative 28 kDa protein	0.74	0.04
RAP2C	RAP2C, member of RAS oncogene family	0.74	0.04
BAMBI	putative transmembrane protein NMA	0.74	0.06
HCCS	holocytochrome c synthase	0.74	0.03
SWAP70	SWAP-70 protein	0.74	0.04
GUCY1B3	guanylate cyclase 1, soluble, beta 3	0.74	0.07
SS18	synovial sarcoma, translocated to X chromosome	0.74	0.04
GTSE1	G-2 and S-phase expressed 1	0.74	0.02
TRAF4	TNFR-associated factor 4	0.74	0.07
PDHX	pyruvate dehydrogenase complex, component X	0.73	0.03
SON	SON DNA binding protein	0.73	0.03
TCEB1		0.73	0.05
STK6	serine/threonine protein kinase 6	0.73	0.05
MAX		0.73	0.02
TAZ	transcriptional co-activator with PDZ-binding motif	0.73	0.06
KIAA0261	KIAA0261	0.73	0.05
LSM2	SMX5-like protein	0.73	0.02
RAB22A	RAS-related protein RAB-22A	0.73	0.05
C2orf6	Mob4B protein	0.73	0.04
TUBB4	tubulin, beta, 4	0.73	0.03
GAS41	glioma-amplified sequence-41	0.73	0.02
MALT1	mucosa assoc. lymphoid tissue lymphoma translocation prot. 1	0.73	0.06
GMNN	geminin	0.73	0.04

Common ID	Gene name	Ratio to control	SEM
KIAA1212		0.73	0.05
RQCD1	required for cell differentiation1	0.73	0.04
BLVRB	biliverdin reductase B	0.73	0.04
MRPL39	mitochondrial ribosomal protein L39	0.73	0.03
TAZ	transcriptional co-activator with PDZ-binding motif	0.73	0.04
SFRS1		0.73	0.03
NFIC	nuclear factor I/C	0.73	0.05
	CDNA FLJ12521	0.73	0.03
TAZ	transcriptional co-activator with PDZ-binding motif	0.73	0.05
SNX24	SBBI31 protein sorting nexing 24	0.73	0.02
TIAM1	T-cell lymphoma invasion and metastasis 1	0.73	0.05
SCAMP1	secretory carrier membrane protein 1	0.72	0.03
BAZ1A	bromodomain adj. to zinc finger domain, 1A	0.72	0.04
TFIP11	tuftelin interacting protein 11	0.72	0.06
SFRS3	splicing factor, arginine/serine-rich 3	0.72	0.02
GC20	translation factor sui1 homolog	0.72	0.02
DDX3X	DEAD box polypeptide 3, X-linked	0.72	0.04
CSPG6	chondroitin sulfate proteoglycan 6	0.72	0.04
KIAA0125	KIAA0125 gene product	0.72	0.04
KCTD14		0.72	0.03
TNFAIP8	TNF alpha-induced protein 8	0.72	0.06
CASP2	caspase 2	0.72	0.06
BCOR	BCL-6 interacting corepressor	0.72	0.03
BAK1	BCL2-antagonist/killer 1	0.72	0.03
RRM2	ribonucleotide reductase M2	0.72	0.04
BAZ1A	bromodomain adj. to zinc finger domain, 1A	0.72	0.02
CGI-79	CGI-79 protein	0.72	0.01
GNE	UDP-N-acetylglucosamine-2-epimerase/N-acetylmannosamine kinase	0.72	0.02
DBR1	debranching enzyme homolog 1	0.72	0.03
AP1S1	adaptor-related protein complex 1, sigma 1	0.72	0.07
NOL5A	nucleolar protein 5A	0.72	0.03
TLE3	transducin-like enhancer of split 3	0.72	0.04
RPS2		0.72	0.05
TFAM	transcription factor A, mitochondrial	0.71	0.03
KNTC2	kinetochore associated 2	0.71	0.02
MRPS12	mitochondrial ribosomal protein S12	0.71	0.03
SFXN1	sideroflexin 1	0.71	0.03
ASPM	abnormal spindle-like, microcephaly assoc.	0.71	0.01
PML	promyelocytic leukemia protein	0.71	0.05
PPP2R1B	protein phosphatase 2 regulatory subunit A, beta	0.71	0.04

Common ID	Gene name	Ratio to control	SEM
TBC1D4		0.71	0.04
DHRS8	dehydrogenase/reductase, SDR family, 8	0.71	0.01
DUSP14	dual specificity phosphatase 14	0.71	0.05
PSCD2	pleckstrin homology, Sec7 and coiled/coil domains 2	0.71	0.03
CHD4	chromodomain helicase DNA binding prot. 4	0.71	0.02
LANCL2	lantibiotic synthetase component C-like 2	0.71	0.03
SGCD	delta-sarcoglycan	0.71	0.07
PEX14	peroxisomal biogenesis factor 14	0.71	0.02
KIF1C	kinesin family member 1C	0.71	0.07
PHLDA1	pleckstrin homology-like domain, family A, 1	0.71	0.07
ARID4A	retinoblastoma-binding protein 1	0.71	0.04
PRPS2	phosphoribosyl pyrophosphate synthetase 2	0.71	0.08
SFRS2	splicing factor, arginine/serine-rich 2	0.71	0.06
C6orf211	chromosome 6 open reading frame 211	0.71	0.03
MAX	MAX protein	0.71	0.02
NCOA1	nuclear receptor coactivator 1	0.71	0.03
SIVA	CD27-binding (Siva) protein	0.71	0.05
BPGM	2,3-bisphosphoglycerate mutase	0.71	0.06
TPRA40	seven transmembrane domain orphan receptor	0.71	0.03
SAFB	scaffold attachment factor B	0.71	0.04
MORF4L1	MORF-related gene 15	0.70	0.02
LIMK2	protein phosphatase 1, regulatory subunit 14B	0.70	0.05
SLC10A3	solute carrier family 10, 3	0.70	0.02
TRIB1	G-protein-coupled receptor induced prot.	0.70	0.02
HSPA14	heat shock protein hsp70-related prot.	0.70	0.06
SURB7	suppressor of RNA polymerase B	0.70	0.02
TEAD3	TEA domain family member 3	0.70	0.07
GBP1	guanylate binding protein 1	0.70	0.03
SFRS3	splicing factor, arginine/serine-rich 3	0.70	0.05
SOX4	sex determining region Y-box 4	0.70	0.07
NDUFS6	NADH-coenzyme Q reductase	0.70	0.04
	IMAGE:4427025	0.70	0.04
LOC51334	mesenchymal stem cell protein DSC54	0.70	0.02
SCLY	selenocysteine lyase	0.70	0.05
ZNF37A	zinc finger protein 37a	0.70	0.07
MTUS1	mitochondrial tumor suppressor gene 1	0.70	0.04
SURB7	suppressor of RNA polymerase B	0.70	0.06
IL6R	interleukin 6 receptor	0.70	0.04
DMD	dystrophin	0.70	0.03
ZNF143	zinc finger protein 143	0.70	0.03
MGC3032		0.70	0.05
KIAA0117		0.70	0.06
MGEA5	meningioma expressed antigen 5	0.70	0.03

Common ID	Gene name	Ratio to control	SEM
HIST1H2BK	H2B histone family, G	0.70	0.03
MRPL22	mitochondrial ribosomal protein L22	0.70	0.06
RAGE	renal tumor antigen	0.70	0.06
RAB14	ras-related protein rab-14	0.70	0.03
POLR3K	DNA directed RNA polymerase III polypeptide K	0.70	0.05
HMGCR	3-hydroxy-3-methylglutaryl-Coenzyme A reductase	0.70	0.04
ALDH3A2	aldehyde dehydrogenase 3A2	0.70	0.06
FLJ13848	hypothetical protein FLJ13848	0.69	0.04
FLJ10846	hypothetical protein FLJ10846	0.69	0.00
HMGB3	high-mobility group box 3	0.69	0.02
PART1	prostate androgen-regulated transcript 1	0.69	0.05
EED	embryonic ectoderm development	0.69	0.05
GNAI3	guanine nucleotide binding prot., α inhibiting, 3	0.69	0.03
FLJ10520	hypothetical protein FLJ10520	0.69	0.03
NUSAP1	nucleolar and spindle associated protein 1	0.69	0.03
SAP18	sin3 associated polypeptide p18	0.69	0.04
FLJ12973	hypothetical protein FLJ12973	0.69	0.02
RY1	putative nucleic acid binding protein RY-1	0.69	0.05
C10orf70	chromosome 10 open reading frame 70	0.69	0.02
UBE2B	ubiquitin-conjugating enzyme E2B	0.69	0.03
SMC5L1	structural maint. of chromosomes 5-like 1	0.69	0.04
CGI-48	CGI-48 protein	0.69	0.07
TLR1	toll-like receptor 1	0.69	0.02
RFK	riboflavin kinase	0.69	0.05
HSPC132	HSPC132	0.69	0.01
THY1	Thy-1 cell surface antigen	0.69	0.05
BUB3	budding uninhibited by benzimidazoles 3	0.69	0.06
KLF3	Kruppel-like factor 3 (basic)	0.69	0.02
MGEA5	meningioma expressed antigen 5	0.69	0.05
HUMBINDC		0.69	0.07
CTRB1	Chymotrypsinogen B precursor	0.69	0.07
SMOX	polyamine oxidase	0.69	0.06
SIAT4C	sialyltransferase 4C	0.69	0.05
TFB2M	transcription factor B2, mitochondrial	0.68	0.02
SAP30	sin3 associated polypeptide p30	0.68	0.02
	CDNA FLJ43274	0.68	0.07
ATF5	activating transcription factor 5	0.68	0.02
MOBP	myelin-assoc. oligodendrocyte basic prot.	0.68	0.04
CGI-37	Saccharomyces cerevisiae Nip7p	0.68	0.06
DR1	down-regulator of transcription 1	0.68	0.04
SIVA	CD27-binding (Siva) protein	0.68	0.06
FANCA	Fanconi anemia, complementation group A	0.68	0.04
CYB5-M		0.68	0.05

Common ID	Gene name	Ratio to control	SEM
NFE2L2	nuclear factor (erythroid-derived 2)-like 2	0.68	0.01
UBN1	ubinuclein 1	0.68	0.02
CDKN2D	cyclin-dependent kinase inhibitor 2D	0.68	0.06
LMNA	lamin A/C	0.68	0.04
C19orf7	chromosome 19 open reading frame 7	0.68	0.01
MAK3	likely ortholog of mouse Mak3p	0.68	0.05
GLS	glutaminase C	0.68	0.04
USP1	ubiquitin specific protease 1	0.68	0.06
PRKCD	protein kinase C, delta	0.67	0.05
SKP2	S-phase kinase-associated protein 2	0.67	0.06
FLJ13910	hypothetical protein FLJ13910	0.67	0.01
NUP54	nucleoporin 54kDa	0.67	0.00
RCP	Rab coupling protein	0.67	0.06
CFLAR	CASP8 & FADD-like apoptosis regulator	0.67	0.02
SCHIP1	schwannomin interacting protein 1	0.67	0.02
AP4S1	adaptor-related prot. complex 4, sigma 1	0.67	0.08
ADM	adrenomedullin	0.67	0.03
C9orf77	chromosome 9 open reading frame 77	0.67	0.06
DR1	down-regulator of transcription 1	0.67	0.05
PSMD12	proteasome subunit, non-ATPase, 12	0.67	0.04
C6orf37	chromosome 6 open reading frame 37	0.67	0.02
TBC1D4	TBC1 domain family, member 4	0.66	0.05
GCA	grancalcin, EF-hand calcium binding prot.	0.66	0.04
TENS1	tensin-like SH2 domain containing 1	0.66	0.03
SP100	nuclear antigen Sp100	0.66	0.03
ADFP	adipose differentiation-related protein	0.66	0.03
KIAA0500		0.66	0.06
DR1	down-regulator of transcription 1	0.66	0.06
HSPC111	hypothetical protein HSPC111	0.66	0.01
CPOX	coproporphyrinogen oxidase	0.66	0.05
ZFR	zinc finger RNA binding protein	0.66	0.05
TGFB1I4	TGF beta 1 induced transcript 4	0.66	0.03
ARHGAP19	Rho GTPase activating protein 19	0.66	0.02
RBM12	copine I	0.66	0.02
ARL6IP	ADP-ribosylation factor-like 6 interacting prot.	0.66	0.05
BAG2	BCL2-associated athanogene 2	0.66	0.02
BTEB1	basic transcription element binding prot. 1	0.66	0.05
IDI1	isopentenyl-diphosphate delta isomerase	0.65	0.06
TUBB4	tubulin, beta, 4	0.65	0.02
ALDH1B1	aldehyde dehydrogenase 1B1 precursor	0.65	0.01
BRD4	bromodomain containing 4	0.65	0.04
CCNE2	cyclin E2	0.65	0.06
SAP30		0.65	0.06
FAM32A	family with sequence similarity 32, A	0.65	0.08

Common ID	Gene name	Ratio to control	SEM
CASP6	caspase 6	0.65	0.05
PTDSR	phosphatidylserine receptor	0.65	0.04
VDR	vitamin D receptor	0.65	0.06
IRF3	interferon regulatory factor 3	0.65	0.02
CCNE1	cyclin E1	0.65	0.03
RIT1	Ras-like without CAAX 1	0.65	0.03
POLR3G	RNA polymerase III, DNA directed	0.65	0.06
HSPB8	heat shock 27kDa protein 8	0.65	0.04
RFC5	replication factor C, 5	0.65	0.02
SERTAD3	RPA-binding trans-activator SERTA domain cont. 3	0.65	0.03
APG12L	APG12 autophagy 12-like	0.65	0.02
TUBA3	tubulin, alpha 3	0.65	0.06
SMAP-1	smooth muscle cell associated protein-1	0.64	0.05
MARCKS	myristoylated alanine-rich prot. kinase C	0.64	0.02
ZNF161	zinc finger protein 161	0.64	0.06
FLJ10349	hypothetical protein FLJ10349	0.64	0.05
RFXANK	regulatory factor X-assoc. ankyrin-cont. prot.	0.64	0.06
MGC22679	hypothetical protein MGC22679	0.64	0.08
PRRX1	paired mesoderm homeobox 1	0.64	0.05
C1orf33	ribosomal protein P0-like protein	0.64	0.03
	IMAGE:3085853	0.64	0.02
IDI1	isopentenyl-diphosphate delta isomerase	0.64	0.06
DACT1	DAPPER1	0.64	0.05
FLJ12969	hypothetical protein FLJ12969	0.64	0.01
HNRPH3	heterogeneous nuclear ribonucleoprot. H3	0.64	0.05
FSHPRH1	FSH primary response 1	0.64	0.06
HMGCS1		0.63	0.08
USP18	ubiquitin specific protease 18	0.63	0.04
HNRPH3	heterogeneous nuclear ribonucleoprot. H3	0.63	0.00
SKP2	S-phase kinase-associated protein 2	0.63	0.06
PIGC	phosphatidylinositol glycan, class C	0.63	0.05
TNFRSF6	TNFR superfamily, 6	0.63	0.01
TMOD3	tropomodulin 3	0.63	0.01
TBDN100	transcriptional coactivator tubedown-100	0.63	0.07
ASF1A	ASF1 anti-silencing function 1, A	0.63	0.03
CASP6	caspase 6	0.63	0.07
POP7	processing of precursor 7	0.62	0.04
NFYB	nuclear transcription factor Y, beta	0.62	0.08
HIST1H4A	H4 histone family, member D	0.62	0.09
Spc25	kinetochore protein Spc25	0.62	0.05
DLX2	distal-less homeo box 2	0.62	0.05
FLJ10350	hypothetical protein FLJ10350	0.62	0.05
ASF1A	ASF1 anti-silencing function 1, A	0.62	0.02

Common ID	Gene name	Ratio to control	SEM
COLEC12	collectin sub-family member 12	0.62	0.05
FBXO5	F-box only protein 5	0.62	0.05
SWAP70	SWAP-70 protein	0.62	0.03
ADNP	activity-dependent neuroprotector	0.62	0.07
KIAA1387	KIAA1387 protein	0.62	0.02
ELF1	E74-like factor 1	0.62	0.05
SGTA	small glutamine-rich tetratricopeptide	0.61	0.05
NUP50	nucleoporin 50kDa	0.61	0.02
EIF4EL3	eukaryotic translation initiation fact. 4E-like 3	0.61	0.02
TIEG	TGFB inducible early growth response	0.61	0.03
TUBA1	tubulin, alpha 1	0.61	0.03
HMGCR	3-hydroxy-3-methylglutaryl-Coenzyme A reductase	0.61	0.01
CBLL1	Cas-Br-M ecotropic retroviral transforming sequence-like 1	0.61	0.01
ZC3HDC7	zinc-finger protein AY163807	0.61	0.01
TWIST1	twist	0.61	0.04
AKAP13	non-ocogenic Rho GTPase-specific GTP exchange factor	0.61	0.04
GABPA	GA binding prot. transcription factor, alpha	0.61	0.04
FLJ23311	FLJ23311 protein	0.61	0.05
IMP-3		0.61	0.07
FZD7	frizzled 7	0.61	0.05
ROCK2	Rho-assoc., coiled-coil cont. prot. kinase 2	0.61	0.02
ARHGEF3	Rho guanine nucleotide exchange factor 3	0.61	0.03
SQLE	squalene epoxidase	0.61	0.05
CDK8		0.61	0.02
RRM2		0.60	0.07
IER5	immediate early response 5	0.60	0.08
CHML	choroideremia-like Rab escort protein 2	0.60	0.02
PC-LKC	protocadherin LKC precursor	0.60	0.07
ARF6	ADP-ribosylation factor 6	0.60	0.02
TSSC4	tumor suppressing subtransferable candidate 4	0.60	0.04
EGFL5	EGF-like-domain, multiple 5	0.59	0.04
GFER	erv1-like growth factor	0.59	0.04
C12orf2	chromosome 12 open reading frame 2	0.59	0.07
SAP18	sin3-associated polypeptide, 18kDa	0.59	0.05
STAU2	staufen homolog 2	0.59	0.03
RBM12		0.58	0.02
INSIG1	insulin induced gene 1	0.58	0.03
NFYA		0.58	0.05
MGC29643	hypothetical protein MGC29643	0.58	0.02
PPARA	peroxisome proliferative activated receptor, α	0.58	0.07
PURA	purine-rich element binding protein A	0.58	0.07

Common ID	Gene name	Ratio to control	SEM
PLAG1	pleiomorphic adenoma gene 1	0.57	0.05
HSU79266	protein predicted by clone 23627	0.57	0.05
ABHD5	abhydrolase domain cont. 5	0.57	0.01
PML	promyelocytic leukemia protein	0.56	0.08
SC4MOL	sterol-C4-methyl oxidase-like	0.56	0.05
CLECSF2	C-type lectin, superfamily, 2	0.56	0.04
TLE4	transducin-like enhancer protein 4	0.56	0.04
DYRK2	dual-specificity tyrosine-phosphorylation regulated kinase 2	0.56	0.03
APAF1	apoptotic protease activating factor	0.55	0.03
GRWD1	glutamate-rich WD repeat containing 1	0.55	0.06
BTEB1	basic transcription element binding protein 1	0.55	0.02
FLRT3	fibronectin leucine rich transmembrane prot. 3	0.55	0.07
DDX6	DEAD box polypeptide 6	0.55	0.02
ADAMTS3	a disintegrin-like & metalloprotease with thrombospondin type 1 motif, 3	0.54	0.04
TIPARP	TCDD-inducible poly(ADP-ribose) polymerase	0.54	0.01
WASL	Wiskott-Aldrich syndrome-like	0.54	0.05
NS3TP2	HCV NS3-transactivated protein 2	0.54	0.05
ABO	ABO blood group	0.53	0.06
IER3	immediate early response 3	0.53	0.04
TNFAIP8	TNF alpha-induced protein 8	0.53	0.05
KLHL5	kelch-like 5	0.53	0.06
HSPC056	HSPC056 protein	0.52	0.03
TLE4		0.51	0.04
GCLM	glutamate-cysteine ligase regulatory protein	0.51	0.03
HSPA1A	heat shock 70kDa protein 1A	0.51	0.04
BCL7C	B-cell CLL/lymphoma 7C	0.49	0.08
HIST1H2BM	H2B histone family, member E	0.48	0.04
NR2F1	nuclear receptor subfamily 2, group F, 1	0.48	0.04
SOX9	sex determining region Y-box 9	0.48	0.09
SOX9	sex determining region Y-box 9	0.48	0.08
CCNE2	cyclin E2	0.46	0.02
CDC42EP3	Cdc42 effector protein 3	0.45	0.01
CDC42EP3	Cdc42 effector protein 3	0.44	0.03
JAK2	Janus kinase 2	0.43	0.04
ARPC4	actin related protein 2/3 complex subunit 4	0.40	0.06
KIAA1449		0.37	0.01
MMP16	matrix metalloproteinase 16	0.36	0.04
IGFBP5	insulin-like growth factor binding protein 5	0.34	0.09
DUSP6	dual specificity phosphatase 6	0.34	0.00
TXNIP	thioredoxin interacting protein	0.33	0.02
TXNIP	thioredoxin interacting protein	0.20	0.02
TXNIP	thioredoxin interacting protein	0.12	0.01

Table 28. The entire list of genes 2-fold increased or decreased in tangeretin-treated MDA-MB-435TAN200H cells. TAN200H cells were treated with tangeretin (0.54 mM) and MDA-MB-435 parental cells with DMSO vehicle control. RNA was isolated and human Affymetrix arrays (HGU95A) were used to assess gene expression as described in *Materials and Methods*. GeneSpring GX 7.3 data mining software was used to obtain lists of genes that were 2-fold up- or downregulated following tangeretin treatment. Gene expression of treated and control samples were normalized to control, and normalized values for treated samples are expressed as fold change. The data shown is from a single analysis.

Common ID	Gene name	Fold change
CRYAB		235.50
CRYAB		186.40
KIAA1201	KIAA1201 protein	49.27
SILV	silver homolog	35.67
GAGE5	G antigen 4	22.15
SMAD6	mothers against decapentaplegic homolog 6	20.13
SEMA3B		20.01
GAGE5	G antigen 5	19.20
CPVL	serine carboxypeptidase vitellogenic-like	14.44
NNMT	nicotinamide N-methyltransferase	13.16
HSPA12A	heat shock 70kDa protein 12A	12.57
TUSC3	tumor suppressor candidate 3	12.32
GAGE2	G antigen 2	12.13
HRH1	histamine receptor H1	11.28
GAGE5	G antigen 7	10.72
ID3		9.99
GAGE6	G antigen 6	9.57
NCK2	NCK adaptor protein 2	8.57
CENTD1	centaurin delta 1	8.16
AXL	AXL receptor tyrosine kinase	7.94
EPHA5	EHK-1 receptor tyrosine kinase	7.44
	Human 18S rRNA gene	7.37
LASS6	hypothetical protein LOC253782	7.18
	cDNA DKFZp586J0323	7.11
FLJ20259	FLJ20259 protein	6.71
COL9A3	alpha 3 type IX collagen	6.64
TM4SF9	transmembrane 4 superfamily, 9	6.62
ID2	inhibitor of DNA binding 2	6.58
RASSF2	Ras association domain family 2	6.46
HYAL1	hyaluronoglucosaminidase 1	6.18
PLXNC1	plexin C1	6.09
GPR34	Human 18S rRNA gene	6.00
AKAP2	A-kinase anchor protein 2	5.97
CDC25A	cell division cycle 25A	5.86
DUSP1	dual specificity phosphatase 1	5.71
DKK1	dickkopf homolog 1	5.51
EDIL3	EGF-like repeats & discoidin I-like dom cont prot 3	5.48
TDRD3	tudor domain containing 3	5.46
DMXL1	Dmx-like 1	5.45
	EUROIMAGE 208948	5.38
GAGE3	GAGE-3 protein	5.07
ITGA7	integrin alpha 7 precursor	5.07
C5orf13	neuronal protein 3.1	5.02

Common ID	Gene name	Fold change
MLANA	melan-A	5.00
LIPT1	lipoyltransferase 1	4.96
KIAA0894	KIAA0894 protein	4.78
MAF	musculoaponeurotic fibrosarcoma oncogene	4.74
IL7	interleukin 7 precursor	4.73
EN2	engrailed homolog 2	4.63
INSIG1	insulin induced gene 1	4.47
KIAA0367	KIAA0367	4.41
EN2	engrailed homolog 2	4.34
PTP4A1	protein tyrosine phosphatase type IVA, 1	4.32
NCALD	neurocalcin delta	4.30
NCAM1	neural cell adhesion molecule 1	4.26
	FBA1 Cri-du-chat region mRNA.	4.21
ANK3	ankyrin 3	4.08
PDLIM3	PDZ and LIM domain 3	4.02
GAGE5	G antigen 5	4.01
DLG1	synapse-associated protein 97	3.97
CREM	cAMP responsive element modulator	3.96
TYRP1	tyrosinase-related protein 1	3.95
PFTK1	PFTAIRE protein kinase 1	3.93
EFNB2	ephrin-B2	3.91
EPM2AIP1	EPM2A interacting protein 1	3.84
TUSC3	tumor suppressor candidate 3	3.81
C16orf34	chromosome 16 open reading frame 34	3.80
MLANA	melan-A	3.79
	Human 18S rRNA gene, complete.	3.76
POLE2	polymerase (DNA directed), epsilon 2	3.75
LOC283824	Clone IMAGE:4791553, mRNA	3.71
NEDD4L	ubiquitin-protein ligase NEDD4-like	3.69
DCT	dopachrome tautomerase	3.65
MLANA	melan-A	3.64
JUN	v-jun avian sarcoma virus 17 oncogene	3.63
MAPRE2	microtubule-associated protein, RP/EB, 2	3.62
KIAA0767	KIAA0767 protein	3.62
DLEU2	deleted in lymphocytic leukemia, 2	3.62
TUBB	tubulin, beta polypeptide	3.61
Spc25	kinetochore protein Spc25	3.61
ID1	inhibitor of DNA binding 1	3.60
FBN1	fibrillin 1	3.59
KPNA1	karyopherin alpha 1	3.57
CDK2	cyclin-dependent kinase 2	3.56
SEMA5A	7 thrombospondin repeats, TM & short cytoplasmic domain, 5A	3.54
	cDNA DKFZp586I1319	3.53
ID1	inhibitor of DNA binding 1	3.52

Common ID	Gene name	Fold change
TNFAIP3	tumor necrosis factor, a-induced protein 3	3.50
DAB2	disabled homolog 2	3.48
RRAGD	Ras-related GTP binding D	3.45
EZH2	enhancer of zeste 2	3.45
Spc25	kinetochore protein Spc25	3.42
RBBP6	retinoblastoma-binding protein 6	3.42
DKFZ	hypothetical protein DKFZp586I1420	3.41
SIAT4A	sialyltransferase 4A	3.41
HSPG2	heparan sulfate proteoglycan 2	3.41
DNCI1	IMAGE:2252136	3.39
LRP8	LDL receptor-related protein 8	3.38
ALCAM	activated leukocyte cell adhesion molecule	3.34
KIAA0485	MRNA, chromosome 1 specific transcript	3.27
CDC45L	CDC45-like	3.26
IL8	interleukin 8 precursor	3.26
HIP1	huntingtin interacting protein 1	3.22
SS18L1	SS18-like protein 1	3.21
KIAA0934	KIAA0934 protein	3.20
CSE1L	CSE1 chromosome segregation 1-like	3.15
T	transcription factor T	3.14
NRD1		3.13
DCT	dopachrome tautomerase	3.13
DCT	dopachrome tautomerase	3.10
	cDNA DKFZp564F133	3.09
	trinucleotide repeat sequence.	3.08
PLCL1	phospholipase C-like 1	3.02
	Human 28S ribosomal RNA gene	3.02
CYR61	cysteine-rich, angiogenic inducer, 61	3.01
DNA2L	DNA replication helicase 2-like	3.01
PPT2	palmitoyl-protein thioesterase 2	3.01
CREM	cAMP responsive element modulator	3.00
CCNE2	cyclin E2	2.97
RBMS1P	MSSP-1	2.97
LONP	retina cDNA randomly primed sublibrary	2.96
BTG3	B-cell translocation gene 3	2.95
KIFC1	kinesin-related protein	2.92
SNRPA1	small nuclear ribonucleoprotein polypep. A'	2.90
SEMA3C	semaphorin 3C	2.90
SNRPD1	small nuclear ribonucleoprotein D1	2.89
CREM	cAMP responsive element modulator	2.88
CDC6	CDC6 homolog	2.88
CTPS	CTP synthase	2.88
NUP93	nucleoporin 93kDa	2.88
NDUFAF1	NADH dehydrogenase 1 alpha subcomplex, assembly factor 1	2.88

Common ID	Gene name	Fold change
MCLC	Mid-1-related chloride channel 1	2.87
ASAH1	N-acylsphingosine amidohydrolase 1	2.87
TOE1	target of EGR1, member 1 (nuclear)	2.85
ACADM	acyl-Coenzyme A dehydrogenase	2.85
BGLAP	OSTEOCALCIN PRECURSOR	2.84
RRM1	ribonucleoside-diphosphate reductase M1	2.83
PPM1H	retina cDNA randomly primed sublibrary	2.82
ZNF124		2.81
CDC7	CDC7 cell division cycle 7	2.80
CAST	calpastatin	2.80
M96	putative DNA binding protein	2.79
	Similar to MGC9515 protein	2.79
LCP2	lymphocyte cytosolic protein 2	2.78
SYNE2	synaptic nuclei expressed gene 2	2.78
SPRY1	sprouty homolog 1	2.77
SMAD5	mothers against decapentaplegic homolog 5	2.76
KPNA5	karyopherin alpha 5	2.76
PRKAR2B	prot. kinase, cAMP-dependent, reg., II, β	2.75
PVT1	cDNA DKFZp686L2129	2.74
DMXL1	Dmx-like 1	2.74
ABLIM1	actin-binding LIM protein 1	2.74
TM4SF1	transmembrane 4 superfamily member 1	2.74
MAP2K6	mitogen-activated protein kinase kinase 6	2.73
IL8	interleukin 8 precursor	2.71
OLFML2A	hypothetical protein LOC169611	2.71
PLK4	polo-like kinase 4	2.70
COL16A1	alpha 1 type XVI collagen precursor	2.69
TM4SF1	transmembrane 4 superfamily member 1	2.69
KIAA0889	KIAA0889 protein	2.69
FNBP3	formin binding protein 3	2.68
DKFZP	DKFZP564F0522 protein	2.67
FLJ12443	hypothetical protein FLJ12443	2.67
RFC5	replication factor C 5	2.67
DNM1L	dynamin 1-like protein	2.66
ZNF330	zinc finger protein 330	2.66
KIAA0186	KIAA0186 mRNA	2.66
IGFBP1	insulin-like growth factor binding protein 1	2.66
TFRC	transferrin receptor (p90, CD71)	2.66
ACAT2	acetyl-Coenzyme A acetyltransferase 2	2.65
	CDNA FLJ12815	2.64
DNCI1	dynein, cytoplasmic, intermediate polypep. 1	2.62
NFIB	nuclear factor I/B	2.62
RBL2	retinoblastoma-like 2 (p130)	2.62
NEDD9	neural precursor cell expressed, developmentally down-regulated 9	2.61

Common ID	Gene name	Fold change
MYH10	myosin, heavy polypeptide 10, non-muscle	2.61
MPDU1	mannose-P-dolichol utilization defect 1	2.60
LMNB1	lamin B1	2.59
MET	met proto-oncogene precursor	2.58
CCT6A	chaperonin containing TCP1, subunit 6A	2.58
PTPN1	prot. tyrosine phosphatase, non-receptor, 1	2.57
RPA1	replication protein A1, 70kDa	2.57
CDC25C	cell division cycle 25C protein	2.57
SMC4L1	SMC4 struct. maint. of chromosomes 4-like 1	2.57
CAP2	adenylyl cyclase-associated protein 2	2.56
ABCE1	ATP-binding cassette, sub-family E, 1	2.55
PLK4	polo-like kinase 4	2.54
	Human 28S ribosomal RNA gene	2.54
FEN1		2.54
RPA1	replication protein A1, 70kDa	2.53
MLLT2	myeloid/lymphoid or mixed-lineage leukemia, translocated to, 2	2.53
SCA1	ataxin 1	2.53
PTPRZ1	prot. tyrosine phosphatase, recept.-type, Z 1	2.53
SLC25A13	solute carrier family 25, member 13	2.53
PTP4A1	protein tyrosine phosphatase type IVA, 1	2.53
IDI1	isopentenyl-diphosphate delta isomerase	2.51
NASP	nuclear autoantigenic sperm protein	2.50
LTBP1	latent TGFβ binding prot. 1	2.50
RAD54L	RAD54-like protein	2.50
PDE4DIP	KIAA0454 protein	2.50
SEMA3C	semaphorin 3C	2.50
TYMS	thymidylate synthetase	2.49
TEF	thyrotrophic embryonic factor	2.48
SLC25A13		2.48
ABCB10	ATP-binding cassette, sub-family B, 10	2.48
SIPA1	signal-induced proliferation-assoc. protein 1	2.47
PLK2	polo-like kinase 2	2.47
KIAA0276	KIAA0276 protein	2.47
MKI67	antigen identified by monoclonal Ab Ki-67	2.47
CDR1	ribosomal protein S15a	2.47
SCG2	secretogranin II precursor	2.46
DICER1	dicer1	2.46
	cytokine receptor-like factor 2	2.46
LRRC14	leucine rich repeat containing 14	2.46
C10orf6	chromosome 10 open reading frame 6	2.45
PRIM1	DNA primase small subunit, 49kDa	2.45
FLNB	filamin B, beta (actin binding protein 278)	2.45
RECQL	RecQ protein-like isoform 1	2.45
SLC16A7	solute carrier family 16, member 7	2.44

Common ID	Gene name	Fold change
LOC113251	c-Mpl binding protein	2.44
	Clone 24627 mRNA sequence	2.44
MCM6	minichromosome maintenance protein 6	2.42
ARL4A	ADP-ribosylation factor-like 4	2.42
SELE	selectin E precursor	2.42
ZNF148	zinc finger protein 148 (pHZ-52)	2.41
KIF2C	kinesin family member 2C	2.41
SMN1		2.41
CCNT1	cyclin T1	2.41
LOC376745	similar to AG02	2.41
DTYMK	deoxythymidylate kinase (thymidylate kinase)	2.41
CDK2	cyclin-dependent kinase 2	2.41
RPL5	ribosomal protein L5	2.41
LBR	lamin B receptor	2.40
PABPC4	poly A binding protein, cytoplasmic 4	2.40
MOX2	OX-2 membrane glycoprotein precursor	2.39
FLJ12443	hypothetical protein FLJ12443	2.38
RAD23A		2.38
ADH5	class III alcohol dehydrogenase 5 chi subunit	2.38
TCF8	ZEB	2.38
KIAA0912	KIAA0912 protein	2.38
ENPP1	ectonucleotide pyrophosphatase / phosphodiesterase 1	2.37
HAT1	histone acetyltransferase 1	2.37
hnRNPA3	FBRNP	2.37
SLC4A8	solute carrier family 4, 8	2.37
MRE11A	meiotic recombination 11 homolog A	2.37
CAST	calpastatin	2.37
NFIB	nuclear factor I/B	2.37
VLDLR	very low density lipoprotein receptor	2.37
	cDNA clone IMAGE:1676509	2.36
AHCYL1	S-adenosylhomocysteine hydrolase-like 1	2.36
FLJ13052		2.36
RALGPS1	Ral guanine nucleotide exchange factor	2.35
APG-1	heat shock protein apg-1	2.35
PDE4B	phosphodiesterase 4B	2.34
CREB1	cAMP responsive element binding protein 1	2.34
PPIG	peptidyl-prolyl isomerase G (cyclophilin G)	2.34
PEG10	KIAA1051 protein	2.33
BARD1	BRCA1 associated RING domain 1	2.33
ITGA2	integrin alpha 2 precursor	2.33
CDKN2C	cyclin-dependent kinase inhibitor 2C	2.32
TMPO	thymopoietin	2.32
POLD3	polymerase (DNA directed), delta 3	2.31
TOP2A	topoisomerase (DNA) II alpha	2.31

Common ID	Gene name	Fold change
SFRS7	splicing factor, arginine/serine-rich 7	2.31
H2AFV	H2A histone family, member V	2.31
DIXDC1	DIX domain containing 1	2.31
GALNT2	N-acetylgalactosaminyltransferase 2	2.31
CENPF	centromere protein F	2.30
API5	apoptosis inhibitor 5	2.30
CRISP3	cysteine-rich secretory protein 3	2.29
RFC2	replication factor C 2	2.29
SFPQ	splicing factor proline/glutamine rich	2.29
TFRC	transferrin receptor (p90, CD71)	2.28
DFNA5	deafness, autosomal dominant 5 protein	2.28
CFDP1	craniofacial development protein 1	2.28
SLC16A1	solute carrier family 16, member 1	2.28
HNRPF	heterogeneous nuclear ribonucleoprotein F	2.27
SLBP	histone stem-loop binding protein	2.27
PTP4A2	protein tyrosine phosphatase type IVA, 2	2.26
KIFC1	kinesin-related protein	2.26
PASK	PAS domain cont. serine/threonine kinase	2.26
PPFIBP2	liprin-beta2	2.26
PCM1	pericentriolar material 1	2.26
RAPGEF5	Rap guanine nucleotide exchange factor 5	2.26
CRYZ	crystallin, zeta	2.25
USP1	ubiquitin specific protease 1	2.25
HIBCH	3-hydroxyisobutyryl-Coenzyme A hydrolase	2.25
IGSF3	immunoglobulin superfamily, member 3	2.25
CREB1	cAMP responsive element binding protein 1	2.25
KIAA0056	KIAA0056 protein	2.24
PCNA	proliferating cell nuclear antigen	2.24
ZZZ3	zinc finger, ZZ domain containing 3	2.24
LOC65243	Human DNA seq. from clone RP1-228H13	2.24
CYC1	cytochrome c-1	2.23
MRPS6	mitochondrial ribosomal protein S6	2.22
NAB1	NGFI-A binding protein 1	2.22
PNN	pinin, desmosome associated protein	2.22
MOBP	myelin-assoc. oligodendrocyte basic protein	2.22
LIG1	DNA ligase I	2.22
RPL26	ribosomal protein L26	2.22
WSB2	WD repeat and SOCS box-containing 2	2.21
KIAA0635	KIAA0635 protein	2.20
ZNF248	zinc finger protein 248	2.20
MSH2	mutS homolog 2	2.20
KIAA0934	KIAA0934 protein	2.20
NPAT	nuclear protein, ataxia-telangiectasia locus	2.20
ARHGAP5	Rho GTPase activating protein 5	2.20
CTSD	cathepsin D preproprotein	2.19

Common ID	Gene name	Fold change
FLJ20297	hypothetical protein FLJ20297	2.19
CDC42BPA	CDC42-binding protein kinase alpha	2.19
PPT2	palmitoyl-protein thioesterase 2	2.19
ZNF267	zinc finger protein 267	2.19
	Human unidentified mRNA, partial sequence.	2.19
NMB	neuromedin B	2.18
MCM7	minichromosome maintenance protein 7	2.18
PCNA	proliferating cell nuclear antigen	2.18
AURKB	aurora kinase B	2.18
WDHD1	WD repeat & HMG-box DNA binding prot. 1	2.18
MAN2A1	mannosidase, alpha, class 2A, member 1	2.18
MRE11A	meiotic recombination 11 homolog A	2.18
RAD23A	UV excision repair protein RAD23 homolog A	2.17
MYLK	myosin light chain kinase	2.17
DCP2	decapping enzyme hDcp2	2.17
C7orf24	chromosome 7 open reading frame 24	2.17
PARG1	PTPL1-associated RhoGAP 1	2.17
PELP1	proline-, glutamic acid-, leucine-rich protein 1	2.16
MSH2	mutS homolog 2	2.16
384D8-2		2.16
CYB5	cytochrome b-5	2.15
PPP3CB	protein phosphatase 3, catalytic subunit, beta	2.15
DNMT1	DNA (cytosine-5-)-methyltransferase 1	2.15
MITF	microphthalmia-associated transcription fact.	2.15
KIAA0830	KIAA0830 protein	2.15
KIF1B	kinesin family member 1B	2.15
SF3B1	splicing factor 3b, subunit 1, 155kDa	2.15
HUMAUANTIG	nucleolar GTPase	2.14
	MRNA; cDNA DKFZp564I153	2.14
HMMR	HA-mediated motility receptor (RHAMM)	2.14
BICD1	Bicaudal D homolog 1	2.14
FNBP3	formin binding protein 3	2.13
CDC2	cell division cycle 2 protein	2.13
ZWINT	ZW10 interactor	2.13
SMAD5	mothers against decapentaplegic homolog 5	2.13
NEXN	nexilin (F actin binding protein)	2.12
SC5DL	sterol-C5-desaturase-like	2.12
CDC2L1		2.12
TFRC	transferrin receptor (p90, CD71)	2.11
ING3		2.11
CFDP1	craniofacial development protein 1	2.11
DHCR24	24-dehydrocholesterol reductase	2.11
TYR	tyrosinase (oculocutaneous albinism IA)	2.10
KIAA0542	KIAA0542 protein	2.10
C4orf15	hypothetical protein MGC4701	2.10

Common ID	Gene name	Fold change
BRCA1	breast cancer 1, early onset	2.10
MARCKS	myristoylated alanine-rich PKC substrate	2.10
ARHGEF12	Rho guanine nucleotide exchange factor, 12	2.10
BUB1	budding uninhibited by benzimidazoles 1	2.10
TNPO1	transportin 1	2.09
AHCYL1	S-adenosylhomocysteine hydrolase-like 1	2.08
PRKCN	protein kinase C, nu	2.08
MYBL2	MYB-related protein B	2.08
RFC4	replication factor C, 37-kDa subunit	2.07
SON	SON DNA-binding protein	2.07
PMS1	postmeiotic segregation 1	2.07
SPTB		2.07
ITGA1	integrin, alpha 1 precursor	2.06
HEXA	hexosaminidase A (alpha polypeptide)	2.06
PIK3R1	phosphoinositide-3-kinase, regulatory, 1	2.06
ERBB3	v-erb-b2 erythroblastic leukemia viral oncogene homolog 3	2.06
PCLO	KIAA0559 protein	2.06
CSDA	cold shock domain protein A	2.05
CDC2	cell division cycle 2 protein	2.05
CCNA2	cyclin A	2.05
SR140	U2-associated SR140 protein	2.05
	Human HepG2 3' region MboI cDNA	2.04
FMR2	fragile X mental retardation 2	2.04
UBE4B	ubiquitination factor E4B	2.04
KIF23	kinesin family member 23	2.04
PDZRN3	KIAA1095 protein	2.04
DDX17	DEAD box polypeptide 17	2.04
CDC20	cell division cycle 20	2.04
PSIP1	PC4 and SFRS1 interacting protein 1	2.03
UGCG	ceramide glucosyltransferase	2.03
MAPK6	mitogen-activated protein kinase 6	2.03
NR2C1	nuclear receptor subfamily 2, group C, 1	2.03
SMA5	Similar to SMA3 protein	2.03
ATP2B4	ATPase, Ca++ transporting, plasma memb. 4	2.03
KCTD12	K channel tetramerisation domain cont. 12	2.03
NDUFA6	NADH dehydrogenase (ubiquinone) 1 alpha subcomplex, 6	2.03
DYRK3	dual-specificity tyrosine-(Y)-phosphorylation regulated kinase 3	2.02
MCM4	minichromosome maintenance protein 4	2.02
CYB5	cytochrome b-5	2.02
DHFR	dihydrofolate reductase	2.02
	cDNA clone EUROIMAGE 35907.	2.02
VRK1	vaccinia related kinase 1	2.02

Common ID	Gene name	Fold change
SH3BP5	SH3-domain binding protein 5	2.02
SNTB2	basic beta 2 syntrophin	2.02
RUTBC1	KIAA0397 protein	2.02
PSMD7	proteasome 26S non-ATPase subunit 7	2.01
SMG1	PI-3-kinase-related kinase SMG-1	2.01
MAD2L1	MAD2 mitotic arrest deficient-like 1	2.01
KIAA0494	KIAA0494 protein	2.01
TYR	Human tyrosinase-related gene segment	2.01
UBB	ubiquitin	2.00
LOC93081	hypothetical protein BC015148	2.00
E2F5	E2F transcription factor 5	-2.00
SLC20A1	solute carrier family 20 (phosph. transp.), 1	-2.00
C20orf18	chromosome 20 open reading frame 18	-2.01
HADH2	hydroxyacyl-Coenzyme A dehydrogenase, II	-2.01
CDK11	cyclin-dependent kinase (CDC2-like) 11	-2.01
PL6	PL6 protein	-2.01
IDH1	isocitrate dehydrogenase 1 (NADP+), soluble	-2.02
FTSJ1	FtsJ homolog 1	-2.02
STK16	serine/threonine kinase 16	-2.02
RCN1	reticulocalbin 1 precursor	-2.02
SLC35B1	solute carrier family 35, member B1	-2.02
SH3BGRL	SH3 dom. binding glutamic acid-rich prot. like	-2.03
PBX1	pre-B-cell leukemia transcription factor 1	-2.03
MYD88	myeloid differentiation primary response 88	-2.03
GSR	glutathione reductase	-2.03
PCTK1	PCTAIRE protein kinase 1	-2.03
EXT2	exostosin 2	-2.03
XBP1	X-box binding protein 1	-2.04
VAMP4	vesicle-associated membrane protein 4	-2.04
IFNG	interferon, gamma	-2.04
CD44		-2.04
ANXA1	annexin I	-2.04
RIOK3		-2.04
PHF16	PHD finger protein 16	-2.04
C9orf16	chromosome 9 open reading frame 16	-2.05
F2R	coagulation factor II receptor precursor	-2.05
MBC2	KIAA0747 protein	-2.05
SDC4	syndecan 4 precursor	-2.05
YWHAZ	tyrosine 3/tryptophan 5 -monooxygenase activation protein, zeta	-2.05
HLA-F	major histocompatibility complex, class I, F	-2.05
CLCN5	chloride channel 5	-2.06
AMOT	angiomotin	-2.06
BCHE	butyrylcholinesterase precursor	-2.06
CD44	CD44 antigen	-2.06

Common ID	Gene name	Fold change
SLC7A11	solute carrier family 7, (cationic amino acid transporter), 11	-2.06
PDXK	pyridoxal kinase	-2.07
RXRA		-2.07
NQO1	NAD(P)H menadione oxidoreductase 1, dioxin-inducible	-2.07
SPP1	secreted phosphoprotein 1	-2.08
HK2	hexokinase II	-2.08
PIK3C3	phosphoinositide-3-kinase, class 3	-2.08
TERF1	telomeric repeat binding factor 1	-2.08
PPP3CB	protein phosphatase 3, catalytic subunit, beta	-2.09
NDUFS7		-2.09
JM5	JM5 protein	-2.09
SLC1A3	solute carrier family 1 (glial high affinity glutamate transporter), 3	-2.10
H1F0		-2.10
D15Wsu75e	DNA segment, Chr 15, Wayne State University 75, expressed	-2.10
ARFGEF2	ADP-ribosylation factor guanine nucleotide-exchange factor 2	-2.10
SUPT4H1	suppressor of Ty 4 homolog 1	-2.11
CYP4F2	cytochrome P450, family 4, subfamily F, 2	-2.11
MKRN4	makorin, ring finger protein, 4	-2.11
SIAT7B	sialyltransferase 7	-2.11
SERPINH1	serine proteinase inhibitor, clade H, 1	-2.11
UGP2	UDP-glucose pyrophosphorylase 2	-2.12
IFI35	interferon-induced protein 35	-2.12
IGBP1	immunoglobulin (CD79A) binding protein 1	-2.13
CSNK2A1	casein kinase II alpha 1	-2.13
RTN2	reticulon 2	-2.13
HMG20B	high-mobility group 20B	-2.14
LOC91966	hypothetical protein LOC91966	-2.14
ADORA2B	adenosine A2b receptor	-2.14
SYBL1	synaptobrevin-like 1	-2.15
MGC52022	Similar to RIKEN cDNA 1810038N08 gene	-2.15
RIN1	ras interactor	-2.15
SRPX	sushi-repeat-containing protein, X-linked	-2.16
CBLB	Cas-Br-M (murine) ecotropic retroviral transforming sequence b	-2.16
SLC1A5	solute carrier family 1 (neutral amino acid transporter), 5	-2.16
ZNF263	zinc finger protein 263	-2.16
DOC-1R	tumor supp. deleted in oral cancer-related 1	-2.16
PTRF	polymerase I and transcript release factor	-2.17
SAT	spermidine/spermine N1-acetyltransferase	-2.17

Common ID	Gene name	Fold change
PSKH1	chymotrypsin-like	-2.17
LTBP4	Latent TGFβ binding protein 4	-2.18
AP3M2	adaptor-related protein complex 3, mu 2	-2.19
LOC151162	cDNA DKFZp686B24166	-2.19
ZNF91	zinc finger protein 91	-2.19
CITED2	Cbp/p300-interacting transactivator, with Glu/Asp-rich carboxy-terminal domain, 2	-2.20
IRS1	insulin receptor substrate 1	-2.20
SLC3A2	solute carrier family 3 (activators of dibasic and neutral amino acid transport), 2	-2.20
TREX2	three prime repair exonuclease 2	-2.20
EMD	emerin	-2.20
C1orf17	chromosome 1 open reading frame 17	-2.21
SLC10A3	solute carrier family 10, member 3	-2.21
ATRX	transcriptional regulator ATRX	-2.21
TBC1D4	KIAA0603 protein	-2.21
CASK	Ca/calmodulin-dependent serine prot. kinase	-2.21
EIF4EBP1	Euk. translation init. fact. 4E binding prot. 1	-2.22
SMURF2	E3 ubiquitin ligase SMURF2	-2.22
UBE2A	ubiquitin-conjugating enzyme E2A	-2.22
JM4	JM4 protein	-2.22
CX3CL1	chemokine (C-X3-C motif) ligand 1	-2.22
PPP1R13B	protein phosphatase 1, reg. subunit 13B	-2.23
MEIS4	Meis1-related protein 2	-2.23
GSN	gelsolin	-2.23
LOC339047	Similar to nucl. pore complex interacting prot.	-2.24
HIST1H2BD	Transcribed sequence with strong similarity to protein histone H2B.1	-2.24
GART	phosphoribosylglycinamide formyltransferase	-2.24
UREB1		-2.25
IFI35		-2.25
PRKACB	protein kinase, cAMP-dependent, catalytic, β	-2.25
LIFR	leukemia inhibitory factor receptor precursor	-2.26
PPAP2A	phosphatidic acid phosphatase type 2A	-2.27
CSNK2A1	casein kinase II alpha 1 subunit	-2.27
DUSP4	dual specificity phosphatase 4	-2.27
SLC1A4	solute carrier family 1 (glutamate/neutral amino acid transporter), 4	-2.27
DNASE1L1	deoxyribonuclease I-like 1	-2.28
CXX1	CAAX box 1	-2.28
PSEN1	presenilin 1	-2.29
ZNF263	zinc finger protein 263	-2.29
CXorf12	chromosome X open reading frame 12	-2.30
RPGR	retinitis pigmentosa GTPase regulator	-2.30
EIF2S3	Euk. translation initiation factor 2, subunit 3	-2.31

Common ID	Gene name	Fold change
EGFL5	MEGF9	-2.32
PEX5	peroxisomal biogenesis factor 5	-2.33
STK4	serine/threonine kinase 4	-2.33
CBLB	Cas-Br-M (murine) ecotropic retroviral transforming sequence b	-2.34
FAH	fumarylacetoacetate hydrolase	-2.34
CRELD1	cysteine-rich with EGF-like domains 1	-2.35
KIAA1539	Soares breast 2NbHBst	-2.35
KIAA0500	chromosome 1 specific transcript KIAA0500.	-2.36
GJB1	gap junction protein, beta 1	-2.37
ARID5B	AT rich interactive domain 5B	-2.37
GK	glycerol kinase	-2.37
BACH1	BTB and CNC homology 1	-2.38
RABAC1	Rab acceptor 1	-2.38
ATF4		-2.39
TNF	tumor necrosis factor alpha	-2.39
FZD2	frizzled 2	-2.39
MOCS3	molybdenum cofactor synthesis 3	-2.39
MGC8721	retina cDNA randomly primed sublibrary	-2.39
RPS6KA4	ribosomal protein S6 kinase, polypeptide 4	-2.39
SPP1	secreted phosphoprotein 1	-2.39
NUCB2	nucleobindin 2	-2.40
SEC63	SEC63-like protein	-2.40
TAZ	tafazzin	-2.42
IL13RA1	interleukin 13 receptor, alpha 1 precursor	-2.42
SLC23A2	solute carrier family 23 (nucleobase transporters), 2	-2.42
ANKS1	ankyrin repeat, sterile α motif domain cont. 1	-2.43
SERPINA3	alpha-1-antichymotrypsin, precursor	-2.43
SPRR2B	small proline-rich protein 2B	-2.43
PLTP	phospholipid transfer protein	-2.44
PHKA2	phosphorylase kinase, alpha 2	-2.44
ZNF217	zinc finger protein 217	-2.44
PRSS7	enterokinase precursor	-2.45
UK114	translational inhibitor protein p14.5	-2.45
GPR21	RAB GTPase activating protein 1	-2.45
SIAT1	sialyltransferase 1	-2.46
EIF2B2	eukaryotic translation init. fact. 2B, subunit 2	-2.46
HLA-DMB	MHC, class II, DM beta	-2.48
RAGE		-2.48
SLC6A8	solute carrier family 6 (neurotransmitter transporter), 8	-2.49
CDKN2A	cyclin-dependent kinase inhibitor 2A	-2.51
MIA	Ras-related protein RAB-4	-2.52
ASMTL	acetylserotonin O-methyltransferase-like	-2.53

Common ID	Gene name	Fold change
DXYS155E	DNA segment on chromosome X and Y (unique) 155 expressed	-2.53
PEX6	peroxisomal biogenesis factor 6	-2.53
HTR2C	5-hydroxytryptamine (serotonin) receptor 2C	-2.53
HIST1H2BM	H2B histone family, member E	-2.53
MYOZ3	myozenin 3	-2.54
TTF1	transcription factor	-2.54
MPPE1	metallophosphoesterase 1	-2.54
XBP1	X-box binding protein 1	-2.54
HMOX1		-2.55
TXNRD1	thioredoxin reductase 1	-2.55
PLAG1	pleiomorphic adenoma gene 1	-2.55
ALDH6A1	aldehyde dehydrogenase 6A1 precursor	-2.56
DJ971N18.2	retina cDNA randomly primed sublibrary	-2.56
HIST1H4I	H4 histone family, E	-2.56
TRIM16	tripartite motif-containing 16	-2.57
RPL23	ribosomal protein L23	-2.57
CUL2	cullin 2	-2.57
GMPR	guanosine monophosphate reductase	-2.58
GPR19	G protein-coupled receptor 19	-2.58
MSC	musculin (activated B-cell factor-1)	-2.59
P2RX5	purinergic receptor P2X5	-2.59
ETV4	ets variant gene 4 (E1A enhancer binding protein, E1AF)	-2.60
CD99	CD99 antigen	-2.60
BTBD2	BTB (POZ) domain containing 2	-2.60
	IMAGE:2470258	-2.61
HDAC5	histone deacetylase 5	-2.62
ETHE1	ETHE1 protein	-2.63
TOSO	regulator of Fas-induced apoptosis	-2.64
CTH	cystathionase	-2.64
EPHB3	ephrin receptor EphB3 precursor	-2.65
WASF1	WAS protein family, 1	-2.65
ZNF183	zinc finger protein 183	-2.65
TNFSF9	tumor necrosis factor superfamily, 9	-2.67
GRP58	glucose regulated protein, 58kDa	-2.69
PDE1C	PDE1C3	-2.70
C21orf107	WD repeat domain 9	-2.70
TIAM1	T-cell lymphoma invasion and metastasis 1	-2.71
RPL23	ribosomal protein L23	-2.72
GSTT1	glutathione S-transferase theta 1	-2.72
EIF5	eukaryotic translation initiation factor 5	-2.73
TGFB2	transforming growth factor B2	-2.73
IKBKG	inhibitor of kappa light polypeptide gene enhancer in B-cells, kinase gamma	-2.74

Common ID	Gene name	Fold change
TRA1	tumor rejection antigen 1	-2.74
ARL7	ADP-ribosylation factor-like 7	-2.74
MGEA6	meningioma expressed antigen 6	-2.75
SERPINB6	cytoplasmic antiproteinase	-2.75
	retina cDNA randomly primed sublibrary	-2.75
ARHGEF6	Rac/Cdc42 guanine nucl. exchange fact. 6	-2.76
	CDNA FLJ41436	-2.76
MRPL28	mitochondrial ribosomal protein L28	-2.77
LOC253982	hypothetical protein LOC253982	-2.77
PTPRF	protein tyrosine phosphatase, receptor, F	-2.77
POU2F3	POU transcription factor	-2.78
TRAF3	TNF receptor-associated factor 3	-2.78
GNG11	guanine nucleotide binding protein, γ 11	-2.79
PTPRG	protein tyrosine phosphatase, receptor, G	-2.80
TIPARP	TCDD-induc. poly(ADP-ribose) polymerase	-2.81
DLX2	distal-less homeo box 2	-2.82
IDS	iduronate-2-sulfatase	-2.82
CBS	cystathionine-beta-synthase	-2.84
C14orf11	chromosome 14 open reading frame 11	-2.84
IRAK1	interleukin-1 receptor-associated kinase 1	-2.84
VEGF	vascular endothelial growth factor	-2.85
SOX9	transcription factor SOX9	-2.85
PIM2	pim-2 oncogene	-2.87
FKBP1A	FK506-binding protein 1A	-2.87
CHN1	chimerin 1	-2.89
RPL23AP7	subtelomeric repeat sequence	-2.90
TACSTD2	tumor-associated calcium signal transducer 2	-2.91
ATP2A2	ATPase, Ca++ transporting, cardiac muscle, slow twitch 2	-2.92
ATP9A	KIAA0611 protein	-2.92
BLVRB	biliverdin reductase B	-2.92
CCND1	cyclin D1	-2.93
HIST2H2AA	H2A histone family, member O	-2.94
GDF15	growth differentiation factor 15	-2.95
PROCR	endothelial protein C receptor	-2.95
DXS9928E	XAP-5 protein	-2.96
HLA-E	lymphocyte antigen	-2.97
RENBP		-2.97
ARD1		-2.98
HSPA5	heat shock 70kDa protein 5	-2.98
CPNE1	copine I	-2.98
VEGF	vascular endothelial growth factor	-2.98
DNAJB9	DnaJ (Hsp40), subfamily B, 9	-2.99
ATF3	activating transcription factor 3	-3.00
HIST1H1C	similar to Histone H1D	-3.00

Common ID	Gene name	Fold change
LYN	v-yes-1 Yamaguchi sarcoma viral related oncogene	-3.00
SLC26A2	solute carrier family 26, 2	-3.00
PPP1R15A	protein phosphatase 1, reg. subunit 15A	-3.01
MYH3	myosin, heavy polypeptide 3	-3.01
PCK2	phosphoenolpyruvate carboxykinase 2	-3.01
C6orf68	YDD19 protein	-3.02
NDP52	nuclear domain 10 protein	-3.03
C9orf61	chromosome 9 open reading frame 61	-3.05
TP53	tumor protein p53	-3.08
PCTK1	PCTAIRE protein kinase 1	-3.11
PTPRJ	protein tyrosine phosphatase, receptor, J	-3.13
COL8A1	alpha 1 type VIII collagen precursor	-3.13
INPP1	inositol polyphosphate-1-phosphatase	-3.16
CRAT	carnitine acetyltransferase	-3.16
KIAA0963		-3.18
TWIST1	twist	-3.19
CCNG2	cyclin G2	-3.19
PRKAB2	protein kinase, AMP-activated, beta 2	-3.21
PCDHGC3	protocadherin gamma subfamily C, 3	-3.21
SLC22A5	solute carrier family 22 member 5	-3.22
CALR	calreticulin precursor	-3.31
WARS	tryptophanyl-tRNA synthetase	-3.31
TCEA1	transcription elongation factor A 1	-3.36
GLRX	glutaredoxin (thioltransferase)	-3.37
MMP16	matrix metalloproteinase 16	-3.39
DDIT4	DNA-damage-inducible transcript 4	-3.39
RPH3A	rabphilin 3A homolog	-3.40
PRKCZ	protein kinase C, zeta	-3.41
ASMTL		-3.41
VAMP5	vesicle-associated membrane protein 5	-3.41
GULP1	engulfment adaptor PTB domain cont. 1	-3.44
DAF	decay accelerating factor for complement	-3.46
	Human chromosome 5q13.1 clone 5G8	-3.46
BIN1	bridging integrator 1	-3.50
EIF4EBP1	glutathione S-transferase theta 1	-3.51
PLXNB3	signal sequence receptor, delta	-3.51
BCAP31	B-cell receptor-associated protein 31	-3.53
VEGF	vascular endothelial growth factor	-3.57
KCNN4	intermediate conductance calcium-activated potassium channel protein 1	-3.58
HLA-C	major histocompatibility complex	-3.60
FHL1	four and a half LIM domains 1	-3.62
PDLIM1	PDZ and LIM domain 1	-3.64
CD74	cell surface glycoprotein	-3.64

Common ID	Gene name	Fold change
IFITM3	interferon-induced transmembrane protein 3	-3.69
PTN	pleiotrophin	-3.69
DXYS155E		-3.69
IER3	immediate early response 3	-3.69
ZAP128	peroxisom. long-chain acyl-coA thioesterase	-3.73
PNRC1	proline-rich nuclear receptor coactivator 1	-3.76
HIST1H2AC	H2A histone family, member L	-3.80
HYOU1	oxygen regulated protein precursor	-3.85
TBL1X	transducin beta-like 1X	-3.86
BTEB1	basic transcription element binding protein 1	-3.88
KATNA1	katanin p60 (ATPase-containing) subunit A 1	-3.91
CTSL	cathepsin L preproprotein	-3.91
IFNGR2	interferon gamma receptor 2	-3.95
DCBLD2	endothelial and smooth muscle cell-derived neuropilin-like protein	-3.97
RPS6KA3	ribosomal protein S6 kinase, polypeptide 3	-3.97
GPR19	G protein-coupled receptor 19	-4.00
SSR4	signal sequence receptor, delta	-4.03
TIMP1	tissue inhibitor of metalloproteinase 1	-4.08
OGT	O-linked GlcNAc transferase	-4.10
KRT18	keratin 18	-4.15
ITGB3	integrin beta chain, beta 3 precursor	-4.17
HERPUD1	homocysteine-inducible, ER stress-inducible, ubiquitin-like domain, 1	-4.17
LYN	v-yes-1 Yamaguchi sarcoma viral related oncogene homolog	-4.22
SCRN1	secernin 1	-4.26
CDC42EP3	Cdc42 effector protein 3	-4.31
CAMP	cathelicidin antimicrobial peptide	-4.31
MAOA	monoamine oxidase A	-4.35
SIM2	single-minded homolog 2	-4.35
C14orf78	retina cDNA randomly primed sublibrary	-4.37
HIST1H4A	similar to HISTONE H4	-4.39
PHLDA1	pleckstrin homology-like domain, family A, 1	-4.44
SERPINB8	serine proteinase inhibitor, clade B, 8	-4.48
HIST2H2BE		-4.52
E2F5	E2F transcription factor 5	-4.57
ZBTB33	kaiso	-4.65
PCTK2	PCTAIRE protein kinase 2	-4.67
SNRPB2		-4.74
RABL4	RAB, member of RAS oncogene family-like 4	-4.81
ANK2	ankyrin 2	-4.85
CAMTA2	calmodulin binding transcription activator 2	-4.88
NT5E	5' nucleotidase, ecto	-4.95
SNTB1	basic beta 1 syntrophin	-5.00

Common ID	Gene name	Fold change
OLIG2	oligodendrocyte lineage transcription factor 2	-5.10
HLA-DRA	MHC, class II, DR alpha precursor	-5.15
SYNE1	nesprin 1	-5.15
CPR8	cell cycle progression 8 protein	-5.15
THBS2	thrombospondin 2 precursor	-5.18
CALR		-5.26
FECH	ferrochelatase	-5.35
L1CAM		-5.35
HLA-DPB1	MHC, class II, DP beta 1	-5.41
EPHA2	ephrin receptor	-5.41
FOXF2	forkhead box F2	-5.41
PRKCL1	protein kinase C-like 1	-5.52
RAI3	retinoic acid induced 3	-5.59
HIST1H2BK	H2B histone family, member T	-5.68
IFITM1	interferon induced transmembrane protein 1	-5.81
SPUVE	protease, serine, 23 precursor	-5.95
TNFRSF21	TNF receptor superfamily, 21	-6.02
ABHD2	alpha/beta hydrolase domain cont. protein 2	-6.02
ASB9	ankyrin repeat and SOCS box-cont. 9	-6.06
DDIT3	TLS-CHOP	-6.29
GSTZ1	glutathione transferase ζ 1	-6.45
THBS2	thrombospondin 2 precursor	-6.58
NDRG1	N-myc downstream regulated gene 1	-6.80
HIST1H2AL	histone 1, H2al	-6.85
BST2	bone marrow stromal cell antigen 2	-6.94
CSTA	cystatin A	-6.99
FST	follistatin	-7.04
CITED1	Cbp/p300-interacting transactivator, 1	-7.35
RAC2	rho family, small GTP binding protein Rac2	-7.46
ERCC6	excision repair cross-complementing, 6	-7.46
PCOLCE	procollagen C-endopeptidase enhancer	-7.52
TM4SF10	transmembrane 4 superfamily, 10	-8.13
MMP1	matrix metalloproteinase 1	-8.33
ELF4	E74-like factor 4	-9.01
HTATIP2	HIV-1 Tat interactive protein 2	-9.09
BCL2A1	BCL2-related protein A1	-9.52
ME1	cytosolic malic enzyme 1	-10.00
RIS1	Ras-induced senescence 1	-10.05
EGR3	early growth response 3	-10.25
HIST1H2AG	H2A histone family, member P	-10.50
HLA-DPB1	MHC, class II, DP β 1	-11.01
APOD	apolipoprotein D precursor	-12.05
KLRC3	killer cell lectin-like receptor subfamily C, 3	-12.14
KLRC2	killer cell lectin-like receptor subfamily C, 2	-12.18
HCG4	HLA complex group 4	-12.72

Common ID	Gene name	Fold change
TMEM16C	transmembrane protein 16C	-13.11
	alpha(1,2)fucosyltransferase	-13.14
COL6A1	collagen, type VI, α 1	-13.81
S100P	S100 calcium binding protein P	-15.46
HIST2H2AA	histone 2, H2aa	-15.48
HLA-DMA	MHC, class II, DM α	-15.48
HOXB2	homeo box B2	-15.87
ZNF330	zinc finger protein 330	-19.34
RAI3	retinoic acid induced 3	-21.65
ARGBP2	Arg/Abl-interacting protein 2	-22.94
HLA-DRB1	MHC, class II, DR β 1	-23.31
DHRS3	dehydrogenase/reductase DR family, 3	-26.46
AZGP1	alpha-2-glycoprotein 1, zinc	-27.25
MGLL	monoglyceride lipase	-40.65
SERPINB1	serine proteinase inhibitor, clade B, 1	-58.82
PRRX1	sequence from clone RP1-79C4	-64.10
ART3	ADP-ribosyltransferase 3	-100.00
SCRG1	scrapie responsive protein 1	-100.00

APPENDIX II

Sample DNA Histogram

Figure 35. Sample DNA histogram obtained from flow cytometry analysis of propidium iodide stained nuclei.

BECKMAN COULTER

COULTER(R) EPICS(R) Acquisition Flow Cytometry Report

17Feb04 12:26:52
KAREN STRIPPED DNA
R0024641
MDA 24 M1

OP ID: MIKE

177 seconds, 51688 events

:l cytosett. from prot. KAREN STRIPPED DNA

Stop Count: 50000 events, histogram 2

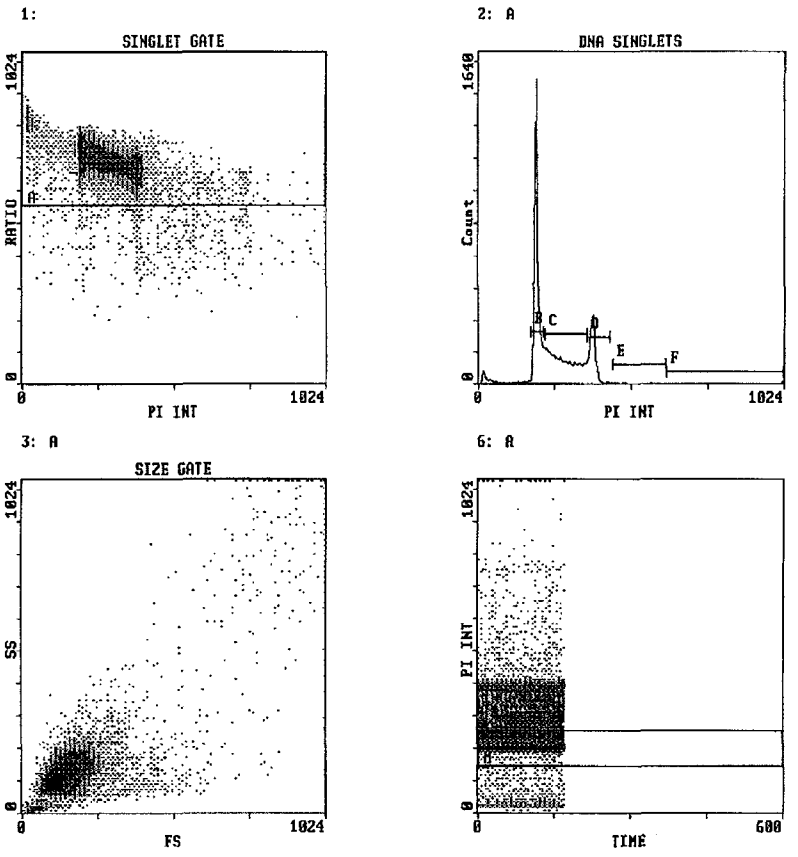

Stats: Normalized, Listgating: Disabled

Hist	Region ID	%	Count	Mn X	Mn Y
1	A RATIO	96.7	50000	261.9	690.0
6	M QC	52.3	26133	147.7	203.9

Hist	Region ID	%	Count	Mn X	Md X	HPCV
2	B G0/G1	40.0	19986	199.5	198.0	1.88
	C S PHASE	35.4	17712	287.1	282.6	18.33
	D G2/M	16.5	8265	387.2	386.6	1.80
	E TRIPLETS	1.53	763	521.4	511.4	2.40
	F QUADRUPLETS	0.78	389	785.3	746.8	**

Curriculum Vitae

Name: Karen Laverne Morley

EDUCATION

2001 – 2007 **Ph.D. Candidate**
Department of Microbiology and Immunology
The University of Western Ontario, London ON
Supervisor: Dr. D. James Koropatnick

1997 – 1999 **Diploma in Honors Standing**
Department of Biochemistry
The University of Western Ontario, London ON

1993 – 1997 **B.Sc.**
Department of Chemistry
The University of Western Ontario, London ON

SCHOLARSHIPS AND AWARDS

2001 – 2006 **Canadian Institute of Health Research**
University-Industry Scholarship

2001 – 2006 **Faculty of Graduate Studies, UWO**
Graduate Tuition Scholarship

2004 **American Association for Cancer Research**
AACR Minority Scholar Award in Cancer Research

2001 **Faculty of Graduate Studies, UWO**
Special University Scholarship

RELEVANT WORK EXPERIENCE

2006 – 2007 **Scientist I**
KGK Synergize Inc., London, ON

1999 – 2001 **Laboratory Technician**
KGK Synergize Inc., London, ON

1997 – 1999 **Research Assistant**
Department of Biochemistry
The University of Western Ontario, London ON
Supervisor: Dr. Elzbieta Kurowska

PUBLICATIONS

Articles in Peer-Reviewed Journals

K. Morley, P.J. Ferguson and J. Koropatnick. 2007. Tangeretin and nobiletin induce G1 cell cycle arrest but not apoptosis in human breast and colon cancer cells. Cancer Lett. 251(1):168-178

E.M. Kurowska, **K. Morley** and A. Gapor. Role of tocotrienols from palm oil in regulation of apo B metabolism in HepG2 cells. Int. J. Food Sci. Nutr., 1999 (submitted)

Book Chapters

N. Guthrie, **K. Morley**, S. Hasegawa, G.D. Manners and T. Vandenberg. Inhibition of human breast cancer cells by citrus limonoids. In: Citrus Limonoids: Functional Chemicals in Agriculture and Food. M.A. Berhow, S. Hasegawa, and G.D. Manners, (Eds.) American Chemical Society, Washington, DC, 2000 pp. 164-174

Published Abstracts

K. Morley, J. Koropatnick. An Investigation of the anticancer mechanism of citrus flavonoids tangeretin and nobiletin. 16th Annual EORTC-NCI-AACR Molecular Targeted Therapies, Geneva, Switzerland, September 29-October 2, 2004.

E.M. Kurowska, **K. Morley** and A. Gapor: Role of tocotrienols from palm oil in regulation of apo B metabolism in HepG2 cells. Experimental Biology 99, Washington, DC, April 17-21, 1999.

E.M. Kurowska, **K. Morley** and A. Gapor: Regulation of apo B production in HepG2 cells by tocotrienols from palm oil. PORIM International Palm Oil Congress, Kuala Lumpur, Malaysia, February 1-6, 1999.